UNIVERSITY OF LONDON THESIS

Degree PhD Year 2007 Name of Author CESCA, Fabrizia

Analysis of the biological functions of Kidins220: from cells to organisms

Fabrizia Cesca

Thesis submitted for the degree of Doctor of Philosophy

at the University of London

July 2007

Molecular Neuropathobiology
Laboratory
Cancer Research UK
London Research Institute
44 Lincoln's Inn Fields
WC2A 3PX London, UK

Department of Biochemistry
and Molecular Biology
University College of London
Gower Street
WC1E 6BT London, UK

ProQuest LLC
789 East Eisenhower Parkway
P.O. Box 1346
Ann Arbor, MI 48106-1346

Ai miei genitori

e alla mia sorellina

To my parents

and my little sister

Perché in questi anni mi avete insegnato

Che le distanze del cuore prescindono

da quelle geografiche.

Abstract

In this work, I have characterised the biological functions of Kidins220 (*K*inase *D in*teracting *s*ubstrate of *220* kDa) in both an *in vitro* and *in vivo* context. Kidins220 is a conserved membrane protein mainly expressed in neuronal cells, which has been implicated in the process of neuronal differentiation in response to neurotrophic stimuli. In the first part of this study, I present an analysis of the molecular mechanism regulating the intracellular trafficking of Kidins220 in a rat pheochromocytoma cell line (PC12), which upon treatment with nerve growth factor (NGF) differentiates into neuronal-like cells resembling sympathetic neurons. Kidins220 transport to neurite tips is driven by the microtubule-dependent motor complex kinesin-1. Perturbation of Kidins220 trafficking in this cellular system reduces the activation of the signalling cascades initiated by NGF and impairs neuronal differentiation.

I was interested in understanding the mechanisms that might modulate the association of Kidins220 to kinesin-1. Kidins220 recruits kinesin-1 via a novel binding motif, which does not share any similarities with the known kinesin-1-interacting signatures. I found that Abelson tyrosine kinase (Abl) phosphorylates Kidins220 at the level of this kinesin interacting motif, thus inhibiting the binding to kinesin light chain. These preliminary results suggest that phosphorylation might act as a molecular switch, to mediate the release of Kidins220 from the kinesin-1 motor complex.

In the second part of this work, I analysed the effects of Kidins220 depletion in living organisms. I tackled this problem by targeting Kidins220 by RNA interference in *Drosophila melanogaster*. In an independent approach, I have generated a construct, based on the Cre/LoxP recombination system, for the conditional knockout of the Kidins220 gene in mice. Kidins220 null animals die at late stages of embryonic development, and display severe cardiovascular and neurological defects. Their phenotype is described in detail using a variety of immunohistochemical and cell biological approaches.

This work therefore presents new evidence supporting the notion that Kidins220 plays an important role in regulating not only neuronal function and differentiation, but also other key developmental processes such as cardiac development.

Acknowledgements

The first and biggest "thank you" is to my parents and my sister, for their love and support, and for always letting me go my own way, even when the way was taking me far from them. Thanks to my old friends Annarita and Gino, for standing at my side at every step of this journey. Thanks to my new friends Mary and Grant, Emma and Tamara, for making my life here a real life. And to my ex-flatmate and friend Arianna, for facing and solving with me countless lab-, life- and housekeeping-related problems. Thanks to all the people I have worked with during these years in CRUK, in particular to Ralf and Susanne Adams for teaching me everything there is to know about making a knock-out mouse, to Colin, Debbie and Alastair in the Light Microscopy Lab for teaching me how to use microscopes, to Clare and Emma and all the members of the Animal Unit for taking such good care of my mice. A special thank you goes to the people in the Experimental Pathology Lab, particularly to Bradley, for the technical, scientific and moral support, for reading my thesis, and for the chocolate.

But above all, I want to thank all the present and past members of the MNP lab. They are (in random order): the Permanent People: crazy Matthew and super Claire; the World Cup Winners (sorry... I meant "the Italians"): Lionel Richie / Aurora, smiley Ale, fashion Alex, and Marco-from-the-mountains; the People from Different Countries: Espanish-billy boy-Guillermo, Sc*u*ttish Lynsey, sweet Veronika, and Calimero Sara; and the People from Different Planets: puositive Olga. Thank you all for making the lab such a great place to work. Thank you for the scientific advice, the moral support in hard times, the jokes in the good times, but above all for the real friendship you have always given to me. There will be other labs and other labmates in my life, but you will always have a special place in my heart (yes, I know... but I'm Italian, I just *have* to have a little bit of melodrama...).

And to conclude, thanks to my supervisor, gipi-the Man from a Different Galaxy, the man that with his powers can transform rabbits into lions and potatoes into caviar... Thank you for giving me the possibility to work in your group, for believing in me, and for your endless attempts to toughen my spirit. The years I spent in your lab have really changed my life.

Table of Contents

List of Figures

List of Tables

List of Videos

Video 1: Kidins220 is actively transported in PC12 cells.

Video 2: mRFP-KIM expression impairs the trafficking of Kidins220.

Video 3: The expression of mRFP-KIM(Y24A) does not alter the trafficking of Kidins220

Abbreviations

aa	amino acid
Abl	Abelson tyrosine kinase
AMPA	α-amino-3-hydroxy-5-methyl-4-isoxazole propionic acid
AP-1	adaptor protein-1
APOER2	apolipoprotein E receptor 2
APP	amyloid precursor protein
APPL1	adaptor protein containing PH domain, PTB domain, and leucine zipper motif
ATP	adenosine-5'-triphosphate
BDNF	brain-derived neurotrophic factor
bp	base pair
BSA	bovine serum albumine
C3G	Crk SH3-binding guanine-nucleotide releasing protein
CaMK	Ca^{2+}-calmodulin regulated protein kinase
cAMP	cyclic adenosine monophosphate
cDNA	complementary DNA
CGN	cerebellar granule neurons
CK	casein kinase
CNS	central nervous system
Cre	cyclisation recombination recombinase
CREB	cAMP response element-binding protein
Crk	chicken tumour virus regulator of kinase
CrkL	Crk-like protein
DAG	diacylglycerol
DIC	differential interference contrast
DMEM	Dulbecco's modified Eagles medium
DMSO	dimethylsulphoxide
DNA	desoxyribonucleic acid
DRG	dorsal root ganglia

DTT	dithiothreitol
EDTA	dimethylenediaminetetraacetic acid
EGF	epithelial growth factor
EGFP	enhanced green fluorescent protein
EGFR	EGF receptor
ELISA	enzyme-linked immunosorbent assay
ELK	Ets-like transcription factor
ERK	extracellular signal regulated kinase
ES cells	embryonic stem cells
Gab	Grb2-associated binding protein
GDNF	glial cell-derived neurotrophic factor
GDNFR	GDNF receptor
GIPC	GAIP-interacting protein, C-terminus adaptor
GluR	glutamate receptor
GPI	glycosylphosphatidylinositol
Grb2	growth factor receptor-bound protein 2
GRIP	GluR-interacting protein
GSK3	glycogen synthase kinase 3
GST	glutathione-S-transferase
HA	hemagglutinin
HR	heptad repeats
HRP	horseradish peroxidase
Ig domain	immunoglobulin-like domain
IP3	inositol(1,4,5)trisphosphate
IPTG	isopropyl-β-D-thiogalacto-pyranoside
Jak	Janus kinase
JIP	JNK-interacting protein
JNK	Jun N-terminal kinase
KC	carboxy terminal tail of Kidins220 (aa 1209-1762)
kDa	kilo Daltons

Kidins220 / ARMS Kinase D interacting substrate of 220 kDa / ankyrin repeat reach membrane spanning

KIF	kinesin superfamily
KIM	KLC-interacting motif (aa 1356-1395)
KHC	kinesin heavy chain
KLC	kinesin light chain
LB	Luria-Bertani medium
loxP	locus of crossing (X-ing) over
LTP	long term potentiation
M6PR	mannose-6-phosphate receptor
MAPK	mitogen-activated protein kinase
MCS	multiple cloning site
MEK	MAP kinase / ERK kinase
MW	molecular weight
NGF	nerve growth factor
NMDA	*N*-methyl-D-aspartate
NMDAR	NMDA receptor
NMJ	neuromuscular junction
NT	neurotrophin
OD	optical density
PBS	phosphate buffer saline
PC12	pheochromocytoma 12 cell line
PCR	polymerase chain reaction
PDGF	platelet-derived growth factor
PDGFR	PDGF receptor
PDZ	postsynaptic density-95 / discs large / zonula occludens-1
PFA	paraformaldehyde
PI-3K	phosphatidylinositol 3-kinase
PKA	cAMP-dependent protein kinase
PKC	protein kinase C
PKD	protein kinase D
PLCγ	phospholipase C γ
PlexA	plexin A
P-MAPK	phosphorylated form of MAPK

polySia	poly-α2,8-sialic acid
Pp5	protein phosphatase 5
PSD-95	postsynaptic density protein 95
Rab	Ras-related in brain
RFP	red fluorescent protein
RNA	ribonucleic acid
RNAi	RNA interference
rpm	rotations per minute
RT	room temperature
S-SCAM	synaptic scaffolding molecule
SAM	sterile alpha motif
SDS	sodium dodecyl sulfate
SDS-PAGE	SDS-polyacrylamide gel electrophoresis
s.e.m.	standard error of the mean
Sema1a	semaphorin 1a
SH2 (3)	Src-homology 2 (3) domain
Shc	SH2-containing sequence
Shp2	SH2 domain-containing protein tyrosine phosphatase
SOS	son of sevenless
STAT	signal transducer and activator of transcription
SyD	Sunday driver
SytI	synaptotagmin I
TGF-α	transforming growth factor α
TGN	trans-Golgi network
Tm	melting temperature
TM	transmembrane region
TNFR	tumor necrosis factor receptor
TPR	tetratricopeptide repeat
Trk	tropomyosin-related kinase
U	unit
UAS	upstream activating sequence
VSV-G	vesicular stomatitis virus G

Publications

Bracale A*, **Cesca F***, Neubrand VE, Newsome TP, Way M, Schiavo G: Kidins220/ARMS is transported by a kinesin-1 based mechanism likely to be involved in neuronal differentiation. Mol Biol Cell. 2007 Jan; 18(1):142-152

* equal contribution

Chapter 1 – Introduction

1 Introduction

1.1 Kidins220

Kidins220 (*Ki*nase *D in*teracting *s*ubstrate of *220* kDa), also known as ARMS (*a*nkyrin repeat *r*each *m*embrane *s*panning), is a transmembrane protein preferentially expressed in neuronal and neuroendocrine cells, which was initially described as substrate for protein kinase D (PKD) (Iglesias et al., 2000), as well as a downstream target of the signalling cascades mediated by neurotrophins and ephrins (Kong et al., 2001).

1.1.1 Structure of Kidins220

Kidins220 is an integral membrane protein, containing four transmembrane segments, and an amino- and a carboxy-terminal tail both exposed to the cytoplasm. Analysis of Kidins220 amino acid sequence revealed the presence of a number of domains, mostly involved in mediating protein-protein interaction (Figure 1-1). A brief description of the structure and function of these domains is provided below.

The N-terminal tail of Kidins220 is almost exclusively formed by eleven ankyrin repeats (aa 37-402). Ankyrin repeats are one of the most common protein motifs in nature, which are able to bind a high number of different molecular partners. An ankyrin repeat consists of 20-40 amino acid residues, folding into a canonical helix-turn-helix structure. Strings of such repeats form a helix bundle, which creates a flexible docking interface. No enzymatic activity has been found associated with ankyrin repeat-containing proteins as yet. They have been shown to act mainly as molecular scaffolds, modulating the assembling of protein complexes

(Li et al., 2006). A prediction of the three dimensional organisation of the ankyrin repeats of Kidins220 is shown in Figure 1-2. The entire region folds in a helical structure, which forms a concave surface offering an easily accessible site of interaction to molecular partners.

P-loop NTPase domains are widely spread protein domains, which are implicated in the most diverse cellular processes. These domains are composed of a Walker A motif, which binds NTPs, and by a Walker B motif, which coordinates a Mg^{2+} ion that splits the bond between the β and γ phosphates of the NTP molecule (Higgins et al., 1988). Both Walker A (aa 467-474) and Walker B (aa 771-775) motifs have been identified in the juxtamembrane regions of the amino- and carboxy-terminal tails of Kidins220. This determined the inclusion of Kidins220 in the new KAP family of P-loop NTP-ases, whose unique feature is the presence of transmembrane helices between the two Walker motifs. Members of this family are predicted to mediate the assembly and disassembly of protein complexes associated with the inner surface of cell membranes (Aravind et al., 2004).

The region spanning residues 500-700 contains four transmembrane domains (TMs), which generate two very short extracellular loops, and a longer (approximately 100 amino acids) internal loop.

A proline-rich region spans the middle segment of the carboxy-tail of Kidins220. It is composed of three poly-proline stretches, starting at residue 1081, 1089, and 1131. Proline-rich regions are common docking sites for various domains, like SH3 or WW domains, and they are usually found in the context of larger multi-domain proteins. A poly-proline stretch folds into a characteristic polyproline type II (PPII) helix, which is a left handed extended helical structure resembling a triangular

prism. This structure is characterised by high rigidity and a very distinctive three-dimensional conformation. Because of these features, proteins usually bind proline stretches with high selectivity and low affinity. The resulting weak interactions usually undergo fast modulation. Phosphorylation is a common way to regulate interactions mediated by polyproline stretches, which often contain several serine and threonine residues (Kay et al., 2000; Zarrinpar et al., 2003). This was shown to be the case for the binding of Kidins220 to CrkL, as discussed below (Arevalo et al., 2006).

After the proline-rich region, the carboxy-terminal tail of Kidins220 contains a sterile alpha motif (SAM) (aa 1152-1221). SAM domains are extremely common in nature, and are found in organisms from yeast to humans. SAM-containing proteins are involved in the most diverse biological processes, from signal transduction to transcriptional regulation. SAM domains have been shown to oligomerise, but they can also bind non-SAM domain proteins, and even RNA (Qiao and Bowie, 2005). Figure 1-3 shows a three-dimensional view of the globular structure of the SAM domain of Kidins220.

Residues 1356-1395 represent the KLC-interacting motif (KIM). As described in Chapter 3, this short stretch of amino acid is responsible for the binding to the kinesin-1 complex, via a new interacting sequence on kinesin light chain (Bracale et al., 2007).

The last four amino acids of Kidins220 (ESIL) constitute a Postsynaptic Density-95 / Discs large / Zonula Occludens-1 (PDZ)-binding motif. PDZ domains are widely diffused protein modules, present from bacteria to humans, which are often found in combination with other protein-protein interaction domains. The most

common PDZ-binding signature is a short stretch of four amino acids at the carboxy-terminus of a protein (following the consensus X-S/T-X-V/L, X-Ψ-X-Ψ, or X-D/E-X-Ψ; where X indicates an unspecified amino acid, and Ψ a hydrophobic amino acid), although PDZ proteins can also bind internal sequences, as well as lipids. In most cases, interactions between PDZ-proteins and their targets are constitutive, and they are often modulated by phosphorylation. PDZ-proteins and their interactors have been often found associated with tyrosine kinase receptors (Nourry et al., 2003). This was demonstrated also for the Kidins220 – α-syntrophin complex, which is based on the interaction between the PDZ-binding motif of Kidins220 and the PDZ domain of α-syntrophin (discussed below). On the basis of co-immunoprecipitation experiments, Kidins220 and α-syntrophin have been shown to be associated *in vivo* with the EphA4 receptor, at the neuromuscular junction. However, the formation of a ternary complex between these three proteins has not been demonstrated as yet (Luo et al., 2005).

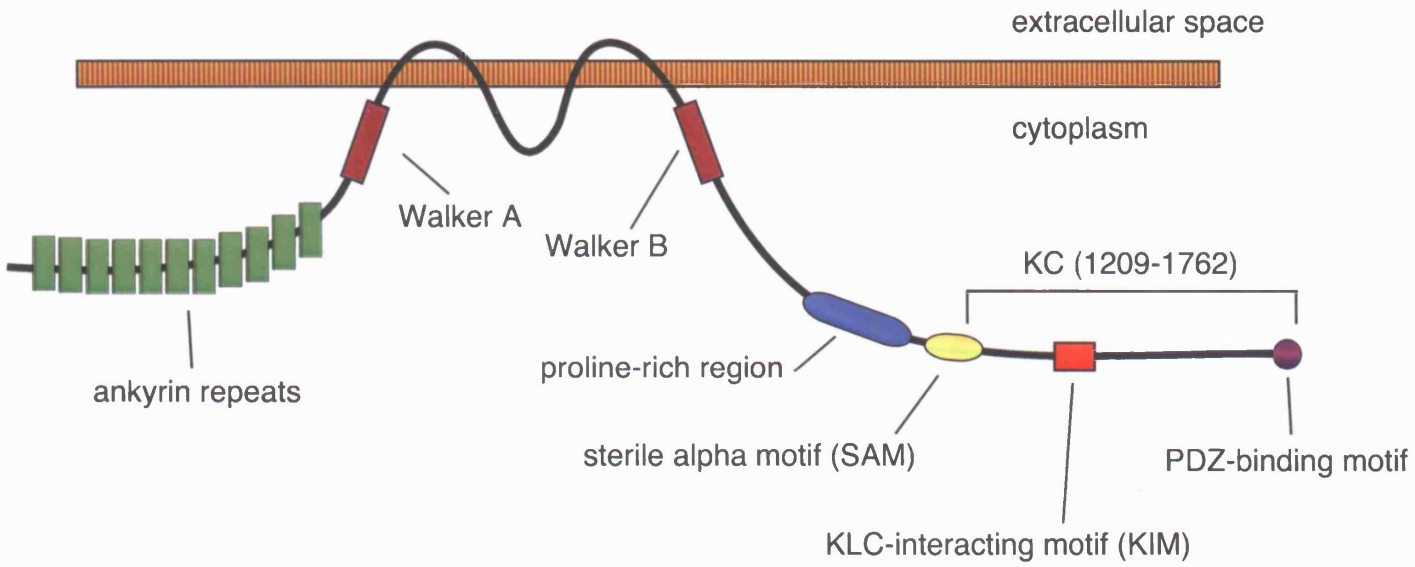

Figure 1-1: *Kidins220 structure*
Schematic representation of the structure of Kidins220. A brief description of the structure and function of the different domains is present in the text.

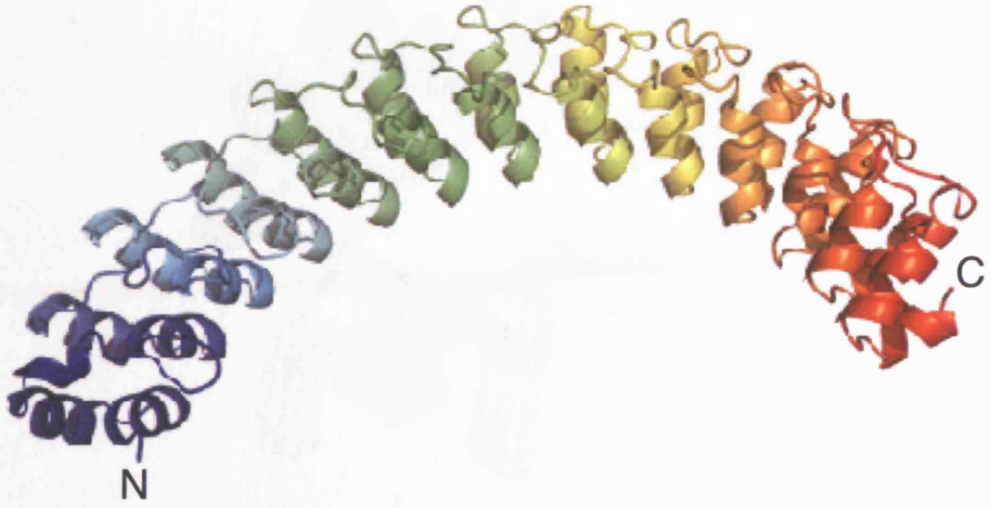

Figure 1-2: *three-dimensional prediction of the ankyrin repeat region of Kidins220*
Three-dimensional view of the ankyrin repeat region (amino acid 6 to 402) of Kidins220. The string of repeats forms a concave surface, which represents a flexible docking site. This model was built using the POPULUS protein refinement protocol (Offman et al., 2006), by Marc Offman, Biomolecular Modelling Laboratory, CRUK.

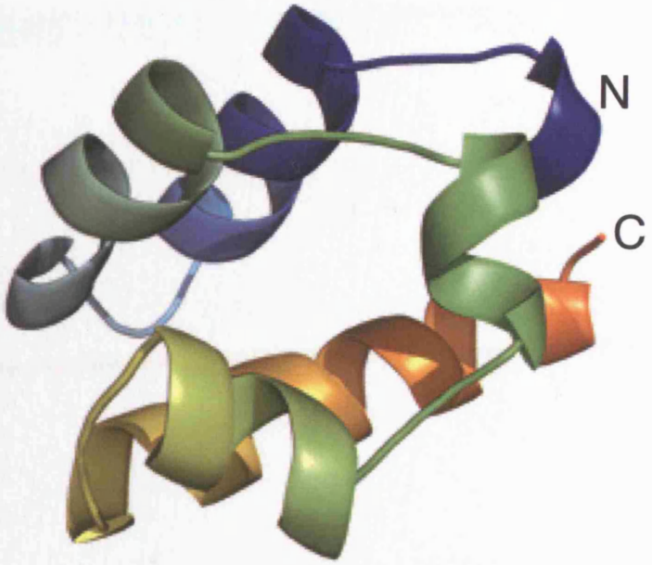

Figure 1-3: *three-dimensional prediction of the SAM domain of Kidins220*
Three-dimensional view of the SAM domain (residues 1150-1240) in the carboxy-terminal tail of Kidins220. The domain shows a globular structure. This model was built using the POPULUS protein refinement protocol (Offman et al., 2006), by Marc Offman, Biomolecular Modelling Laboratory, CRUK.

1.1.2 Kidins220-interacting proteins

1.1.2.1 Interaction with Trio: connection with the actin cytoskeleton

The amino-terminal region of Kidins220 interacts with Trio (Dr. V.E. Neubrand and C.L. Thomas, unpublished data), a guanine nucleotide exchange factor that modulates actin cytoskeletal reorganisation during cell migration and growth (Debant et al., 1996; Bellanger et al., 2000). Axon growth is one of the first responses to neurotrophic stimuli, triggered by signalling cascades activated at the level of the growth cone (see Figure 1-10). However, it is still not completely understood how neurotrophin signalling is coupled to the actin remodelling events that are required for axonal growth. The PI3K pathway has been implicated in the processes mediating chemoattraction to NGF, in *Xenopus* spinal neurons (Ming et al., 1999). In addition, it is required for the NT-4 dependent migration of mouse cortical interneurons (Polleux et al., 2002). Thus, PI3K signalling seems to control the cytoskeletal changes mediating growth cone attraction to neurotrophins. NGF signals have been shown to act through PI3K to activate Rac1 (Nusser et al., 2002), a cascade known to involve the small GTPase RhoG (Katoh et al., 2000), to promote neurite outgrowth in PC12 cells. Interestingly, Trio has also been shown to act through RhoG in response to NGF, to induce differentiation in the same cellular system (Estrach et al., 2002). However, a link between Trio and TrkA has not been demonstrated as yet. On the basis of these considerations, it is possible that Kidins220 may provide the missing link between neurotrophin stimuli and actin rearrangement, by connecting neurotrophin receptors and Trio at the growth cone.

1.1.2.2 Interaction with the neurotrophin receptors and CrkL: connection with the MAPK signalling

Kidins220 has been shown to interact with the three Trk receptors (Arevalo et al., 2004). Furthermore, it is part of a ternary complex, together with TrkA and $p75^{NTR}$ (Chang et al., 2004). The interaction between Kidins220 and TrkA is mediated by the fourth transmembrane domain of Kidins220 and the transmembrane domain of the receptor (Arevalo et al., 2004). The interaction with $p75^{NTR}$ involves the intracellular domain of the receptor (aa 327-342) (Chang et al., 2004), and the last 250 amino acids of Kidins220 (Kong et al., 2001). The interaction of Kidins220 with TrkA was shown to be NGF-dependent, and persisted for up to 25 h of NGF treatment (Kong et al., 2001). In contrast, the formation of a ternary complex between Kidins220, TrkA and $p75^{NTR}$ was found to be NGF-independent. Interestingly, increased levels of Kidins220 protein caused a reduction in the formation of a complex between TrkA and $p75^{NTR}$, suggesting that Kidins220 might regulate the formation of different receptor complexes, with different neurotrophin binding affinities (Chang et al., 2004).

Kidins220 is tyrosine phosphorylated in response to NGF as well as BDNF stimulation. The time course of Kidins220 phosphorylation follows the kinetics of Trk receptor autophosphorylation, suggesting that Kidins220 might be phosphorylated directly by the Trks, without involvement of intermediate factors (Kong et al., 2001). In addition, tyrosine phosphorylation of Kidins220 appears at the same time as Shc and PLC-γ phosphorylation, indicating that Kidins220 is amongst the first proteins to be activated in response to NGF stimuli (Arevalo et al., 2004). The adaptor protein CrkL constitutively binds the second polyproline stretch

of Kidins220 via its SH3 domain (Arevalo et al., 2004). Upon NGF treatment, Kidins220 is phosphorylated on tyrosine 1096, at the level of the CrkL-interacting region. This causes a conformational change in the CrkL-Kidins220 complex, which allows the recruitment of C3G and other downstream activators of the MAPK pathway (Arevalo et al., 2006). Kidins220 therefore mediates the assembly of the CrkL/C3G/Rap1 complex, which promotes the sustained activation of the MAPK pathway. This effect is highly specific, as perturbing Kidins220 function by means of RNAi or dominant negative constructs does not affect either the transient MAPK activation initiated by EGF, the initial phases of MAPK activation mediated by Ras, or Akt activation (Arevalo et al., 2004).

1.1.2.3 Interaction with PKD: formation of a membrane raft-based signalling platform

Lipid rafts are specialised microdomains of the plasma membrane, enriched in cholesterol and sphingolipids (Brown and London, 1998). They are proposed to represent a protected environment where signalling complexes can assemble and initiate intracellular cascades in response to extracellular stimuli (Simons and Toomre, 2000). Although the concept of membrane rafts is controversial, several studies have identified and characterised a number of proteins and signalling complexes allegedly localised to these microdomains. Proteins with high affinity for membrane rafts include glycosylphosphatidylinositol (GPI)-anchored proteins, cholesterol-linked or palmitoylated proteins, and a subset of transmembrane proteins (Simons and Toomre, 2000). The first transmembrane receptors to be associated with membrane rafts were the platelet-derived growth factor receptor (PDGFR) (Liu et

al., 1996) and the epithelial growth factor receptor (EGFR) (Mineo et al., 1996). Subsequently, both ephrins (Bruckner et al., 1999; Davy et al., 1999) and Eph-receptors (Wu et al., 1997) were found to be associated with rafts, together with the complement of proteins required for their downstream signalling. More recently, the glial cell-derived neurotrophic factor (GDNF) receptor α (GFRα) (Tansey et al., 2000), as well as TrkA (Huang et al., 1999; Peiro et al., 2000), TrkB (Suzuki et al., 2004) and $p75^{NTR}$ (Huang et al., 1999; Higuchi et al., 2003), have been added to the list of raft-associated proteins. In all cases, localisation to membrane microdomains was shown to be a prerequisite to the activation of the downstream signalling events.

PKD is a serine/threonine kinase involved in the modulation of several cellular processes, such as proliferation and Golgi trafficking (Ghanekar and Lowe, 2005). Kidins220 constitutively interacts with PKD, and upon phorbol ester stimulation is phosphorylated by this kinase on serine 919 (Iglesias et al., 2000). Kidins220 has been shown to associate with lipid rafts at the leading edge of motile immature dendritic cells (Riol-Blanco et al., 2004), as well as in PC12 cells and primary cortical neurons (Cabrera-Poch et al., 2004). In all cases, the raft-associated pool of Kidins220 was found to colocalise with PKD. In addition, Kidins220 and PKD colocalise at the level of the trans Golgi network (TGN). The expression of a kinase-dead form of PKD was shown to alter Kidins220 distribution, causing its accumulation in intracellular clusters positive for TGN markers. Therefore, PKD localisation and activity control the trafficking of Kidins220 from the TGN to the plasma membrane, likely by modulating the recruitment of PDZ proteins at the TGN, in a phosphorylation-dependent fashion (Sanchez-Ruiloba et al., 2006). The

interaction with PKD could control the formation of a signalling platform at the cell surface, containing Kidins220 and possibly neurotrophin or ephrins receptors.

1.1.2.4 Interaction with kinesin light chain: connection with the microtubule cytoskeleton

As discussed in Chapter 3, the KLC-interacting motif mediates the binding to the kinesin-1 complex. The kinesin-1 dependent transport of Kidins220 is important for the establishment of a correct response to neurotrophic stimuli, in PC12 cells (Bracale et al., 2007). Although a complex between Kidins220, kinesin-1 and Trk/p75^{NTR} has not been demonstrated as yet, it is tempting to speculate that Kidins220 might link Trk-bearing vesicles to the kinesin motor, thus modulating the anterograde trafficking of the receptors, and their targeting to the axon terminal.

1.1.2.5 Interaction with α-syntrophin: connection to ephrin signalling at the neuromuscular junction

Syntrophins are a family of PDZ-containing adaptor proteins, which have signalling and structural roles at the neuromuscular junction (NMJ) (Kramarcy and Sealock, 2000). The interaction between Kidins220 and α-syntrophin is mediated by the PDZ binding motif of Kidins220. These two proteins have been shown to interact in cortical neurons as well as in muscle, and co-localise at NMJs at various developmental stages. Interestingly, the expression pattern of Kidins220 closely follows the distribution of Eph and Trk receptors during muscle development. It has been suggested that the complex Kidins220-α-syntrophin may regulate oligomerisation of the ephrin receptor EphA4 in response to ephrin-A1 stimulation.

According to this hypothesis, Kidins220 and α-syntrophin cooperate to enhance EphA4-induced Jak/Stat signalling, thus coordinating the molecular events required for synapse development (Luo et al., 2005).

1.1.2.6 Kidins220 at the junction between many different signalling pathways

Kidins220's role in mediating the response to different trophic stimuli is now becoming clearer. To date, the best characterised function of Kidins220 is the modulation of the intracellular signalling pathways activated in response to neurotrophins. Kidins220 is involved in multiple interactions with different neurotrophin receptors (Arevalo et al., 2004; Chang et al., 2004). Upon neurotrophin binding, Kidins220 recruits to the activated receptors a range of adaptor molecules, which in turn transmit the signal to specific intracellular effectors. Amongst the many different pathways that are activated in response to neurotrophins, the MAPK cascade has been shown to be the most affected by the inhibition of Kidins220 function (Arevalo et al., 2004). Thus, these data indicate that neuronal cells require Kidins220 to undergo differentiation in response to trophic signals. The molecular and functional characterisation of the interaction between Kidins220 and the guanine nucleotide exchange factor Trio is underway (V.E. Neubrand et al., manuscript in preparation). The results of this analysis might provide the missing link to connect neurotrophin signalling to the molecular events leading to actin cytoskeleton remodelling, in the processes of neuronal growth and migration. The functional interaction with α-syntrophin and EphA4 at the NMJ implicates Kidins220 in the intracellular pathways triggered by ephrins (Luo et al., 2005). Further studies might unveil a new role for Kidins220 as mediator of ephrin signalling during synapse

development. PKD-mediated phosphorylation of Kidins220 regulates its trafficking from the TGN to specialised microdomains of the plasma membrane (Sanchez-Ruiloba et al., 2006). Targeting to membrane rafts might be necessary for Kidins220 to come in contact with ephrins and/or neurotrophin receptors, and recruit their specific effectors upon stimulation. On the basis of all these considerations, it is possible to define a role for Kidins220 in mediating the assembly of multiple signalling complexes, via its many protein-protein interaction domains.

Figure 1-4: *Kidins220 interactors*
Schematic representation of the different protein that have been shown to interact with Kidins220, and the signalling pathways to which they have been associated. The different Kidins220 domains are represented as in Figure 1-1.

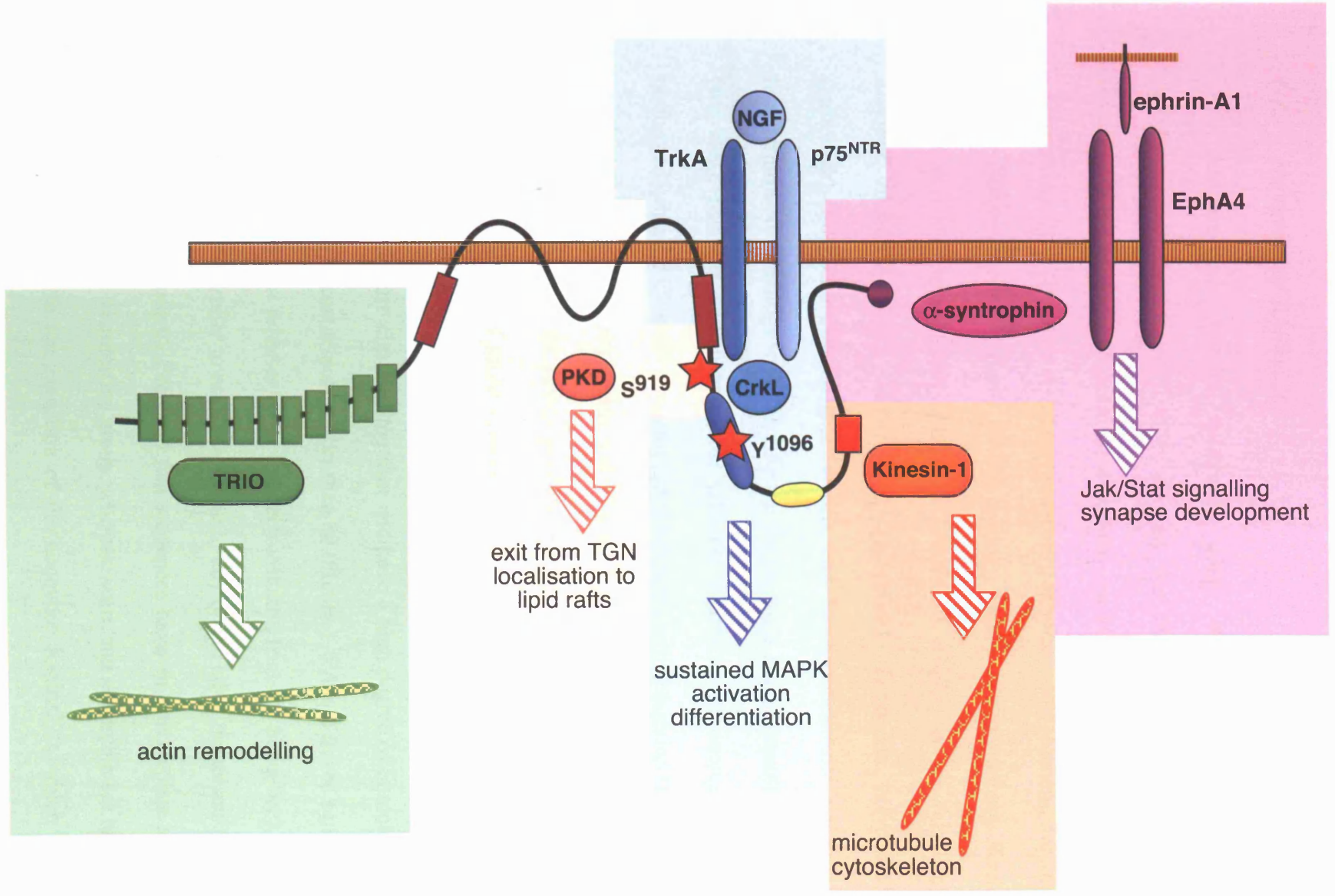
NGF
TrkA
p75NTR
ephrin-A1
EphA4
α-syntrophin
PKD
S919
CrkL
Y1096
Kinesin-1
TRIO
exit from TGN
localisation to
lipid rafts
sustained MAPK
activation
differentiation
Jak/Stat signalling
synapse development
actin remodelling
microtubule
cytoskeleton

1.1.3 Evolution of Kidins220

Analysis of protein databases using the BLASTP algorithm (http://www.ncbi.nlm.nih.gov/BLAST) allowed the identification of Kidins220 orthologs in the following organisms: *Anopheles gambiae* (mosquito), *Drosophila melanogaster* (fruit fly), *Apis mellifera* (honeybee), *Homo sapiens* (human), *Macaca mulatta* (Rhesus monkey), *Canis familiaris* (dog), *Mus musculus* (mouse), *Rattus norvegicus* (rat), *Monodelphis domestica* (opossum), *Gallus gallus* (chicken), *Xenopus tropicalis* (frog), *Danio rerio* (zebrafish), *Tetraodon nigroviridis* (pufferfish), *Caenorhabditis elegans* (worm), and *Strongylocentrotus purpuratus* (sea urchin). No orthologs were identified in the molluscs *Loligo* (squid) or *Aplysia* (sea slug). Multiple alignment of the different Kidins220 sequences was then performed using the ClustalW program (http://www.ebi.ac.uk/clustalw) (Figure 1-5), which also generated a phylogram tree (Figure 1-6 A) and a pairwise alignment score matrix (Figure 1-6 B). It was possible to identify two clusters of sequences, highlighted by the red and green squares in both the phylogram (Figure 1-6 A) and the matrix (Figure 1-6 B). Mammalian (human, monkey, dog, mouse, rat, opossum) and chicken proteins are clustered together and have a high degree of homology, as indicated by a phylogenetic score higher than 80 (Figure 1-6 A and B, red square). A second cluster could be represented by insects (mosquito, fruit fly, honeybee), whose sequences are more similar to each other than to any of the other organisms (Figure 1-6 A and B, green square). Frog and fish sequences have an intermediate level of homology towards the mammalian group, whereas worm and sea urchin are the most divergent species. With the exception of the honeybee Kidins220, which has an

N-terminal insert of about 600 aa, the amino terminal region of the protein shows a good conservation between the different organisms, whereas the carboxy-terminal portion is more divergent. The presence and conservation of Kidins220 sequences throughout different species point towards an evolutionary conserved function for this protein. Interestingly, Kidins220 is present also in species for which a canonical neurotrophin pathway has not been identified, such as *Drosophila* and *C. elegans*. In these organisms Kidins220 might have an equivalent function, possibly interacting with different receptors involved in neuronal development.

Figure 1-5: *alignment of Kidins220 orthologs*

Multiple protein alignment of different Kidins220 orthologs: *A.g.*, Anopheles gambiae (XP_320386); *D.m.*, Drosophila melanogaster (NP_611574); *A.m.*, Apis mellifera; *H.s.*, Homo sapiens (NP_065789); *M.m.*, Macaca mulatta (XP_001083592); *C.f.*, Canis familiaris (XP_532865); *Mus*, Mus musculus (XP_914251); *R.n.*, Rattus norvegicus (NP_446247); *M.d.*, Monodelphis domestica (XP_001381222); *G.g.*, Gallus gallus (XP_419939); *X.t.*, Xenopus tropicalis (jgi_Xentr4_273441); *D.r.*, Danio rerio (NP_956276); *T.n.*, Tetraodon nigroviridis (CAG10502); *C.e.*, Caenorhabditis elegans (NP_001076687); *S.p.*, Strongylocentrotus purpuratus (Genescan). Red squares highlight the transmembrane regions. The alignment was performed using the ClustalW program (http://www.ebi.ac.uk/clustalw). The sea urchin homolog of Kidins220 was identified with the help of Mike Mitchell, Bioinformatics and Biostatistics Service (CRUK), by using the GeneScan gene prediction from draft assembly Baylor release 3.

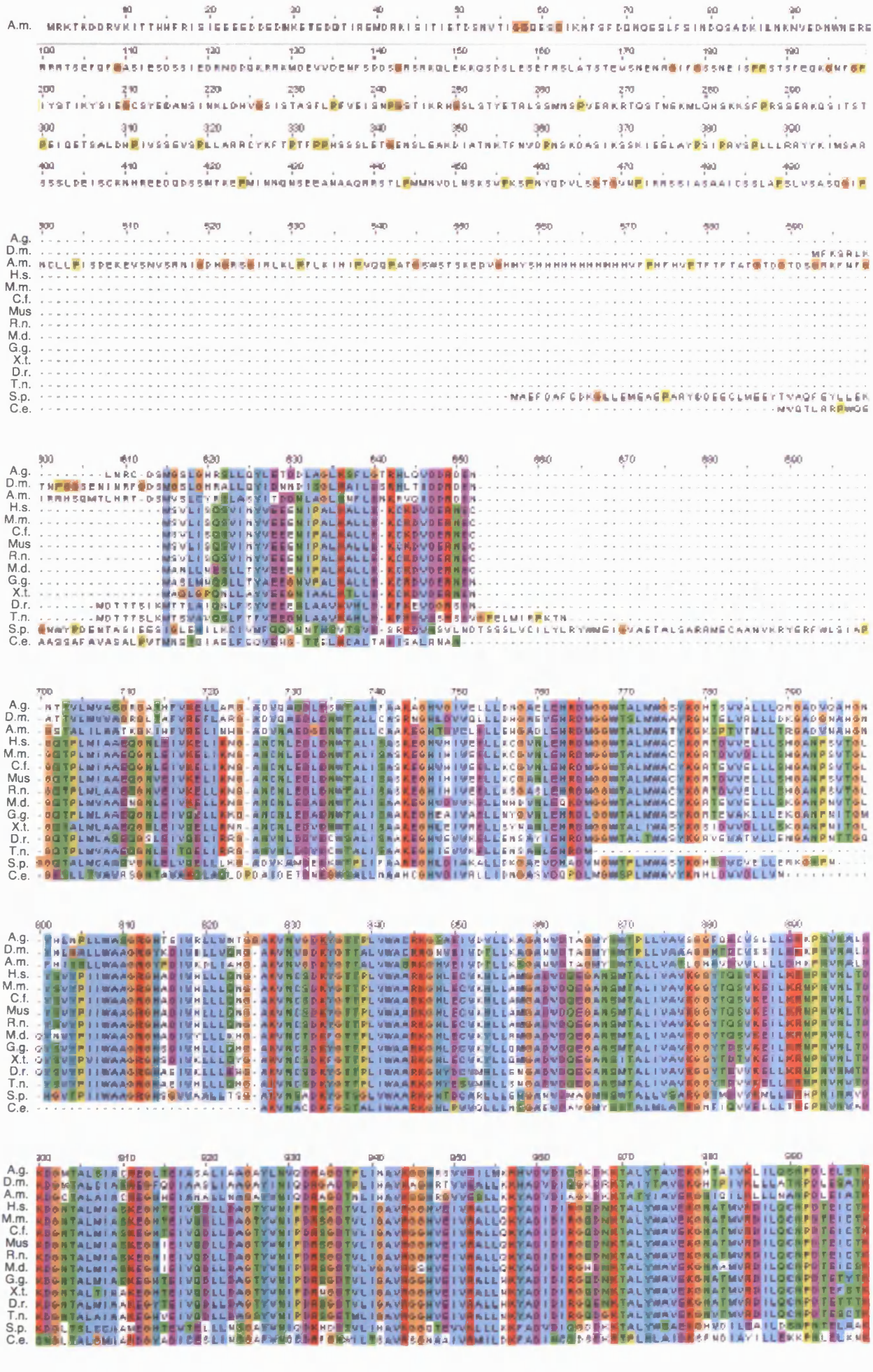
A.m.
A.g.
D.m.
A.m.
H.s.
M.m.
C.f.
Mus
R.n.
M.d.
G.g.
X.t.
D.r.
T.n.
S.p.
C.e.

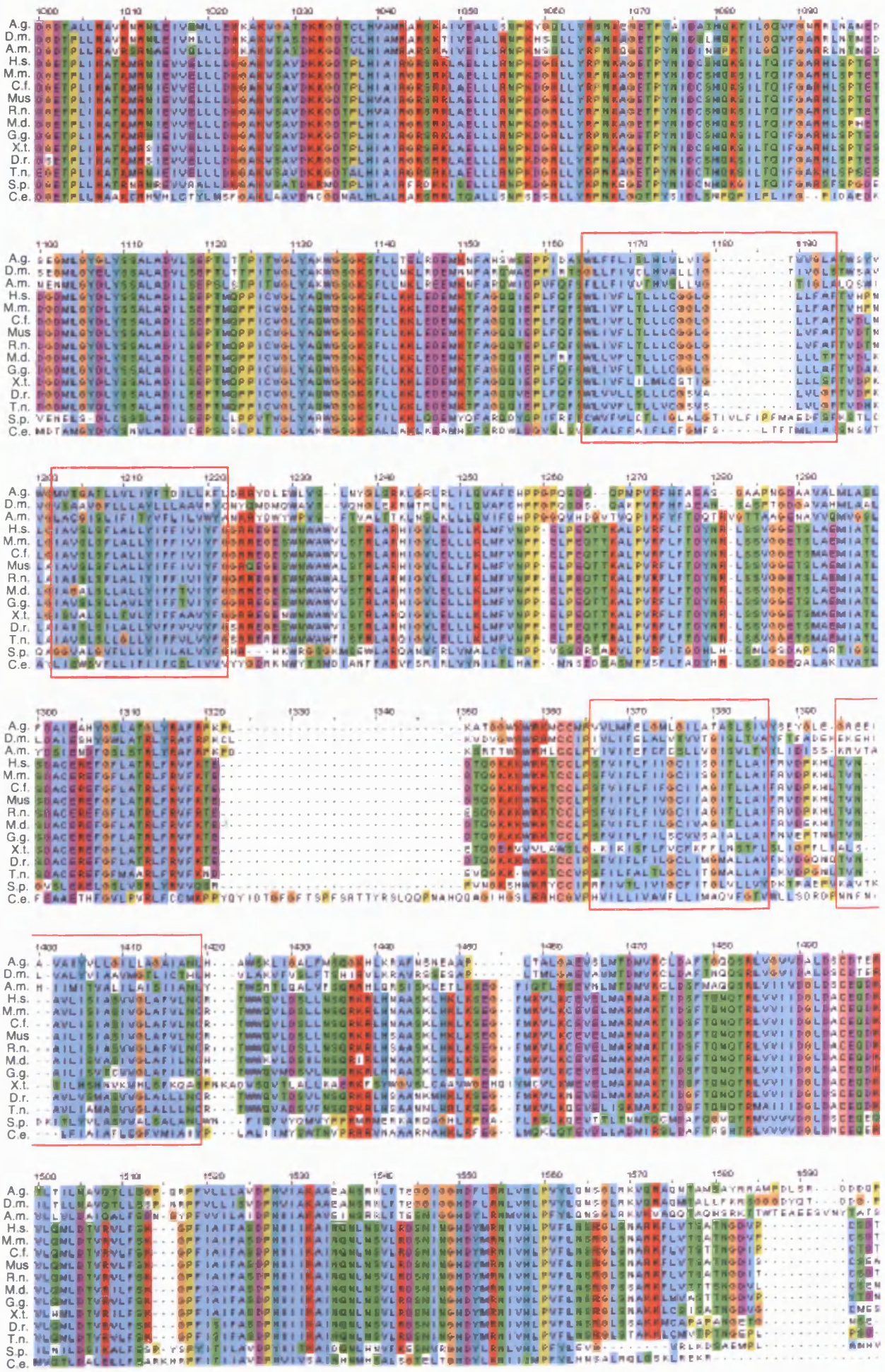
A.g.
D.m.
A.m.
H.s.
M.m.
C.f.
Mus
R.n.
M.d.
G.g.
X.t.
D.r.
T.n.
S.p.
C.e.

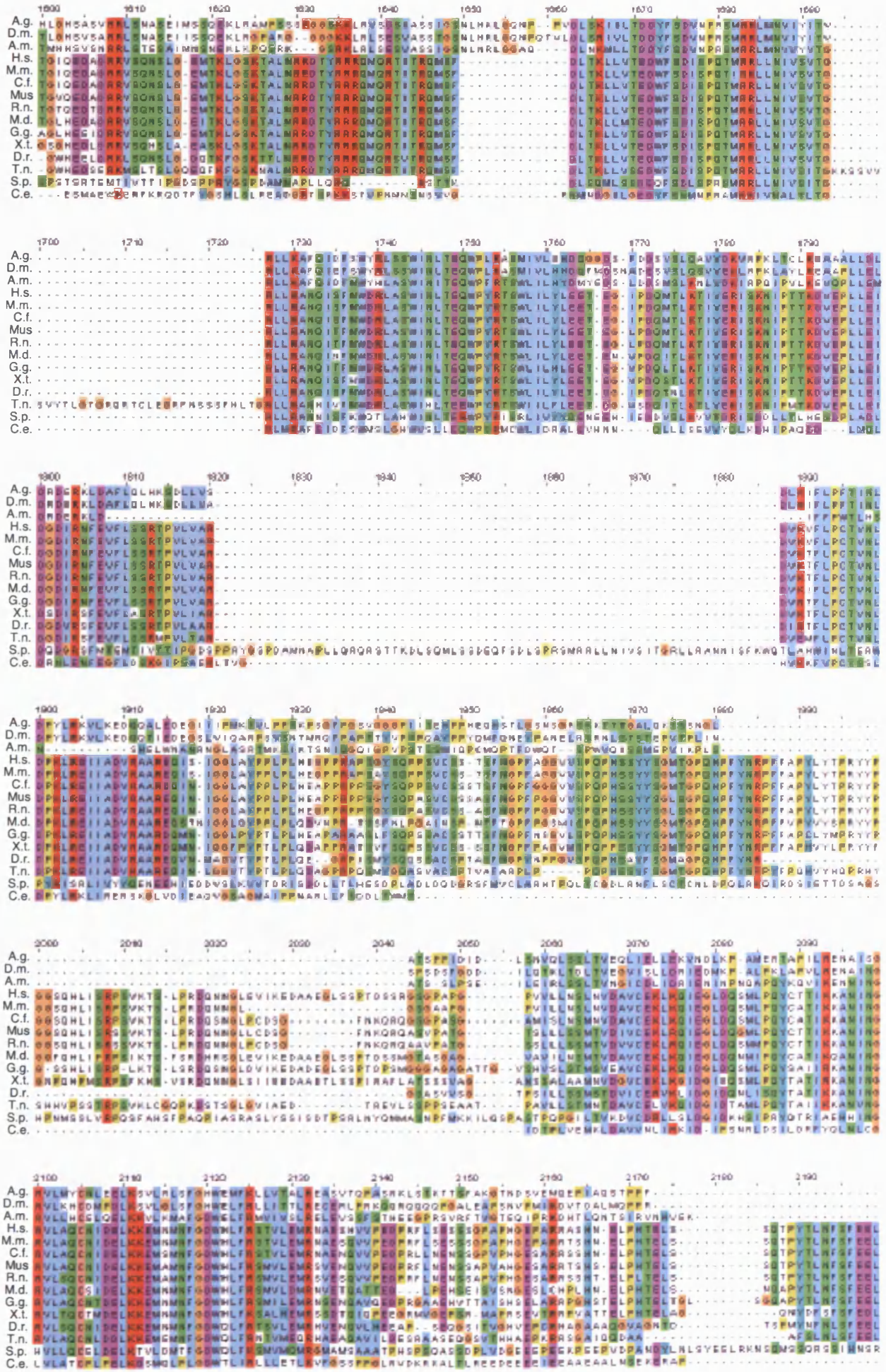
A.g.
D.m.
A.m.
H.s.
M.m.
C.f.
Mus
R.n.
M.d.
G.g.
X.t.
D.r.
T.n.
S.p.
C.e.

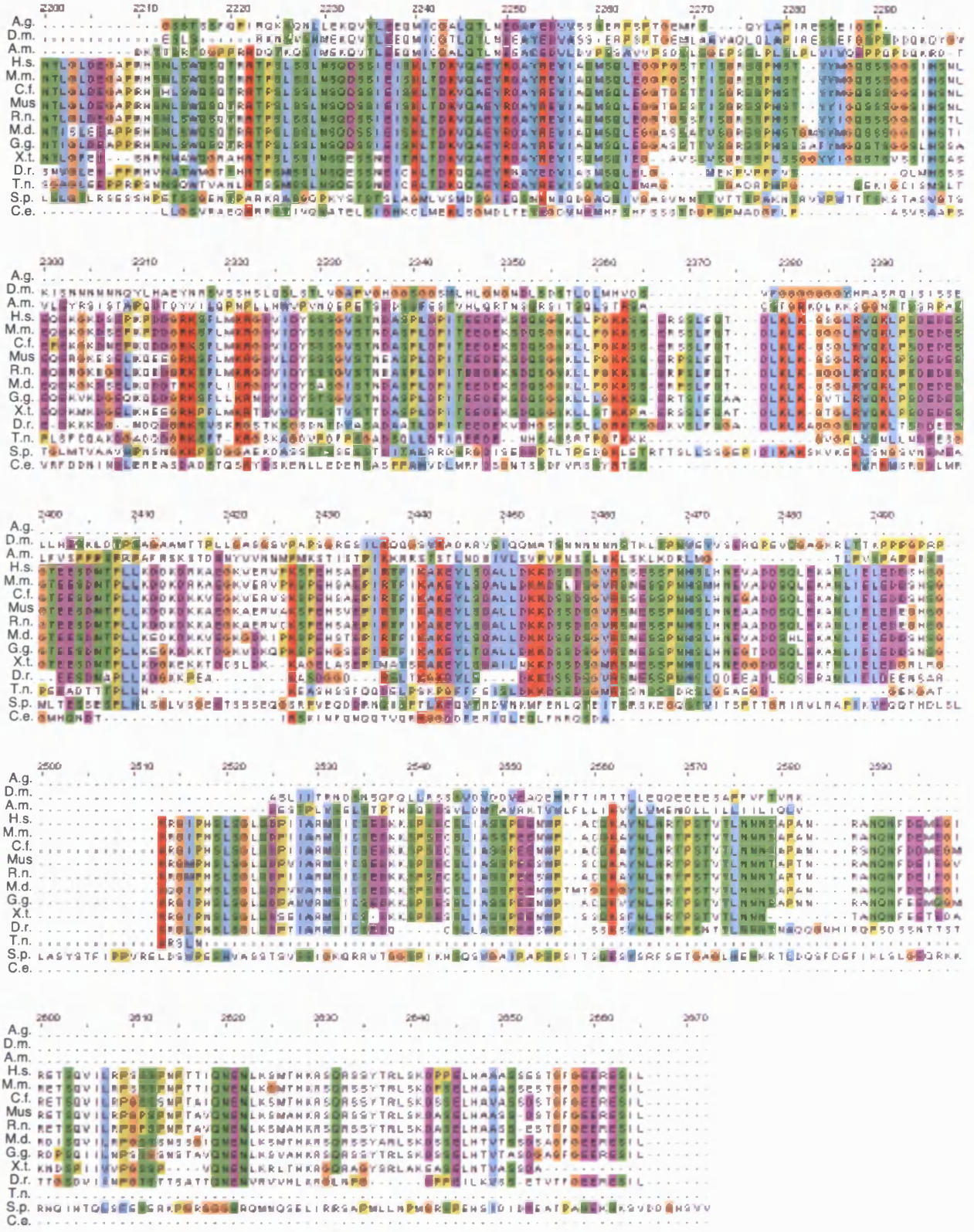
A.g.
D.m.
A.m.
H.s.
M.m.
C.f.
Mus
R.n.
M.d.
G.g.
X.t.
D.r.
T.n.
S.p.
C.e.

Figure 1-6: *phylogram and pairwise alignment scores of different Kidins220 orthologs*

(A) Phylogram of the sequences used in Figure 1-5. The branch lengths are proportional to the amount of inferred evolutionary change between the different sequences (values for each branch are indicated on the right). (B) Pairwise alignment scores. Pairwise scores are calculated as the number of identities in the best alignment divided by the number of residues compared (gap positions are excluded). Red squares highlight the mammalian cluster; green squares highlight the insect cluster. For this analysis, default ClustalW parameters were used. Details about the algorithms used to generate the phylogram and the pairwise scores are available in the ClustalW website (http://www.ebi.ac.uk/clustalw). Abbreviations for the different species are as in Figure 1-5.

A Phylogram

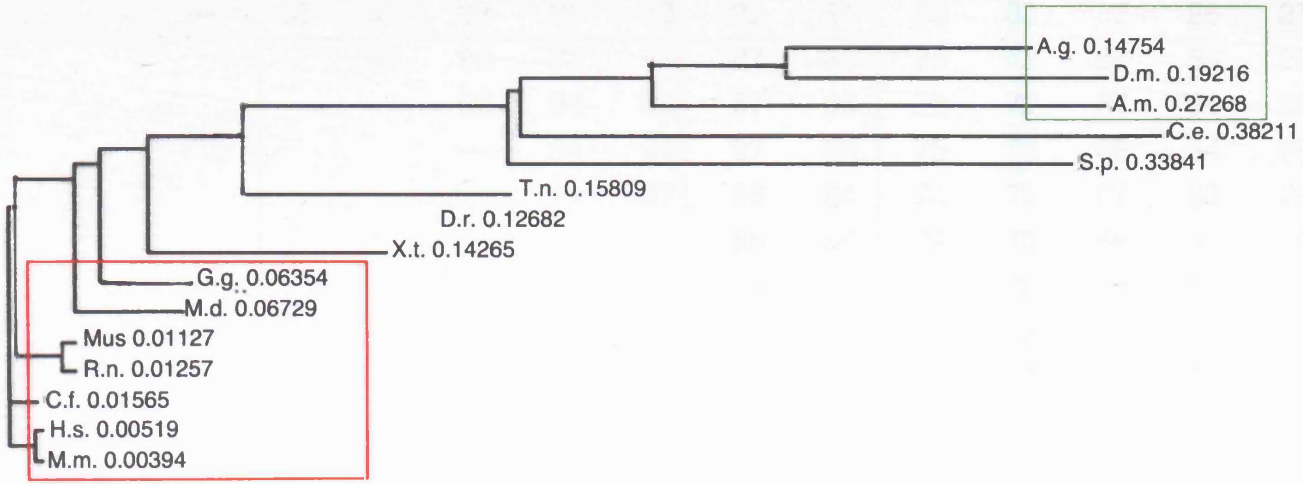
A.g. 0.14754
D.m. 0.19216
A.m. 0.27268
C.e. 0.38211
S.p. 0.33841
T.n. 0.15809
D.r. 0.12682
X.t. 0.14265
G.g. 0.06354
M.d. 0.06729
Mus 0.01127
R.n. 0.01257
C.f. 0.01565
H.s. 0.00519
M.m. 0.00394

B Phylogenetic score (%)

	A.g.	D.m.	A.m.	H.s.	M.m.	C.f.	Mus	R.n.	M.d.	G.g.	X.t.	D.r.	T.n.	S.p.	C.e.
A.g.	---	66	51	36	36	37	37	36	36	38	36	35	34	35	28
D.m.		---	44	32	33	32	32	31	32	31	31	30	30	31	26
A.m.			---	32	32	32	32	32	33	31	30	33	32	26	27
H.s.				---	99	96	93	93	87	86	75	72	68	34	28
M.m.					---	96	94	94	87	86	75	72	67	34	28
C.f.						---	94	94	87	86	75	72	68	34	28
Mus							---	97	86	84	74	73	67	33	29
R.n.								---	85	84	74	73	66	33	29
M.d.									---	85	74	70	66	34	29
G.g.										---	77	73	68	32	28
X.t.											---	67	63	33	28
D.r.												---	71	36	27
T.n.													---	35	29
S.p.														---	28
C.e.															---

1.2 Molecular mechanisms of neurotrophin signalling

1.2.1 Neurotrophins and neurotrophin receptors

The correct development of the nervous system relies on the ability of axons and dendrites to recognise their targets. During this highly regulated process, neurons migrate and differentiate in response to gradients of specific growth factors, collectively termed neurotrophins, which regulate multiple neuronal functions, including cell survival, differentiation, synaptic function, and plasticity (Bibel and Barde, 2000; Chao, 2003; Huang and Reichardt, 2003). The complex network of signalling pathways triggered by neurotrophic stimuli is initiated at the neuronal surface by the specific interaction between neurotrophins and their receptors. The mammalian family of neurotrophins is composed by nerve growth factor (NGF), brain derived neurotrophic factor (BDNF), neurotrophin-3 (NT-3) and neurotrophin-4/5 (NT-4/5). Each neurotrophin preferentially binds to one of the tropomyosin-related kinase (Trk) receptors: NGF to TrkA, BDNF and NT-4/5 to TrkB, NT-3 to TrkC. Although these interactions are, in general, highly specific, a certain degree of cross-talk has been demonstrated for NT-4/5, which in some experimental conditions can bind TrkA, and for NT-3, which is also able to interact with TrkA and TrkB (Figure 1-7) (Roux and Barker, 2002). In addition, all neurotrophins bind to the p75 neurotrophin receptor ($p75^{NTR}$). As shown in Figure 1-7, Trk receptors are type-I transmembrane proteins characterised by an intracellular conserved kinase domain. The extracellular region is composed by two IgG-like domains, and a series of leucine-rich motifs flanked by two cysteine

clusters. Deletion studies on different Trk receptors have shown that the IgG-like domain adjacent to the membrane is the region that determines ligand specificity (Urfer et al., 1995). $p75^{NTR}$ is also a type-I transmembrane receptor. Its extracellular domain is composed of four cysteine-repeat motifs, which are responsible for neurotrophin binding, whereas the intracellular region contains a type-II death domain, a protein module originally identified in pro-apoptotic members of the tumor necrosis factor receptor (TNFR) superfamily (Roux and Barker, 2002).

A number of differently spliced isoforms have been identified for all the receptors. These alternative isoforms include TrkA and TrkB receptors that lack a short amino acid region in the extracellular domain, TrkB and TrkC isoforms that completely lack the intracellular kinase domain, as well as a TrkC isoform with an insertion in the kinase domain. A truncated isoform has also been characterised for $p75^{NTR}$. This variant contains only the first cysteine-rich domain, and is incapable of binding neurotrophins (Figure 1-7) (Roux and Barker, 2002). Truncated and inactive isoforms have different affinity for their ligands, and might play an important role in modulating the activity of the full-length receptors during development, as discussed in section 1.4.2.4.

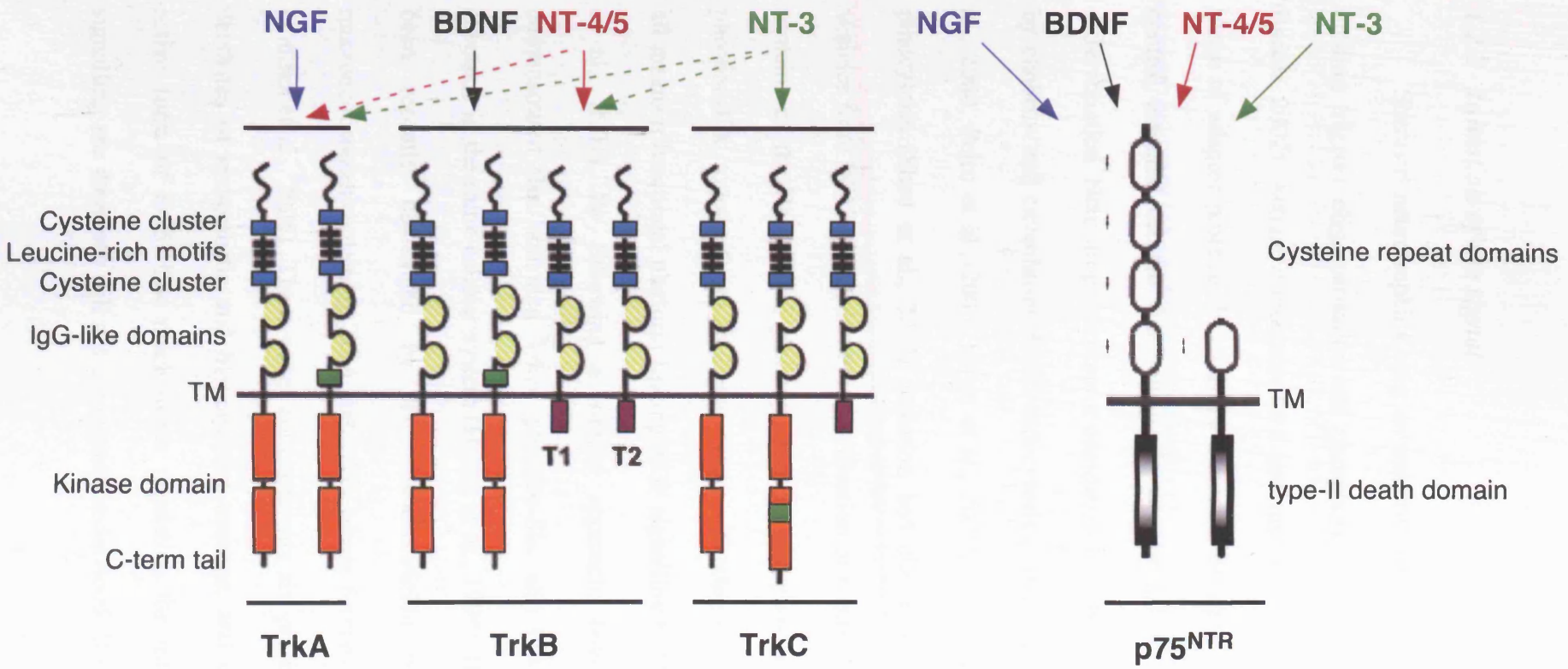

Figure 1-7: *neurotrophin receptors and their ligand specificity*

Schematic representation of the domain structure of the different Trk and $p75^{NTR}$ isoforms, and their ligand specificity. Different domains are represented as follow: orange boxes, intracellular kinase domains; green boxes, small amino acid insertions in the juxtamembrane region of TrkA and TrkB, or in the kinase domain of TrkC; purple boxes, truncated intracellular domains of TrkB and TrkC; yellow-striped circles, IgG-like domains; blue boxes, cysteine clusters; black boxes, leucine-rich motifs; black-shaded boxes, type-II death domain of $p75^{NTR}$; white ovals, cysteine-repeat domains. TM, transmembrane region; T1, T2, truncated intracellular domain 1 and 2. Adapted from Roux and Barker, 2002 and Huang and Reichardt, 2003.

1.2.2 Initiation of the signal

Secreted neurotrophins exist as non-covalently bound dimers. Neurotrophin binding triggers oligomerisation and phosphorylation of the receptors (Roux and Barker, 2002). Activated receptors then undergo internalisation, and by recruiting a range of adaptor proteins they initiate a number of signalling cascades that would control essential cellular functions such as neuronal survival, proliferation and differentiation. Neurotrophin-receptor complexes have been shown to be internalised by clathrin- and caveolin-mediated endocytosis (Bilderback et al., 1999; Beattie et al., 2000; Peiro et al., 2000; Howe et al., 2001), as well as by Pincher-mediated pinocytosis (Shao et al., 2002). Isolation and characterisation of clathrin-coated vesicles from PC12 cells led to the identification of a number of activated signalling proteins of the Ras-MAPK pathway, such as phospho-Mek1/2, phospho-Erk and phospho-Elk, together with NGF and TrkA, indicating that this compartment is by all means a functional platform linking NGF signalling to MAPK activation (Howe et al., 2001). By following a similar approach, however, Mobley's group demonstrated that activated TrkA, phospho-Shc and PLCγ are associated with caveolae in the same cellular system (Huang et al., 1999). Both these findings have been recently challenged by the characterisation of clathrin-independent macroendosomes containing TrkA and TrkB, whose formation is Pincher-dependent (Valdez et al., 2005). These novel compartments are present in soma, axons and dendrites of sympathetic and hippocampal neurons, and are associated with the active form of Erk5. The mechanisms regulating the initiation of neurotrophin signalling are therefore still not completely understood. It is possible that different

signalling platforms modulate Trk internalisation in different types of neurons, or in response to different neurotrophins. In addition, whether Trk activation is required for internalisation, or whether the internalisation *per se* can influence the signalling ability of the receptors, is still debated (Zweifel et al., 2005).

Neurotrophin-mediated activation of Trks leads to the recruitment of a range of proteins, which specifically recognise phosphorylated residues in the cytoplasmic domain of the receptors. The main signalling cascades that are initiated following Trk activation are the phospholipase C-γ1 (PLC-γ1), the mitogen-activated protein kinase / extracellular regulated kinase (MAPK/Erk) and the phosphatidylinositol 3-kinase (PI-3K) pathways (Figure 1-8). PLC-γ1 acts by hydrolising phosphatidylinositol-(4,5)bisphosphate (PtdIns(4,5)P_i), to generate inositol (1,4,5)trisphosphate (IP3) and diacylglycerol (DAG). IP3 promotes calcium release from intracellular stores, which in turn activates a series of kinases like protein kinase C (PKC) or Ca^{2+}-calmodulin regulated protein kinase (CaMK). DAG also triggers the activation of several enzymes, such as PKC. The PLC-γ1 pathway has been involved in important physiological processes like long term potentiation (LTP) in hippocampal neurons. Activation of MAPK signalling can be transient, via a mechanism involving Shc-Grb2/SOS-Ras, or prolonged, via the Crk-C3G-Rap1 complex. These two different pathways ultimately lead to proliferation and differentiation, respectively. Activated PI3K generates P3-phosphorylated phosphoinositides. Amongst those, phosphatidylinositol(3,4,5)-trisphosphate [PtdIns(3,4,5)P_3, or PIP3] in turn activates the protein kinase Akt, whose downstream targets include several proteins involved in the promotion of cell

survival. A comprehensive review of these signalling pathways is present in Huang and Reichardt, 2003.

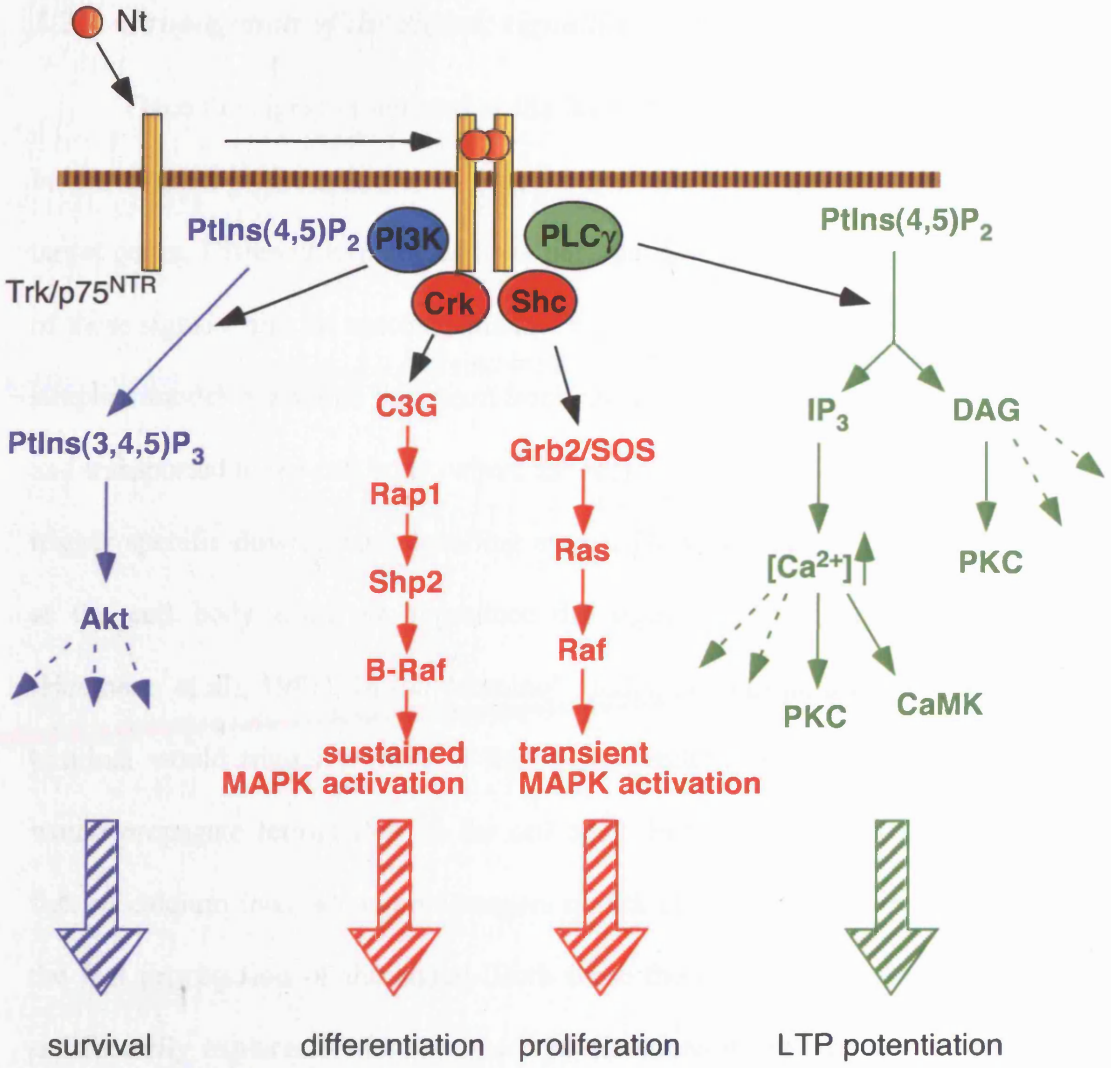

Figure 1-8: *schematic representation of the main signalling pathways initiated by neurotrophin stimuli*

Neurotrophin (Nt) binding leads to receptor dimerisation and subsequent activation by phosphorylation. Activated receptors recruit a series of adaptors, which specifically recognise phosphorylated residues in the intracellular domain. These adaptors in turn activate three main signalling cascades. The PI3K pathway (blue) promotes cell survival through activation of Akt. Sustained or transient activation of the MAPK pathway (red) promote differentiation or proliferation, respectively. Pathways activated by PLCγ (green) have been implicated in physiological processes such as long term potentiation in the hippocampus.

1.2.3 Propagation of the signal: signalling endosomes?

Once the signal is initiated at the level of the plasma membrane, it needs to be transmitted to the nucleus, in order to activate transcription of the appropriate target genes. Different hypotheses have been put forward, to try to define the nature of these signals, and the mechanisms that regulate their retrograde propagation. The simplest model maintains that neurotrophins are internalised at the nerve terminal and transported to the cell body, where they come in contact with their receptors and trigger specific downstream signalling events. However, injection of neurotrophins at the cell body does not reproduce the signals initiated at the growth cone (Heumann et al., 1981). In the "domino" model, neurotrophin binding at the axon terminal would trigger a wave of ligand-independent Trk phosphorylation, which would propagate retrogradely to the cell body. In the "retrograde effector" model, flux of calcium ions, second messengers or Trk effectors would be responsible for the fast propagation of the signal. Both these theories however do not provide a satisfactorily explanation for the observed directionality of receptor transport. The most accredited theory maintains that control of Trk signalling is regulated via membrane trafficking. This is also known as the "signalling endosome" model. According to this hypothesis, activated Trk receptors are internalised in a specific endosomal compartment, where they recruit the complement of molecular partners required for the propagation of the signal. The endosomes, bearing the receptors and all the interacting proteins, are then retrogradely transported to the cell body. At this level new downstream effectors can be recruited, which would ensure the transmission of the signal to the nucleus (Ginty and Segal, 2002). Kinetic analysis

shows that signal propagation via a signalling endosomes-mediated transport is more efficient than simple diffusion or even wave-like transmission of ions or phosphorylation. In addition, signalling endosomes are directionally selective and target-specific, thus combining the efficiency of the transport with a minimal amount of non specific cross-talk (Howe and Mobley, 2004).

The identities of the proteins that may be associated and transported with signalling endosomes are still under intense investigation. One of the first questions to be addressed was whether ligands are transported together with the receptors. On the basis of antibody neutralisation experiments, retrogradely transported NGF-TrkA complexes were shown to promote sympathetic neuron survival (Ye et al., 2003). These findings were challenged by the work of Campenot and collegues. By using NGF covalently cross-linked to beads, they showed that neuronal survival signals can reach the cell bodies unaccompanied by the NGF that initiated it (MacInnis and Campenot, 2002). Segal's group similarly demonstrated that the same holds true for the BDNF-TrkB complex (Heerssen et al., 2004). It is possible to speculate that multiple mechanisms of retrograde signalling exist, activated under different conditions, which may or may not require the co-transport of neurotrophins with the activated receptors (Campenot and MacInnis, 2004).

Several studies have attempted to identify protein complexes that are associated with signalling endosomes. NGF and activated TrkA were co-precipitated with the C3G/CrkL/Shp2/Gab2 complex, which mediates the sustained activation of the MAPK pathway, in PC12 cells (Wu et al., 2001). Similar studies conducted in dorsal root ganglia neurons revealed the presence of endosomes containing NGF, activated TrkA, and signalling proteins of the Rap1/Erk1/2, p38MAPK and

PI3K/Akt pathways (Delcroix et al., 2003). The small GTPase Rab7 has been recently added to the number of signalling endosome-associated molecules. Rab (Ras-related in brain) proteins are known mainly for their involvement in the regulation of distinct steps of membrane trafficking (Stenmark and Olkkonen, 2001). However, new findings have implicated Rabs in the processes of signal transduction, by characterising their role in modulating receptor trafficking. A dominant negative form of Rab7 has been shown to induce endosomal accumulation of TrkA and a subsequent increase of Erk1/2 activation upon NGF treatment, thus suggesting a role for this protein in the regulation of the TrkA retrograde trafficking (Saxena et al., 2005). In accordance with these findings, Rab7 has been identified as a key regulator of axonal retrograde transport of neurotrophins in motor neurons (Deinhardt et al., 2006). Two independent studies have recently identified APPL1 (adaptor protein containing PH domain, PTB domain, and leucine zipper motif) as a TrkA interactor. APPL1 might play a role in the modulation of TrkA signalling, as its depletion decreases the activation of the Erk1/2 and Akt pathways in response to NGF (Lin et al., 2006; Varsano et al., 2006). Figure 1-9 shows a possible representation of a signalling endosome.

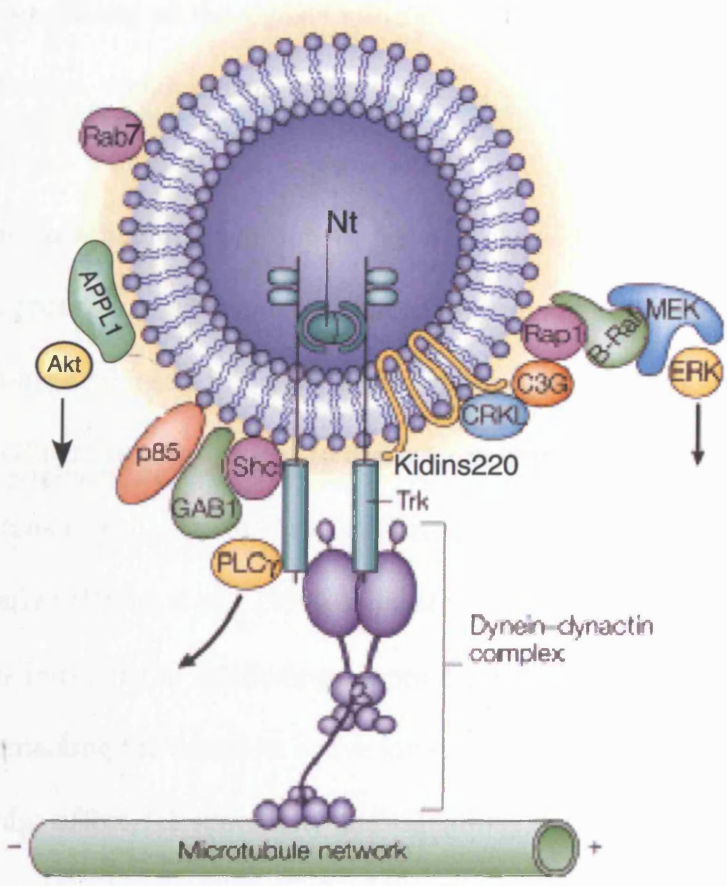

Figure 1-9: *possible representation of a signalling endosome*
Following Nt binding, activated Trk receptors are internalised in specific endosomal compartments, or signalling endosomes. Signalling endosomes are retrogradely transported to the cell body, likely via interaction with the dynein-dynactin complex. They contain a variety of signalling molecules associated to the receptor complex, which are associated with the MAPK/Erk, PLCγ and Akt pathways (arrows). Adapted from Zweifel et al., 2005.

1.2.4 Multiple levels of complexity in the regulation of neurotrophin responses

The specificity of the signals initiated by Trk receptors is finely tuned by a number of factors, which create several levels of complexity. Firstly, the repertoire of Trk receptors expressed by a particular neuron will determine the subset of neurotrophins to which that neuron will respond. An additional level of regulation is given by the presence of alternatively spliced isoforms of the receptors. The presence of a short amino acid insert in the juxtamembrane region of TrkA and TrkB has been shown to modulate responsiveness to different neurotrophins (Clary and Reichardt, 1994; Strohmaier et al., 1996). Trk isoforms lacking the catalytic domain can act both as negative (Palko et al., 1999) or positive (Stoilov et al., 2002) regulators of the signal, by impairing or facilitating the presentation of the ligand to the full-length receptors, containing the complete active kinase domain. The presence or absence of $p75^{NTR}$ can also affect Trk specificity and signalling ability (Hapner et al., 1998). At the intracellular level, expression and availability of different substrates or adaptors can play an important role in controlling the signalling pathways activated downstream of Trks (Lee et al., 2001). Studies in PC12 cells have shown that Trk receptors at the plasma membrane are able to promote neuronal survival, whereas internalised receptors induce differentiation. Thus, the intracellular localisation of the activated receptors is crucial to select a specific subset of interactors, which will determine the final response to the neurotrophic stimulus (Zhang et al., 2000).

Finally, the response to neurotrophic signals depends on the temporal and spatial pattern of stimulation. In PC12 cells, transient or sustained activation of the

MAPK pathway upon NGF treatment has been associated with proliferation and differentiation, respectively (Marshall, 1995). Studies conducted in dorsal root ganglia and sympathetic neurons have characterised a local and fast response at the growth cone, involving the activation of the PI3K and Erk1/2 pathway, which ultimately promotes axonal growth. A long-distance and slow response, requiring trafficking of the activated receptors to the soma, has been shown to rely on nuclear Erk5 and PI3K/Akt signalling (Kuruvilla et al., 2000; Watson et al., 2001). The transcription factor cyclic adenosine monophosphate (cAMP) response element-binding protein (CREB) is the main target of these long-distance signalling cascades, whose final outcome is the activation of CREB-mediated transcription of genes promoting neuronal survival (Ginty et al., 1994; Bonni et al., 1995) (Figure 1-10). Therefore, the repertoire of Trk receptors and spliced isoforms, the presence of $p75^{NTR}$, the availability of downstream effectors, membrane sorting and transport of activated receptors are all factors that provide additional steps controlling the specificity of the neurotrophic response.

Figure 1-10: *local versus long-distance signalling in neurons*

(A) Neurotrophin binding triggers retrograde transport of activated receptors. Neurotrophins (pink spheres) released from the target tissue (T) bind to their receptors (blue) at the axon terminal. Activated receptors (starred) are then internalised and retrogradely transported to the cell body. The nature of the signalling cascades that are subsequently activated depends, amongst other factors, on the location of the receptors. (B) At the growth cone, the activation of the PI3K and Erk1/2 pathways promotes axon growth. (C) Upon retrograde transport of the activated receptors, nuclear activation of the PI3K/Akt and Erk5 pathways initiates CREB-mediated transcription of genes promoting neuronal survival. MEF2, myocyte-specific enhancer factor 2; Rsk/MSK, ribosomal S6 kinase / mitogen- and stress-activated kinase. Adapted from Heersen and Segal, 2002.

A

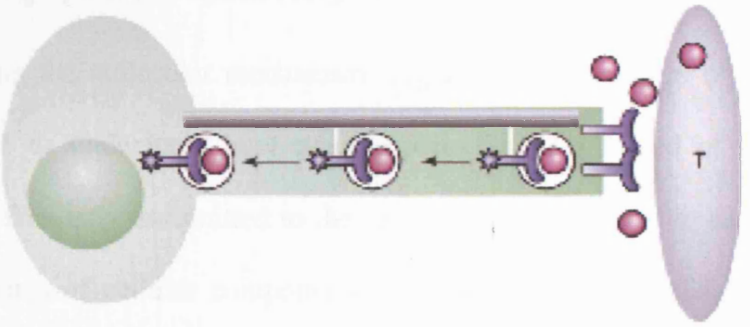
T

B

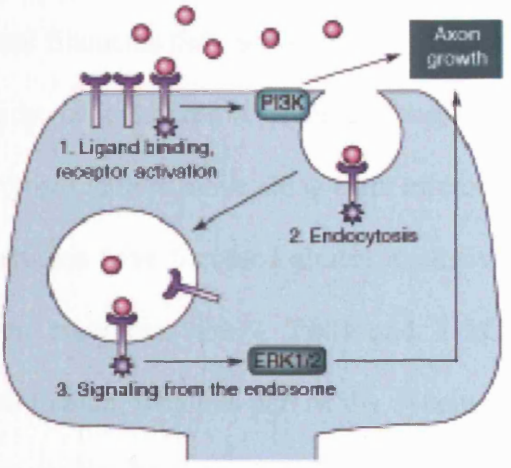
Axon growth
PI3K
1. Ligand binding, receptor activation
2. Endocytosis
ERK1/2
3. Signaling from the endosome

C

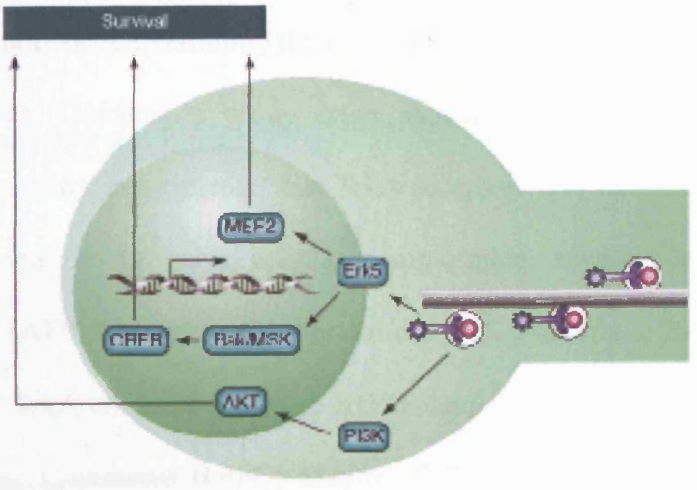
Survival
MEF2
ERK5
CREB
RSK/MSK
AKT
PI3K

1.2.5 Trafficking of neurotrophin receptors

Unravelling the molecular mechanisms regulating the transport of Trks and $p75^{NTR}$ is crucial to understand how neurotrophic signals initiated at the axon terminal can be efficiently transmitted to the cell body. As discussed in section 1.3, vectorial movements of cellular components are mediated by specialised proteins called molecular motors, which exploit ATP hydrolysis to move along cytoskeletal fibres. There are three classes of motors, which differ in the directionality of their movement and cytoskeletal filaments that they interact with. Motors belonging to the kinesin (KIF) superfamily or cytoplasmic dynein transport their cargoes along microtubules, whereas myosin motors move along actin microfilaments.

In recent years, studies have focussed almost exclusively on the retrograde transport of neurotrophin receptors. TrkA, TrkB and TrkC were found to be associated with the Tctex-1 chain, which is part of the dynein motor complex (Yano et al., 2001). Independent studies have characterised in detail the dynein-dependent trafficking of TrkA (Bhattacharyya et al., 2002; Heerssen et al., 2004). In contrast, surprisingly little is known about the molecular motors responsible for the anterograde transport of the neurotrophin receptors, and their targeting to the axon terminal. However, Goldstein's group have shown, using nerve ligation and subcellular fractionation experiments, that TrkA receptors and the kinesin-1 motor complex are present in the same cellular compartment, together with amyloid precursor protein (APP), β-secretase and presenilin-1 (Kamal et al., 2001). Another possibility is that TrkA could be linked to KIF1B and/or myosin VI via the GAIP-interacting protein, C-terminus (GIPC) adaptor. GIPC has been shown to interact

with TrkA (Lou et al., 2001), as well as with KIF1B and myosin VI (Bunn et al., 1999), but a ternary complex of Trk-GIPC-KIF1B (or myosin VI) has not yet been demonstrated (Figure 1-11) (Yano and Chao, 2004). Altogether, the mechanisms that regulate the anterograde transport of neurotrophin receptors remain to be elucidated.

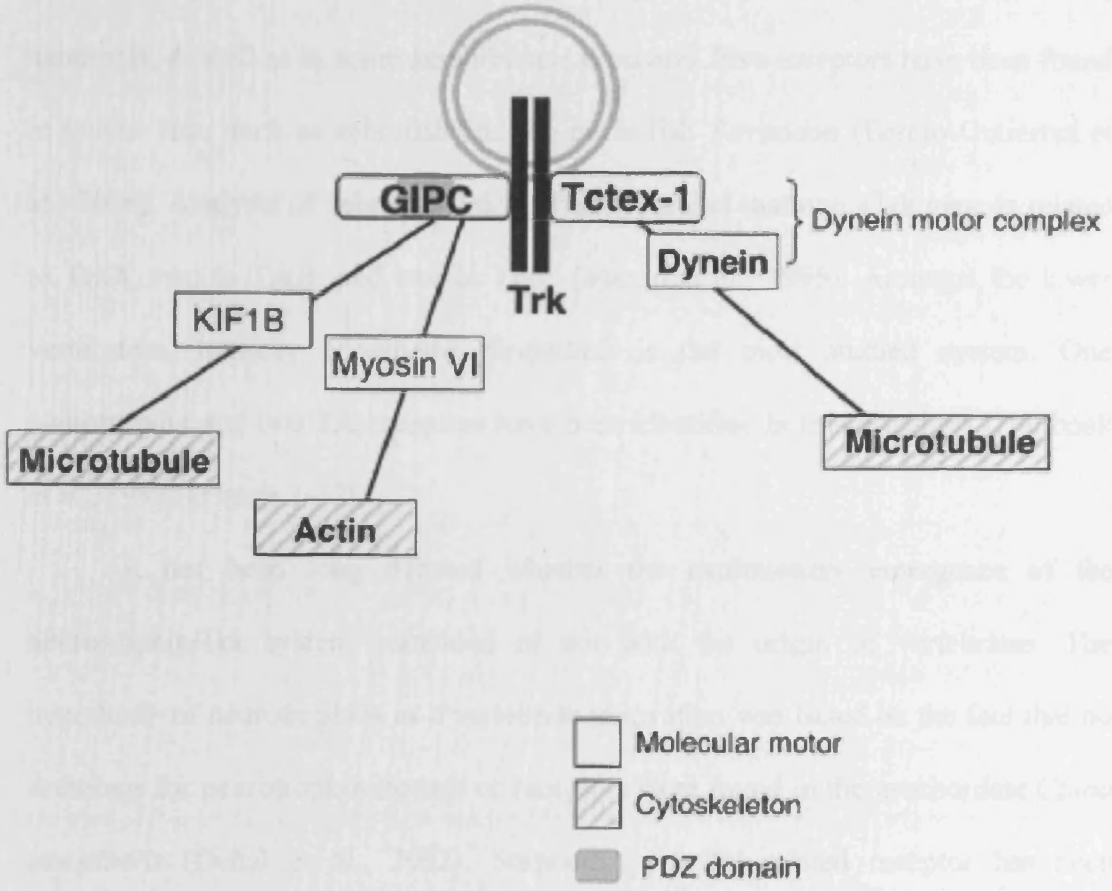

Figure 1-11: *possible connection between Trk-bearing vesicles and molecular motors*
Trk receptors have been shown to interact with the Tctex-1 component of the cytoplasmic dynein motor complex (Yano et al., 2001), as well as with the GIPC adaptor (Lou et al., 2001). GIPC binds both KIF1B and myosin VI (Bunn et al., 1999). However, a ternary complex of Trk-GIPC-KIF1B (or myosin VI) has not been demonstrated as yet. Adapted from Yano and Chao, 2004.

1.2.6 Evolution of neurotrophins

Neurotrophins and their receptors play a fundamental role in the development and maintenance of the vertebrate nervous system. Three Trk receptors have been identified in placental (human, dog, cow, chimpanzee) and non-placental (opossum) mammals, as well as in some amphibians (*Xenopus*). Five receptors have been found in teleost fish, such as zebrafish and the pufferfish *Tetraodon* (Benito-Gutierrez et al., 2006). Analysis of zebrafish Trks (zTrks) revealed that one zTrk gene is related to TrkA, two to TrkB, and two to TrkC (Martin et al., 1995). Amongst the lower vertebrates, lamprey (*Lampetra fluviatilis*) is the most studied system. One neurotrophin and two Trk receptors have been identified in this organism (Hallbook et al., 1998) (Figure 1-12).

It has been long debated whether the evolutionary emergence of the neurotrophin/Trk system coincided or not with the origin of vertebrates. The hypothesis of neurotrophins as a vertebrate innovation was based on the fact that no orthologs for neurotrophin ligands or receptors were found in the urochordate *Ciona intestinalis* (Dehal et al., 2002). Surprisingly, a Trk-related receptor has been recently isolated in amphioxus (*Branchiostoma floridae*), an organisms belonging to the cephalochordate group. This receptor, AmphiTrk, is highly homologous to vertebrate Trks both in its intracellular and in the extracellular domain. AmphiTrk is equally related to TrkA, TrkB and TrkC, and is able to transduce signals initiated by all mammalian neurotrophins (Benito-Gutierrez et al., 2005). These findings thus brought the emergence of a neurotrophin-based system back to the chordata phylum (Figure 1-12). The sequencing of the *Strongylocentrotus purpuratus* (sea urchin)

genome, completed last year (Sodergren et al., 2006), has placed neurotrophin origin farther back in evolution. A phylogenetic analysis of the genome of this organism has unexpectedly revealed *bona fide* orthologues of vertebrate neurotrophin-, Trk- and $p75^{NTR}$ genes, denominated *Sp-Nt*, *Sp-Trk* and *Sp-p75^{NTR}*. *Sp-Nt* is predicted to have a cysteine knot-based structure closely resembling vertebrate neurotrophins. *Sp-Trk* displays two IgG-like domains and a leucine-rich repeat region, as well as an intracellular tyrosine kinase domain, which are all distinctive features of vertebrate Trks (see Figure 1-7). On the basis of these recent data, therefore, it seems that the neurotrophin system might be a common feature of all deuterostomes, rather than a vertebrate acquisition (Burke et al., 2006).

The first invertebrate proteins related to Trk receptors were identified in *Drosophila*, on the basis of similarities in their kinase domain (Benito-Gutierrez et al., 2006). However, their extracellular domains did not show any homology with vertebrate Trks. The domain structure of two of these proteins, Dror and DTrk/OffTrk, is shown in Figure 1-13. Surprisingly, no genes related to neurotrophins or their receptors have been found in *C. elegans* (Ruvkun and Hobert, 1998). A Trk-related receptor has been isolated in the snail *Lymnaea stagnalis* (L-Trk). L-Trk is most similar to Trk receptors in its kinase domain, and its extracellular domain has leucine-rich motifs flanked by cysteine stretches, like vertebrate Trks. However, L-Trk has an N-terminal extension not found in vertebrate receptors. Most importantly, it completely lacks the IgG-like domains, which in vertebrates are the main determinants for neurotrophin binding (Figure 1-13) (van Kesteren et al., 1998). On the basis of the evidence currently available, protostomes (i.e. molluscs, insects and nematodes) are likely to lack a canonical neurotrophin system. In

nematodes, nervous system development relies on basic interactions between neural precursors. The simple mechanisms regulating these developmental processes therefore do not require the fine regulation provided by the neurotrophin-Trk pathways. On the contrary, development of the nervous system in insects is a fairly complex process, for which a neurotrophin-like mechanism could be required. One hypothesis in this regard suggests that steroid hormones are the principal regulators of neuronal development in *Drosophila* (Jaaro et al., 2001). An alternative theory maintains that in absence of neurotrophins, other growth factors could accomplish equivalent functions. A possible candidate pathway is represented by the epithelial growth factor receptor (EGFR) and its ligands *vein* and *spitz*, the *Drosophila* homologs of the growth factors neuregulin and transforming growth factor α (TGF-α), which in vertebrates ensure the survival of oligodendrocytes and motor neurons, respectively. Both *vein* and *spitz* have been shown to promote glial survival in a paracrine fashion, thus resembling the mode of action of neurotrophins (Hidalgo, 2002).

From an evolutionary point of view, it is noteworthy that neurotrophins and Trk receptors are expressed in neural crest and their derivatives, which are exclusive vertebrate features (Bibel and Barde, 2000). Neurotrophins are also involved in distinctive developmental processes, like tooth development in jawed vertebrates (Luukko et al., 1996), or the formation of lateral line ganglia of fish and amphibians (Martin et al., 1998). It has been suggested that short-lived, "simple" species would not require neurotrophins for the development and maintenance of their nervous systems (Barde, 1994). However, it is still not known what level of complexity represents the limit beyond which a neurotrophin-based system is required.

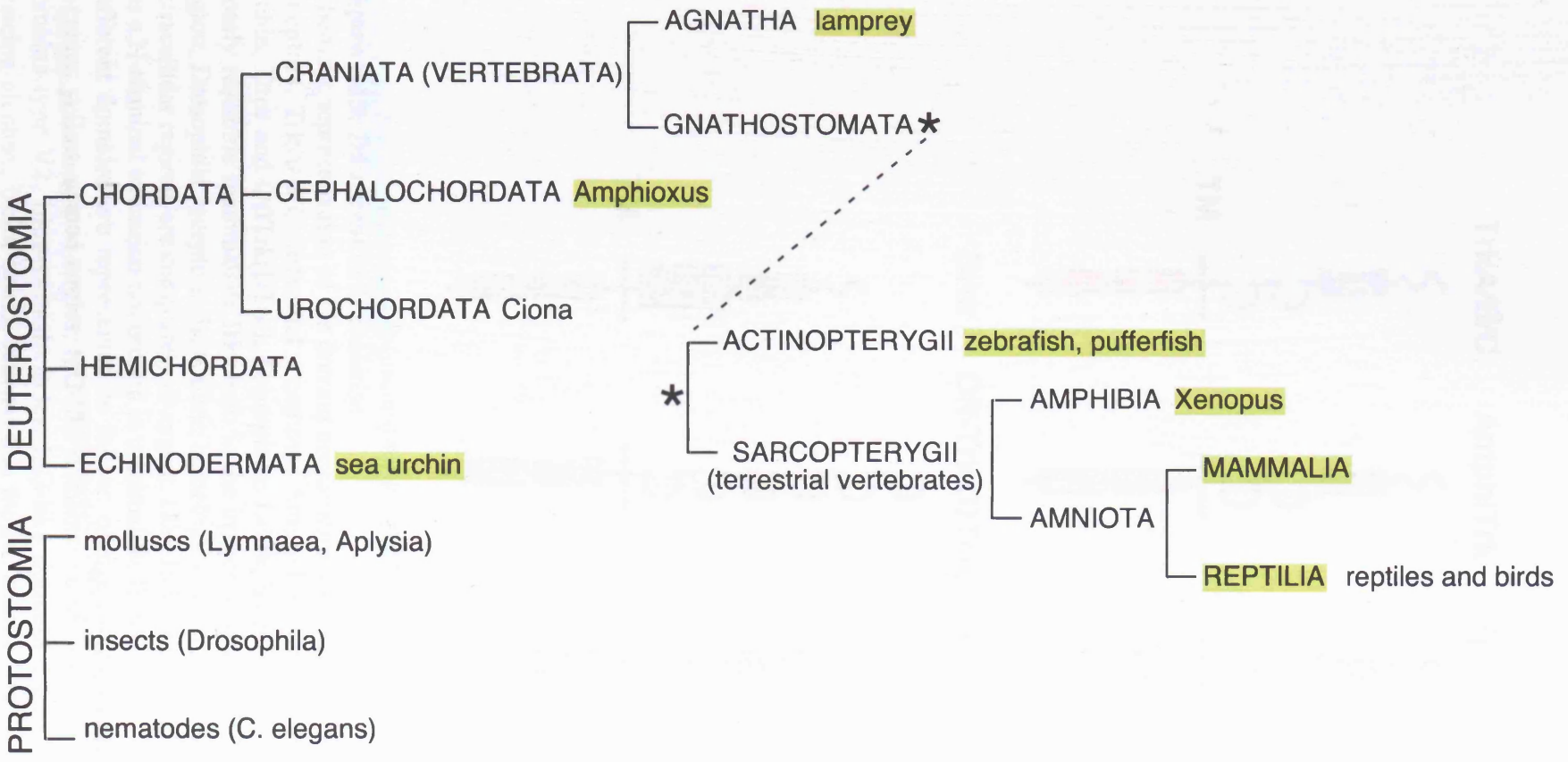

Figure 1-12: *schematic representation of the main groups of organisms*
Schematic representation of the animal groups discussed in the text, and their evolutionary relationships. Animals for which a neurotrophin-based system has been identified are highlighted in yellow.

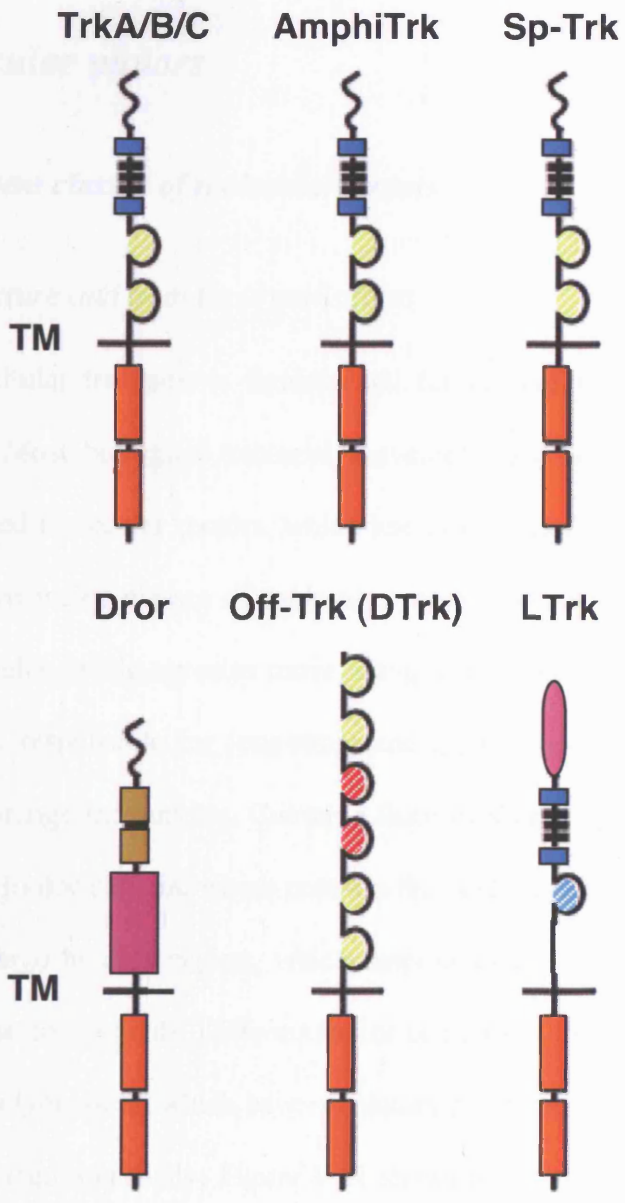

Figure 1-13: *Trk receptors in evolution*
Schematic representation of the domain organisation of putative orthologues of Trk receptors. TrkA/B/C, mammal receptors; AmphiTrk, amphioxus; Sp-Trk, sea urchin; Dror and OffTrk(DTrk), *Drosophila*; L-Trk, snail. AmphiTrk and Sp-Trk closely resemble mammalian Trks both in the intracellular and in the extracellular region. Drosophila receptors show some homology in the kinase domain, but their extracellular regions are completely divergent. LTrk lacks the IgG-like domains, and has a N-terminal extension not present in mammalian Trks.
Different domains are represented as follow: orange boxes, intracellular kinase domains; yellow-striped circles, IgG-like domains; purple-striped circles, IgG-like domains type V2; blue-striped circles, IgG-like domains type C1; blue boxes, cysteine clusters; black boxes, leucine-rich motifs; purple box, Kringle domain; brown boxes, Ror-like cysteine clusters; pink oval, N terminal extension of LTrk. TM, transmembrane region.

1.3 Molecular motors

1.3.1 Different classes of molecular motors

1.3.1.1 Structure and domain organisation

Intracellular transport is fundamental for cellular morphogenesis, function and survival. Most biological vectorial movements are accomplished by specific proteins, termed molecular motors, which use cytoskeletal fibres as cellular tracks. There are three major classes of molecular motors: kinesins and dyneins interact with microtubules, while myosins move along actin filaments. Microtubule motors are commonly responsible for long-range transport, whereas actin motors mainly mediate short-range movements. Common features shared by all molecular motors are a catalytic motor domain, which contains the ATP- and the cytoskeleton-binding sites, and a cargo-binding region, which determines the selective interaction with specific cellular components. Different motor complexes are associated with a range of accessory polypeptides, which have regulatory functions and also contribute to the definition of cargo specificity. Figure 1-14 shows a schematic representation of the domain organisation in three representative members of the different classes of molecular motors.

The cytoskeletal organisation of a particular cell influences how different molecular motors are organised and how their action is coordinated. The arrangement of cytoskeletal fibres varies considerably between different cell types. Microtubules are polarised filaments that radiate from a structure called centrosome, usually located close to the nucleus. In non-polarised cells, the minus ends of

microtubules are anchored to the centrosome, whereas the plus ends extend towards the periphery of the cell. In these cells, kinesin motors are usually responsible for the transport of cellular components from the nucleus to the cell surface, whereas cytoplasmic dyneins move from the periphery to the cell centre (Figure 1-15 A). Polarised epithelial cells have parallel arrays of microtubules, with the minus ends towards the apical side, and the plus ends towards the basal membrane. In this case, therefore, kinesins are expected to drive transport to the basal side, and dyneins to the apical (Figure 1-15 B). Although experimental data generally support this model, the contribution of the different classes of motors to vesicle trafficking in epithelial cells is still under investigation (Musch, 2004). A different situation is represented by ciliated cells. In cilia and flagella, microtubules are uniformly oriented with their plus ends towards the tip. In these structures, kinesins move anterogradely away from the cell body, whereas dyneins move retrogradely (Figure 1-15 C). Neurons have a more complex organisation, with a different cytoskeletal arrangement in the axonal and in the dendritic compartment. In the axon microtubules are uniformly oriented with the plus end towards the growth cone, whereas in the dendrites they display a more mixed polarity. As for ciliated cells, kinesins are generally associated to axonal anterograde transport, and dyneins to retrograde movements (Figure 1-15 D)(Goldstein and Yang, 2000).

In non-muscular cells, actin microfilaments are mostly concentrated just beneath the cell membrane, where they form a dense meshwork. The actin cytoskeleton regulates cell shape and motility, by modulating the formation of specialised structures such as filopodia and lamellipodia (Welch et al., 1997). In neurons, microfilaments play a particularly important role in the regulation of

growth cone dynamics. Processes like migration, retraction, turning and branching are all mainly driven by actin remodelling events, in response to environmental cues (Kalil and Dent, 2005). Myosins are responsible for short-range movements in the cellular regions close to the plasma membrane, or in the peripheral domains of the growth cones, where they haul their cargoes through the actin network. At least 18 classes of myosins have been characterised in mammalian cells. They share a common motor domain, but significantly diverge in their cargo-binding tail (Soldati and Schliwa, 2006). Motors belonging to the kinesin superfamily mostly move towards the plus end of microtubules, although a few subfamilies have been shown to go in the opposite direction. As for the myosin motors, all kinesins share a conserved motor domain, but they display a wide array of tail regions, which in mammals originate up to 100 different motors. Dynein motors are big multimeric complexes composed by two (cytoplasmic dynein) or three (axonemal dynein) heavy chains, and several intermediate, intermediate-light and light chains. The core components of the dynein motor complex are not as diverse as for the kinesin superfamily. In this case, cargo specificity is determined by association of different accessory proteins (Woehlke and Schliwa, 2000b). All known dynein motors move towards the minus end of microtubules, in a centripetal/retrograde direction, although recent evidence have shown that dynein-dynactin complexes can move bi-directionally *in vitro* (Ross et al., 2006).

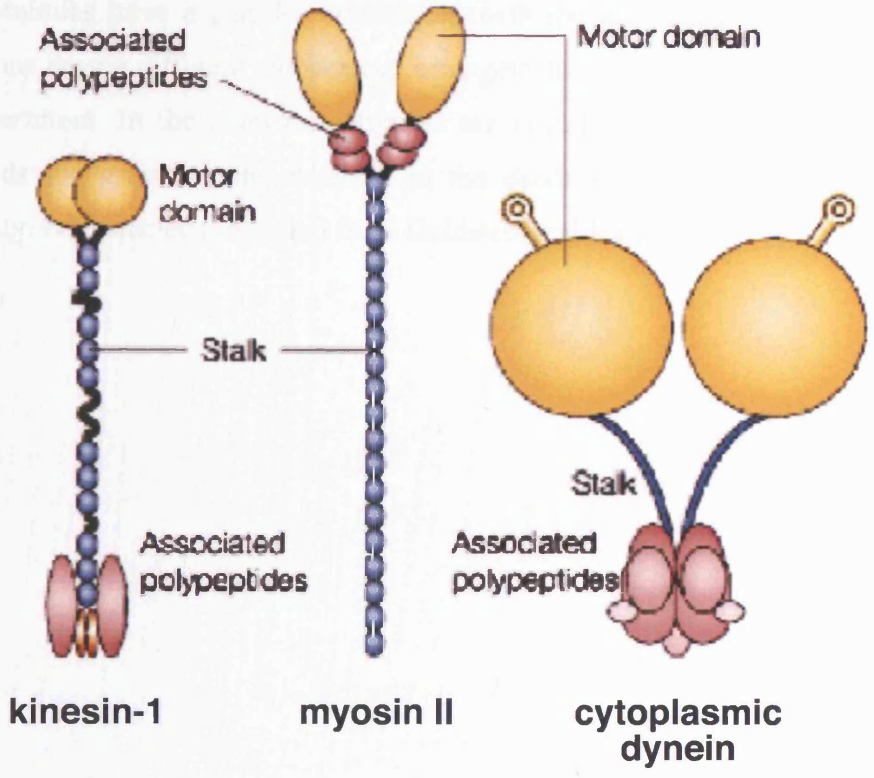

Figure 1-14: *general domain organisation in different molecular motors*
Schematic representation of the most representative motors involved in vesicular transport: kinesin-1 for the kinesin superfamily, myosin II (skeletal muscle myosin) for myosins, and cytoplasmic dynein for the dynein group. The core component of these motors is a dimer of two heavy chains, which consist of a catalytic domain (yellow) and a stalk domain (blue). Associated polypeptides (purple) are two light chains in the kinesin-1 complex, four light chains in skeletal muscle myosin, and a complex of intermediate, light-intermediate and light chains for cytoplasmic dynein. Adapted from Woehlke and Schliwa, 2000.

Figure 1-15: *microtubule organisation in different cell types*

(A) In non-polarised cells, microtubules radiate from the centrosome, in proximity to the nucleus, to the cell surface, where their plus ends are located. (B) In polarised cells, microtubules are oriented with the plus ends towards the basolateral membrane, and the minus ends towards the apical surface. (C) In cilia and flagella microtubules have a parallel orientation, with the plus ends towards the tip. (D) Neurons have a different cytoskeletal arrangement in the axonal and in the dendritic compartment. In the axon microtubules are uniformly oriented with the plus end towards the growth cone, whereas in the dendrites they display a more mixed polarity. Nuc, nucleus. Adapted from Goldstein and Yang, 2000.

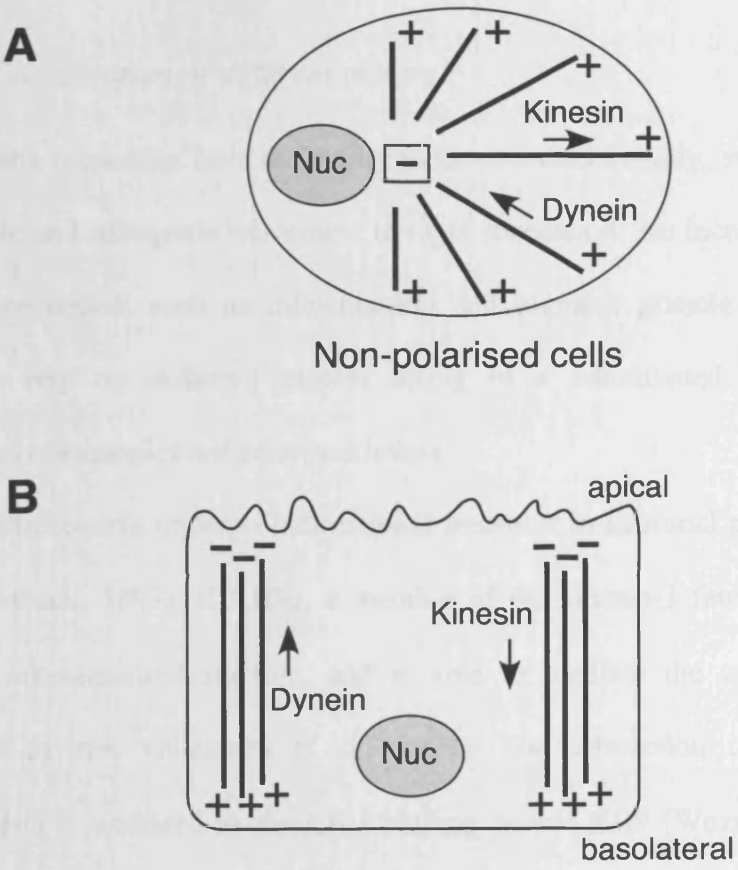
A
Kinesin
Nuc
Dynein
Non-polarised cells
B
apical
Kinesin
Dynein
Nuc
basolateral
Polarised cells
C
Kinesin
Nuc
Dynein
Ciliated cells
D
Nuc
Kinesin
Dynein
axon
dendrites
Neurons

1.3.1.2 Coordination of different motors

Many organelles have the ability to move bidirectionally, switching between anterograde and retrograde movement in rapid succession. An increasing number of transport processes, such as mitochondria and pigment granule movements, are shown to rely on different motors acting in a coordinated fashion. A few representative examples are presented below.

Mitochondria undergo bidirectional transport in neuronal processes (Morris and Hollenbeck, 1993). KIF1Bα, a member of the kinesin-3 family, is associated with the mitochondrial fraction, and is able to mediate the transport of these organelles *in vivo* (Nangaku et al., 1994). The interaction of KIF1Bα with mitochondria is mediated by the KIF1 binding protein KBP (Wozniak et al., 2005). More recently, kinesin-1 and dynein were identified as the molecular motors responsible for mitochondria movement in *Drosophila* motor axons, regulating each other activity through a mechanism most likely based on reciprocal coordination (Pilling et al., 2006). In *Drosophila*, the binding of the kinesin-1 complex to mitochondria requires the adaptor protein Milton and the mithocondrial Rho-like GTPase Miro (Glater et al., 2006). Due to their large size, mitochondria can easily bind many different plus- and minus- end directed motors, whose coordination would determine their trafficking dynamics.

Lipid droplets are storage organelles for neutral lipids. They display a regulated bidirectional transport during the development of *Drosophila* embryos (Welte et al., 1998), as well as in tissue culture cells (Valetti et al., 1999). In

Drosophila, the coordination of opposite polarity motors on lipid droplets is most likely mediated by the Klar protein (Welte et al., 1998).

Transport of melanosomes is an example of how coordination can be achieved not only between different microtubule motors, but also between microtubule- and actin-dependent motors. Several studies have shown that cytoplasmic dynein, kinesin-2, and myosin V bind the melanosome surface, acting in a coordinated fashion to modulate the complex trafficking of this organelle (reviewed in Soldati and Schliwa, 2006).

In principle, three possible scenarios could be depicted to explain how coordination of different polarity motors is achieved. In the first situation, only one type of motor is bound to its cargo at any given time, although several studies do not support this hypothesis. For example, dynein-associated structures were shown to move bidirectionally in *Dictyostelium*, indicating that the dynein motors stay associated with their cargoes even when they move in the opposite direction (Ma and Chisholm, 2002). Alternatively, opposite polarity motors can be attached to the cargo at the same time, either opposing each other's action in a "tug-of-war", or coordinating their activities, so that only one motor is active at any time. A kinetic analysis of the trafficking of lipids droplets in *Drosophila* supports a coordination model versus a tug-of war (Gross et al., 2002). In addition, neutralising antibodies against kinesin (Brady et al., 1990) or dynactin (Waterman-Storer et al., 1997) block organelle trafficking in both directions in squid axoplasm, indicating that the activities of anterograde and retrograde motors are closely linked. However, inhibition of kinesin-1 activity does not always result in an impairment of retrograde transport, as shown by a study from Morfini and colleagues, where the authors show

that GSK3-mediated phosphorylation of KLC affects anterograde movements, leaving retrograde trafficking unaffected (Morfini et al., 2002). Altogether, these data support a model where opposite-polarity motors are simultaneously bound to the same cargo, and reciprocally modulate their activity in order to coordinate cargo movements in different directions. The molecular mechanisms responsible for motor coordination are far from being understood. The main candidate for a motor coordinator is dynactin. Disruption of components of the dynactin complex impairs axonal trafficking in both directions (Martin et al., 1999). In addition, a direct interaction has been detected between dynactin and the KAP subunit of *Xenopus* KIF3 (Deacon et al., 2003). On the basis of this evidence, dynactin has been suggested to act as a molecular switch, which alternatively activates kinesin or dynein motors on the surface of cargoes, thus mediating their plus- or minus-end directed movements.

Two recent studies have characterised the ability of dynein (Reck-Peterson et al., 2006) or the dynein-dynactin complex (Ross et al., 2006) to move bidirectionally *in vitro*. Although the *in vivo* significance of these processes is not known as yet, these studies add a new level of complexity to the concept of bidirectional transport. Despite these recent findings, many open questions still remain regarding how motor activity is coordinated, and how directionality is determined in long-range movements such as the ones involved in axonal transport.

1.3.2 The kinesin superfamily

The kinesin superfamily (KIF) comprises a large number of microtubule motors, encoded by 45 loci in mice and humans, originating more than 60 KIF

transcripts (Miki et al., 2001). Different kinesins are classified on the basis of the position of their motor domain: amino-, middle- or carboxy-terminal domains characterise N-, M- and C-kinesins, respectively. As shown in Figure 1-16, kinesins share a common motor domain, but outside this domain their structure significantly diverge. Likewise, the speed of these motors varies considerably, from 0.02 $\mu m\ s^{-1}$ for the C-kinesin KIFC1, to 3.0 $\mu m\ s^{-1}$ for conventional kinesin (Woehlke and Schliwa, 2000b).

Kinesins have been implicated in the transport of the most diverse cellular components. For example, kinesin-1 motors transport mitochondria (Tanaka et al., 1998), lysosomes (Nakata and Hirokawa, 1995) and tubulin oligomers (Terada et al., 2000). They regulate the trafficking of vesicles containing APP (Kamal et al., 2000) or apolipoprotein E receptor 2 (APOER2) (Verhey et al., 2001) towards the axonal compartment, whereas vesicles bearing AMPA (α-amino-3-hydroxy-5-methyl-4-isoxazole propionic acid) receptors (Setou et al., 2002) and RNA-containing granules (Kanai et al., 2004) are directed to dendrites. Selective translocation of kinesin-1 has been recently shown to be a marker of axonal specification (Jacobson et al., 2006). KIF3 motors (belonging to the kinesin-2 family) have been involved in intraflagellar transport in node cells, which determines the establishment of the left-right symmetry during development (Nonaka et al., 1998). KIF17, another member of the kinesin-2 family, transports NMDA (*N*-methyl-D-aspartate) receptor-bearing vesicles to dendrites, thus playing an important role in the processes related to memory and learning (Setou et al., 2000). Motors of the kinesin-3 family transport mitochondria (Nangaku et al., 1994) and mannose-6-phosphate receptors (M6PR) (Nakagawa et al., 2000). Members of the kinesin-13 family (KIF2) are characterised

by a unique microtubule-depolymerising activity, which is involved in the suppression of axon collateral elongation (Homma et al., 2003).

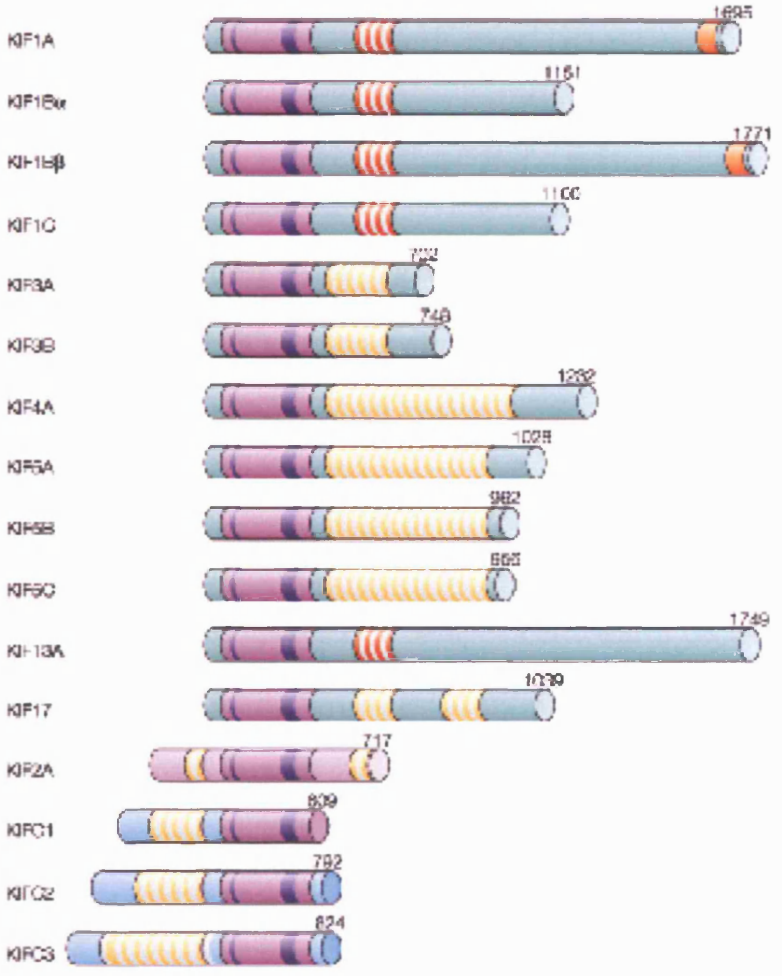

Figure 1-16: *the kinesin superfamily*
Schematic representation of the structure of some kinesin families. Motor domains are in pink, ATP-binding sequences are indicated by a thin purple line, microtubule-binding sequences by a thick purple line, dimerisation domains by yellow stripes, forkhead-associated domains by red stripes, pleckstrin homology domains by orange stripes. N-kinesins are in green, M-kinesins in pale pink, C-kinesins in blue. Adapted from Hirokawa et al., 2005.

1.3.3 Kinesin-1

1.3.3.1 Historical overview and structure

Conventional kinesin was originally identified in 1985 by two groups, which independently purified the motor from squid axoplasm and chicken brain (Brady, 1985; Vale et al., 1985). The purification was based on the property of the protein to form a very stable complex with microtubules in the presence of adenylyl imidodiphosphate (AMP-PNP), a non-hydrolysable ATP analog. Purified kinesin was able to mediate microtubule gliding on glass as well as beads gliding along microtubules (Vale et al., 1985).

Kinesin-1 is a heterotetramer of two heavy chains (KHC) and two light chains (KLC). KHCs are composed of a catalytic core, which contains the ATPase motor domain responsible for the movement along microtubules, a short neck region involved in dimerisation, and a long stalk region that can bind KLCs, as well as specific cargoes (Figure 1-17) (Schnapp, 2003). Three KHC isoforms have been identified, coded by three *KIF5* genes: KIF5A (Aizawa et al., 1992) and KIF5C (Kanai et al., 2000) are neuronally enriched, whereas KIF5B (Gudkov et al., 1994; Meng et al., 1997) is ubiquitously expressed. Although the majority of the kinesin-1 cargoes bind to KLCs, as discussed below, a growing number of proteins interacting with KHCs have been characterised, including the synaptosome-associated proteins SNAP25 and SNAP23 (Diefenbach et al., 2002), the disrupted in schizophrenia protein 1 (DISC1) (Taya et al., 2007), the scaffolding protein β-dystrobrevin (Macioce et al., 2003), the glutamate receptor interacting protein (GRIP) (Setou et al., 2002), the actin polimerisation factor Ena (Martin et al., 2005), and the

microtubule-associated protein syntabulin (Su et al., 2004). In general, KHC can bind both cargoes and light chains via non-overlapping domains, however, it is able to function even in the absence of KLCs. For example, the kinesin-mediated transport of specific mRNAs and dynein in the *Drosophila* oocyte is unaffected in KLC mutant flies, thus suggesting that the heavy chains are sufficient to target these components to their correct location (Palacios and St Johnston, 2002). Mitochondria transport in *Drosophila* is dependent on the kinesin motor. In this case, the association between mitochondria and KHC is mediated by the adaptor protein milton, which competes with KLC for the binding to KHC. In KLC *Drosophila* mutants, mitochondria localise normally in photoreceptor axons, indicating that KHCs act independently of KLC in mediating mitochondria transport in this organism (Glater et al., 2006). An additional example of KHC-mediated trafficking is provided by the *Drosophila* fragile X mental retardation protein (dFMR), a component of RNA-containing granules, whose transport is independent of KLCs (Ling et al., 2004). In lower organisms, such as the fungus *Neurospora crassa*, light chains are absent (Steinberg and Schliwa, 1995), and the C-terminal region of the heavy chain is sufficient for cargo binding (Seiler et al., 2000). Similarly, sea urchin KHCs bind membrane cargoes via their C-terminal tail, independently of the light chains (Skoufias et al., 1994).

With the exception of the cases above, KLCs are involved in the modulation of KHC activity and cargo binding. Four genes encoding KLCs have been identified in mice: *KLC1* is enriched in the nervous system, while *KLC2* and *KLC4* are ubiquitously expressed, and *KLC3* shows a restricted expression to spermatids and photoreceptors (Rahman et al., 1998; Junco et al., 2001; Yang et al., 2002; Carninci

et al., 2005). At least 19 splice isoforms have been identified for KLC1, which mainly differ at the level of their C-terminal region (McCart et al., 2003). These variants have been proposed to play a role in targeting KLC1 to different intracellular compartments or cargoes. In support of this hypothesis, KLC1B or -C are found associated with mitochondria (Khodjakov et al., 1998) and rough endoplasmic reticulum (RER)-derived membranes (Wozniak and Allan, 2006), whereas KLC1D or -E localise to Golgi-derived vesicles (Gyoeva et al., 2000; Wozniak and Allan, 2006). KLCs are composed of a heptad repeat region (HR) in the N-terminal portion, and a tetratricopeptide (TPR) repeat region, at the C-terminus (Figure 1-17) (Schnapp, 2003). The HR region binds the stalk domain of KHCs, whilst the TPRs are involved in the recruitment of specific cargoes. Although the majority of the cargoes bind the TPR region, a few exceptions have been identified, such as rootletin, the component of the ciliary rootlets in ciliated cells, which binds the HR region (Yang and Li, 2005), the glycogen synthase kinase 3 (GSK)- binding protein (GPB/Frat), which interacts with the short region upstream of the HR (Weaver et al., 2003), and the 14-3-3 protein, which binds to the carboxy-terminal tail of KLC2 (see also below) (Ichimura et al., 2002).

1.3.3.1.1 Kinesin-1 cargoes in non-neuronal systems

The function of the kinesin-1 motor complex has been extensively studied in the contest of axonal transport, neuronal development and survival; however, kinesin-1 also plays a fundamental role in non-neuronal cells. Some representative examples of kinesin-1 cargoes in non-neuronal systems are presented below.

The ER integral membrane proteins kinectin (Toyoshima et al., 1992), and the ribosome receptor p180 (Diefenbach et al., 2004) have been described as kinesin-1 interactors. Although in both cases the interactions were originally characterised in neuronal systems, they might reflect a more general role for kinesin-1 in maintaining a functional ER by regulating the trafficking of ER-derived vesicles. As previously mentioned, rootletin is the component of ciliary rootlet, a cytoskeleton-related structure that provides support to cilia in ciliated cells. Rootletin interacts with KLC3 (Yang et al., 2002), as well as KLC1 and -2 (Yang and Li, 2005) by binding the HR region, however the physiological significance of this interaction is still unclear. Kinesin-1 mediates the trafficking of p120-catenin, which interacts with and regulates cadherin-mediated adhesion in epithelial cells, thus modulating cell motility. Kinesin-1 is responsible for the targeting of p120-catenin to cell-cell junctions, as well as for its nucleo-cytoplasmic shuttling (Yanagisawa et al., 2004). Recently, kinesin-1 has been shown to interact with Smad2 in *Xenopus* animal cap explants and zebrafish embryos. Similar to p120-catenin, kinesin-1 mediates the nucleo-cytoplasmic shuttling of Smad2 in response to TGF-β stimuli, thus suggesting a role for kinesin-1 in TGF-β signalling during early developmental processes (Batut et al., 2007). This section will focus on the role played by kinesin-1 in the context of neuronal survival and differentiation. The properties of neuronal kinesins are however likely to be shared by other cell types.

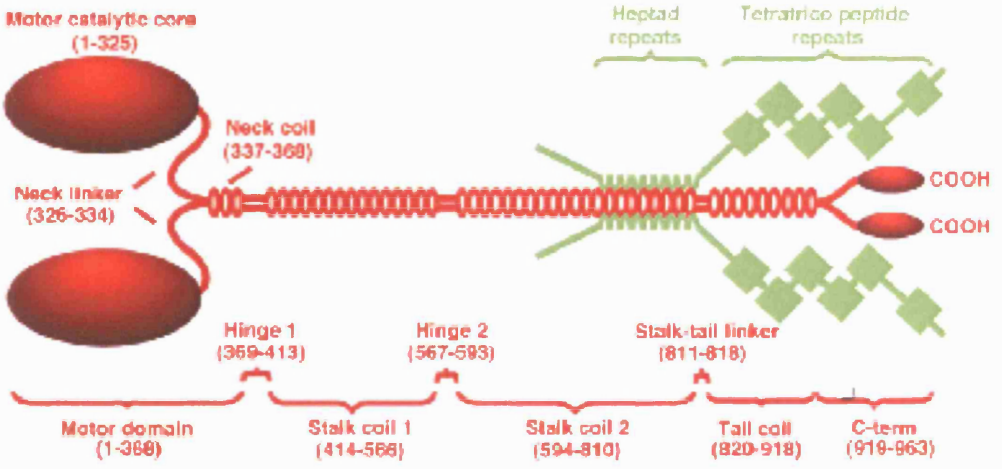

Figure 1-17: *structure of kinesin-1*
Schematic representation of the kinesin-1 motor complex. Heavy chains are in red, light chains are in green. Amino acid residues for the different domains are indicated. Adapted from Schnapp, 2003.

1.3.3.2 Axonal versus dendritic transport

Maintaining a functional distinction between axon and dendrites requires the differential targeting of proteins and organelles to these two compartments. Different hypotheses have been put forward to explain how neuronal compartmentalisation is created and maintained. In principle, the sorting between axonal and dendritic proteins could happen at the exit from the Golgi, or alternatively the selection could take place at a later stage. In the latter case, cargoes might be selectively degraded / stabilised in specific compartments, or retained in membrane microdomains through interaction with other proteins or cytoskeletal anchors (Stowell and Craig, 1999).

Molecular motors have been suggested to play a role in the processes of axon/dendrite specification, by recognising different MT modifications, or amino acid sequences in the cargo proteins. As mentioned in section 1.3.1.1, in the axonal compartment MTs are uniformly oriented with their plus end towards the growth cone, whereas in the proximal part of the dendrites they display a mixed polarity. Due to this organisation, minus-end motors such as dyneins can actively move only into dendrites, whereas plus-end motors would be able to enter both compartments (Baas et al., 1988; Foletti et al., 1999). It has been suggested that kinesins are "smart" motors, in that they could recognise MTs going into different compartments on the basis of different post-translational modifications (Burack et al., 2000). In support of this hypothesis, microtubule-associated proteins (MAPs) have been shown to affect the ability of kinesin-1 to attach to MTs, but not its speed or processivity once the motor is engaged (Seitz et al., 2002). Furthermore, MT

acetylation facilitates kinesin-1 binding and transport (Reed et al., 2006). The KIF5 motor domain was shown to preferentially recognise MTs in the initial segment of the axon, thus selectively directing a subset of Golgi-derived vesicles to the axonal compartment (Nakata and Hirokawa, 2003).

Besides the ability of motors to distinguish between different sets of MTs, the cargo itself can provide information about its final destination. Specific signals have been identified, which would direct proteins to axons or dendrites. Dendrite-targeting sequences have been mapped in the cytoplasmic domain of the transferrin receptor (TfR) (West et al., 1997), and the adhesion molecule neuroligin-1 (Rosales et al., 2005). Axon-targeting signals have been found in the C-terminal domain of Glu receptors (Stowell and Craig, 1999), KCNQ (Chung et al., 2006) Kv channels (Gu et al., 2003), and VAMP2 (Sampo et al., 2003), as well as in the ectodomain of β-APP (Tienari et al., 1996) and NgCAM/L1 (Sampo et al., 2003).

The role of kinesin-1 in the context of dendritic/axonal transport has been intensively investigated. Kinesin-1 has been identified as an early marker of axonal fate (Jacobson et al., 2006), however it has also been suggested that cargo binding to KLC might direct transport towards the axon, whereas the interaction with KHC would ensure transport into the dendritic compartment (Hirokawa and Takemura, 2004). KHC-mediated transport to dendrites has indeed been shown for both GRIP (Setou et al., 2002) and RNA granules (Kanai et al., 2004), although the exact mechanism by which the motor-cargo complex is able to distinguish between the axonal and dendritic compartment is unclear. The role of GRIP in dendritic morphogenesis has recently been characterised by Hoogenraad and colleagues. In their study, they have shown that GRIP connects EphB receptors to kinesin-1, thus

contributing to the formation and maintenance of the dendritic tree. These findings are in accordance with the observations made on the triple EphB1-EphB2-EphB3 knock out mice, which display a severely defective dendritic morphogenesis (Hoogenraad et al., 2005). Altogether, these data suggest that kinesin-1 might play different roles in targeting specific proteins to the dendritic and axonal compartments.

In recent years, several groups have identified and studied signalling pathways involved in axon specification, which rely on the activity of molecular motors. In this case, motors are responsible for the differential targeting of pre-assembled signalling complexes to either the axonal or the dendritic compartment. Some of the most recent findings in this field are summarised below. The KIF3A-mediated transport of the polarity complex PAR-3/PAR-6/aPKC to the growing axon is required for the establishment of neuronal polarity (Nishimura et al., 2004). Collapsin response mediator protein 2 (CRMP2) links the kinesin-1 motor to either tubulin (Kimura et al., 2005), or the Sra-1/WAVE1 complex, a regulator of actin cytoskeleton, thus mediating their targeting to developing axons (Kawano et al., 2005). The guanylate kinase-associated kinesin (GAKIN), a kinesin-related protein belonging to the kinesin-3 family, transports PIP_3-containing vesicles to the longest neurite, through interaction with the PIP_3-binding protein PIP_3BP. Disruption of this interaction leads to loss of polarisation (Horiguchi et al., 2006). KIF5B is responsible for the axonal targeting of Kv1 channels, possibly by binding to their axon-targeting sequence (Rivera et al., 2007). The mitotic kinesin, kinesin-5, has instead a negative effect on axon growth, due to its inhibitory activity on MT sliding (Myers and Baas, 2007).

1.3.3.3 Folding and inhibition of kinesin-1 activity

Despite kinesin-1 being implicated in the intracellular transport of several cargoes and organelles, up to 70% of the kinesin-1 cellular motor pool is represented by soluble proteins in the cytoplasm (Vale et al., 1985; Hollenbeck, 1989). This observation prompted the hypothesis that the cytoplasmic pool of kinesin could be in an inactive conformation, ready to become engaged in cargo transport in response to the appropriate stimulus. This inhibition would accomplish the double role of avoiding the futile hydrolysis of ATP in absence of cargoes, as well as the accumulation of kinesin motors at the distal microtubule ends (Verhey et al., 1998; Coy et al., 1999). Several studies have now contributed to the characterisation of the mechanisms that modulate the switch between the active and inactive state of the motor. In absence of cargoes, kinesin-1 is "switched off" by a self-inhibition mechanism, which is induced by KLC binding (Verhey et al., 1998). In this conformation, the N-terminal region of KLC binds to the hinge region and the first part of the tail region of KHC, and at the same time the tail domain of KHC folds back on the motor domain, thus impairing its ability to come into contact with the cytoskeleton. A 65 amino acid long sequence in the KHC tail was shown to be sufficient to mediate the inhibition of the motor activity in the folded conformation (Verhey et al., 1998; Coy et al., 1999; Friedman and Vale, 1999; Stock et al., 1999). Motor activation could be triggered by cargo binding (Coy et al., 1999; Friedman and Vale, 1999; Blasius et al., 2007), post-translational modification such as phosphorylation (discussed in more details in section 1.3.5), or slightly acidic pH (Verhey et al., 1998). More recently an alternative scenario has been proposed, where kinesin-1 can be in a folded (inhibited) conformation while still bound to

membrane cargoes. In this situation, both KHCs and KLCs would be required to participate in cargo binding (Wozniak and Allan, 2006). The role of KLCs in KHC activation and targeting is supported by the analysis of the KLC1 knock out mice, which display abnormal localisation of KIF5A and KIF5B (see section 1.3.6) (Rahman et al., 1999).

1.3.4 Kinesin motors and signalling pathways

The number of proteins known to interact with different members of the kinesin superfamily is constantly increasing. For many years it was believed that "kinesin receptors" were molecules whose only purpose was to link the kinesin motor to specific cargos. However, evidence coming from several studies has now established that molecules acting as kinesin-cargo linkers are adaptors or scaffolds that have also many other functions. As a consequence, the definition of cargo has broadened from single proteins, to include organelles and entire pre-assembled signalling complexes. In many cases, molecular partners do not come in contact with each other at their final destination, but they are rather transported together in pre-assembled modules, which contain information about the signal, but also about the location where the cascade should become activated. Molecular motors play a key role in determining the appropriate response to external stimuli, by delivering signalling complexes to specific domains of the plasma membrane, as well as by targeting activated receptors to local and long-range trafficking routes. The best known examples of connection between molecular motors, cargoes and signalling pathways are discussed below.

Vesicles containing APP, β-secretase and presenilin-1 (one of the catalytic subunits of the γ-secretase complex) undergo KIF5 mediated axonal transport. β-secretase and presenilin-1 mediate the proteolytic processing of APP to produce amyloid-β peptide, which is the main constituent of extracellular amyloid plaques in Alzheimer's disease. However, it is still unknown whether kinesin-1 interacts directly with APP (Kamal et al., 2000), or the interaction is mediated by the JNK-interacting protein-1 (JIP-1) (Inomata et al., 2003; Matsuda et al., 2003) (Figure 1-18 A). In any case, these observations suggest that APP processing might occur on a particular subset of transport vesicles. The kinesin-1 motor might be involved in the pathogenesis of Alzheimer's disease, as impaired APP transport might contribute to the onset of this neurodegenerative pathology.

Mammalian JIPs are scaffolds for the MAPK pathway that activates Jun N-terminal kinase (JNK) (Davis, 2000). More specifically, JIPs bind the Reelin receptor APOER2, which is implicated in JNK signalling and plays a fundamental role in neurogenesis (Rice and Curran, 2001). JIP proteins bind the TPR domains of KLC, thus connecting the kinesin-1 complex to APOER2-bearing vesicles. The KIF5-mediated transport of JIP therefore ensures the correct targeting of different components of this pathway to the neurite tips (Figure 1-18 B)(Bowman et al., 2000; Verhey and Rapoport, 2001).

The AMPA receptor subunit GluR2 interacts with the GluR-interacting protein GRIP1, a multi-PDZ-domain protein that mediates the clustering of AMPA receptors at excitatory synapses in the brain (Dong et al., 1997). GRIP1 also binds KHC of KIF5, thus modulating the transport of AMPA-bearing vesicles to dendrites (Figure 1-18 C) (Setou et al., 2002). AMPA receptors have been shown to be

transported also by KIF1A, through the neuronal scaffolding protein Liprin-α (Shin et al., 2003). As in the case of the NMDA receptor (see below), it is possible that redundant transport mechanisms exist for this type of cargoes, or that the activity of KIF5 and KIF1A is specific for different neurons or neuronal compartments.

Hirokawa's group has recently isolated and characterised large RNase-sensitive granules that are directed to the dendritic compartment via an interaction with the heavy chain of the KIF5 complex. Components of these granules included mRNA molecules, RNA-transporting proteins as well as the machinery for protein synthesis and regulators of translation. However, the protein(s) linking kinesin to these granules have not been identified as yet. These finding shed new light on the role played by motors in local mRNA synthesis, which is of crucial importance especially in response to nerve injuries (Figure 1-18 D)(Kanai et al., 2004).

A subset of Golgi-derived clathrin-coated vesicles, containing M6PR, is transported along microtubules from the trans Golgi cisternae to the plasma membrane. Transport of M6PR-containing vesicles is mediated by KIF13A, through an interaction with the clathrin-adaptor complex AP-1 (Nakagawa et al., 2000). AP-1 thus on one side interacts with the transmembrane M6P-receptor, modulating its sorting from the TGN into specific cargo vesicles, and at the same time recruits the clathrin molecules necessary for vesicle budding, as well as KIF13A, which will ensure the transport of these vesicles to the plasma membrane (Figure 1-18 E).

A similar mechanism regulates the transport of NMDAR-containing vesicles. In this case, KIF17 binds the PDZ protein LIN-10, which is part of a bigger complex containing also the NMDAR 2B subunit (NR2B). The LIN complex therefore binds KIF17 on one side, and the transmembrane protein NR2B on the other side (Setou et

al., 2000). KIF17-mediated transport of these carriers is responsible for the establishment of postsynaptic clusters of glutamate receptors, which are involved in fundamental functions such as synaptic plasticity and neuronal morphogenesis (Figure 1-18 F) (Setou et al., 2000). Interestingly, Mok and co-workers showed that NMDAR can be transported also by the KIF1B motor, through interaction with PSD-95 or S-SCAM (Mok et al., 2002). These observations suggest that redundant mechanisms might exist to regulate the transport of physiologically relevant cargoes.

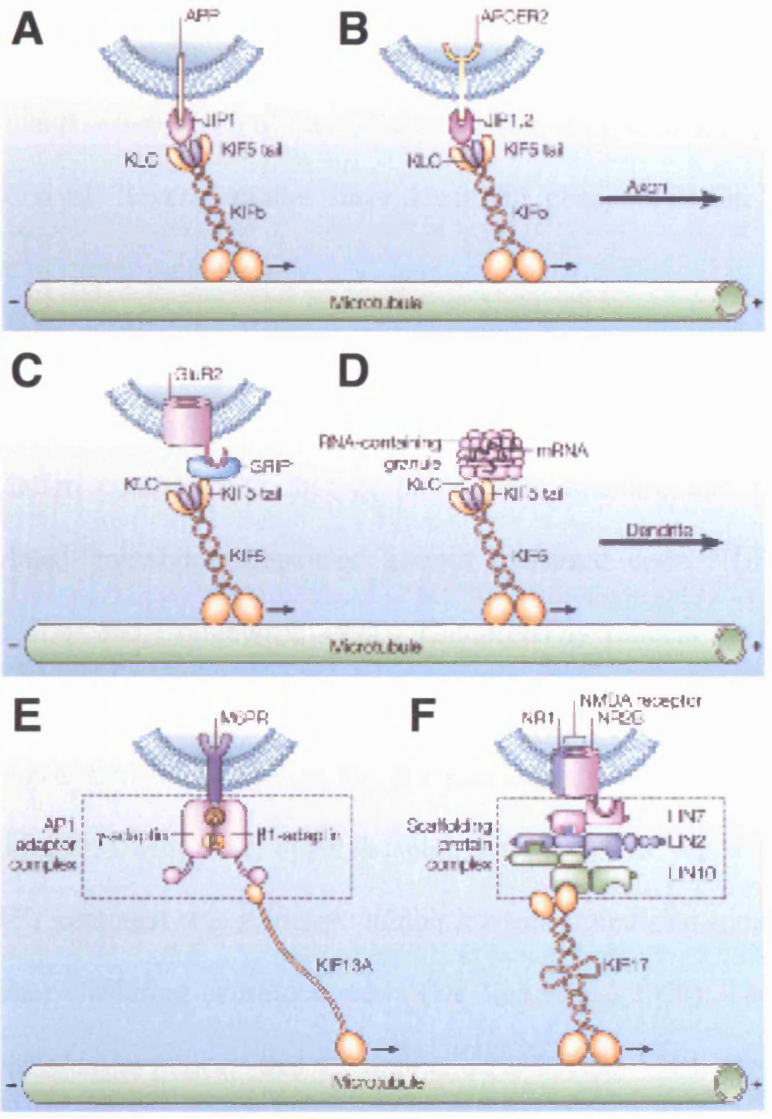

Figure 1-18: *molecular motors and signalling pathways*
(A) APP-containing vesicles are transported by KIF5. (B) JIP proteins link KIF5 to the Reelin receptor APOER2. (C) The AMPA receptor subunit GluR2 is connected to the KIF5 motor by GRIP1. (D) mRNA-containing granules are transported into the dendritic compartment by KIF5, via KHC binding. (E) KIF13A mediates the transport of M6PR-containing vesicles, through the interaction with the AP-1 adaptor complex. (F) The LIN complex links KIF17 to NMDAR-containing vesicles. Adapted from Hirokawa and Takemura, 2005.

1.3.5 Modulation of motor activity by phosphorylation

Given the increasing number of biological processes whose correct functioning is shown to rely on the activity of motor proteins, it is clear that modulation and coordination of the different classes of molecular motors are crucial for cell survival. Several studies have identified phosphorylation as a common mechanism of motor regulation.

Both the heavy and the light chains of kinesin-1 are phosphorylated *in vivo* (Hollenbeck, 1993). Membrane-associated KHC showed an increased phosphorylation compared to that in the soluble fraction, and the amount of phosphorylated / membrane-associated kinesin increased upon NGF-treatment, in PC12 cells (Lee and Hollenbeck, 1995). This probably reflects the increase in the transport rate during the process of differentiation, thus supporting the idea that the phosphorylated form of kinesin is the one mediating vesicle trafficking (Lee and Hollenbeck, 1995). However, hyperphosphorylation of KLC upon tumor necrosis factor (TNF) treatment was shown to inhibit kinesin-1-mediated transport, resulting in perinuclear clustering of mitochondria (De Vos et al., 2000). These contrasting observations seem to indicate that the regulation of kinesin-1 activity is achieved by coordination of multiple pathways, which can have opposite effects depending on the cellular environment and the type of stimulus. The Hsc70 chaperones actively relase kinesin-1 from membranes, possibly by interacting with KLCs (Tsai et al., 2000). GSK3 phosphorylation of KLC also mediates detachment of kinesin-1 from membranes, and specifically impairs fast anterograde transport in squid axoplasm, leaving retrograde transport unaffected. It has been proposed that GSK3

phosphorylation might cause conformational changes in the three-dimensional structure of KLC, which would make the Hsp70 binding site more accessible, and consequently facilitate the detachment (Morfini et al., 2002). *In vitro* experiments showed that phosphorylation of kinesin-1 by cAMP-dependent protein kinase (PKA) inhibits its binding to synaptic vesicles (Sato-Yoshitake et al., 1992). Phosphorylation of KLC2 on Ser575 is necessary and sufficient for the binding to the 14-3-3 protein (Ichimura et al., 2002). Phosphorylation seems to be a general mechanism to modulate the activity of molecular motors. In fact, phosphorylation of the light intermediate chain of cytoplasmic dynein by cdc2-CyclinB1 kinase causes the release of dynein from membranes (Addinall et al., 2001). In a similar way, phosphorylation of myosin V by CaMKII also regulates the attachment/detachment of the motor to its cargoes, in a cell cycle-dependent manner (Karcher et al., 2001).

Interestingly, binding of some cargoes could be itself phosphorylation dependent, as shown for the Ena/VASP proteins, which regulate actin polimerisation and branching (Krause et al., 2003). In its unphosphorylated (active) form, Ena binds KHC and impairs axonal transport in *Drosophila*. Abl kinase phosphorylates and inhibits Ena activity (Krause et al., 2003), therefore indirectly exerting a positive effect on kinesin-1-mediated transport. The functional connection between Abl, Ena and kinesin-1 has been confirmed by genetic interaction tests in flies (Martin et al., 2005). Phosphorylation is also thought to be the mechanism underlying the accumulation / dispersion of melanosomes in melanophores (Thaler and Haimo, 1990; Reilein et al., 1998). As mentioned in section 1.3.1.2, melanosome transport relies on the coordinated activity of kinesin, dynein and myosin motors. Phosphorylation by a still unknown kinase could modulate myosinVa detachment

from the melanosome to allow organelle aggregation. The observation that kinesins and dyneins do not antagonise each other whilst bound to the same organelle raised the idea that phosphorylation of one or both of these motors could determine which one is active at any stage, thus determining the net direction of transport (Nascimento et al., 2003), although other scenarios are also possible, as discussed in section 1.3.1.2.

Phosphorylation could therefore represent a general mechanism to ensure the release of motor complexes from their cargoes, once they have reached their final destination. The association of motors with signalling complexes could allow signalling pathways to regulate motor activity. Phosphorylation of the motor itself or of an intermediate protein could modulate the recruitment/activation of the motor at the point of departure, or its detachment/inactivation once the complex has reached its final destination (Figure 1-19).

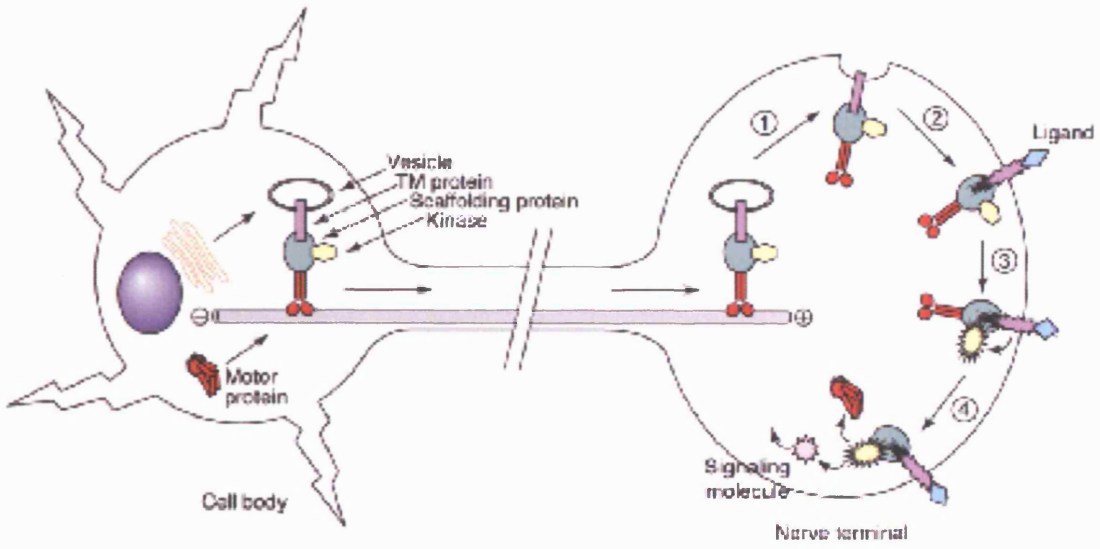

Figure 1-19: *possible modulation of kinesin activity by phosphorylation*
(steps 1-2) Pre-assembled signalling complexes are transported by molecular motors from the cell body to the axon terminal. Motor proteins are represented in red; blue ovals, scaffolding proteins; purple boxes, transmembrane (TM) receptors; yellow hexagons, kinases. (steps 3-4) Upon ligand binding (blue rhombus), receptors are activated (purple stars) and would in turn activate the associated kinases (yellow stars). Activated kinases could directly or indirectly mediate the detachment of the kinesin motor, as well as activate intracellular signalling molecules. Adapted from Verhey and Rapoport, 2001.

1.3.6 In vivo *targeting of KHCs and KLCs*

Results from gene targeting studies in *Drosophila* support a role for kinesin-1 in nervous system development. KHC mutations cause paralysis and death at the larval or pupal stage (Saxton et al., 1991), due to impairment of axon potential propagation and neurotransmitter release (Gho et al., 1992). Mutant neurons display a characteristic phenotype, with axonal swellings packed with cargoes of fast axonal transport, such as synaptic membrane proteins, which progressively affect neuronal functionality (Hurd and Saxton, 1996). In order to eliminate the contribution of maternal kinesin during development, mosaic female flies have been generated, which lack KHC in the germline. In this situation, embryogenesis fails at early stages because of mistargeting of mRNAs in the embryo (Brendza et al., 2000). KLC mutations phenocopy the defects of the KHC targeted flies: KLC mutants display paralysis and death at larval stage, as well as the axonal swelling phenotype (Gindhart et al., 1998).

The phenotypes resulting from the genetic targeting of the different KHC genes in mice reflect the characteristic distribution of the specific isoforms, as well as their ability to compensate for each other. KIF5A null mice die at birth due to their inability to breathe, with no obvious defects in nervous system development, apart from enlarged motor neuron bodies (Xia et al., 2003). Cre-mediated ablation of KIF5A in postnatal neurons results in seizures, sensory and motor neuron degeneration, and hind limb paralysis, thus suggesting a KIF5A-specific function in the maintenance of neuronal homeostasis as well as during development (Xia et al., 2003). KIF5C mutant mice show the less severe phenotype: they are viable, with a

slightly smaller brain compared to wild type littermates, and a moderate loss of motor neurons (Kanai et al., 2000). This mild phenotype is probably due to the ability of the other two isoforms to compensate for KIF5C absence. The deletion of the ubiquitous KIF5B heavy chain by contrast is lethal between E9.5 and E11.5, with severe growth retardation of the knock out embryos. This result is not surprising, given that KIF5B has a much broader distribution than the other two isoforms, which are only expressed in the nervous system. KIF5B mutant cells show impaired dispersion of lysosomes and perinuclear clustering of mitochondria (Tanaka et al., 1998).

KLC1 null mice are viable, but smaller than the wild type and with impaired motor functions. In addition, the intracellular localisation of KIF5A and KIF5B is altered in sensory and motor neurons derived from KLC1 mutant animals, thus supporting the idea that KLCs are necessary for activation and targeting of the heavy chains (Rahman et al., 1999).

1.4 In vivo *function of neurotrophins and their receptors*

1.4.1 Neurotrophins: more than neuronal growth factors

Expression of neurotrophins and their receptors is not limited to development, nor is restricted to neuronal cells. NGF and its receptors TrkA and $p75^{NTR}$ have been extensively studied, and their expression monitored at different developmental stages as well as in adult life, in a number of different tissues (Sofroniew et al., 2001). A very interesting example is represented by $p75^{NTR}$ expression in motor neurons. Motor neurons transiently express high levels of

$p75^{NTR}$ during development, at the time of axon elongation, when a significant portion of them would undergo a naturally occurring cell death (Hamburger, 1975). After this developmental stage, and throughout adulthood, the expression of this receptor is reduced to minimal levels. Several studies have shown a dynamic regulation of NGF and its receptor in response to injury: $p75^{NTR}$ expression is significantly upregulated around one week after the injury took place, and would go down again once regeneration is complete (Ernfors et al., 1989; Wood et al., 1990). In addition, Schwann cells were also shown to increase NGF and $p75^{NTR}$ expression in response to nerve injury (Taniuchi et al., 1986). These observations suggest that $p75^{NTR}$ could provide trophic support to injured motor neurons, or it could play a role in the modulation of axon guidance during regeneration. $p75^{NTR}$ has been also implicated in the pathogenesis of neurodegenerative diseases. For example, increased levels of this receptor were found in oligodendrocytes and macrophages associated with multiple sclerosis plaques (Dowling et al., 1999). In addition, $p75^{NTR}$ has been suggested to mediate amyloid β-induced toxicity in Alzheimer's disease, via a direct interaction with the amyloid peptide (Yaar et al., 1997).

An increasing number of genetically modified mice are now available, in which neurotrophin receptors or their ligands have been altered or removed. The ablation of components of the neurotrophic system has often resulted in perinatal lethality. With the exception of the NT-4/5 knock-out, the removal of all the other neurotrophins, as well as their receptors, is eventually lethal. Although these knock-out models have been useful to dissect the function of neurotrophins during development, they can provide only a limited amount of information about the function of these molecules in adulthood. The generation of conditional knock-out

animals would allow the removal of components of the neurotrophic system selectively in the postnatal period, thus bypassing early lethality. It would then be possible to achieve a better understanding of the mechanisms at the base of many neurological conditions, like Alzheimer's and other neurodegenerative diseases, which have been linked to malfunctioning of the neurotrophin machinery. As discussed below, the removal of a ligand and the corresponding receptor do not always give an identical phenotype. This is mainly due to the fact that some neurotrophins are able to interact with multiple receptors (Figure 1-7). Functional redundancy thus represents an additional level of complexity in the analysis of the knock-out phenotypes.

1.4.2 Knock-out models for neurotrophins and their ligands

1.4.2.1 DTrk/Off-Trk

As discussed in section 1.2.6, the *Drosophila* DTrk/Off-Trk receptor was identified as a possible Trk homolog, on the basis of similarities in the intracellular kinase domain. DTrk is expressed during embryogenesis in several region of the fly nervous system. It was shown to promote cell adhesion in a homophilic, Ca^{2+}-independent manner (Pulido et al., 1992). Generation of DTrk loss-of-function alleles in *Drosophila* resulted in axon guidance defects in the CNS as well as in motor neurons. Mutants were characterised by disruption of axonal projections to the target muscles, coupled to defective defasciculation (Winberg et al., 2001). Interestingly, there was a genetic interaction between DTrk, semaphorin 1a (Sema1a) and plexinA (PlexA) mutants. Plexin receptors and their ligands semaphorins are signalling proteins involved in axon guidance, immune cell

regulation, as well as vascular growth and remodelling (Kruger et al., 2005). Genetic analysis on *Drosophila* mutants showed that DTrk and PlexA act downstream of Sema1a, thus opening the possibility that DTrk is involved in the Semaphorin/plexin pathway to control axon guidance events (Winberg et al., 2001).

1.4.2.2 NGF/TrkA

Mice lacking NGF are viable at birth, although smaller than their littermates, but they are not able to feed properly and fail to gain weight. The majority of the animals die within the first three days of life. However, some of them can survive up to one month. Knock-out mice show severe cell loss in sympathetic ganglia, which disappear completely by two weeks of age. In addition, dorsal root ganglia (DRGs) from NGF-deficient animals show a selective loss of small TrkA-positive nociceptive neurons (Figure 1-20 b). As a consequence, both heterozygous and knock-out animals display a reduced responsiveness to pain (Crowley et al., 1994).

Mice defective for the TrkA receptor can survive up to one month of age. They show severe sensory and sympathetic defects, probably due to neuronal loss in the trigeminal, sympathetic and dorsal root ganglia. The similarities in the phenotype displayed by NGF- and TrkA-deficient mice indicate that TrkA is required to accomplish most of the trophic effects mediated by NGF in the peripheral nervous system (Smeyne et al., 1994). In the central nervous system, TrkA expression is restricted to some regions of the basal forebrain. Accordingly, in TrkA -/- mice, projections emanating from this part of the brain are severely decreased. This is in contrast with observations made in NGF -/- mice, which do not show major abnormalities in the same area (Crowley et al., 1994). This suggests that TrkA could

bind different ligands in addition to NGF, to accomplish its trophic effects in this region of the brain.

1.4.2.3 BDNF/NT-4/5/TrkB

Most of the BDNF-deficient mice die by the second week of age, although some of them can survive up to one month. They display movement defects, like spinning, head bobbing and hindlimb extension during attempted locomotion. This severe phenotype is due to drastic loss of neurons in vestibular ganglia, which are responsible for balance and locomotion. In addition, many other sensory ganglia appear significantly smaller, including DRGs. Interestingly, BDNF -/- mice lack slowly adapting mechanoreceptors terminating on Merkel cells (Figure 1-20 c) (Carroll et al., 1998). In contrast with the observations made on the TrkB-null mice (see below), motor neurons appear normal both in size and number, suggesting that in absence of BDNF, NT-3 or NT-4/5 could activate TrkB receptors in this neuronal population. The brains of mutant animals show mild defects, restricted to some regions of the substantia nigra, hippocampus and cortex. However, an important function of BDNF was uncovered by the analysis of the hippocampal synapses of BDNF -/- animals. BDNF-deficient synapses showed a significant decrease in the number of vesicles docked at presynaptic active zones, thus suggesting a role for BDNF in the mobilisation and/or docking of these structures (Pozzo-Miller et al., 1999). In addition, LTP is seriously compromised in BDNF -/- as well as BDNF +/- animals (Korte et al., 1995; Patterson et al., 1996). Although the molecular basis of these actions is not completely understood as yet, all the available data point towards a fundamental role of BDNF in hippocampal physiology. It is clear that BDNF

action requires TrkB activity, as postnatal ablation of this receptor in the forebrain region also compromises LTP (Minichiello et al., 1999), most likely by affecting LTP signalling at the presynaptic level (Xu et al., 2000a). The same animals show impairment in spatial learning behaviour, worsening with age, which is reminiscent of the phenotype associated with hippocampal lesions (Minichiello et al., 1999). BDNF +/- mice also display abnormalities in eating behaviour, with a tendency to become obese. These dysfunctions are normally associated with hypothalamic defects, as the hypothalamus is the region of the brain controlling eating behaviour. These observations suggest a role for BDNF in hypothalamic physiology (Kernie et al., 2000). BDNF -/- mice do not show any obvious abnormalities outside of the nervous system (Ernfors et al., 1994a; Jones et al., 1994).

Mice carrying a catalytically inactive TrkB receptor have a more severe effect: the homozygous animals die 24 to 48 hours after birth due to their inability to feed. This phenotype is likely related to a significant loss of trigeminal ganglia and facial motor neurons. As for the BDNF -/- mice, DRGs appear smaller. In addition, however, TrkB-deficient animals show a reduction in the number of lumbar motor neurons (Klein et al., 1993). The fact that TrkB -/- mice show a more severe phenotype than the BDNF -/- animals, suggests that TrkB might act as a receptor for other neurotrophins *in vivo*. Analysis of the central nervous system of TrkB -/- mice showed an increase in apoptotic cell death in different regions of the brain, such as the dentate gyrus, some of the cortical layers, the striatum, and the thalamus (Alcantara et al., 1997). A subsequent study confirmed that dorsal thalamic neurons develop a dependence on BDNF at late stages of embryonic development (E19). At this time, BDNF is produced by the cerebral cortex, which is the main target of

thalamic projections. TrkB deficient thalamic neurons are unable to sense this particular neurotrophin, and as a consequence they undergo apoptosis (Lotto et al., 2001). The post-natal, conditional excision of TrkB has been shown to cause a reduction in the size of the cerebral cortex. More detailed analysis revealed reduction in the length of dendrites of pyramidal neurons in this region, implicating TrkB in the cellular events leading to growth of neuronal processes (Xu et al., 2000b). Conditional deletion of TrkB in cerebellar precursors was shown to affect the development of inhibitory interneurons, which expressed a reduced amount of GABAergic markers and were severely impaired in their ability to establish synaptic contacts (Rico et al., 2002).

NT-4/5 null mice appear normal, and do not have any major neurological or physical defects. The only structure affected by NT-4/5 deletion is the nodose-petrosal complex, which controls respiration, heart rate, blood pressure and other autonomic functions (Conover et al., 1995; Liu et al., 1995). More in-depth studies of these mutant animals have showed that NT-4/5 -/- mice lack a specific subpopulation of sensory neurons, identified in the down-hair receptors (Figure 1-20 d) (Stucky et al., 1998). In addition, they display deficiency in gustatory papillae and taste bud formation (Liebl et al., 1999). Mice lacking both BDNF and NT-4/5 did not appeare to be more seriously affected than the BDNF knock-out animals (Conover et al., 1995).

1.4.2.4 NT-3/TrkC

The majority of NT-3 knock-out mice die shortly after birth, with a small percentage surviving up to three weeks. They show severe movement defects, ataxia

and inability to position the limbs properly when trying to move. Analysis of the mutant animals revealed a reduced number of neurons in all sensory and sympathetic ganglia. The most distinctive feature of the NT-3 null mice, however, is the complete absence of proprioceptive organs, like muscle spindles and Golgi tendons, which is reflected in the loss of big proprioceptive neurons in the DRGs (Figure 1-20 a). This is clearly at the base of the locomotion problems displayed by the mutant mice, characterised by abnormal movements and postures (Ernfors et al., 1994b) The loss of spinal sensory neurons was shown to be due to high level of neuronal apoptosis, coupled to a premature differentiation of precursor cells to the neuronal phenotype (Farinas et al., 1996). The perinatal lethality characterising most of the NT-3 -/- mice is however unrelated to neuronal defects, but it is due to severe cardiovascular abnormalities, including ventricular septal defects, pulmonary stenosis, overriding aorta and right ventricular hypertrophy, which are the characteristic features of a heart malformation known as tetralogy of Fallot (Donovan et al., 1996). This cardiac phenotype is present also in TrkC -/- mice, as discussed below, suggesting an essential role for the NT-3/TrkC signalling in heart development.

The TrkC deficient mice recapitulate the defects caused by the NT-3 deletion. Most of the mutant mice die by three weeks of age, but some can survive up to four months. They have difficulties in locomotion, and hold their limbs in abnormal postures. Not surprisingly, mutant DRGs lack proprioceptive neurons (Klein et al., 1994). Also in the case of the TrkC -/- mice, early postnatal lethality is due to cardiac malformations, like atrial and ventricular septal defects, and valvular defects including pulmonary stenosis (Tessarollo et al., 1997).

The *trkC* locus encodes several different isoforms of the TrkC receptor, some of them lacking the kinase domain (Figure 1-7). Tessarollo and co-workers created a mouse model, where a physiological truncated TrkC isoform is overexpressed. Transgenic mice show a phenotype reminiscent of the NT-3 and TrkC null animals, with severe cardiac defects and abnormalities in the peripheral nervous system. These observations suggest that truncated receptors might function by neutralising NT-3, maybe in a dominant negative fashion (Palko et al., 1999).

The cardiac defects found in both NT-3 and TrkC null mice involve structures of neural crest origin. Studies conducted on neural crest cells derived from TrkC -/- mice have identified a precocious fate restriction, coupled to premature neurogenesis. Premature differentiation into neuronal lineages causes a reduction in migratory capacity, and probably originates the defects in the cardiac outflow of the mutant mice (Youn et al., 2003).

1.4.2.5 $p75^{NTR}$

$p75^{NTR}$-null mice are viable and fertile. By four months of age, however, they develop skin alterations and ulcers in the distal extremities. These defects have been linked to decreased sensory innervation in the skin, which correlates to loss of heat sensitivity in these animals. Consistent with the reduced cutaneous innervation, DRGs were found to be smaller in $p75^{NTR}$ -/- mice (Lee et al., 1992). $p75^{NTR}$-deficient DRGs, superior cervical ganglia and trigeminal neurons show reduced sensitivity to NGF stimulation, and consequently display an increase cell death. On the basis of these observations, $p75^{NTR}$ has been suggested to play a role in the modulation of TrkA activity during the development of sensory and sympathetic

neurons (Davies et al., 1993; Lee et al., 1994). In contrast, $p75^{NTR}$ deletion did not seem to affect motor neuron development (Murray et al., 1999). Subsequent studies have shown that neuronal defects in $p75^{NTR}$ null mice were at least in part due to an impairment of Schwann cells migration, which resulted in a decreased ensheathment of developing axons (Bentley and Lee, 2000). The understanding of the role of $p75^{NTR}$ during development was however challenged by the observation that transgenic mice overexpressing the intracellular domain of the receptor show high neuronal cell death in the developing CNS (Majdan et al., 1997). It therefore seems that $p75^{NTR}$ action is the result of a fine modulation of anti- and pro-apoptotic signals.

$p75^{NTR}$ is widely expressed in many tissues of the developing embryo. As a consequence, the deletion of this receptor was expected to cause important developmental defects. Surprisingly, however, $p75^{NTR}$ -/- mice showed a relatively mild phenotype, with no major deficits in the main organ systems. It is possible that $p75^{NTR}$ is not essential during embryonic development, and that its role could be compensated by other molecules. A shorter isoform of $p75^{NTR}$ was later identified, which was not targeted in the first $p75^{NTR}$-null animals. The removal of this isoform, in addition to the full-length receptor, resulted in a stronger phenotype. About 40% of the knock-out mice die at late stages of development or at birth, and the surviving animals show impaired motility and ataxia. The perinatal lethality is caused by dilation and rupture of blood vessels, thus implicating $p75^{NTR}$ in the development of the vascular system (von Schack et al., 2001).

Figure 1-20: *specific subpopulations of sensory neurons depend on different neurotrophins during development*

Development of proprioceptive neurons (a) relies on NT-3/TrkC signalling; small nociceptive neurons (b) depend on NGF; BDNF modulates the survival of mechano-receptors (c); deep-hair cell afferents (d) require NT-4/5. Adapted from Bibel and Barde, 2000.

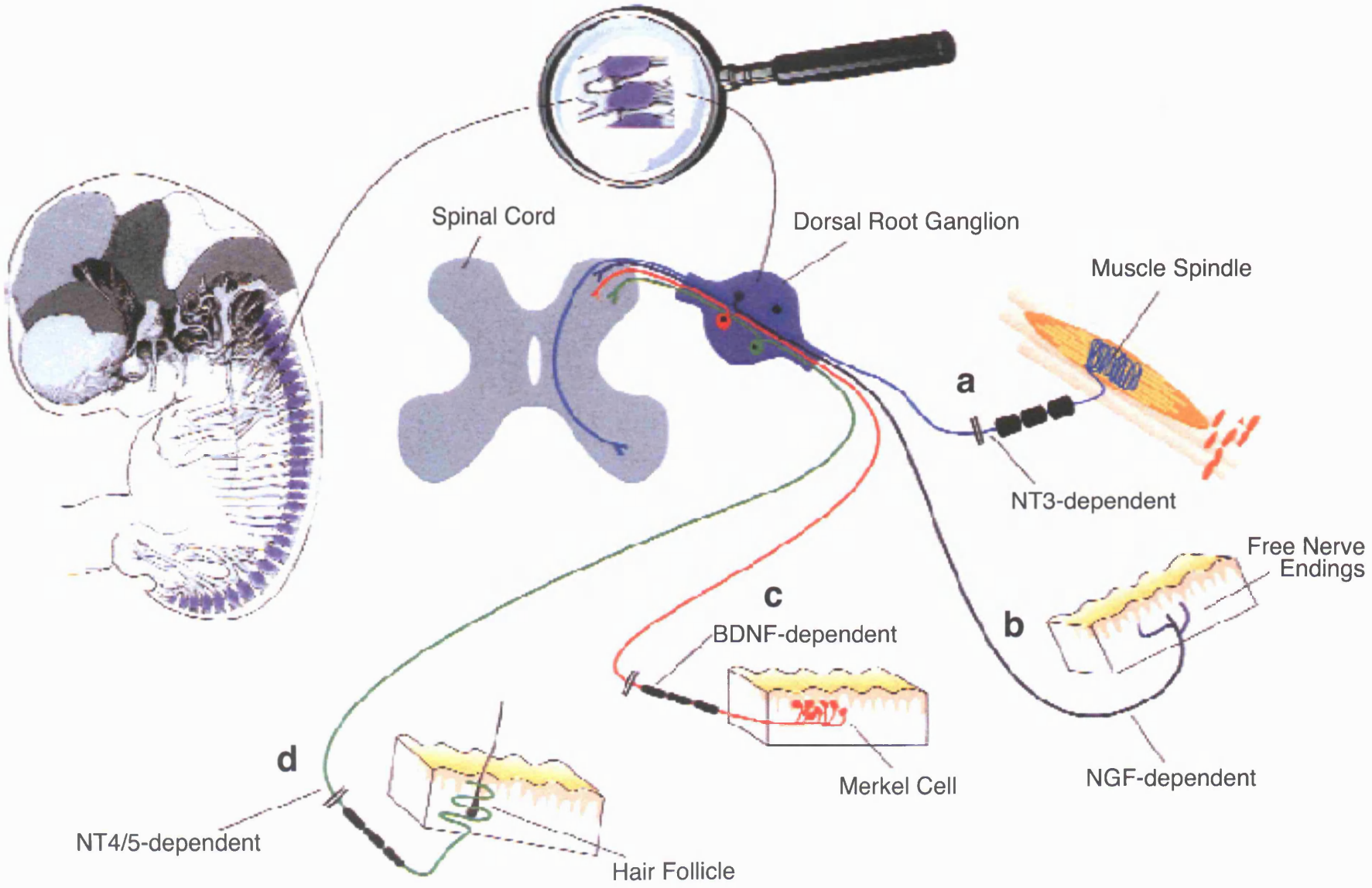
Spinal Cord
Dorsal Root Ganglion
Muscle Spindle
a
NT3-dependent
Free Nerve
Endings
b
c
BDNF-dependent
Merkel Cell
NGF-dependent
d
NT4/5-dependent
Hair Follicle

1.5 Molecular mechanisms of Eph / ephrin signalling

1.5.1 Eph receptors and ephrins

The Eph receptors, named after the *e*rythropoietin-*p*roducing *h*epatocellular carcinoma cell line from which the first receptor was isolated, constitute the largest known family of receptor tyrosine kinases (Hirai et al., 1987). They have the typical structure of transmembrane kinase receptors: an extracellular portion involved in ligand binding, a single transmembrane region and an intracellular kinase domain (Figure 1-21). Eph receptors bind to a group of membrane-bound ligands called ephrins. All ephrin ligands share an extracellular core domain, involved in receptor binding, but differ in the way they are tethered to the membrane: ephrin-As are glycosylphosphatidylinositol (GPI)-anchored proteins, whereas ephrin-Bs have a transmembrane region and a short intracellular sequence (Figure 1-21). Eph receptors are divided in two subgroups, EphA and EphB, on the basis of sequence similarity in their extracellular domain. This classification however also reflects their ligand specificity: EphA receptors preferentially bind ephrin-As, while EphB receptors preferentially bind ephrin-Bs, although a certain degree of crosstalk has been demonstrated between the two groups. At present 16 Eph receptors (EphA1-10 and EphB1-6) and 9 ephrins (ephrin-A1-6 and ephrin-B1-3) have been characterised in vertebrates (Menzel et al., 2001; Pasquale, 2005).

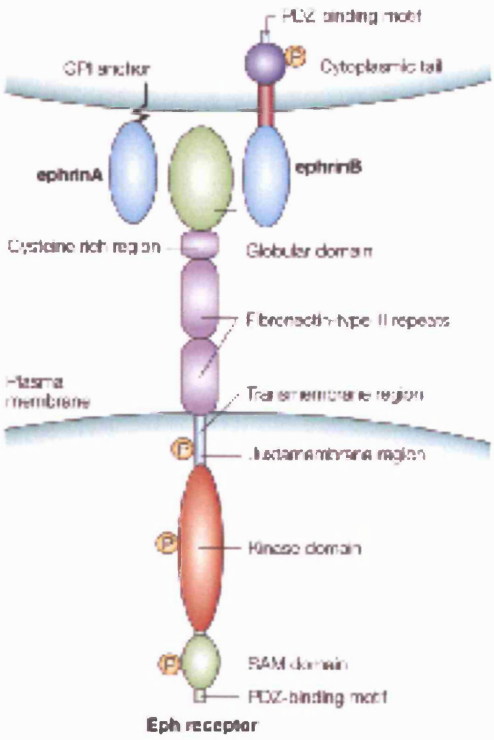

Figure 1-21: *Eph receptors and ephrins*
Schematic representation of the structure of Eph receptors, ephrin A and ephrin B ligands. Eph receptors are transmembrane proteins composed of an extracellular domain responsible for ligand binding, a transmembrane region and an intracellular kinase domain. Ephrin ligands are also membrane proteins, anchored to the lipid bilayer via a GPI tail, in case of ephrin As, or via a transmembrane stretch for ephrin Bs. The principal tyrosine phosphorylation sites in both receptor and ligand intracellular domains are indicated. Adapted from Kullander and Klein, 2002.

1.5.2 Forward and reverse signalling

As Eph and ephrins are membrane-associated proteins, the initiation of the signal requires receptor- and ligand-expressing cells to come into contact with each other. Eph-ephrin complexes then group into larger clusters, which initiate signal transduction into the neighbouring cells (Pasquale, 2005).

Ephrin binding triggers autophosphorylation and activation of the receptors, which subsequently recruit specific adaptors and initiate a number of intracellular signalling cascades. The formation of the Eph-ephrin complex also induces clustering and conformational changes of the ligands. These modifications activate the ephrins, so that they become competent to recruit a distinct complement of interactors and transmit the signal "backwards", i.e. into the ligand-expressing cell. This distinctive feature of the Eph-ephrin system is known as bidirectional signalling, as each component of the complex behaves simultaneously as a receptor and as a ligand (Pasquale, 2005).

Eph-ephrin signalling has been implicated in the regulation of cell migration and adhesion in different tissues, such as the nervous and the vascular systems. In recent years, great effort has been put into studying the molecular basis of the Eph-ephrin system, which is now becoming progressively clear. The following paragraphs will summarise some of the better characterised pathways activated by the Eph receptors ("forward signalling") and by ephrins ("reverse signalling").

1.5.2.1 Forward signalling

One of the better characterised responses to Eph signalling is the modulation of actin dynamics, via the Rho family of small GTPases (Rho, Rac and Cdc42). In

neuronal cells, Eph receptors can induce opposite effects on the actin cytoskeleton, depending on the cellular environment and on the type of stimulus. The guanine nucleotide exchange factor (GEF) Ephexin binds the EphA kinase domain receptors. Upon ephrin-A stimulation, Ephexin triggers Rho activation, which ultimately promotes actin depolimerisation and growth cone collapse (Wahl et al., 2000; Shamah et al., 2001). EphB2 receptors have been shown to activate Cdc42, via the GEF intersectin (Irie and Yamaguchi, 2002), and Rac, through the GEF kalirin (Penzes et al., 2003). In both cases, EphB2 signalling has been suggested to modulate the morphogenesis and maturation of dendritic spines in hippocampal and cortical neurons (Irie and Yamaguchi, 2002; Penzes et al., 2003). Very recently, the Rac-GAP α-chimaerins have been shown to act downstream of EphA4. Upon binding of ephrin-B3, -A1 or -A5, α-chimaerins trigger Rac inactivation, actin depolimerisation and consequently growth cone collapse. Interestingly, chimaerin-null mice phenocopy the ephrin-B3 and EphA4-knock-out mice. Mutants display a very characteristic hopping gait, which is a consequence of midline crossing defects affecting the corticospinal tract, as explained below in more detail (Beg et al., 2007; Iwasato et al., 2007; Wegmeyer et al., 2007).

Activation of the Erk/MAPK pathway plays a crucial role in establishing either a proliferative or differentiative response upon growth factor stimulation, as discussed in the context of neurotrophin signalling (see section 1.2.2). Eph-ephrin signalling has been shown to either up- or downregulate this pathway, presumably depending on the intracellular effectors available in a certain cellular environment. For example, ephrin-A1 stimulation of neuronal precursor cells triggers MAPK activation via Rap1. This effect is mediated by EphA receptors and promotes

neuronal commitment of brain stem cells (Aoki et al., 2004). On the other hand, EphB2 receptors have been shown to inhibit the MAPK pathway, through downregulation of H-Ras activity, ultimately leading to growth cone collapse and neurite retraction in NG108 neuronal cells (Elowe et al., 2001).

Eph-ephrin signalling has also been associated with modulation of integrin-mediated adhesion. Once more, Eph receptors can both activate or inhibit this response, in a cell-specific fashion. For example the focal adhesion kinase (FAK), an important player in integrin signalling, is differentially targeted by Eph receptors in different cell types to accomplish opposite responses. In prostate carcinoma cells, FAK is dephosphorylated downstream of EphA2, which results in negative regulation of integrin-mediated adhesion (Miao et al., 2000). In contrast, the same stimulus enhances FAK phosphorylation and promotes cell adhesion and spreading in NIH3T3 cells (Carter et al., 2002).

1.5.2.2 Reverse signalling

The idea that ephrins could be active signalling molecules, rather than just ligands for Eph receptors, was prompted by the observation that the extracellular portion of EphB receptors is able to trigger phosphorylation of the intracellular domain of ephrin-Bs (Holland et al., 1996; Bruckner et al., 1997). Similarly to what has been described for the receptors, ephrin-mediated signalling can have opposite effects, depending on cell type and experimental context. Ephrin-Bs have been shown to inhibit the attraction of cerebellar granule cells to the stromal cell derived factor-1 (SDF-1), via the GTPase activating protein PDZ-RGS3. This pathway could play an important role during development, as it might allow granule cells to

correctly migrate towards the different cerebellar layers (Lu et al., 2001). Several *in vivo* studies support the importance of ephrin "reverse" signalling. For example, the removal of the intracellular portion of ephrin-B2 (ephrin-B2ΔC) in mice recapitulates the vascular phenotype of the ephrin-B2 knock out animals, as discussed below (Adams et al., 2001). Despite the lack of a cytoplasmic domain, ephrin-As have also been shown to initiate reverse signalling. Upon EphA binding, ephrin-As recruit the Src family kinase Fyn to lipid rafts, which results in MAPK activation and, ultimately, in increased cell adhesion (Davy et al., 1999).

1.5.2.3 Crosstalk with other receptors

Besides being able to directly activate signalling pathways in both the ligand- and the receptor-expressing cells, Eph and ephrins can also influence the activity of other receptors, thus broadening their range of action. A direct interaction has been described between EphB and NMDA receptors at neuronal synapses, which could play an important role in synaptic development and maturation (Dalva et al., 2000) (see also below). As mentioned in section 1.1.2.6, Kidins220 could provide a functional link between the Eph and Trk families, possibly by modulating EphA4 and neurotrophin pathways at the NMJ (Luo et al., 2005).

1.6 In vivo *function of Eph receptors and ephrins*

The function of Eph receptors was initially characterised in the context of neuronal development, but several studies have now contributed to define the importance of Eph-ephrin signalling in the development of different tissues, such as the heart and the vascular system. It is becoming clear that Eph and ephrins play a

general role in the modulation of cell attraction and repulsion, which represent the basis of developmental processes like the segmentation of body structures, or the generation and maintenance of boundaries between adjacent cells. Ephs and ephrins are often differentially expressed on neighbouring cell populations, so that interactions occur at the interface between different territories, preventing Eph- and ephrin-bearing cells from mixing with each other (Wilkinson, 2001).

Several mouse models have been generated in the past decade, in an attempt to define the biological roles of the different members of the Eph and ephrin families. Similar to the neurotrophin knock out models (described in section 1.4), the functional analysis of the resulting phenotypes has often proved to be more difficult than expected. Two features of the Eph-ephrin system can account for this complicated scenario. Firstly, due to functional redundancy between different Ephs and ephrins, some molecules can compensate for each other, and secondly, each member of the family may mediate completely different functions when acting as a receptor or a ligand. For the purposes of this work, the focus will be on the most relevant *in vivo* studies, which have characterised the role of Eph-ephrin signalling in the development of the nervous and cardiovascular systems, as well as in neural crest cell migration.

1.6.1 Cardiovascular patterning

EphB receptors and ephrin-B ligands have been described as key players during the processes of angiogenesis and heart development. Ephrin-B2 knock out mice, and a percentage of EphB2/EphB3 double knock out mice, die at E11.5 due to cardiovascular defects (Wang et al., 1998; Adams et al., 1999). In addition, EphB4

null-animals phenocopy the vascular problems of the ephrin-B2 knock out, thus supporting a role for EphB4-ephrin-B2 signalling in angiogenesis (Gerety et al., 1999). The two mouse models also display very similar defects in heart morphogenesis, i.e. developmental delay, incomplete looping, and defects in the endocardium organisation (Gerety et al., 1999). The molecular mechanisms underlying the observed phenotypes were only partially explained by the expression pattern of EphB4 and ephrin-B2, which were found to be restricted to veins and arteries, respectively (Adams et al., 1999).

1.6.2 Neural crest cell migration

Neural crest cell migration is a tightly regulated process, in which a combination of repulsive and adhesive signals guides the cells along defined routes from the dorsal neural tube to their final destination. At the cranial level, neural crest cells migrate in several streams to invade the head and branchial arches, to give rise to cranial ganglia as well as the bone and cartilage structures of the head. The knock-out of ephrin-B2 results in the absence or reduction of the second branchial arch, thus suggesting that ephrin signalling could provide some of the attractive or repulsive cues necessary for the migration of this particular cell population (Adams et al., 2001). Along the spine, somites pattern the migration of neural crest cells, which will generate several structures including all peripheral ganglia. Interestingly, EphB2 and EphB3 receptors have been found on migrating cells, whereas the corresponding ligands (ephrin-B1 and -B2) are present on the flanking somites (Wang and Anderson, 1997; Flanagan and Vanderhaeghen, 1998). Surprisingly, no defects in periferal ganglia have been described in EphB2 or EphB3 null mice or the

EphB2/EphB3 double knock-outs, presumably because of functional redundancy with other receptors. However, a fraction of the double knock-out animals die at birth due to cleft palate, which is a developmental defect related to problems in neural crest cell migration (Henkemeyer et al., 1996; Orioli et al., 1996).

1.6.3 Nervous system development

1.6.3.1 Segmental patterning

Hindbrain development relies on the formation and functional specialisation of six metameric structures known as rhombomeres. Many Ephs and ephrins are expressed in a rhombomere-specific pattern, thus raising the possibility that Eph-ephrin signalling could play a role in the creation and/or maintenance of boundaries between these structures (Flanagan and Vanderhaeghen, 1998). Support for this hypothesis comes from experiments conducted in *Xenopus* and zebrafish, where EphA4 receptors were inactivated via a dominant negative approach. In the targeted embryos, abnormal mixing occurred between cells belonging to adjacent rhombomeres, suggesting that the normal functioning of the receptors might be required for the separation of cells from neighbouring segments (Xu et al., 1995).

1.6.3.2 Topographic mapping

The term "topographic mapping" refers to neuro-developmental processes in which the spatial relation between neuronal cell bodies is maintained at the level of their axonal extensions to the target tissue. This is made possible by the presence of gradients of specific molecules, or "topographic labels", several of which belong to the Eph / ephrin family. The best characterised example of topographic mapping are

the retinotectal projections from retinal axons to the *superior colliculus* (*tectum* in the chicken). Several different ephrins are presented in dorso-ventral and rostro-caudal gradients in the *tectum / superior colliculus*, while Eph receptors are expressed in similar dorso-ventral and nasal-temporal gradients by the migrating retinal ganglion cells and their axons (Cheng et al., 1995; Drescher et al., 1995). The interaction with the ephrin-expressing tissue triggers the repulsion of the Eph-bearing axons, which arrest their growth within the targt tissue at levels determined by the relative amount of signalling. The role of ephrins in retinotectal mapping is supported by the analyis of ephrin-A2 and ephrin-A5 knock out mice, which show patterning abnormalities in the connections of the retinal axons and a synergistic phenotype in the double knock-out animals (Feldheim et al., 2000).

Spinal motor neurons are organised in longitudinal columns that run along the spinal cord and make connections with specific muscles. At the brachial and lumbar levels, MNs form the lateral motor column (LMC), which innervates the limb buds and, at later stages, the limb muscles. Inside the LMC, MNs are subdivided in motor pools, which target individual muscles (Landmesser, 1978). The relationship between a given motor pool and its corresponding target muscle, provides another example of topographic mapping. Similar to what has been described for the retinotectal system, Eph receptors are expressed on migrating LMC axons, whereas their ligands are found in the targeted limb buds (Flenniken et al., 1996; Gale et al., 1996; Ohta et al., 1997). Furthermore, EphA4 was shown to modulate MN pathfinding towards the hindlimbs, in chicken embryos (Eberhart et al., 2002). In accordance with these observations, EphA4 null mice display muscular atrophy due to the absence of the peroneal nerve, the main dorsal nerve of the

hindlimbs. In these mice, dorsal motor axons do not defasciculate properly and join the ventral nerve, thus leaving the dorsal limb muscles denervated. In addition, a 40% loss of lumbar motor neurons was reported in the same mutant model (Helmbacher et al., 2000).

1.6.3.3 Axon guidance across the midline

Eph-ephrin signalling has been implicated in the modulation of axon guidance in several neuronal circuits. The analysis of the EphB2 and EphB3 knock out mice provided some of the first evidence for an *in vivo* role of Eph receptors in axon pathfinding. The most obvious phenotype of these animals was the lack of a portion of the anterior commissure, which connects the two hemispheres of the cerebral cortex, due to defective migration of commissural neurons (Henkemeyer et al., 1996; Orioli et al., 1996).

More recently, Eph and ephrins have been implicated in the formation of the corticospinal tract. Neurons forming the corticospinal tract are born in either the right or left lobe of the cortex. Their processes cross the midline at the junction between brain and spinal cord, and extend down the spine along the controlateral side, where they make contact with specific MN pools and thereby establish neuronal circuits required for the central control of body movements. In normal conditions, corticospinal axons project to only one side of the spinal cord, whereas in EphA4 and ephrin-B3 null mice they can re-cross the midline, and establish connections with MNs on both sides of the spine. This results in a very characteristic hopping phenotype, with synchronous movements of the hindlimbs due to the inability of the mice to control the right and the left side of the body independently

(Dottori et al., 1998; Kullander et al., 2001). Subsequent studies have shown that ephrin-B3 is expressed in the spinal cord midline, acting as a repellent for the EphA4-expressing corticospinal axons (Yokoyama et al., 2001).

1.6.3.4 Ephs and ephrins in hippocampal development and functioning

The development of the hippocamposeptal system requires the coordinated action of several attractive and repulsive molecules, which guide hippocampal axons to their appropriate target in the septal region of the cortex. Amongst these molecules, Eph receptors and ephrins are expressed in a complementary pattern on migrating hippocampal neurons and their target cortical regions, respectively (Zhou, 1997). Ablation of EphB2 or both EphB2 and EphB3 in mice results in abnormal bundling of hippocampal axons, which fail to defasciculate close to the target region (Chen et al., 2004).

Besides their role in axon guidance, Ephs and ephrins have been shown to modulate hippocampal physiology. A direct interaction has been demonstrated between EphB2 and NMDA receptors. Upon ephrin-B stimulation, the two receptors cluster at the synapse, thus raising the possibility that signalling downstream of EphB2 might affect synapse formation and plasticity (Dalva et al., 2000). A subsequent study has established that EphB2 triggers Src-mediated phosphorylation of the NMDA receptor, which potentiates the NMDA-dependent influx of calcium at excitatory synapses (Takasu et al., 2002).

Dendritic spines are the postsynaptic targets of excitatory synapses, and changes in their morphology have been associated to synaptic plasticity as well as to the physiological processes associated with learning and memory. EphB2 regulates

the process of dendritic spine formation by binding and phosphorylating the proteoglycan syndecan-2 (Ethell et al., 2001). EphB2 null mice have normal spine morphology, suggesting functional redundancy with other Eph receptors, however they show impaired LTP and LTD (Grunwald et al., 2001). The double and triple EphB1/EphB2/EphB3 knock out have no dendritic spines, and in addition they display a reduction of excitatory synapses and AMPA and NMDA clustering (Henkemeyer et al., 2003).

1.7 Possible roles of Kidins220 in development and adulthood

Both the neurotrophin-Trk and ephrin-Eph systems play crucial roles in nervous system development and homeostasis. Different members of the Trk and Eph receptor families pursue specific tasks in different neuronal populations, at different stages of development and in adulthood (discussed in sections 1.4 and 1.6). As a downstream effector of these pathways (Kong et al., 2001), Kidins220 might be involved in the differentation of specific subpopulations of neurons. Kidins220 interacts with TrkA, TrkB and TrkC (Arevalo et al., 2004), and it is therefore possible that it could act downstream of different receptors in different tissues. The knock-out of Kidins220 could therefore affect the ability of subsets of neurons to respond to neurotrophic stimuli, or could affect axon pathfinding in Eph-ephrin mediated processes such as midline crossing of commissural neurons. This could potentially lead to cell death of specific neuronal populations, or to defects in axon bundling / defasciculation, in the central as well as in the peripheral nervous system.

Furthermore, Kidins220 may also act upstream of these growth factor receptors, influencing their targeting to the correct membrane compartments.

Besides being highly expressed in the nervous system during embryonic development, Kidins220 is also expressed in the adult brain, in particular in the hippocampus and cerebellum (Kong et al., 2001). These regions preside over fundamental processes such as motor coordination, learning and memory, and it is therefore possible that Kidins220 might play a role in the modulation of higher brain functions in adulthood. Interestingly, both neurotrophins and ephrins have been shown to modulate synaptic plasticity in various hippocampal circuits, thus supporting the idea that Kidins220 might act downstream of these pathways also postnatally. As discussed in sections 1.4 and 1.6, the role of neurotrophins and ephrins is not restricted to the nervous system, but their action extends to a range of other organs such as the cardiovascular system. Our analysis of the Kidins220 knock-out animals might therefore reveal unexpected functions of Kidins220 within and outside the nervous system.

1.8 Objectives

Knock-out mice lacking neurotrophins or their receptors have been of paramount importance for the understanding of the events regulated by the different neurotrophic pathways during development. The analysis of these animals has often given surprising results, unveiling unexpected roles for neurotrophins in the development of structures outside the central and peripheral nervous system. From the molecular perspective, neurotrophin signalling relies on the precise modulation of the intracellular trafficking of Trks and $p75^{NTR}$ proteins. Inactive receptors are transported anterogradely from the cell body to the axon terminal, where, upon neurotrophin binding, they become activated (Roux and Barker, 2002). Activated receptors are subsequently endocytosed and, by recruiting specific subsets of adaptor proteins, initiate different intracellular cascades that trigger a fast response at the growth cone, as well as a late response involving transcription activation of survival genes (Heerssen and Segal, 2002). This long-term effect requires the retrograde transport of activated receptors with associated factors on the surface of a "signalling endosome" to the cell body (Ginty and Segal, 2002). Extensive studies have shed light on the events leading to receptor activation, characterising in detail the phosphorylation and subsequent recruitment of specific interactors. Some information starts to be available about the mechanisms and dynamics of the retrograde transport of signalling endosomes, which is mediated by the dynein motor complex (Yano et al., 2001; Bhattacharyya et al., 2002; Heerssen et al., 2004). In contrast, very little is known about the anterograde transport of the neurotrophin receptors, and about the mechanisms that ensure their correct targeting to specific

domains of the plasma membrane. Kidins220 has been implicated in the sustained activation of the MAPK pathway in response to neurotrophin stimuli, by mediating the recruitment of specific adaptors downstream of the Trks and $p75^{NTR}$ receptors (Arevalo et al., 2004; Arevalo et al., 2006). In this thesis, I have characterised the mechanisms directing the intracellular trafficking of Kidins220, thus improving our understanding of the events leading to the activation of neurotrophin-dependent pathways at the plasma membrane.

In the second part of this work, I have analysed the mechanisms regulating kinesin-1 detachment from Kidins220 at the neurite tips. Several studies have identified phosphorylation as a mechanism mediating the detachment/inactivation of molecular motors from their cargoes, once they have reached their final target (Sato-Yoshitake et al., 1992; Addinall et al., 2001; Karcher et al., 2001; Morfini et al., 2002). I was interested in understanding whether phosphorylation is responsible for the detachment of the kinesin-1 complex from Kidins220 at the plasma membrane, thus enabling this protein to play its role in mediating the signalling events downstream of the neurotrophin receptors.

The generation of a Kidins220 knock-out model could add important details to this complex scenario. Analysis of the phenotype of Kidins220 null mice both during development or in adulthood will define the role of this protein in the response to different neurotrophins, thus providing an invaluable tool for dissecting the mechanisms underlying neurotrophin signalling.

The hypotheses at the onset of this study and the objectives of this research can be summarised as following:

Hypothesis – 1: the intracellular trafficking of Kidins220 is mediated by kinesin-1. The correct targeting of Kidins220 is required for the establishment of a correct response to neurotrophic stimuli, downstream of Trk receptors.

Objective – 1: to characterise the intracellular trafficking of Kidins220, using PC12 cells. This will require the mapping of the domains involved in the interaction, the characterisation of the kinetic of Kidins220 transport, and the analysis of the role of Kidins220 trafficking in the contest of neurotrophin signalling.

Hypothesis – 2: phosphorylation modulates the interaction between Kidins220 and kinesin-1.

Objective – 2: to screen a range of kinases, using an *in vitro* kinase assay, with the aim of finding possible candidates that can phosphorylate Kidins220.

Hypothesis – 3: the conditional targeting of the Kidins220 gene can provide useful information about the function of this protein *in vivo*.

Objective – 3: to target Kidins220 expression in *Drosophila*, via RNAi, and in mouse, by homologous recombination. This will be followed by the analysis of the emerging phenotype of the knock-out mice.

Chapter 2 – Materials and Methods

2 Materials and Methods

2.1 Materials

2.1.1 Reagents and Media

Reagents were purchased from the following companies, unless stated otherwise: Amersham Biotech, Sigma, Fluka, BDH, Calbiochem. Molecular biological reagents were purchased from Qiagen, Promega, New England Biolabs and Clontech. Enzymes were obtained from New England Biolabs unless otherwise specified.

Distilled water (dH_2O), Phosphate buffer saline (PBS), Hanks' buffer, 20X SSC buffer, 1 M Sodium-Phosphate buffer pH 6.8, 0.5 M EDTA pH 8.0, Dulbecco's Modified Eagle's Medium lacking phenol red, riboflavin, penicillin/streptomycin and folic acid ($DMEM^-$), E4 medium for cell culture, yeast growth medium (YPD), bacterial growth media (LB, SOC and 2YT), glutamine, penicillin/streptomycin and PCR sequencing mix were all supplied by Cancer Research UK Laboratory Services.

2.1.2 Antibodies

All fluorescently-conjugated secondary antibodies were from Molecular Probes and all HRP-conjugated secondary antibodies were from Amersham Pharmacia or Dako. All the antibodies used in this work are listed in Table 1.

Table 1: *list of antibodies*

Antibodies used in this work (Mo: mouse; Rb: rabbit; Go: goat; M: monoclonal; P: polyclonal). WB: Western Blot; IF: immunofluorescence; IHC: immunohistochemistry on paraffin-embedded sections; WM: whole mount staining of embryos.

Antigen	Antibody name	Species	Supplier	Dilution	
				WB	IF
GST fusion of Kidins220 C-term domain (1209-1762)	1F8	Mo M	Monoclonal antibody facility, Cancer Research UK	1:500	1:100
Kidins220 C-term peptide	Gsc16	Rb P	Biological Resources, Cancer Research UK	1:500	1:300
Phosphorylated Kinesin Interacting Motif on Kidins220	KIM	Rb P	Custom made by Harlan UK Limited	1:100	
Synaptotagmin-I C2A domain	Syt#253	Rb P	Biological Resources, Cancer Research UK		1:100
Synaptotagmin-I	Syt#M48	Mo M	Monoclonal antibody facility, Cancer Research UK		1:100
Kinesin Heavy Chain	H2	Mo M	Chemicon International	1:500	1:100
Kinesin Light Chain	L1	Mo M	Chemicon International	1:500	1:100
Phospho-mitogen-activated protein kinase	P-MAPK	Rb P	#9101S, Cell Signaling Technology		1:100
Sunday Driver/c-Jun NH2-terminal kinase interacting protein-3	SyD/JIP-3	Rb P	Gift from Dr. V. Cavalli (Washington University, St. Louis, MO)(Cavalli et al., 2005)	1:1000	1:100
Kinesin family member 1A (KIF1A)	Kinesin-3	Go P	Santa-Cruz Biotechnology	1:200	1:100
Amyloid Precursor Protein	APP	Rb P	Cell Signaling Technology		1:100
$p75^{NTR}$ extracellular domain	$p75^{NTR}$	Rb P	Custom made by BioGene, UK (Deinhardt et al., 2006)		1:5000

Antigen	Antibody name	Species	Supplier	Dilution	
				WB	IF
GST-TrkA fusion protein	Pan-Trk	Mo M	Invitrogen		1:100
Hemagglutinin epitope	HA	Rat M	Roche		1:100
Glutathione S-transferase	GST	Mo M	Monoclonal antibody facility, Cancer Research UK	1:3000	
Phospho-tyrosine	4G10	Mo M	Upstate (Millipore)	1:500	
				IHC	WM
Human/mouse active caspase-3	Caspase-3	Rb P	#AF835, R&D	1:600	
calbindin	calbindin	Rb P	Chemicon	1:300	
neurofilament	2H3	Mo M	Developmental Studies Hybridoma Bank at the University of Iowa (DSHB)		1:40
Homeobox 9	HB9/ HLXB9	Rb P	AbCam	1:1500	

2.1.3 Plasmids

Plasmids and constructs used in this work are described in Table 2.

Table 2: *list of plasmids*

Plasmids and constructs used in this work

Plasmid	Company	Application
pGBKT7	Clontech	Yeast two-hybrid screening (baits)
pGADT7	Clontech	Yeast two-hybrid screening (preys)
pPCR-Script Amp SK(+)	Stratagene	Cloning of KLC1 deletion mutants
pPCR-Script™	Stratagene	Cloning of EGFP-Kidins220 and HA-Kidins220
pEGFP-C2	BD Biosciences (Clontech)	Cloning of EGFP-Kidins220
pGEX-KG	GE Healthcare	Cloning of KC

Plasmid	Company	Application
pGEX-4T3-HA	(Lalli et al., 1999)	Cloning of KC deletion mutants
pmRFP	(Bracale et al., 2007)	Cloning of KIM and KIM(Y24A)
pE/L	(Frischknecht et al., 1999)	Cloning of KIM and KLC-TPR
pGEX-6P2	GE Healthcare	Cloning of KIM mutants for phosphorylation assays
pGEM-T easy	Promega	Cloning of KLC1
pWIZ	Gift from Dr. H. McNeill (Samuel Lunenfeld Research Institute, Toronto, Canada) (Lee and Carthew, 2003)	RNAi in *Drosophila*
pTURBO	Gift from Dr. H. McNeill (Samuel Lunenfeld Research Institute, Toronto, Canada)	RNAi in *Drosophila*
pBluescript II KS (+)	Gift from Dr. R. Adams (Cancer Research UK, London, UK)	Subcloning of mouse constructs
pBK-CMV	Gift from Dr. R. Adams (Cancer Research UK, London, UK)	Subcloning of mouse constructs
pFlrt+lacZ1.gck	Gift from Dr. R. Adams (Cancer Research UK, London, UK)	Kidins220 mouse conditional knock-out
Full-length EGFP-Kidins220	Described below	Microinjection and transfection
pcDNA3-HA-KLC-HR	Gift from Dr. K.J. Verhey (Harvard Medical School, Boston, MA) (Verhey et al., 1998; Verhey et al., 2001)	GST-pull down experiments with Kidins220-KC
pcDNA3-HA-KLC-TPR	Gift from Dr. K.J. Verhey (Harvard Medical School, Boston, MA) (Verhey et al., 1998; Verhey et al., 2001)	GST-pull down experiments with Kidins220-KC
EGFP-DNKHC	Gift from Dr. K. Mikoshiba (University of Tokyo, Japan) (Bannai et al., 2004)	Transfection of PC12 cells
Full-length SyD/JIP-3	Gift from Dr. V. Cavalli (Washington University, St. Louis, MO)	Yeast two-hybrid controls
Full-length protein phosphatase 5 (Pp5)	Gift from Dr. D. Barford and Dr. J.Yang (The Institute of Cancer Research, London, UK)	Yeast two-hybrid controls
pmCRABP-I	Gift from Dr. R. Adams (Cancer Research UK, London, UK) (Leonard et al., 1995)	Expression of CRABP-I probe for *in situ* hybridisation

Plasmid	Company	Application
pMC-Cre	Gift from Ian Rosewell, Transgenic Services, CRUK	Transfection of ES cells

2.1.4 Oligonucleotides

All oligonucleotides were obtained from Sigma-Genosys Ltd (London, UK). "fw" and "rv" indicate 5' primer and 3' primer, respectively. Oligonucleotides used in this work are described in Table 3 and Table 4.

Table 3: *list of primers – 1*

Primers for the truncated and point mutants used in biochemical and phosphorylation assays

name	Primer sequence (5' to 3')
EGFP-Kidins220	
Afe fw	gaagcgctccagttacacaaggc
Pac Cla Pme rv	gagtttaaacatcgattcgaattaattaaagaatgctctctctctcttctccaaag
Not Age BsrG Sac	acgtgcggccgccaccggtatgtacaagtccgcggggtcagttcttatatcacagag tgtgataaatt
Xcm	gaccagattgcagttggctccattc
HA-Kidins220	
HA5	gtacccctacgacgtgcccgactacgccgc
HA3	gggatgctgcacgggctgatgcggcg
KLC truncated mutants	
KLC1-D fw	acatgggatccaacctggtggaggagaagtcc
KLC1-D rv	tgctcgagtcacacagatccaaactcc
KLC1-E fw	tgatgggatccctgagcgaggcgcagctgatgg
KLC1-F fw	tcatgggatccgaagacaaagactctgattc
KLC1-G fw	taggatccatgcatgcatgacaacatgtcc
KLC1-G rv	ttctcgagtcacacagatccaaactcc
KLC1-H rv	agctcgagttacaccgcagggtgatctcg
KLC1-I rv	acctcgagttagtcgtggccggaagtcttctcc
Kidins220 truncated mutants	
KC fw	taatgaattccgagaaactgagacagatagaag
KC rv	tagcggccgctcagagaatgctctctctctc
B rv	atgcggccgctcaggatttcttgcctgggag
C rv	atgcggccgctcactttagctcaccctccttcc
D rv	atgcggccgctcacgaccctgtgcccccttc
E rv	atgcggccgctcactgggaattgagactcg
F fw	taatgaattcccaggactccagtattg

name	Primer sequence (5' to 3')
G fw	taatgaattccacaataagcggcagatcttctcc
H fw	taatgaattcccaggaggatgggcgg
L fw/EGFP-Kidins220ΔKIM fw	cccaggactccggaggcacagggtcg
L rv/EGFP-Kidins220ΔKIM rv	cgaccctgtgcctccggagtcctggg
KIM point mutants	
KIM(Y20A) fw	ggtgcaggccgaggctagagacgcc
KIM(Y20A) rv	ggcgtctctagcctcggcctgcac c
KIM(Y24A) fw	gccgagtatagagacgccgctagagagtacattgctcag
KIM(Y24A) rv	ctgagcaatgtactctctagcggcgtctctatactcggc
KIM(Y27A) fw	gcctatagagaggccattgctcagatgtcc
KIM(Y27A) rv	ggacatctgagcaatggcctctctataggc
KIM(E19A) fw	ggtgcaggccgcgtatagagacgcc
KIM(E19A) rv	ggcgtctctatacgcggcctgcacc
KIM(E26A) fw	gacgcctatagagcgtacattgctcagatgtcc
KIM(E26A) rv	ggacatctgagcaatgtacgctctataggcgtc
KIM(Y20F) fw	ggtgcaggccgagtttagagacgcctatag
KIM(Y20F) rv	ctataggcgtctctaaactcggcctgcacc
KIM(Y20P) fw	gataaggtgcaggccgagcctagggacgcctatagagagtac
KIM(Y20P) rv	gtactctctataggcgtccctaggctcggcctgcaccttatc
KIM(Q17A) fw	caaagcttactgataaggtggcggccgagtatagagacg
KIM(Q17A) rv	cgtctctatactcggccgccaccttatcagtaagctttg
KIM(Y24A, E26A, Y27A) fw	gccgagtatagagacgccgctagagcggccattgctcagatgtcc
KIM(Y24A, E26A, Y27A) rv	ggacatctgagcaatggccgctctagcggcgtctctatactcggc
Yeast two-hybrid pairwise testing	
SyD/JIP-3 fw	atgaattcgagatccagatggacgagggagg
SyD/JIP-3 rv	aagcggccgcctcaggggtgtaggacacctgc
KLC fw	tagaattccatgacaacatgtccacaatgg
KLCDN fw	atgaattcctgagcgaggcgcaggtgatgatgg
KLCTPR fw	atgaattcgaagacaaagactctgattc
KLC/KLCDN/KLC TPR rv	atctcgagtttaaccagcccgagcttcatc
Pp5TPR fw	atgaattccccccggctgatggagctctgaagc
Pp5 TPR rv	atctcgagcacggagcgcttgtgctcg
Cloning of KIM in pGEX-6P2	
KIDpGEX6P2 fw	taggatccattgaaatttcaaagcttactg
KIDpGEX6P2 rv	atgcggccgcttattctaactgggacatctgagc

Table 4: *list of primers – 2*

Primers for the constructs for Kidins220 RNAi in *Drosophila*, and Kidins220 conditional knock-out in mouse

name	Primer sequence (5' to 3')
Drosophila RNAi	
Fw1	acgttctagacgcggaaacgttgagattgtgg
Rv1splice	aactcacctagagcacaatctccaagttgcgg
Fw2	acgttctagacctgcctgcacatcgcaatgcg
Rv2splice	aactcacctagagcagataggcgagcagc
Sequencing PAC clones	
ex9 fw	tgtcatacgcagaaggttgc
ex9 rv	ccacacagccaatgcattaggg
ex10 fw	gaagattgatatttcccacc
ex10 rv	tggcagaatgtttcctgacc
ex11 fw	aaatcactggttgggaaagc
ex11 rv	tcactcagaaattaaaggcc
ex12 fw	attgtctgctttgtagaggc
ex12 rv	acacacgtatacatgaaagc
ex13 fw	tcaagataaggtttcccacc
ex13 rv	aagacagctactcacagagc
ex14 fw	gtgcccagcacaagtttatg
ex14 rv	ctagagtgactgaagacagc
ex15 fw	gctctcctttacttgctacg
ex15 rv	aactaagagactaaggtagc
ex16-17 fw	catgtgtatgctagaaacgc
ex16-17 rv	ttaacatttcgagagcatgc
ex18 fw	tggatggatttctcttgtgc
ex18 rv	gatagtttgtgaagtcatgc
ex19 fw	atagcaccaaaggatagtac
ex19 rv	ttatccctttggagcatagc
ex20 fw	caagcagcagcctcaagtgg
ex20 rv	tcaaccccaacactctaagg
ex21 fw	tctgttttgttggtcttacc
ex21 rv	tagcacaacattcacagagc
ex22 fw	ctgtagtataaacaagtggc
ex22 rv	gaaggagagactgtgtgcgc
Kidins220 construct in pFlrt vector	
short fw	actgctcgaggtgggaatatgctgctgtcc
short rv	tacgctcgaggatagtttgtgaagtcatgc
splice fw	catactcgaggtttaaacggtggttcacagccatctg
splice rv	acatgtcgacggccggcctcttcagtcttaaatactcg
flox fw	attactcgaggtttaaacggtggttcacagccatctg
flox rv	gatgtcgacggcgcgccactagttcttcagtcttaaatactcg
long fw	actggcggccgcatacctatattataaaagac

name	Primer sequence (5' to 3')
long rv	ttacgtcgacatgtgggtgctgggaatcc
Site directed mutagenesis on the NruI site	
sdm fw	ggctgaaatgatcgcgaccctctcagatgc
sdm rv	gcatctgagagggtcgcgatcatttcagcc
Primers for ES screening and mouse genotyping	
pflrt-s-neo fw	gttgttagtgaagtaggtctc
short-as rv	gagagattcactagagaaagc
long-s fw	gagcacagacttctcttatgg
flox-as rv	gcgtttctagcatacacatg
splice-as	cagatggctgtgaaccaccgtttaaac
PGK-Cre fw	gcctgcattaccggtcgatgcaacga
PGK-Cre rv	gtggcagatggcgcggcaacaccatt
Primer for southern blot	
Southern short rv	ttctttcatccctttgtagc
Primers for RT-PCR	
5' KNAP 136787	atgtcagttcttatatcacagagt
3' GAP1 142201	gtgaaagcaaacactaggccgagc
5' GAP2 142199	ctcatagtgttcctcaccctgc
3' GAP2 142202	agaattcaggagagagtccagcac

2.1.5 Radioactive isotopes

Redivue $\alpha[^{32}P]$-dCTP, $\gamma[^{32}P]$-dATP and $[^{35}S]$-Methionine were from GE Healthcare. All radioactive experiments were conducted in authorised areas, and radioactive waste was disposed of following Cancer Research UK safety regulations.

2.1.6 Mouse PAC library, IMAGE and PAC clones

The mouse PAC (RPCI21) library, the IMAGE clones 30096863, 30543572, 2192152 (5418-A17), 5363668 (11925-D05), 5363780 (11925-H21), and the mouse PAC (RPCI21) clones 515-K9 and 542-I24 were obtained from MRC Geneservice (Cambridge, UK)

2.1.7 Peptides and peptide arrays

Peptides and peptide arrays were provided by the Peptide Synthesis Laboratory at Cancer Research UK.

2.1.8 Bacterial strains

The following strains were used for amplifying DNA plasmids: *E. coli* BL21, *E. coli* XL10, *E. coli* XL1Blue. *E. coli* TG1 strain was used for protein expression.

2.1.9 Yeast strains

The AH109 yeast reporter strain (Clontech) was used for the yeast two-hybrid screen and for all the control experiments.

2.1.10 Eukaryotic Cell lines

PC12 cells (ATCC number: CRL-1721), rat pheocromocytoma cells, adherent. Primary rat motor neurons and dorsal root ganglia neurons were kindly provided by Dr. S. Salinas, Cancer Research UK, London. Primary rat cerebellar neurons were kindly provided by Dr. M. Rigoni, University of Padova, Italy.

2.1.11 Animals

All the mice used in this study are on the C57BL/6 background, and they were provided by the Transgenic Services Unit at Cancer Research UK. The embryonic stem cells used to generate chimeras are derived from 129 animals.

2.2 Methods

All the experiments performed on mouse primary neurons and embryos were under licence from the UK Home Office (Animals Scientific Procedures Act 1986), approved by the Cancer Research UK Ethical Committee.

2.2.1 Bacterial cultures

Antibiotics were added to cooled media, final concentrations were the following: Ampicillin (100 μg/ml), Kanamycin (25 μg/ml).

2.2.1.1 Preparation of electrocompetent bacteria

Bacteria were streaked from a frozen stock (25% glycerol, stored at -80°C) onto an agar plate and incubated at 37°C overnight. A single colony from the agar plate was inoculated into 5 ml Luria-Bertani (LB) medium. After overnight incubation at 37°C and 250 rpm, 800 ml of LB medium was added. Cultures were grown at 37°C and 200 rpm to an A_{600} of 0.6, incubated on ice for 30 min and pelleted by centrifugation at 4000 *g* for 20 min at 4°C using a JA10 rotor (Beckman). The bacterial pellet was washed twice with 400 ml ice-cold water to reduce the ionic strength, and resuspended in 40 ml ice-cold 10% glycerol. Electroporation competency was measured by transforming 50 μl of bacteria with 1 μg supercoiled plasmid DNA and counting the resulting colonies. Only preparations that gave more than 10^8 colonies/μg plasmid in test transformations were used. Electrocompetent bacteria were aliquoted, snap-frozen in liquid nitrogen and stored at -80°C.

2.2.1.2 Bacterial transformation

50 µl of the appropriate electrocompetent bacteria were thawed on ice, mixed with 50 to 500 pg of plasmid DNA and incubated for 1 min. Mixtures were transferred into cold 2 mm electroporation cuvettes (Equibio), and transformations were performed at 200 Ω, 25 µF and 2.5 kV in a BioRad *E. coli* pulser. Immediately after electroporation, 1 ml of SOC medium without antibiotics was added. Cell suspensions were placed into polypropylene tubes, shaken at 250 rpm for 30 min at 37°C and then plated onto pre-warmed LB-agar plates containing the appropriate antibiotic. Picked colonies were grown in 2 ml LB medium with the appropriate antibiotic overnight and subsequently analysed. Colonies containing the correct DNA were stored at -80°C in 25% glycerol.

2.2.2 DNA techniques

2.2.2.1 DNA and RNA agarose gel electrophoresis

Agarose gels were prepared by dissolving 0.8 to 2% agarose in TBE buffer (90 mM Tris-OH, 90 mM boric acid, 2 mM EDTA pH 8.0). Ethidium bromide was added to a final concentration of 0.5 µg/ml. DNA or RNA samples were mixed with 10X loading buffer (10% Ficoll 400, 25% glycerol, 10 mM Tris-HCl pH 7.6, 1 mM EDTA pH 8.0 with either 0.25% Bromophenol Blue, 0.25% Xylene cyanol, or 0.10% Orange-G) and electrophoresed at 80 to 150 V/cm in TBE buffer.

2.2.2.2 Gel purification of DNA fragments

Gel slices containing DNA fragments were isolated and purified using the QIAquick gel extraction kit (QIAGEN®) following the manufacturer's instructions.

2.2.2.3 *Isolation of plasmid DNA*

Isolation of small amount of plasmid DNA (miniprep) or high amount of plasmid DNA (maxiprep) were performed using the QIAprep® Spin Mini Prep Kit, or the QIAfilter™ Plasmid Maxi Kit (QIAGEN®), respectively, following the manufacturer's instructions.

Isolation of plasmid DNA from P1 Artificial Chromosome (PAC) clones was performed alkaline lysis. Single bacterial colonies were grown overnight at 37°C, with shaking, in 4 ml of LB medium supplemented with the appropriate antibiotic. Bacteria were centrifuged at 4000 *g* for 10 min at RT, and pellets were resuspended in 0.3 ml of ice-cold P1 solution (15 mM Tris-OH pH 8, 10 mM EDTA, 100 μg/ml Rnase A, filter sterilised). 0.3 ml of P2 solution (0.2 N NaOH, 1% SDS, filter sterilised) were added, the solution mixed and incubated at RT for 5 min. 0.3 ml of ice-cold P3 solution (3 M potassium-Acetate pH 5.5, autoclaved) were slowly added, gently shaking the tubes during the addition, and samples were incubated for 5 min at RT, to allow the formation of a precipitate of protein and *E. coli* DNA. Samples were centrifuged at 10,000 *g* for 30 min at 4°C. Supernatants were transferred to fresh tubes containing 0.8 ml ice-cold isopropanol, mixed, incubated on ice for 5 min, and centrifuged at maximum speed for 15 min at 4°C. Supernatants were discarded, 0.5 ml of 70% ethanol were added to each DNA pellet, and samples were centrifuged at maximum speed for 5 min at 4°C. Supernatants were discarded, pellets air dried and resuspended in 40 μl TE.

2.2.2.4 *DNA precipitation*

DNA was precipitated by addition of 1/10 volume of 3 M Sodium-Acetate pH 5.2 and 2.5 volumes 100% ethanol, incubation for at least 1 h at -80°C, and centrifugation for 30 min at maximum speed at 4°C. The pellet was then washed with 70% ethanol, centrifuged again, let air-dry and resuspended in an appropriate volume of dH_2O.

2.2.2.5 *Measure of nucleic acid concentration*

Nucleic acids were resuspended in water and OD_{260} and OD_{280} were measured in a Nanodrop® spectrophotometer (Labtech International). An OD_{260} of 1 corresponds to 50 mg/ml double stranded DNA. The level of impurity was measured at 280 nm, where proteins have their maximum absorption. With this value the quotient of OD_{260}/OD_{280} was determined. Ratio values below 1.8 were taken as impure and discarded.

2.2.2.6 *Restriction digestion*

0.5-3 µg DNA were incubated in the appropriate buffer with 1 U/µg restriction endonuclease at 37°C for 1 h or overnight. If compatible DNA ends were generated after digestion, vectors were dephosphorylated using 0.5 U/µg alkaline phosphatase for 30 min at 37°C, to prevent re-circularisation.

2.2.2.7 *Ligation*

Vector and insert were gel purified (see section 2.2.2.2) and ligations were performed using 200-300 ng of total DNA and 400 U T4 DNA ligase in a total volume of 10 µl, for 1 h at RT or overnight at 16°C. The molar ratio of vector to

insert was usually between 1:2 and 1:10. After ligation, 2 µl of the reaction were transformed into *E. coli* by electroporation as described (section 2.2.1.2).

2.2.2.8 Polymerase chain reaction (PCR)

Using PCR it is possible to amplify DNA molecules specifically, yielding a 10^6-10^9 fold increase in the target sequence. The steps in PCR amplification consist of (1) denaturation of double-stranded target DNA into two single strands by heat, (2) annealing of specific primers to the target DNA by cooling down and (3) extension by the action of the thermostable *Taq* DNA polymerase (Saiki et al., 1988). The components of a conventional PCR reaction mix are listed in Table 5; a typical PCR program is described in Table 6.

Table 5: *components of a conventional PCR reaction mix*

Reagent	Volume (µl)		Company
	Pfu	Taq	
10X Pfu buffer or 10X Taq buffer – $MgCl_2$	5	5	Stratagene Invitrogen
50 mM $MgCl_2$	---	1.5	Invitrogen
10 mM dNTPs	1	1	Promega
100 µM Primer fw	0.3	0.5	Sigma-genosys
100 µM Primer rv	0.3	0.5	Sigma-genosys
Pfu/Taq	0.5	1	Stratagene/Invitrogen
DNA	100-150 ng		
dH_2O	to 50 µl		

Taq DNA polymerase was from Invitrogene, Pfu turbo DNA polymerase was from Stratagene.

Table 6: *scheme of a conventional PCR cycle*

1	denaturation	94°C	2 min
2	denaturation	94°C	1 min
3	annealing	2-5°C less than the lower Tm	1 min
4	extension	72°C (Pfu) 68°C (Taq)	1 min/kb DNA
5	Go to step (2) 34 times		
6	Final extension	72/68°C	5 min
7	cooling	12°C	∞
8	end		

Specific PCR reactions and cycles, required for the engineering of the construct for the conditional knock-out of Kidins220 in mouse, are described in section 6.4.1. PCR reactions were performed on a MJ Research PTC-200 Peltier Thermal Cycler (GMI, Inc.)

2.2.2.9 DNA sequencing

For DNA sequencing, ~250 ng of DNA, 3.2 pmol of specific primer and 8 µl of BigDye® Terminator Cycle Sequencing Kit (Applied Biosystems) were brought to a volume of 20 µl with H_2O. The polymerase chain reaction was done under the conditions described in Table 7. PCR products were purified using the DyeEx™ 2.0 Spin Kit (QIAGEN) following manufacturer's instructions, and dried in a speed vac DNA concentrator. The sequencing was performed by the Cancer Research UK sequencing facility. Sequence alignment was performed using DNA strider (version 1.4f2) or 4Peaks (version 1.5).

Table 7: *PCR cycle for sequencing*

1	denaturation	96°C	2 min
2	denaturation	96°C	30 sec
3	annealing	47°C	15 sec
4	extension	60°C	4 min
5	Go to step (2) 24 times		
6	cooling	12°C	∞
7	end		

2.2.2.10 DNA preparation for microinjection in Drosophila embryos

A solution containing 4.5 µg of the RNAi vector (pWIZ) and 1.5 µg of the helper vector (pTURBO) was prepared. The DNA was precipitated with Sodium-Acetate/ethanol, washed twice with 70% ethanol and resuspended in 18 µl of nuclease free water. The solution was centrifuged at maximum speed for 1 min, 4.5 µl were removed and added to 0.5 µl PBS, mixed and centrifuged at maximum speed for 1 min. The supernatant was transferred to a new tube and used for microinjection.

2.2.2.11 DNA preparation for ES cells electroporation

~400 µg of the final construct were linearised overnight, with the NotI enzyme. The DNA was then precipitated with Sodium-Acetate/ethanol, washed twice with 70% ethanol and resuspended in 180 µl of nuclease free water. 1 µl of the solution was run on a TBE agarose gel to check the efficiency of the digestion. DNA concentration was measured and volume was adjusted to a final concentration of 1 mg/ml with nuclease free water.

2.2.2.12 Southern Blotting

2.2.2.12.1 Digestion and transfer.

20 µg of DNA were digested overnight with 40 U of the appropriate enzyme, in a final volume of 100 µl. A small aliquot was run in a 0.8% TBE agarose gel to check the efficiency of the digestion, and then the remaining sample was electrophoresed in a 0.8% TBE gel. The DNA was then depurinated in-gel in 0.25 M HCl for 20 min under shaking, washed shortly with 0.5 M NaOH/1.5 M NaCl, and denaturated with 0.5 M NaOH/1.5 M NaCl for 30 min under shaking. The DNA was blotted overnight on a Hybond N+ Nylon membrane (GE Healtcare) in a standard blotting apparatus. After the transfer, the membrane was incubated in 50 mM Sodium-Phosphate buffer pH 6.8 for 10 min on the bench and for 10 additional min under shaking, placed on a Whatman 3 mm paper and baked for 2 hrs at 80°C.

2.2.2.12.2 Hybridisation

The nylon membrane was pre-hybridised with Church's buffer (0.5 M Sodium-Phosphate pH 6.8, 7% SDS, 1 mM EDTA pH 8.0) at 65°C for 1 h. The buffer was discarded and replaced with Church's buffer containing a denatured radioactive DNA-probe in a concentration of $1.5x10^6$ cpm/ml (for details about the preparation of the probe, see section "Probe preparation and labelling"). The membrane was hybridised overnight at 65°C.

2.2.2.12.3 Post-hybridisation washes

After discarding the hybridisation mix, the membrane was rinsed with pre-warmed wash buffer (20 mM Sodium-Phosphate pH 6.8, 1% SDS), and then washed

twice (for 15 min and for 30 min) in pre-warmed wash buffer at 65°C. The membrane was then wrapped into plastic foil, exposed to an auto-radiography film (MR Film, Kodak® BioMax) and incubated at -80°C for 2 to 7 days.

2.2.2.12.4 Probe preparation and labelling

50 ng of template DNA were labelled with $\alpha[^{32}P]$-dCTP using the Prime-It® II Random Primer Labeling Kit (Stratagene), and subsequently purified with NICK™ columns (GE Healthcare) following manufacturer's instructions. 2 µl of the purified mix were transferred in a scintillation vial and the amount of incorporated radioactivity was quantified. The appropriate amount of radioactive probe was then denatured by adding 1/5 volume of 2 M NaOH, and incubating at RT for 5 min.

2.2.2.13 Hybridisation of mouse PAC library (RPCI21)

A mouse PAC (RPCI21) library was hybridised following the procedure for Southern blotting described above. For probe preparation, 300 ng of template DNA were labelled and purified.

2.2.2.14 DNA extraction

2.2.2.14.1 From yeast

Yeast transformant colonies were inoculated in 5 ml of the appropriate medium, and grown overnight at 30°C. Cultures were centrifuged at 1000 *g* for 5 min at RT, and resuspended in 0.2 ml of yeast lysis solution (10 mM Tris-HCl pH 8.0, 2% Triton X-100, 1% SDS, 100 mM NaCl, 1 mM EDTA). Cells were lysed by addition of 0.2 ml of phenol/chloroform/isoamyl alcohol (25:24:1), 0.3 g of acid

washed glass beads, and vortexing for 2 min. The mixture was centrifuged at 13000 *g* for 5 min at RT. The supernatant was transferred to a clean tube; DNA was precipitated by Sodium-Acetate/ethanol and resuspended in 20 µl dH_2O.

2.2.2.14.2 From ES cells

Cells were washed twice in PBS, and lysed overnight at 60°C in Lysis buffer (10 mM Tris-HCl pH 7.5, 10 mM EDTA, 10 mM NaCl, 0.2% SDS, 0.1 mg/ml proteinase K), in a humid atmosphere. After lysis, an equal volume of isopropanol was added, and the mixture was incubated at RT for 45 min to allow DNA precipitation. DNA was then pelleted by centrifugation at 1200 *g* for 15 min at RT, washed 3 times in 70% ethanol, let dry and resuspended in dH_2O.

2.2.2.14.3 From tissues

Tails or ear snips were incubated in 200 or 150 µl of DirectPCR (Tail) (*V*iagen) with 0.1 mg/ml proteinase K, overnight at 55°C, under shaking. Tubes were centrifuged for 1 min at 13000 *g*, and 2 µl were used for PCR.

2.2.3 RNA techniques

2.2.4 RNA extraction

Embryonic tissues or cells were resuspended in TRIzol® (Invitrogen) and incubated at RT for 5 min. After the incubation, chloroform was added and the solution was mixed and incubated for 10 min at RT. The mixture was centrifuged for 15 min at 4°C at 11000 rpm in a tabletop centrifuge, and the supernatant was transferred to a clean tube. RNA was precipitated by adding isopropanol and

incubating for 10 min at RT, and pelleted by centrifugation at 11000 rpm, for 10 min at 4°C. The pellet was washed in 75% ethanol in DEPC-treated H_2O (see below), dried and resuspended in DEPC H_2O. 6 ml of TRIzol® were used to extract RNA from a E15 mouse embryo, 1 ml of TRIzol® was used to extract RNA from cells on a 60 mm dish. For every ml of TRIzol®, the following volumes were used in the subsequent steps: 0.3 ml chloroform, 0.75 ml isopropanol, 1.5 ml 75% ethanol, 100 µl of DEPC H_2O. 2 µl of RNA were loaded in a 2% agarose gel, to check for degradation. RNA concentration was then measured.

To prepare DEPC water, diethyl pyrocarbonate (DEPC) was added to dH_2O to a final concentration of 0.1%, the solution was incubated at 37°C overnight and subsequently autoclaved.

2.2.5 cDNA synthesis

cDNA was synthesised from total mRNA, by using the SuperScript™ II RNase H⁻ Reverse Transcriptase Kit (Invitrogen), following manufacturer's instructions.

2.2.6 Cloning strategies

All plasmids and vectors used in this study are elencated in Table 2. All the Kidins220 constructs used in Chapter 3 are derived from the rat Kidins220 cDNA (Iglesias et al., 2000). The construct used for Kidins220 targeting by RNAi in *Drosophila* is based on the sequence of *Drosophila* Kidins220 cDNA. The construct used for Kidins220 targeting in mouse is based on the sequence of the mouse Kidins220 genomic and cDNA.

2.2.6.1 Constructs for the Yeast Two-Hybrid

Constructs used in the yeast two-hybrid pairwise testing were amplified using the primers listed in Table 3, and then subcloned into the EcoRI/NotI site of the pGBKT7 vector (baits), or in the EcoRI/XhoI sites of the pGADT7 vector (preys). KC(Y1379A) was derived from the pGBKT7 vector encoding KC, using the QuikChange® XL Site-Directed Mutagenesis Kit (Stratagene) and the same primers used for mRFP-KIM(Y24A) (see Table 3).

2.2.6.2 HA-Kidins220 and EGFP-Kidins220

Both HA-Kidins220 and EGFP-Kidins220 were derived from the plasmid pcDNA3-Kidins220-VSVG-HisA (Iglesias et al., 2000). As first step, the VSVG-His tag was removed. To this purpose, the C-terminal portion of Kidins220 was amplified by PCR, using the primers listed in Table 3, adding the PacI, ClaI and PmeI restriction sites at the C-terminus, as indicated in Figure 2-1 A. The PCR fragment was subcloned in pPCR-Script™, by using the PCR-Script™ Amp Cloning Kit (Stratagene), and verified by direct sequencing. The fragment was then inserted into the AfeI/PmeI sites of pcDNA3-Kidins220-VSVG-HisA. In the resulting construct (*pcDNA3-Kidins220-untagged*, Figure 2-1 B), the VSVG-6xHis tag is replaced by a short sequence, containing new unique restriction sites. The PacI site contains a in frame stop codon (see Figure 2-1 A). In order to insert the HA and EGFP sequences, a short polylinker region was added at the N-terminus of Kidins220. As indicated in Figure 2-1 B, the N-terminal portion of Kidins220 was amplified by PCR, adding the NotI, AgeI, BsrGI and SacII restriction sites, with the primers listed in Table 3. An ATG start codon was added between the AgeI and

BsrGI sites. The PCR fragment was subcloned in pPCR-Script™, by using the PCR-Script™ Amp Cloning Kit (Stratagene), and verified by direct sequencing. The small linker was then inserted in the NotI/XcmI sites of pcDNA-Kidins220-untagged. In the resulting construct (*pcDNA3-Kidins220-untagged-Nins*, Figure 2-1 C), new unique restriction sites, as well as a new start codon, are present at the N-terminus of the Kidins220 sequence. The HA sequence was then inserted in the BsrGI/SacII sites of pcDNA3-Kidins220-untagged-Nins. To this purpose, we used two custom made oligonucleotides encoding the two complementary strands of the HA sequence (see Table 3), designed to overlap with the BsrGI and SacII sites at the 5'- and 3'-end, respectively (Figure 2-2 A). Firstly, 300 pmol of each primer were phosphorylated using 1 µl of T4 polynucleotide kinase (PNK), in a total reaction volume of 50 µl. The reaction was incubated at 37°C for 30 min, and T4 PNK was subsequently inactivated by incubating the mixture at 65°C for 20 min. 30 pmol of each primer were then annealed in 30 µl of annealing buffer (50 mM NaCl, 20 mM Tris-HCl pH 7.5, 20 mM $MgCl_2$). The solution was incubated at 100°C for 5 min in a metal block, the block was then let cool down to RT, and finally incubated at 4°C overnight. The annealed fragment was then inserted in the BsrGI/SacII of pcDNA3-Kidins220-untagged-Nins. In the resulting construct (*pcDNA3-HA-Kidins220*, Figure 2-2 B), the HA sequence is inserted at the N-terminus of Kidins220. To obtain *pcDNA3-EGFP-Kidins220*, the EGFP sequence from pEGFP-C2 was inserted in frame in the AgeI/BsrGI sites of pcDNA3-Kidins220-untagged-Nins (Figure 2-2 C, D).

The plasmid EGFP-Kidins220ΔKIM was derived from the vector encoding pcDNA3-EGFP-Kidins220, using the QuikChange® XL Site-Directed Mutagenesis Kit (Strategene) and the primers listed in Table 3.

Figure 2-1: *cloning of untagged Kidins220 and Kidins220-untagged-Nins*
(A) Removal of the VSVG-His tag. To obtain *pcDNA3-Kidins220-untagged*, the C-terminal portion of *pcDNA3-Kidins220-VSVG-HisA* was first amplified by PCR, adding new restriction sites, as indicated. The PCR fragment was then inserted into the AfeI and PmeI sites (arrows) The PacI site contains an in frame stop codon, highlighted in bold (empty arrowheads in B and C). (B) Addition of a N-terminal polylinker region. To obtain *pcDNA3-Kidins220-untagged-Nins*, the N-terminus of *pcDNA3-Kidins220-untagged* was first amplified by PCR, adding new restriction sites, as indicated. The PCR fragment was then inserted into the NotI and XcmI sites (arrows). A new start codon is present, between the AgeI and BsrGI sites (arrowhead in C). (C) Scheme of *pcDNA3-Kidins220-untagged-Nins.*

Figure 2-2: *HA-Kidins220 and EGFP-Kidins220*
(A) Addition of the HA tag. To obtain *pcDNA3-HA-Kidins220*, the HA sequence was inserted into the BsrGI and SacII sites (arrows) of *pcDNA3-Kidins220-untagged-Nins*, following the procedure described in the text. (B) Scheme of *pcDNA3-HA-Kidins220.* (C) Insertion of the EGFP sequence. To obtain *pcDNA3-EGFP-Kidins220*, a fragment encoding EGFP was inserted into the AgeI and BsrGI sites (arrows) of *pcDNA3-Kidins220-untagged-Nins*, as described in the text. (D) Scheme of *pcDNA3-EGFP-Kidins220.*

A

pcDNA3-Kidins220-VSVG-HisA

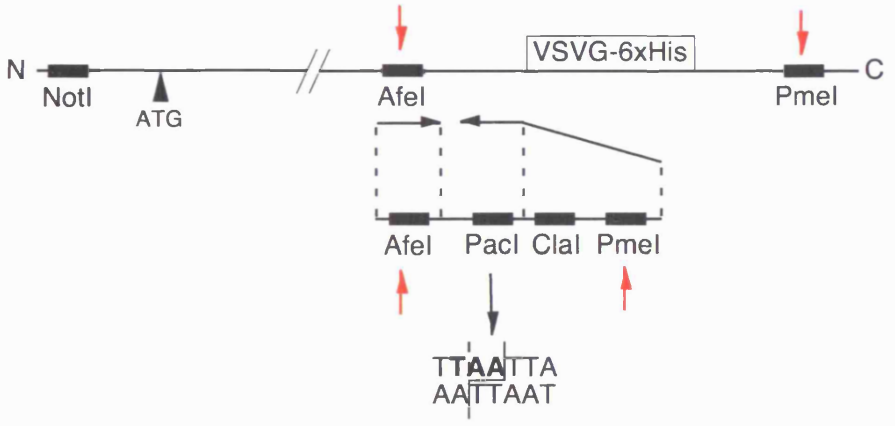

B

pcDNA3-Kidins220-untagged

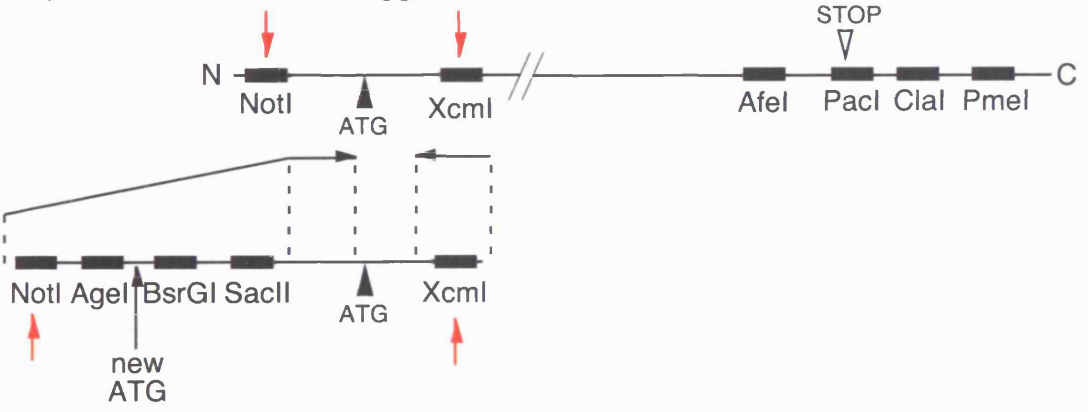

C

pcDNA3-Kidins220-untagged-Nins

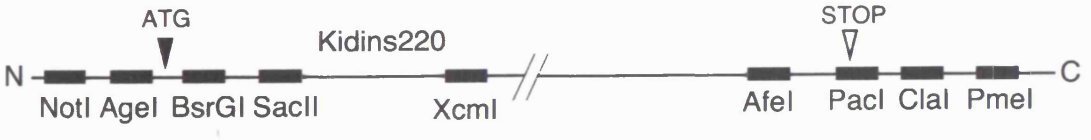

A

pcDNA3-Kidins220-untagged-Nins

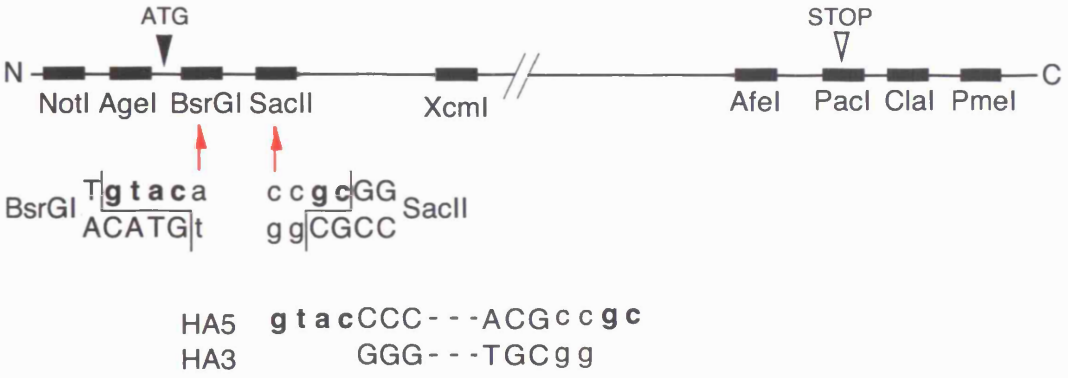

B

pcDNA3-HA-Kidins220

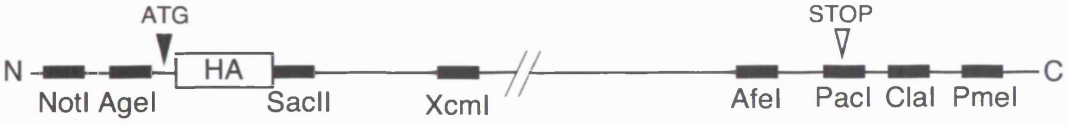

C

pcDNA3-Kidins220-untagged-Nins

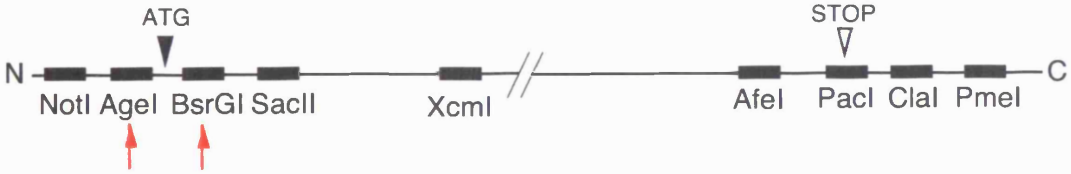

D

pcDNA3-EGFP-Kidins220

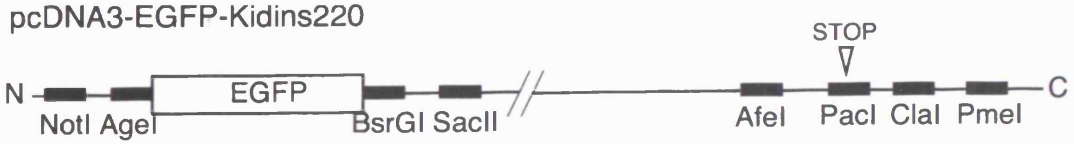

2.2.6.3 Constructs for the KLC1 mutants

KLC1 deletion mutants were amplified using the primers listed in Table 3, and then subcloned into the pPCR-Script™ Amp SK(+) cloning vector using the PCR-Script™ Amp Cloning Kit (Stratagene), according to the manufacturer's instructions.

2.2.6.4 Constructs for the Kidins220 mutants

The C-terminal region (1209-1762) of Kidins220 (KC) was amplified by PCR using rat Kidins220 cDNA (Iglesias et al., 2000) as template, and inserted in frame in the pGEX-KG vector. KC deletion mutants were amplified using the primers listed in Table 3, and then sub-cloned into the EcoRI/NotI sites of pGEX-4T3-HA.

2.2.6.5 RFP-constructs

Monomeric red fluorescent protein (mRFP)-KIM was prepared using a vector derived from pEGFP-C2, where the sequence encoding EGFP had been substituted with the one of mRFP (Campbell et al., 2002). pmRFP-KIM(Y24A) was derived from the vector encoding mRFP-KIM, using the QuikChange® XL Site-Directed Mutagenesis Kit (Stratagene) and the primers listed in Table 3.

2.2.6.6 Constructs for point mutations

The mutants KIM(Y20A), KIM(Y24A), KIM(Y27A), KIM(E19A), KIM(E26A), KIM(Y20F), KIM(Y20P), KIM(Q17A), KIM(Y24A, E26A, E27A)

were derived from KC-K (see Figure 3-11) using the QuikChange® XL Site-Directed Mutagenesis Kit (Stratagene) and the primers listed in Table 3.

2.2.6.7 Cloning in the pGEX-6P2 vector

The sequences encoding for KIM, KIM(Y20A), KIM(Y24A) and KIM(Y27A) were amplified by PCR from the corresponding constructs in pGEX-4T3-HA, using the primers listed in Table 3, adding the EcoRI site and the EcoRV site at the 5'- and 3'-end, respectively. The resulting fragments were inserted in frame in the EcoRI/EcoRV sites of pGEX-6P2, and verified by direct sequencing.

2.2.6.8 Cloning in the pE/L vector

The plasmid pE/L-KIM was obtained by inserting the coding sequence of KIM into the EcoRV/NotI sites of the vector bearing the pE/L virus promoter.

2.2.6.9 Cloning in the pWIZ vector

The selected region was amplified from genomic DNA using the primers listed in Table 3, adding the XbaI restriction site both at the 5'- and 3'-end. The PCR product was ligated first in the AvrII site, which is compatible with the XbaI site, at the 5' splice site in the pWIZ vector. After the insertion, both the AvrII and XbaI sites are destroyed. Colonies were screened by BamHI digestion, to verify the orientation of the insert, and verified by direct sequencing. As second step, the same fragment was ligated in the NheI site, which is compatible with the XbaI site, at the 3' splice site in the pWIZ vector. After the insertion, both the NheI and XbaI sites are destroyed. Colonies were screened by NotI digestion, to find a clone where the fragments were inserted in opposite orientation (see Figure 5-3 and Figure 5-4). One

clone was selected and prepared for microinjection in *Drosophila* embryos (see section 2.2.2.10)

2.2.7 Protein techniques

2.2.7.1 Protein extracts

Cells were scraped in ice-cold PBS, centrifuged at 1200 *g* for 10 min and lysed in lysis buffer (10 mM Tris-HCl, pH 8.0, 150 mM KCl, 1% NP-40, 1% glycerol, 1 mM EDTA, 0.1 mM DTT and protease inhibitor cocktail (Roche)) for 30 min 4°C under constant agitation. Rat or mouse tissues were extracted in the same buffer using a teflon dounce homogeniser (Wheaton) and then incubated as before. After centrifugation at 16,000 *g* for 60 min at 4°C, the concentration of the extracts was quantified (see below).

2.2.7.2 Protein quantification

Protein concentrations were determined using the Bradford assay (BIO-RAD Protein Assay Reagent). Sample dilutions and Bovine Serum Albumine (BSA) standards were incubated with 1 ml BIO-RAD Protein Assay Reagent diluted 1:4 at RT for 5 min. Absorption was measured at OD_{595} in a spectrophotometer (*Bio* Photometer, Eppendorf).

2.2.7.3 SDS-Polyacrylamide Gel Electrophoresis (SDS-PAGE)

Protein samples were mixed with the appropriate volume of 5x SDS-PAGE sample buffer (20% glycerol, 5% β-mercaptoethanol, 2.5 mg Bromophenol Blue, 10% SDS, 120 mM Tris-HCl pH 6.8) and boiled for 5 min or incubated at RT for

10 min. After a short spin to collect all the liquid at the bottom of the tube, samples were loaded on a polyacrylamide proteanIII™ minigel (BIO-RAD). These freshly prepared gels consisted of a separating gel (8 to 15% acrylamide [ratio of acrylamide:bis-acrylamide 37.5:1], 0.1% SDS, 375 mM Tris-HCl pH 8.8), overlaid with a stacking gel (4.5% acrylamide, 0.1% SDS, 125 mM Tris-HCl pH 6.8). Gels were polymerised with 3 mM ammonium persulphate (AMPS) and 0.1% N,N,N',N'-tetramethyl-ethylenediamine (TEMED). Samples were run at 20 mA in running buffer (190 mM glycine, 0.1% SDS, 25 mM Tris-OH pH 8.3). When appropriate, proteins were fixed and stained with Coomassie staining solution (50% methanol, 10% acetic acid, 0.1% Coomassie Brilliant Blue) for 15 min at RT, followed by de-staining in de-staining buffer (10% acetic acid, 10% isopropanol, in water) overnight.

2.2.7.4 Western Blotting

Proteins were transferred onto PROTRAN® nitrocellulose membranes (Schleicher & Schuell), using a BIO-RAD wet blotting system, at 4°C in transfer buffer (20 mM Tris-OH, 150 mM glycine, 20% methanol for 1 h at 100 V or overnight at 30 V. The membranes were stained with Ponceau S to assess the efficiency of protein transfer. Blots were blocked with blocking solution (5% skimmed milk (Marvel) in PBS 0.1% Tween-20 (PBST)) for 1 h at RT or overnight at 4°C, followed by incubation with primary antibody diluted in antibody buffer (2.5% skimmed milk in PBST). Membranes were washed with PBST for 15 min and incubated with HRP-conjugated secondary antibody in antibody buffer. After

extensive washing in PBST, immunoreactivity was detected using enhanced chemiluminescence (ECL, GE Healthcare).

For competition experiments, the primary antibody was incubated with 1000x excess of the appropriate peptide, in antibody buffer, for 30 min prior to addition to the membrane.

To test the anti-phosphoKIM antibodies, the blocking step and all the subsequent washes and incubations were carried out in presence of 100 μM Sodium-orthovanadate.

2.2.7.5 Probing of peptide arrays

The membranes were incubated for 5 min in 100% Ethanol, washed 6 times in PBS 0.05% Tween-20 (PBST), and incubated in PBST 3% BSA for 2 h at RT. Membranes were then incubated with purified KLC1 0.2 μg/ml in binding buffer (20 mM Hepes-KOH pH 7.6, 100 mM KCl, 0.1 mM DTT, 0.25% Triton X-100, 3% BSA) for 1 h at RT. After extensive washing with PBST, membranes were incubated with anti-KLC1 antibodies diluted 1:1000 in PBST 3% BSA for 1 h at RT, washed in PBST, incubated with HRP-conjugated secondary antibodies diluted 1:5000 in PBST 3% BSA, washed again with PBST, and once with PBST 0.5M NaCl. Immunoreactivity was detected using ECL (GE Healthcare).

2.2.7.6 Expression and Purification of GST-recombinant Proteins

Recombinant GST-fusion proteins were espressed in the *E. coli* TG1 strain. Bacteria from glycerol stocks were used to inoculate 1 ml of LB medium containing the appropriate antibiotic and incubated overnight at 37°C. Cultures were then diluted in 10 ml of pre-warmed 2YT medium (10 g bacto-tryptone, 10 g yeast

extract, 5 g NaCl in 1 l H_2O, pH 7.2) with antibiotic and grown to an A_{600} of 0.8-1.1 at 37°C and 200 rpm. 1 mM isopropyl-β-D-thiogalacto-pyranoside (IPTG) was added for protein induction. After 4 h incubation at 30°C at 200 rpm, bacteria were centrifuged for 5 min at 1000 rpm in a Megafuge 1.0 R (Heraeus) and the supernatant was discarded.

All the following steps were carried out at 4°C. The bacterial pellet was resuspended in 50 ml of pre-chilled PBST and the bacterial suspension was centrifuged for 5 min at 4000 *g*. The pellet was washed again with PBST and centrifuged as before, and the bacteria were subsequently resuspended in 1 ml resuspension buffer (2 mM EDTA, 4 µg/ml pepstatin, 0.1% β-mercaptoethanol, EDTA-free protease inhibitor cocktail (Roche)). The cell suspension was sonicated (3 x 10 sec cycles) in a Vibra Cell™ instrument (Sonics) and the bacterial lysates were centrifuged for 15 min at 16000 *g* in a table-top centrifuge. The supernatants were mixed with 50% GSH-resin agarose (pre-swollen in PBST) at a ratio of 1:20 and incubated for at least 1 h with agitation. The bacterial supernatants were then removed and the beads were washed twice with PBST, once with PBST 250 mM NaCl, and once more with PBST. Protein-coupled beads were stored at 4°C for up to two weeks.

2.2.7.7 Phosphorylation assays

GST or recombinant GST-proteins bound to glutathione-Sepharose beads were washed twice in phosphorylation buffer and subsequently incubated with the appropriate kinase in presence of cold ATP (experimental conditions are described in Table 8). In selected experiments, Redivue™ [^{32}P]-ATP was added at the ratio of

1 mCi per µmol cold ATP. The phosphorylation mix was incubated at 30°C for 30 min under constant agitation, and the reaction was blocked by cooling on ice. Beads were washed 3 times with phosphorylation buffer and resuspended in loading buffer. Eluted proteins were then analysed by SDS-PAGE and autoradiography.

Table 8: *experimental conditions for phosphorylation assays with different kinases*

	Abl	CK1	CK2
Phosphorylation buffer	50 mM Tris-HCl pH 7.5, 10 mM $MgCl_2$, 2 mM DTT	50 mM Tris-HCl pH 7.5, 10 mM $MgCl_2$, 5 mM DTT	20 mM Tris-HCl pH 7.5, 50 mM KCl, 10 mM $MgCl_2$
Cold ATP (µM)	100	200	200

2.2.7.8 In vitro *GST-pull down with [^{35}S]- labelled proteins or purified KLC1*

[^{35}S]-labelled proteins were generated using TnT Quick coupled transcription/translation system (Promega) and Redivue™ L-[^{35}S] Methionine 15 mCi/ml (GE Healthcare). Alternatively, 20 µg of purified KLC1 were used for each sample. In selected experiments, recombinant GST-proteins were phosphorylated as described in 2.2.7.7. For pull-down assays, protein-coupled beads were washed in Hank's buffer (20 mM Hepes-NaOH pH 7.4, 0.44 mM KH_2PO_4, 0.42 mM NaH_2PO_4, 5.36 mM KCl, 136 mM NaCl, 0.81 mM $MgSO_4$, 1.26 mM $CaCl_2$, 6.1 mM glucose) containing 0.1% BSA (Hank's-BSA), blocked with 2% BSA in Hank's for 1 h at 4°C, and washed with Hank's-BSA. *In vitro* transcribed/translated proteins were pre-cleared on glutathione-sepharose beads for 1 h at 4°C and then incubated with either pre-bound GST-proteins or GST alone for 2 h at 4°C in Hank's-BSA. Beads were then washed six times with ice-cold Hank's-

BSA in the presence of 250 mM NaCl, 0.1% Triton X-100, and resuspended in loading buffer. Eluted proteins were then analysed by SDS-PAGE and autoradiography.

2.2.7.9 GST-pull down and Immunoprecipitation (IP) assays from lysates

Cell or tissue extracts were incubated with immobilised GST-proteins or GST overnight at 4°C. Alternatively, cell lysates were incubated with the appropriate antibodies and immunocomplexes were isolated by the addition of protein G-Sepharose Fast Flow (GE Healthcare) for 1 h at 4°C. After six washes with lysis buffer, bound proteins were eluted in loading buffer and analysed in SDS-PAGE followed by Western Blot.

2.2.7.10 Generation of Antibodies

2.2.7.10.1 Polyclonal antibody against Drosophila Kidins220

Two rats were immunised with a peptide corresponding to the last 24 amino acids of *Drosophila* Kidins220. All procedures were performed in the Harlan UK laboratories (Oxon, England), on behalf of the Biological Resources Unit, Cancer Research UK.

2.2.7.10.2 Polyclonal antibody against phosphorylated KIM

Two rabbits were immunised with a peptide corresponding to the KIM sequence, phosphorylated on tyrosine 20. All procedures were performed in the Harlan UK laboratories (Oxon, England), on behalf of the Biological Resources Unit, Cancer Research UK.

2.2.7.11 Affinity purification of Antibodies

The interactions of antigens with their antibodies provide a method to purify specific, active antibodies. Here the antigen is first bound to activated sepharose beads, followed by binding of the antibody to the immobilised antigen.

2.2.7.11.1 Coupling of the antigen

The most widely used method of antigen immobilisation is to couple the protein to Sepharose 4B (AP Biotech), which has been activated with cyanogen bromide. First 2 g of CNBr-activated Sepharose 4B were weighed out. They were washed and reswelled with 50 ml of 1 mM HCl. The gel was then washed three times with 40 ml coupling buffer (0.1 M carbonate buffer, 0.5 M NaCl, pH 8.3. Carbonate buffer: ~7 ml 0.5 M Na_2CO_3 pH 11, in 0.5 M $NaHCO_3$ pH 8, final volume ~200 ml, pH 8.3) by centrifuging for 5 min at 4000 *g*, the supernatant discarded and the pellet again resuspended in coupling buffer.

Meanwhile 10 mg of purified peptide were dissolved in 1 ml of coupling buffer in a 2 ml Eppendorf tube. 1 ml of the washed gel solution was added. This was incubated for 2 h at room temperature and then overnight at 4°C on an end-over-end mixer. The next day the beads were pelleted for 2 min at 3000 *g* in a 4°C cold table-top centrifuge. The supernatant was removed and retained. This step was repeated once more with another 1 ml of coupling buffer. The second supernatant was also retained and both supernatants combined before measuring their OD at 280 nm (Ultrospec 3000). Excess peptide was washed away by resuspending the beads with 10 ml of coupling buffer. The beads were pelleted and the supernatant

removed, but still kept to measure its OD. The peptide left in these supernatants was subtracted from the input protein and the coupling efficiency calculated.

2 ml of 0.2 M glycine-NaOH pH 8.5 were added to the suspension and incubated for 2 h at room temperature to block the remaining active groups. Excess blocking reagent and non-covalently adsorbed protein were washed away by three cycles of washing with 14 ml coupling buffer followed by 14 ml of acetate buffer (0.1 M Na-acetate, 0.5 M NaCl, pH 8.0). Each step contained a centrifugation step for 5 min at 2500 *g*. After the last centrifugation step with the acetate buffer, this supernatant was discarded and the peptide-coupled beads were used for antibody purification.

2.2.7.11.2 Purification of the antibody

Antigen-coupled beads were incubated with 10 ml of the antiserum, 2 ml PBS and 12 µl Triton X-100 overnight at 4°C with gentle mixing. The beads were then pelleted, but the supernatant retained and tested for remaining activity. The beads were washed three times with 10 ml PBS (5 min centrifugation at 3000 rpm) and resuspended in 10 ml PBS. This solution was packed in an appropriate column and washed with PBS until the OD_{280} of the eluate had reached ~0. Bound antibodies were eluted in 10 x 500 µl aliquots of 100 mM glycine-HCl pH 2.8, into 55 µl of 3 M Tris-HCl pH 8.0 to neutralise. Six further 500 µl aliquots were made with 100 mM glycine-HCl pH 2.2, into 60 µl of 3 M Tris-HCl pH 8.0.

The absorbance of each aliquot was measured at 280 nm. The peak fractions were snap frozen in liquid nitrogen in 5 µl aliquots and stored at -20°C.

2.2.7.12Peptide-directed ELISA

In order to bind the peptide to the plate, 0.01 to 10 ng of peptide in 50 µl/well TBS were aliquoted into a flat-bottom polyvinylchloride 96-well plate (FALCON®) and incubated overnight at RT under a fume hood. The plate was blocked for 1 h with TBST (20 mM Tris-OH, 137 mM NaCl, 0.05% Tween-20) 1% BSA at RT, and washed twice with TBST. The plate was subsequently incubated with the primary antibody diluted in TBST 1% BSA for 2 h at RT, washed five times with TBST, and then incubated with the secondary HRP-conjugated antibody diluted in TBST 1% BSA for 1 h at RT. After the incubation, the plate was washed five times in TBST, blocked for 10 min in TBST 1% BSA, and rinsed in water. The Sigma Fast™ O-phenylenediamine dihydrochloride (OPD) peroxydase substrate was added to the plate and incubated until the solution turned yellow. The reaction was stopped by adding 2 M HCl, and the absorption was measured at A_{490} in a plate reader (Molecular Devices).

2.2.7.13 Structure prediction

KIM 3D structure prediction was obtained from the Robetta server (http://robetta.bakerlab.org/). The submitted sequence corresponds to amino acid 1336 – 1415 of rat Kidins220.

2.2.8 Yeast techniques

2.2.8.1 Yeast two-hybrid screening

The yeast two-hybrid screening was performed by Dr. A. Bracale, University of Naples, Italy. The screen was carried out using a Matchmaker System 2

(Clontech) following manufacturer's instructions. The KC fragment of Kidins220 fused with GAL4-binding domain in pGBKT7 was used as bait to screen a rat brain cDNA library in the pACT2 vector using the AH109 yeast reporter strain. Approximately 7 x 10^5 transformants were screened. Positive interacting clones were selected for growth on Ade-/His-/Trp-/Leu-/X-α-gal plates and analysed by direct sequencing.

2.2.8.2 Yeast transformation

The binding of KC to KLC1 was verified by an independent pairwise yeast two-hybrid analysis. For this test, a small scale Litium-Acetate (Li-Ac) yeast transformation was first performed on the AH109 yeast strain, with plasmids encoding the constructs used as baits (pGBKT7-KC, -KIM(Y24A), -JIP-3/SyD). Transformed yeast was grown on Trp-plates. A few colonies were picked, plasmid DNA was extracted (see section 2.2.2.14.1) and screened by endonuclease digestion to check for the integrity of the construct. Yeast clones containing the correct constructs were kept as glycerol stocks at -80°C. A second small scale LiAc transformation was then performed on the three transformed strains, with plasmids encoding the constructs used as preys (pGADT7-KLC1, -ΔNKLC1, -TPRKLC1, -TPRPp5). Transformed yeast was grown on high stringency (Ade-/His-/Trp-/Leu-) plates containing 5-Bromo-4-Chloro-3-indolyl-α-D-galactopyranoside (X-α-Gal). The number of colonies was counted for each co-transformation, and the β-galactosidase activity was measured using the yeast β-galactosidase assay kit (PIERCE, see section 2.2.8.3).

Yeast transformations were performed as described in the Yeast Protocol Handbook (Clontech). Briefly, yeast was inoculated in 50 ml of the appropriate medium and grown overnight at 30°C with shaking to stationary phase (OD>1.5). Part of the culture was transferred to 300 ml of medium, to reach a starting OD of 0.2-0.3, and the diluted culture was grown at 30°C with shaking to an OD of 0.4-0.6. Cells were centrifuged at 1000*g* for 5 min at RT, resuspended in 50 ml water, and centrifuged again, and resuspended in 1.5 ml of sterile TE buffer (200 mM Tris-OH pH 7.5, 20 mM EDTA). 100 µl of yeast competent cells were first mixed with a solution containing 0.1 µg DNA and 0.1 mg herring testes carrier DNA, and 0.6 ml of PEG/LiAc solution (40% polyethylene glycol, 100 mM lithium acetate pH 7.5, in TE buffer) were subsequently added. After a 30 min incubation at 30°C with shaking, 70 µl DMSO were added, and the cells were heat shocked for 15 min in a 42°C water bath. Cells were then chilled on ice for 1-2 min, centrifuged for 5 s at 14000 rpm at RT, resuspended in 100 µl of medium and plated.

2.2.8.3 β-galactosidase assay

A quantitative measure of β-galactosidase activity was obtained by using the Yeast β-Galactosidase Assay Kit (Pierce). Briefly, cells were grown in the appropriate medium to mid-log phase (OD_{660} 0.5-1.0). The exact OD_{660} for each culture was recorded. 350 µl of working solution were prepared following manufacturer's instructions, and added to 350 µl of culture. The mixture was incubated at 37°C until a colour change was observed, and the total reaction time was recorded. 300 µl of stop solution were added, the cultures were centrifuged at 13000x*g* for 30 s and the supernatants OD_{420} was determined. A measure of

β-galactosidase activity is given by the ratio (1000 x OD_{420})/(t x V x OD_{660}), where t = total incubation time (min), and V = volume of cells (ml) used in the assay.

2.2.9 Tissue culture techniques

2.2.9.1 PC12 cells culture conditions

PC12 rat pheochromocytoma cells were cultured at 37°C in DMEM supplemented with 7.5% fetal calf serum, 7.5% horse serum, and 2 mM glutamine in a humidified atmosphere containing 10% CO_2. When required, PC12 were treated with 100 ng/ml nerve growth factor (NGF, Alomone Labs) in DMEM.

2.2.9.1.1 Coating of coverslips and glass-bottom dishes

Glass-bottom dishes (MatTek Corporation) and coverslips were coated with 0.2 mg/ml poly-L-lysine in PBS, for 30 min to 1 h at RT. The solution was then removed and the dishes/coverslips air-dried in a sterile hood.

2.2.9.1.2 Transfection

PC12 cells were transfected with 0.5 μg DNA and 1-2 μl Lipofectamine (Invitrogen) in OptiMEM (Gibco). 5 h after transfection, the medium was replaced with DMEM containing 100 ng/ml NGF and the cells were incubated for the required amount of time before fixation or lysis. In selected experiments, HeLa cells were infected with the A36R-YdF recombinant vaccinia virus (Rietdorf et al., 2001). In order to induce high levels of protein expression in infected cells, all transfected genes were under the control of the viral pE/L promoter. At 4 h post infection, cells were transfected with pE/L mRFP, pE/L mRFP-KIM, or pE/L mRFP-TPR (Rietdorf et al., 2001) using Lipofectin (Invitrogen) according to manufacturer's instructions,

and processed for immunofluorescence after 4 h. Virus particles were visualised by labelling infected cells without permeabilisation with an anti-B5R antibody (Schmelz et al., 1994), followed by incubation with AlexaFluor®488-conjugated anti-rat antibodies.

2.2.9.1.3 Microinjection

For microinjection, PC12 cells were plated on MatTek dishes and differentiated for 2-4 days in DMEM containing 100 ng/ml NGF, 0.1% fetal calf serum, 0.1% horse serum. Cells were microinjected using an Eppendorf microinjector system. Borosilicate glass capillaries (GC120TF-10; Harvard Appartus Ltd.) were used to pull needles on a Sutter Instrument needle puller (Model P97) using the following settings: P = 300, heat = 510-540 (adjusted depending on filament condition); pull = 200; vel = 200; t = 250. Cells were microinjected with EGFP-Kidins220 plasmid alone (50 µg/ml) or in combination with mRFP-KIM(Y24A) (20 µg/ml) or mRFP-KIM (20 µg/ml). DNA was centrifuged through a 0.22 µm filter before loading into the injection needle. After overnight recovery, cells were washed with non-fluorescent DMEM without phenol red, riboflavin, folic acid, penicillin/streptomycin and supplemented with 30 mM Hepes-NaOH, pH 7.3 (DMEM$^-$), and imaged by low-light time lapse microscopy.

2.2.9.1.4 Processing for Immunofluorescence

For immunocytochemistry experiments, cells were fixed with 3.7% paraformaldehyde in PBS for 15 min at room temperature, washed with PBS, incubated with 50 mM NH_4Cl for 10 min, rinsed and permeabilised with blocking buffer (2% BSA, 0.25% porcine skin gelatin, 0.2% glycine, 15% fetal calf serum,

0.1% Triton X-100, in PBS) for 1 h. Primary antibodies were diluted in PBS containing 1% BSA, 0.25% porcine skin gelatin, 3% fetal calf serum (antibody dilution buffer) and incubated for 1 h at RT. After rinsing with PBS, secondary antibodies diluted in antibody dilution buffer were applied for 30 min at RT. Cells were then washed and mounted with Mowiol 4-88 (Harco).

2.2.9.2 ES cell culture conditions

Kidins220 +/lox ES cells were routinely grown on gelatin-coated plastic dishes, and maintained using standard methods in ES cell growth medium: Glasgow Minimal Essential Medium (GMEM, Invitrogen) supplemented with 5% ES cell grade fetal calf serum, 5% Serum Replacement (Invitrogen), 2 mM glutamax, 100 μM β-mercaptoethanol, and 1000 U/ml Leukemia Inhibitory Factor (LIF), at 37°C and 10% CO_2.

2.2.9.2.1 Selection in G418

Homozygous Kidins220 lox/lox ES cells were derived from Kidins220 +/lox ES cells by selecting colonies that were resistant to a high concentrationi of G418 (3.75 mg/ml) over a three week period.

2.2.9.2.2 Electroporation

Kidins220 lox/lox ES cells were transiently transfected with a Cre recombinase expression plasmid (pMC-Cre) as follows: cells were seeded at 90% confluence the day before electroporation, trypsinised and counted. 5×10^6 cells were then washed twice in serum free DMEM, resuspended in 1 ml of DMEM and placed into a 4 mm gap electroporation cuvette (Bio-Rad). 20 μg of pMC-Cre

plasmid were added to the cells, mixed gently and left at RT for 5 min. Electroporation (1 pulse of 240 V and 500 μF) was performed using a Gene Pulser II (Bio-Rad) and the cells were left to recover for 5 min at RT before resuspending in 10 ml of ES cell growth medium. The cells were then seeded onto 10 cm culture dishes (2000 – 4000 cells per dish), maintained under standard conditions for 1 – 2 weeks and the resulting colonies were picked and genotyped using standard methods.

2.2.10 Mouse techniques

All embryos used in this study were obtained from natural matings of Kidins220 +/ko mice, on the C57BL/6 background. Mice were mated overnight and separated in the morning. The development of the embryos was timed from the detection of a vaginal plug, which was considered day 0.5.

2.2.10.1 Dissection and genotyping of embryos

Embryos were dissected in ice-cold PBS, and the yolk sac was kept for genotyping.

2.2.10.2 Whole mount staining

All the steps were carried out at 4°C, unless otherwise indicated. After dissection, embryos were fixed in 4% paraformaldehyde in PBS for 4 h to overnight (depending on the size), washed in PBS, and then dehydrated through a series of 30 min-washes in increasing concentrations of methanol in PBS (15%, 30%, 50%, 75%, 100% methanol). Once dehydrated, samples were either stored at -20°C or immediately processed. Prior to immunostaining, embryos were transferred into

methanol containing 5% hydrogen peroxide for 4 to 6 h at RT, to bleach embryos and to inactivate endogenous peroxidases. They were then washed in 100% methanol and rehydrated through a series of methanol/PBS washes (85%, 70%, 50%, 30%, 15%, 0% methanol). Embryos were incubated overnight in blocking buffer (20% normal goat serum (NGS), 1% Triton-X100 in PBS), to block non-specific binding sites, and then incubated for 2 to 3 d with primary antibody diluted in antibody buffer (0.2% NGS, 0.1% Triton-X100). Embryos were then washed 5 times for 1 h each with antibody buffer, and then incubated overnight with the appropriate HRP-conjugated secondary antibody in PBS containing 0.2% NGS, 0.5% NP-40. After this incubation, samples were extensively washed with PBS. In the meantime, the SG substrate was prepared using the Vector® SG substrate Kit for peroxidase (Vector Laboratories), following manufacturer's instructions. The substrate was applied to the embryos, and the reaction was monitored under the microscope (usually about 2 to 5 min) until the staining reached the desired intensity. The reaction was then stopped by adding PBS, and the samples were washed with increasing concentrations of glycerol in PBS (30%, 50%, 100% glycerol). Embryos were stored in 100% glycerol at RT.

2.2.10.3 In situ hybridisation

2.2.10.3.1 Fixation, pre-treatment and hybridisation of samples

After dissection, embryos were fixed in 4% paraformaldehyde in PBS overnight at 4°C, washed in PBT (0.1% Tween-20 in PBS), and then dehydrated through a series of 30 min-washes in increasing concentrations of methanol in PBT (15%, 30%, 50%, 75%, 100% methanol). Once dehydrated, samples were either

stored at -20°C or immediately processed. Samples were rehydrated through a series of methanol/PBT washes (85%, 70%, 50%, 30%, 15%, 0% methanol), washed in PBT, and then treated with 10 µg/ml proteinase K in PBT at RT for 15 to 45 min, depending on the size. Proteinase K digestion removes proteins unmasking the target RNA and helps to permeabilise the tissues, allowing the riboprobe to access its mRNA target during subsequent hybridisation. After this treatment, embryos were post-fixed for 20 min in 4% PFA, 0.1% glutaraldehyde in PBT at RT, then rinsed once with a 1:1 solution of PBT/hybridisation mix (50% formamide, 6.5% SSC, 5 mM EDTA pH 8.0, 50 µg/ml yeast RNA, 0.2% Tween-20, 0.5% 3-[(3-Cholamidopropyl)dimethylammonio]-1-propanesulfonate (CHAPS), 100 µg/ml heparin, in distilled water), then rinsed with pre-warmed hybridisation mix, and finally incubated with hybridisation mix for at least 1 h at 70°C. After this step, embryos were either stored at -20°C up to few weeks, or directly processed. Hybridisation mix was replaced with pre-warmed hybridisation mix containing 0.1-0.2 µg/ml DIG-labelled RNA probe (see section 2.2.10.3.4) and incubated on a rocker overnight at 70°C.

2.2.10.3.2 Post-hybridisation washes

Samples were washed twice in hybridisation mix for 30 min at 70°C, then washed once in pre-warmed 1:1 PBT/hybridisation mix for 20 min at 70°C, and extensively washed in TBST. Embryos were rinsed twice with MABT buffer (100 mM maleic acid-HCl pH 7.5, 150 mM NaCl, 1% Tween-20,), pre-incubated for at least 1 h in MABT 10% heat-treated sheep serum, and then incubated overnight at 4°C in MABT containing 10% heat-treated sheep serum and 1:2000 dilution of anti-

digoxigenin antibody. Samples were washed with MABT over day at RT, and overnight at 4°C, on a rocker.

2.2.10.3.3 Colour development

Embryos were washed twice for 10 min in NTMT buffer (100 mM NaCl, 100 mM Tris-HCl pH 9.5, 50 mM $MgCl_2$, 0.1% Tween-20, 2 mM levamisole, in distilled water), and then incubated in the dark with 1.5 ml NTMT containing 9 µl/ml Nitrotetrazolium Blue chloride (NBT) and 7 µl/ml 5-Bromo-4-chloro-3-indolyl phosphate dipotassium salt (BCIP), both from 100 mg/ml stocks in dimethyl-formamide. Samples were rocked for the first 20 min, then monitored under the microscope. When the colour developed to the desired extent (30 min to overnight), embryos were washed 3 times with PBT and stored in PBT containing 10 µg/ml thimerosal.

2.2.10.3.4 Preparation of digoxigenin-labelled RNA probes

To prepare the template, 10 µg of the appropriate plasmid DNA were digested with 100 U of the linearising restriction enzyme, in a final volume of 100 µl. After 2 h at 37°C, the efficiency of the digestion was checked by running a small volume of the mixture in a 1% agarose gel. Linearised DNA was purified as described in section 2.2.2.2. The concentration was estimated by running a small aliquot in an agarose gel, together with a standard marker of known concentration. The RNA probe was synthesised by mixing the following components in a RNase-free tube, to a final volume of 25 µl: 10 µl nuclease-free water, 5 µl transcription buffer 5X, 1 µl DTT 0.75 M, 2.5 µl DIG-NTP mix 10X (Boeringer), 1 µg linearised

template, RNasin (Stratagene), SP6, T7 or T3 RNA polymerase (50 U/µl, Stratagene). The reaction was incubated at 37°C for 3 h, and then the following components were added: 20.5 µl nuclease-free water, 2 µl EDTA 0.5 M, 2.5 µl LiCl 8 M, 150 µl 100% EtOH. The mixture was incubated at -20°C for 2 h and centrifuged for 20 min at maximum speed at 4°C. The pellet was washed with 1 volume 70% ethanol and centrifuged for 10 min at maximum speed, ethanol was removed, and pellet was centrifuged again for 1 min. The remaining ethanol was carefully removed and the pellet resuspended in 100 µl EDTA 10 mM and stored at -20°C. The amount of probe was quantified by running 2 µl in an agarose gel, together with a standard of known concentration.

2.2.10.4 Paraffin embedding and sections

Tissues or embryos were embedded in hot wax in the appropriate orientation, left to solidify and stored at RT until ready for cutting. Blocks were then trimmed to remove excess wax using a blunt knife, and further trimmed on the microtome using the coarse feed control, to obtain a good cutting surface. Blocks were placed on an ice tray for at least 5 min before section cutting. Sections were cut with a new blade at the required thickness (usually 4 µm) and laid out on the waterbath using forceps. Chosen sections were placed on slides, drained from excess water, and placed in slide racks. Racks were left in a slide drying oven at 37°C overnight.

2.2.10.5 Haematoxylin and eosin staining

Sections were washed twice in xylene to remove the wax, then washed twice in 100% ethanol and twice in 70% ethanol, always for 3 min at RT. They were then

washed in tap water, incubated in Harris Haematoxylin solution (Sigma) for 8 min, and washed again in running tap water for 5 min. They were subsequently differentiated by incubation in 1% acid alcohol (1 ml hydrochloric acid in 100 ml 70% ethanol) for 20-30 sec, and washed in tap water for 1 min. Sections were then incubated in lithium carbonate solution (saturated) (1.54 g lithium carbonate in 100 ml distilled water) for 30 s-1 min, and washed in tap water for 1 min. They were subsequently stained in 1% Eosin solution (Sigma) for 5-10 min, and washed in tap water. Sections were than dehydrated by washing in 70% ethanol, 100% ethanol, xylene, each step for 5 min, mounted in depex (BDH) and analised.

2.2.10.6 IHC on sections

Paraffin-embedded sections on glass slides were washed with xylene, 100% ethanol, 70% ethanol and twice with PBS, always for 5 min at RT. If required, sections were microwaved in citrate buffer (0.1 M tri-sodium acetate pH 6, 4.5 mM HCl) for 10 min until boiling, allowed to cool for 15 min, washed with water and then with PBS. A wax pen was used at this point to draw around sections. Samples were incubated for 10 min in 1.6% H_2O_2 in PBS, washed with water and then with PBS, and incubated for at least 30 min in 10% serum in 1% BSA/PBS. After this step, the primary antibody was applied, diluted in 1% BSA/PBS, for at least 1 h at RT. The sections were washed twice in PBS and subsequently incubated with the appropriate biotin-conjugated secondary antibody diluted in 1% BSA/PBS, for 45 min at RT. After incubation, samples were washed twice in PBS, incubated with ABC elite reagent (Vector Laboratories) for at least 30 min, and washed again twice in PBS. The DAB reagent (Biogenix) was prepared and added on the sections, the

reaction was monitored under the microscope and stopped when the staining reached a good intensity by adding water for at least 5 min. Sections were then stained with Haematoxylin for 1 min, washed in water for 1 min, and then washed in 70% ethanol, 100% ethanol, xylene, each step for 5 min. Finally, sections were mounted in depex (BDH) and analised.

2.2.11 Imaging techniques

2.2.11.1Time-lapse low-light microscopy

For time-lapse low-light imaging, cells were placed in a humidified chamber and maintained at 37°C in DMEM$^-$ medium. Fluorescent images were acquired every 2 s with a Nikon Diaphot 200 inverted microscope equipped with a Nikon 100X 1.25A Plan Fluor DIC oil-immersion objective using XF102.2 (Omega Optical) to detect EGFP-tagged proteins, XF100-3 filters to detect mRFP-tagged proteins, and a Hamamatsu C4742-95 Orca1 cooled charge-coupled device (CCD) camera (Hamamatsu Photonic Systems) controlled by AQM Advance6 Kinetic Acquisition Manager 2000 software (Kinetic Imaging Limited). Exposure times varied between 55 and 333 ms.

Images were assembled into movies using Kinetc Imaging software in a Microsoft Video 1, 100% compression quality algorithm format, and played at 10 frames/s.

2.2.11.2Confocal microscopy

Fluorescent images were acquired using a Zeiss LSM 510 confocal microscope equipped with a Zeiss 63X, 1.40 NA DIC Plan-Apochromat oil-

immersion objective. A region of interest was chosen and simultaneously excited using the 488, 543 and 633 nm lines of a krypton-argon and two helium-neon lasers, respectively. Prior to specimen imaging, the detector gain was set to black using control samples, which have been treated with secondary AlexaFluor antibodies only. Images were averaged four times in each focal plane.

2.2.11.3 Analysis of sections and embryos

Tissue sections were analysed using a Nikon eclipse E1000 equipped with a Nikon digital camera DXM1200F, and the following objectives: Nikon 4X 0.2 NA DIC Plan-Apochromat, Nikon 10X 0.45 NA DIC Plan-Apochromat, Nikon 20X 0.75 NA DIC Plan-Apochromat, Nikon 40X 0.95 NA DIC Plan-Apochromat.

Embryos from whole mount and *in situ* hybridisation experiments were analysed using a Nikon SMZ1500 equipped with a Nikon 1X HR Plan-Apochromat objective.

2.2.12 Data quantification and statistical analysis

All the data from immunofluorescence and biochemical assays presented in this study were confirmed in at least two independent experiments. Where a statistical analysis was performed, the number of experiments / samples considered is indicated in the corresponding figure legend. For the histological analysis presented in Chapter 6, the number of embryos / samples analysed in each experiment is indicated in the corresponding figure legend.

2.2.12.1 Tracking analysis

Moving carriers were tracked using the MetaMorph software and the point tracking data were imported into a Mathematica 5.2 (Wolfram Research) notebook, custom-written by Alastair Nicol (Light Microscopy Unit, Cancer Research UK), which identifies the extremes of the tracked particles and the linear displacement from their origin. The notebook also calculates the total distance travelled (obtained by summation of the distances between tracked points), and the average speed (obtained from "total distance travelled"/time). The length of the movies analysed was constant, and all the visible particles were tracked. For the speed analysis, we considered only tracking data from carriers that were moving more than 4 μm from their origin.

2.2.12.2 Immunofluorescence analysis

For quantitation of the P-MAPK signalling, mean fluorescence intensity of individual cells was measured using ImageJ 1.34S (http://rsb.info.nih.gov/ij/). The average value for untransfected cells was set to 100% and compared to the mean fluorescence intensity of transfected cells. To determine the basal fluorescence intensity of P-MAPK (corresponding to 0%), cells were fixed and stained for P-MAPK after 5 h incubation in complete growth medium. The specificity of the P-MAPK signal was verified by pre-incubating cells for 30 min with MEK inhibitor PD98059 (5 mg/ml; Calbiochem) and performing the NGF treatment in the presence of the inhibitor, followed by fixing and staining for P-MAPK. The P-MAPK mean fluorescence intensity of these cells was similar to the basal fluorescent intensity described above (data not shown).

2.2.12.2.1 Co-localisation

For the quantification of co-localisation, the co-localisation macro of the LSM 510 software (Zeiss) was used following manufacturer's instructions. For each couple of proteins analysed, the percentage of Kidins220, SyD/JIP-3 or SytI positive pixels that overlapped with KHC or KIF1A positive pixels was calculated.

2.2.12.3Differentiation analysis

For the quantitative analysis of neurite outgrowth, PC12 cells were transfected with mRFP, mRFP-KIM(Y24A) or mRFP-KIM and differentiated with 100 ng/ml NGF for 3 days. Images were acquired by confocal microscopy (LSM510, Zeiss) using a 40x Plan-Apochromat oil-immersion objective. We considered differentiated cells as those with at least one neurite longer than twice the diameter of the cell body.

2.2.12.4Western blot quantification

Intensity of the bands in Coomassie-stained protein gels, Ponceau-stained nitrocellulose membranes and immunoblots were quantified by using the NIH Image software. The amount of GST-fusion protein loaded in each lane was normalised to the amount of GST in the corresponding control, taking into consideration the different molecular weights. For quantitation of KLC1 binding on peptide arrays, the amount of KLC1 bound to wild type KIM was set to 100%.

2.3 Supplemental Material

2.3.1 Description of videos

Video 1: Kidins220 is actively transported in PC12 cells

Cells were injected with EGFP-Kidins220 and imaged as described in 2.2.11.1. The cell body is located on the left. Frames were taken every 2 s and correspond to a field of 32.8 μm x 25 μm. The video consists of 150 frames played at 10 frames/s.

Video 2: mRFP-KIM expression impairs the trafficking of Kidins220

Cells were coinjected with EGFP-Kidins220 and mRFP-KIM and imaged as described in 2.2.11.1. In the presence of mRFP-KIM, EGFP-Kidins220-positive structures are mainly stationary or undergo short range movements. Frames were taken every 2 s and correspond to a field of 13 μm x 21.7 μm. The video consists of 100 frames played at 10 frames/s.

Video 3: the expression of mRFP-KIM(Y24A) does not alter the trafficking of Kidins220

Cells were coinjected with EGFP-Kidins220 and mRFP-KIM(Y24A) and imaged as described in 2.2.11.1. The trafficking of EGFP-Kidins220-positive carriers is unaffected by the expression of mRFP-KIM(Y24A). Frames were taken every 2 s and correspond to a field of 51.09 μm x 31.2 μm. The video consists of 100 frames played at 10 frames/s.

Chapter 3 – Interaction between Kidins220 and the kinesin-1 complex

3 Interaction between Kidins220 and the kinesin-1 complex

3.1 Introduction

Kidins220 has been shown to play an important role in establishing the correct cellular response to neurotrophic signals. Upon NGF stimuli, Kidins220 is rapidly phosphorylated and provides a docking site for the CrkL-C3G complex. The formation of this signalling platform results in the sustained activation of the MAP kinase pathway, which ultimately ensures neuronal survival (Arevalo et al., 2004). Despite the recent studies elucidating the role of Kidins220 in neurotrophin response (Arevalo et al., 2004; Chang et al., 2004; Arevalo et al., 2006), many questions remain open regarding how the targeting of this protein to growth cones and/or specific domains of the plasma membrane relates to its biological function. To elucidate this issue, a yeast two-hybrid was performed, which allowed us to identify kinesin light chain 1 (KLC1), a subunit of conventional kinesin, as Kidins220-interacting partner, and to investigate the role of this complex in NGF-dependent events.

3.2 Kidins220 and neurotrophin receptors

Biochemical studies have shown that Kidins220 interacts with the neurotrophin receptors Trk-A, -B, and -C, as well as with the co-receptor $p75^{NTR}$ (Arevalo et al., 2004). Confocal microscopy analysis has revealed a good co-localisation of Kidins220 with TrkA in sympathetic neurons (Kong et al., 2001), and

with TrkB in primary cortical neurons (Arevalo et al., 2004). I therefore assessed the co-distribution of Kidins220 and the different neurotrophin receptors in our cellular system. To this purpose, I used polyclonal (Iglesias et al., 2000) and monoclonal (Bracale et al., 2007) antibodies against Kidins220. The specificity of these antibodies had been previously confirmed by C.L. Thomas, who performed competition experiments both in immunofluorescence and in western blot assays. For all the immunofluorescence assays shown in this chapter, cells treated only with fluorophore-tagged secondary antibodies were used as negative controls.

I stained undifferentiated (Figure 3-1 A *a-c*) and NGF-differentiated (Figure 3-1 A *d-k*) PC12 cells with antibodies for Kidins220 and $p75^{NTR}$. In undifferentiated cells, I observed a good co-localisation of the two proteins mainly at the plasma membrane (Figure 3-1 A *a-c*). In differentiated cells, Kidins220 and $p75^{NTR}$ co-localised on an internal compartment, both along the neurites (Figure 3-1 A *d-g*, arrowheads) and in the cell bodies (Figure 3-1 A *h-k*, arrowheads). Unfortunately, I could not find any antibodies that would satisfactorily recognise TrkA or TrkB receptors by immunofluorescence, in our cellular system. I therefore used a pan-Trk antibody, raised against an epitope common to TrkA, TrkB and TrkC, to stain differentiated PC12 cells, together with a Kidins220 antibody. I could detect a very small amount of co-localisation between Kidins220 and Trk receptors, confined to specific regions of the plasma membrane (Figure 3-1 B *a-d*, arrowheads). The good overlap between Kidins220 and $p75^{NTR}$ staining correlates well with the published biochemical data (Kong et al., 2001). The difficulties that I encountered in visualising the co-localisation of Kidins220 with TrkA and TrkB are likely to be due to poor efficiency of the Trk-antibodies in our cellular system.

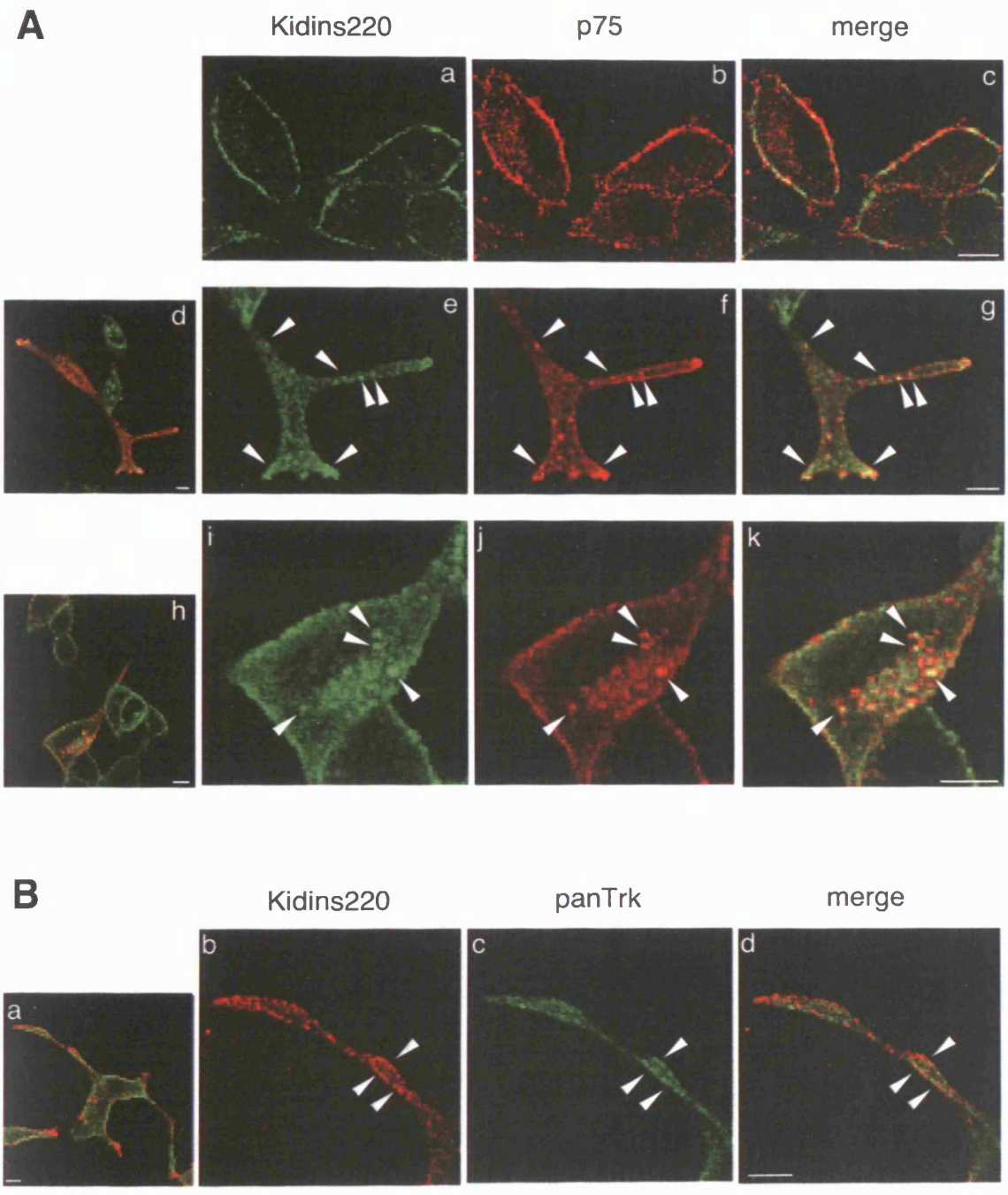

Figure 3-1: *Kidins220 co-localises with p75^{NTR}, and to a less extent with Trk receptors, in PC12 cells*

(A) PC12 cells were stained with monoclonal anti-Kidins220 (*a*, *e*, *i*), or polyclonal anti-p75^{NTR} (*b*, *f*, *j*) antibodies, prior differentiation (*a-c*) or after 3 days of NGF treatment (*d-k*). Kidins220 and p75^{NTR} co-localise at the plasma membrane in undifferentiated cells. In differentiated cells, they co-localise on an internal compartment along the neurites (*d-g*, arrowheads) as well as in the cell bodies (*h-k*, arrowheads). (B) NGF-differentiated PC12 cells were stained with polyclonal anti-Kidins220 (*b*) and monoclonal anti-panTrk (*c*) antibodies. A very small amount of co-localisation between Kidins220 and Trk receptors was detected, confined to limited regions of the plasma membrane (*b-d*, arrowheads). Scale bars = 10 μm.

3.3 Kidins220 directly interacts with KLC

3.3.1 Yeast two-hybrid

The yeast two-hybrid screen described in this section was performed by Dr. A. Bracale.

Yeast two-hybrid is an experimental approach commonly used to reveal direct interactions between two known proteins, or to find new interacting partners for a candidate protein (Fields and Song, 1989). Dr. A. Bracale decided to use the C-terminal portion of Kidins220 (KC, see Figure 1-1) as bait in a yeast two-hybrid screen of a rat brain cDNA library. KC does not contain any classical amino acid domains, with the exception of the PDZ-binding motif (ESIL) at the C-terminal end. Three proteins have been described in the literature to interact with the carboxy-terminal domain of Kidins220: the neurotrophin receptor $p75^{NTR}$, which interacts with the last 250 amino acids of Kidins220 (Kong et al., 2001), α-syntrophin, a PDZ-domain protein that binds the ESIL motif (Luo et al., 2005), and the adaptor protein CrkL, which associates with the polyproline stretch at the level of tyrosine 1096 (Arevalo et al., 2006). The carboxy-tail of Kidins220 seems therefore to play a role in mediating responses to both neurotrophin and ephrin receptors. The identification of new binding partners for this region might further our understanding of the mechanisms underlying these signalling pathways. Among other hits, Dr. A. Bracale found KLC1 splice variant C, a subunit of kinesin-1, also known as conventional kinesin (Figure 1-17). Given the cellular distribution of Kidins220, which concentrates at the neurite tips in differentiated PC12 cells (Iglesias et al.,

2000), and displays a punctate pattern along axons and dendrites of primary neurons (see Figure 3-2), it is therefore possible that Kidins220-positive intracellular structures might be transported along neuronal processes via a kinesin-dependent mechanism. On the basis of this hypothesis, Kidins220 trafficking might be mediated by kinesin-1 via a direct interaction with KLC.

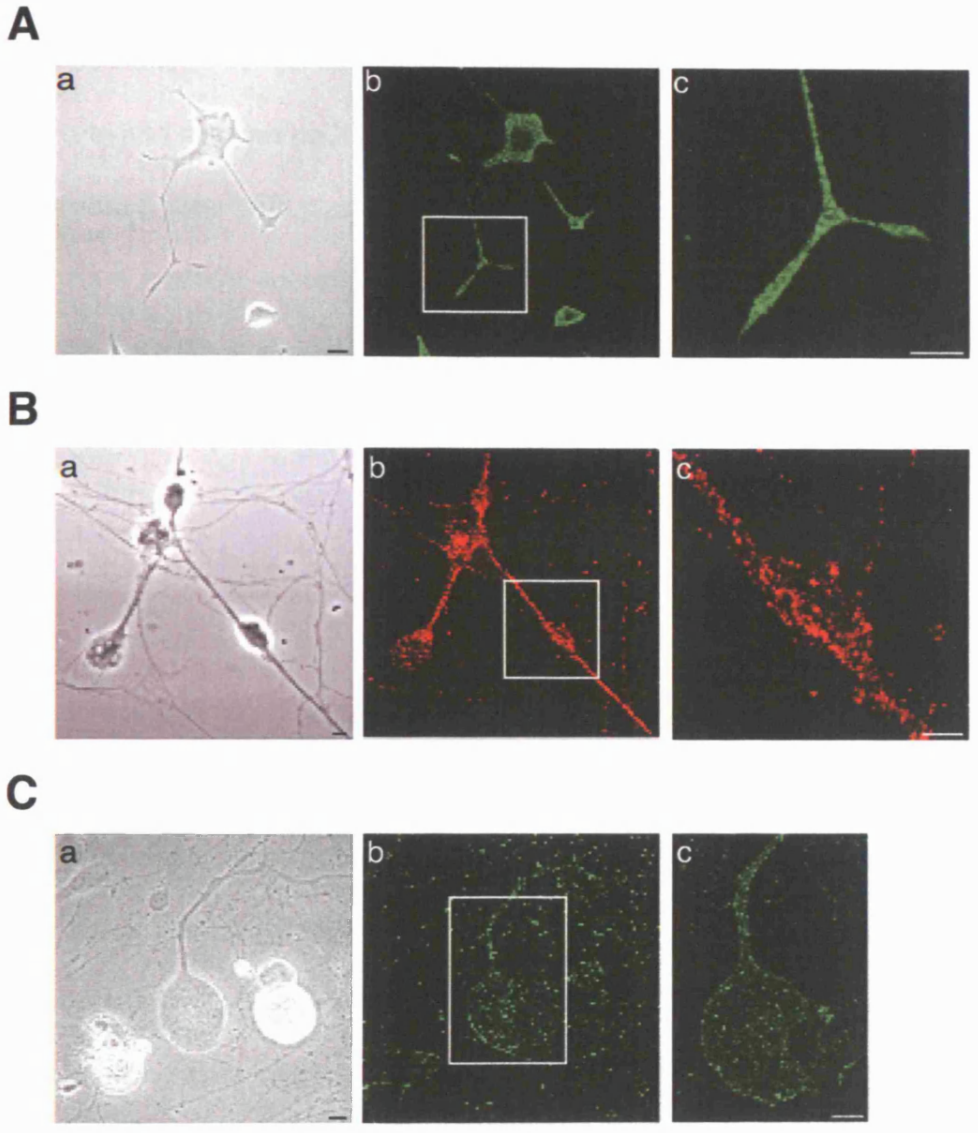

Figure 3-2: *localisation of Kidins220 in PC12 cells and primary neurons*

(A) PC12 cells after 3 days of NGF treatment, (B) Cerebellar Granule Neurons (CGNs) after 3 days in vitro, or (C) Dorsal Root Ganglia neurons (DRGs) after 7 days in vitro, stained with polyclonal antibodies for Kidins220. In all cases, Kidins220 accumulates in discrete intracellular structures both in the cell bodies and along the neurites. Scale bars = 10 μm

3.3.2 Kidins220 directly interacts with KLC

The binding of KC to KLC1 was first verified by an independent pairwise yeast two-hybrid analysis on high stringency medium (see Figure 3-3). To this end, I co-transformed yeast with plasmids encoding KLC1 and KC, as described in section 2.2.8.2. As a positive control, I co-transformed yeast with the plasmids encoding KLC1 and SyD/JIP-3, a well-known KLC1 binding protein (Verhey et al., 2001). The TPR domain of protein phosphatase 5 (Pp5-TPR, Das et al., 1998), an unrelated TPR-containing protein, was used as a negative control, as discussed also in section 3.5. In this kind of assay, the number of colonies growing on high stringency medium is indicative of the strength of the protein interaction. It was therefore possible to compare the binding affinity of different proteins for KLC1. The number of colonies obtained by co-transformation of yeast with KC and KLC1 encoding plasmids was about 70% of that obtained with SyD/JIP-3 and KLC1, suggesting that the interaction between Kidins220 and KLC1 is relatively strong. The interaction was then confirmed via a biochemical approach, by GST pull-down, using a GST-KC fusion protein and *in vitro* translated rat KLC1 (Bracale et al., 2007). This approach demonstrates that KC binds KLC1 directly. GST pull-down experiments were also performed on PC12 cell lysates and rat brain extracts. In both cases, it was possible to detect a specific interaction between GST-KC and the native KLC. Importantly, the entire kinesin-1 holocomplex was found associated with KC, since both the heavy and light chains of the motor complex were recovered with the GST-KC beads (Bracale et al., 2007).

The ability of the endogenous Kidins220 to interact with the kinesin-1 motor complex was then assessed in PC12 cell lysates by co-immunoprecipitation with an antibody directed against KHC, and immunoblotting with a Kidins220 antiserum as well as with anti-KHC and anti-KLC antibodies. Confirming the results obtained with GST-pull downs, the endogenous full length Kidins220 associated with KHC, KLC1 and KLC2. By comparing the amount of bound versus unbound protein, Dr. V. Neubrand estimated that only a fraction of Kidins220 (about 1%) is bound to kinesin-1 under these conditions, whilst she could recover about 5% of SyD/JIP-3 (Bracale et al., 2007). This difference could be due to the fact that only a small fraction of the endogenous Kidins220 is bound to the kinesin-1 complex at any time. Alternatively, the binding between kinesin-1 and Kidins220 might be weaker than the one with SyD/JIP-3, leading to a reduced recovery of Kidins220 with the kinesin-1-coupled beads. Unfortunately, we were unable to co-immunoprecipitate kinesin-1 with either polyclonal (Gsc16) or monoclonal (1F8) anti-Kidins220 antibodies. This negative result may be due to sterical hindrance, as both these antibodies bind the KC region: Gsc16 antibodies were raised against a peptide corresponding to the last 12 carboxy-terminal amino acids of Kidins220, whereas the epitope recognised by 1F8 antibodies is in the region spanning amino acids 1434-1488. Although Gsc16 and 1F8 do not directly bind to the KIM region, their binding to Kidins220 might interfere with the interaction with KLC. The interaction of Kidins220 with kinesin-1 was observed in lysates from PC12 cells either treated or untreated with NGF, indicating that the formation of this complex is independent of neurotrophin stimulation in this cellular system (data not shown). These data confirm

the interaction detected by the yeast two-hybrid screen and suggest that the endogenous Kidins220 and kinesin-1 form a complex in PC12 cells and rat brain.

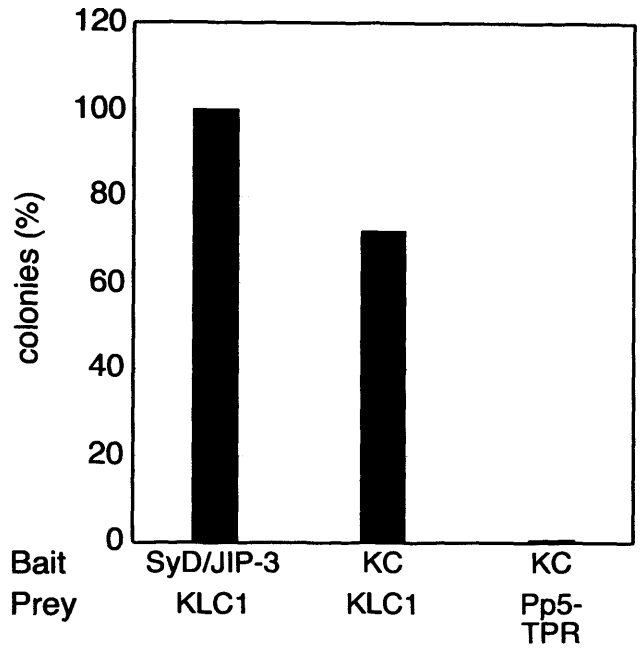

Figure 3-3: *verification of the interaction between KC and KLC1, by yeast two-hybrid analysis*

Relative strength of interactions between KC and KLC1, together with positive and negative controls, were measured by colony growth on high stringency medium. Growth of yeast co-transformed with KC and KLC1 encoding plasmids is about 70% of that of SyD/JIP-3 and KLC1 (set to 100%). No colonies were observed for the co-transformation with Pp5 (Pp5-TPR), an unrelated TPR-containing protein.

3.4 Kidins220 and kinesin-1 co-localise in differentiated PC12 cells

3.4.1 Analysis of Kidins220 localisation by confocal microscopy

Analysis of cells by confocal microscopy allows to assess the intracellular localisation of proteins, as well as other cellular components. By conjugating the proteins of interest to different fluorophores, it is possible to visualise the distribution of two or more proteins at the same time, and to quantify the extent of their overlapping, or co-localisation. Although the co-localisation of two proteins is not a proof of their physical interaction, a good overlap provides some indications about the presence of these proteins on proximal compartments, where they might come in contact with each other. Kidins220 and KHC displayed a punctate distribution in cell bodies as well as neurites of PC12 cells, characterised by extensive clustering at the neurite tips (Figure 3-4 A *a-d*, also Figure 3-1 and Figure 3-2). To provide a quantitative analysis of the level of co-distribution of Kidins220 and the kinesin-1 complex, I determined the degree of co-localisation of Kidins220, as well as that of a range of control proteins, with different members of the kinesin family (Figure 3-4 B). The parameters that I considered for this analysis are described in the Materials and Methods section. SyD/JIP-3, used here as a positive control, exhibited an 82% overlap with KHC (Figure 3-4 A *e-h*), whereas synaptotagmin I (SytI), which is known to be transported by kinesin-3/KIF1A and not by kinesin-1 (Okada et al., 1995), showed only 28% co-localisation with KHC (Figure 3-4 A *i-l*). I found that 58% of Kidins220 co-localised with kinesin-1 (Figure

3-4 A *a-d*), while only 28% overlapped with kinesin-3 (Figure 3-4 A *m-p*). A partial overlap between the distribution of Kidins220 and both KHC and KLC was also observed in motor neurons (MNs), mainly in dendrites and growth cones (see Figure 3-5). Altogether, these results indicate that Kidins220 and kinesin-1 largely co-distribute to internal compartments targeted to neuronal processes in PC12 cells and primary neurons.

3.4.2 Antibodies for other kinesin cargoes

During the analysis described above, I tested a panel of antibodies for cargoes of kinesin-1 and other members of the kinesin family, on NGF-differentiated PC12 cells. Although many of those reagents did not give satisfying results when used in immunofluorescence, two antibodies proved to be valid tools. Figure 3-6 A shows the intracellular localisation of APP, a known interactor for kinesin-1 (Kamal et al., 2000). APP displays a punctate staining in the cell bodies as well as along the neurites of the cells. In Figure 3-6 B I used a custom made monoclonal antibody (#M48) to assess the distribution of SytI, a cargo for kinesin-3/KIF1A. SytI shows a diffuse staining in the cell bodies, and an extensive accumulation at the neurite tips.

Figure 3-4: *Kidins220 and kinesin-1 co-localise in PC12 cells*

(A) PC12 cells treated for 3 days with NGF were stained with polyclonal (*b*) or monoclonal (*n*) anti-Kidins220, polyclonal anti-SyD/JIP-3 (*f*), polyclonal anti-SytI (*j*), monoclonal anti-KHC (*c*, *g*, *k*) or polyclonal anti-kinesin-3 (*o*) antibodies, and analysed by confocal microscopy. Scale bars = 5 μm. (B) The percentage of co-localisation of the indicated proteins in neurites is shown. For each couple of proteins analysed, the percentage of Kidins220, SyD/JIP-3 or SytI-positive pixels that overlapped with KHC or KIF1A positive pixels was calculated, by using the co-localisation macro of the LSM510 software (Zeiss). Kidins220 : KHC, n = 16 neurites; SyD/JIP-3 : KHC, n = 11 neurites; Syt : KHC, n = 16 neurites; Kidins220 : kinesin-3, n = 22 neurites, from two independent experiments. Error bars represent s.e.m.

A

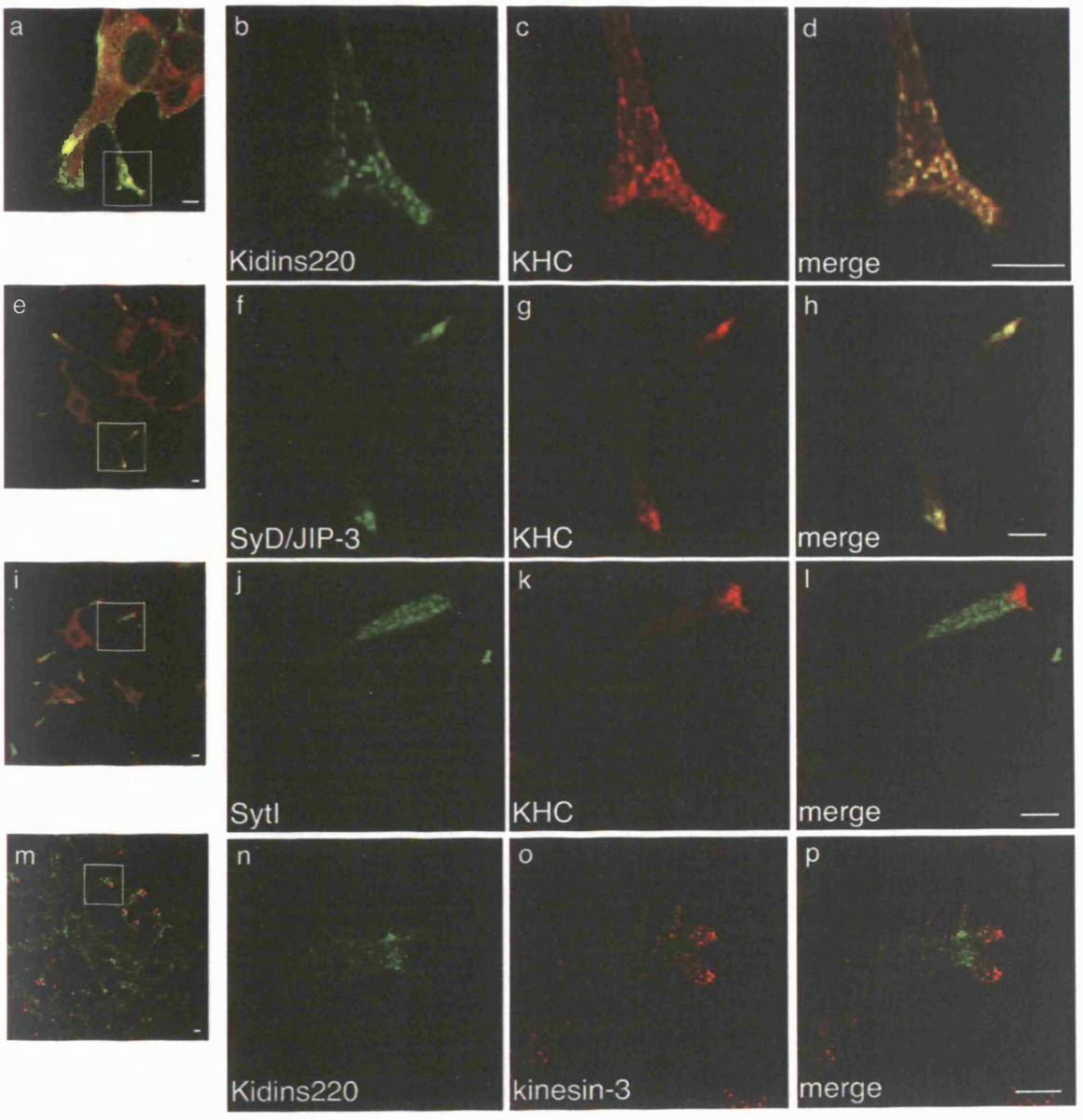
a
b
Kidins220
c
KHC
d
merge
e
f
SyD/JIP-3
g
KHC
h
merge
i
j
SytI
k
KHC
l
merge
m
n
Kidins220
o
kinesin-3
p
merge

B

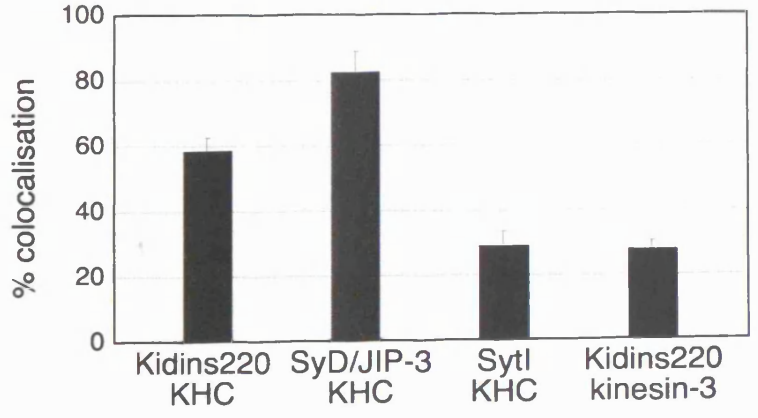
% colocalisation
100
80
60
40
20
0
Kidins220
KHC
SyD/JIP-3
KHC
SytI
KHC
Kidins220
kinesin-3

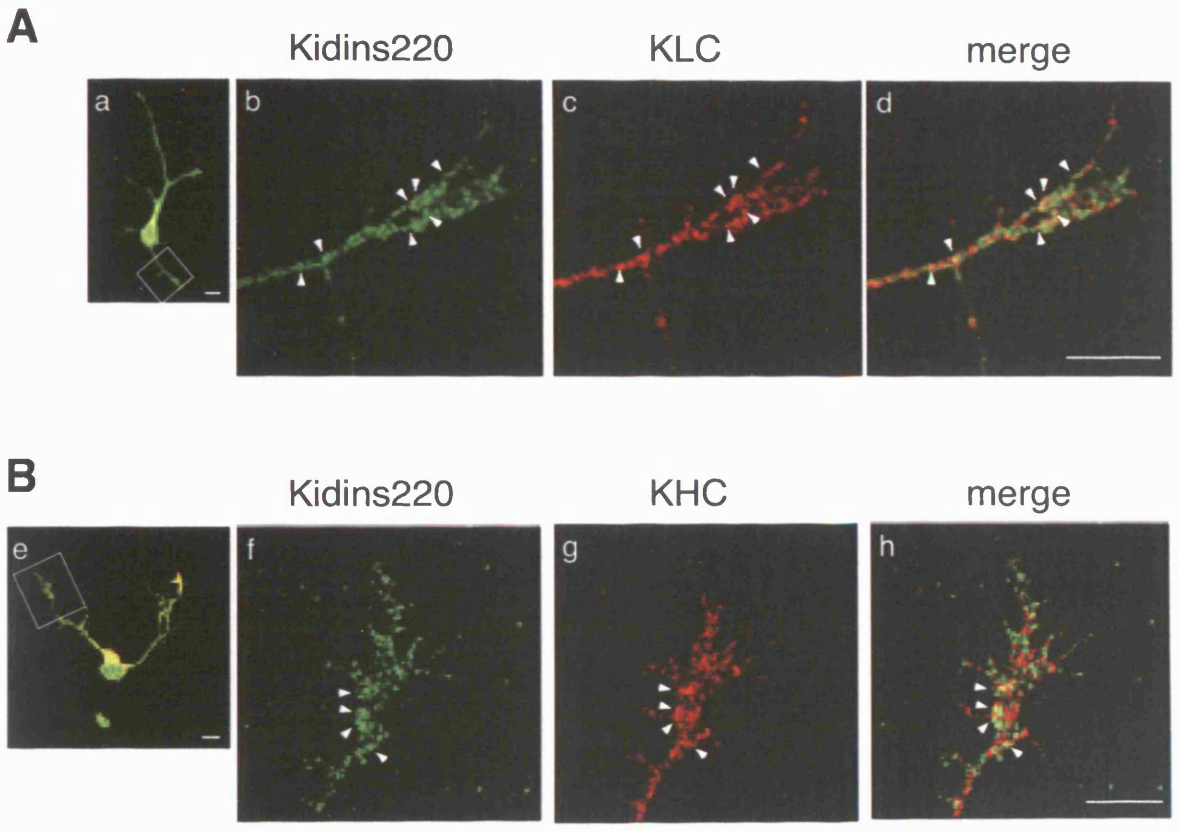

Figure 3-5: *Kidins220 and kinesin-1 partially co-localise in primary MNs*
Differentiating rat spinal cord MNs (1 day in culture) were stained with Kidins220 antibodies (*b*, *f*), and anti-KLC (*c*) or anti-KHC (*g*) antibodies, and analysed by confocal microscopy. Structures containing both Kidins220 and KLC (*d*) or KHC (*h*) appear in yellow (arrowheads). Scale bars = 5 μm. This experiment was performed by Dr. A. Bracale.

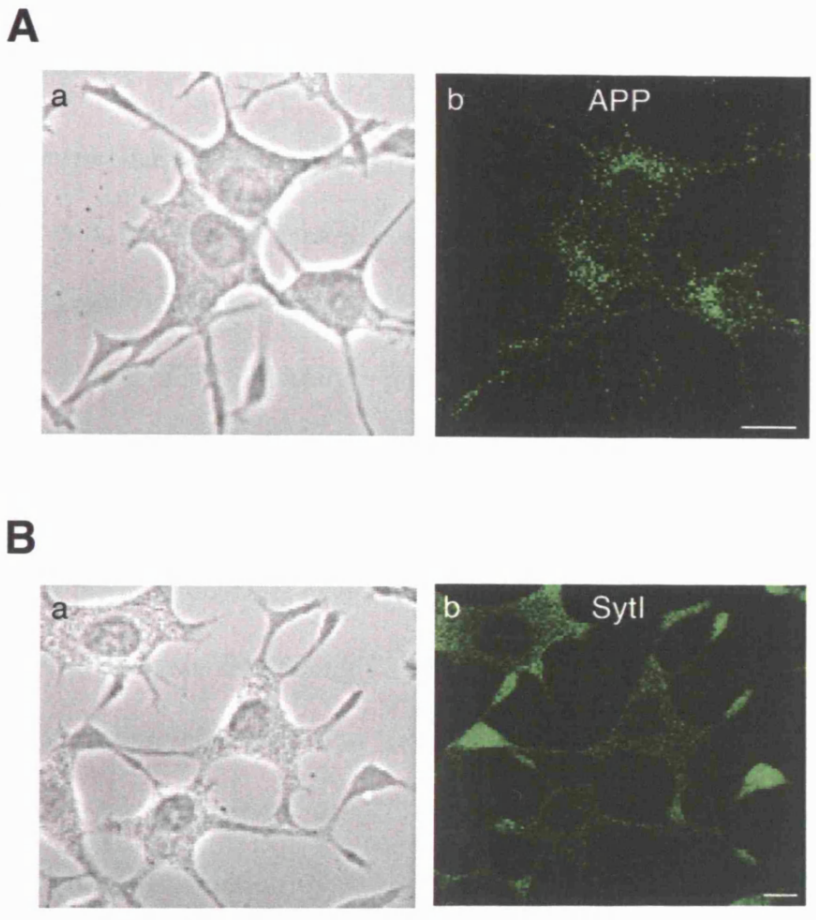

Figure 3-6: *localisation of APP and SytI in differentiated PC12 cells*
(A) Phase image (*a*) and staining with polyclonal anti-APP antibodies (*b*). APP displays a punctate staining in the cell bodies as well as along the neurites of the cells. (B) Phase image (*a*) and staining with monoclonal anti-SytI antibodies (*b*). SytI shows a diffuse staining in the cell bodies, and an extensive accumulation at the neurite tips. Scale bars = 10 µm.

3.5 The region 83-296 of KLC1 mediates the binding to Kidins220

KLCs are characterised by two main regions: a series of heptad repeats (HR) at the N-terminus, and six tetratricopeptide repeats (TPRs) at the C-terminus (Figure 3-8) (Gindhart and Goldstein, 1996). The HR-containing region is known to mediate the interaction with KHC, although recent evidence has shown that it can also connect kinesin-1 to cargo proteins (Yang and Li, 2005), whereas the TPR motifs dock kinesin-1 to specific cargoes (Karcher et al., 2002; Hirokawa and Takemura, 2005). I tested the ability of KC to interact with the TPR motifs of KLC by pairwise yeast two-hybrid analysis. Surprisingly, growth of yeast co-transformed with KC and KLC-TPR expressing plasmids was severely reduced, compared to the growth obtained by co-transformation of KC and full length KLC1 (set to 100%). Furthermore, co-transformation of KC and the TPR domain of Pp5 (Pp5-TPR), an unrelated TPR-containing protein (Das et al., 1998), completely abolished yeast growth (Figure 3-7 A). This first set of experiments indicate that the interaction between Kidins220 and KLC is mediated not exclusively by the TPR repeats, but a different portion of KLC is required to obtain a full binding efficiency. In order to identify the region of KLC involved in the binding to Kidins220, I generated a series of truncated versions of rat KLC1 (illustrated in Figure 3-8) and tested them in pull-down experiments using recombinant GST-KC (Figure 3-9). In agreement with the data obtained from the yeast two-hybrid analysis, I found that the KLC region containing the TPR motifs (KLC1-C and -F, Figure 3-9) binds KC with very low efficiency, and that a portion of the HR domain and the linker region (aa 83-199)

together with the first two TPR motifs (199-296) are required for maximal interaction (KLC1-H, Figure 3-9). The need of a portion of the HR region for the binding to KC has been independently confirmed by pairwise yeast two-hybrid analysis (KLC1ΔN, Figure 3-7 A and B). In this assay, the relative strength of the interaction between KC and different KLC1 truncated mutants was assessed by both colony growth and β-galactosidase activity. Interestingly, the removal of the region 1-63 from KLC1 seems to enhance the binding to KC above the levels observed with full length KLC1 in GST-pull down, raising the possibility that this N-terminal portion might act *in vivo* as a regulatory region (Figure 3-9). Altogether, these results suggest that Kidins220 binds to the kinesin-1 complex using a novel docking site on KLC1, which includes the carboxy-terminal portion of the heptad repeats, the linker region and the first two TPR motifs.

Figure 3-7: *pairwise testing of interactions by yeast two-hybrid analysis*
Relative strength of interactions between different Kidins220 and kinesin-1 constructs, together with positive and negative controls, was measured by colony growth on high stringency medium (A) and by quantifying β-galactosidase activity associated with the resulting colonies (B). (A) A reduced number of colonies was observed for yeast co-transformed with KC and the TPR regions of KLC1 (KLC1-TPR, corresponding to KLC1-F in Figure 3-8), compared to the number of colonies obtained from the co-transformation of KC and full length KLC1 (set to 100%). No colonies were observed for the co-transformation with Pp5 (Pp5-TPR). These results indicate that TPR motifs are not sufficient to bind Kidins220. The addition of a portion of the HR repeats (KLC1-ΔN, corresponding to the construct KLC1-E in Figure 3-8) partially rescued the interaction (see also B), suggesting that Kidins220 interacts with KLC1 via a novel docking site, which includes both HR and TPR regions. The mutation Y1379A, which corresponds to Y24 in KIM(Y24A), strongly impairs the interaction between Kidins220 and KLC1, as shown by both yeast growth (A) and β-galactosidase activity (B), and is in agreement with the GST-pull down results shown in Figure 3-12. (B) Quantitative β-galactosidase assay on single yeast colonies (see Materials and Methods) confirmed that the TPR domain alone (KLC1-TPR) is unable to bind Kidins220, and that a portion of the HR repeats (KLC1-ΔN) is required. The β-galactosidase activity of the yeast co-transformed with KC and KLC1 encoding plasmids was set to 100%, whereas 0% corresponds to the activity of yeast transformed with KC alone. n = 3 colonies were measured for each couple. Error bars represent s.e.m.

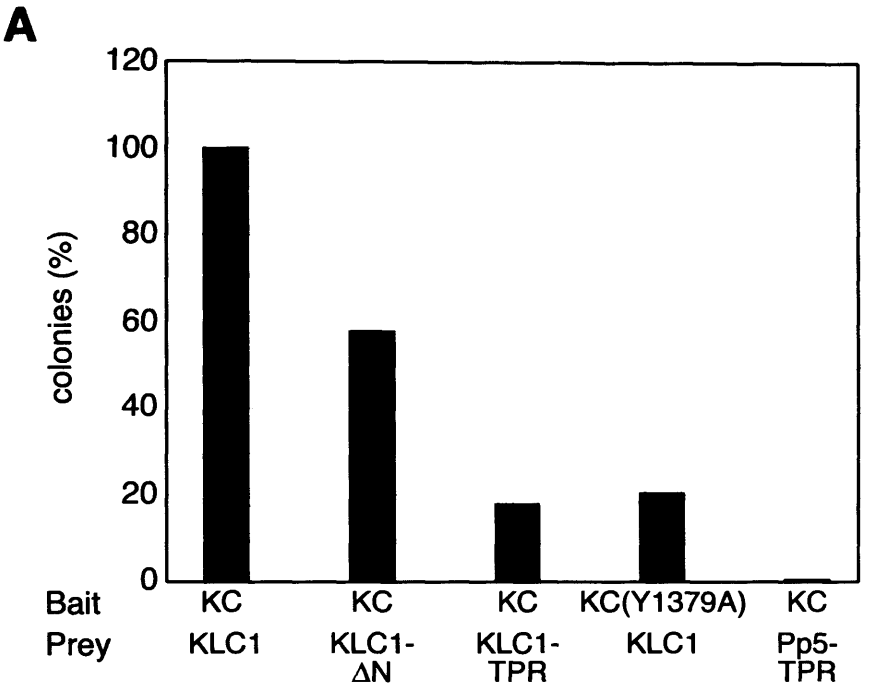
A
120
100
80
60
40
20
0
colonies (%)
Bait
Prey
KC
KLC1
KC
KLC1-ΔN
KC
KLC1-TPR
KC(Y1379A)
KLC1
KC
Pp5-TPR

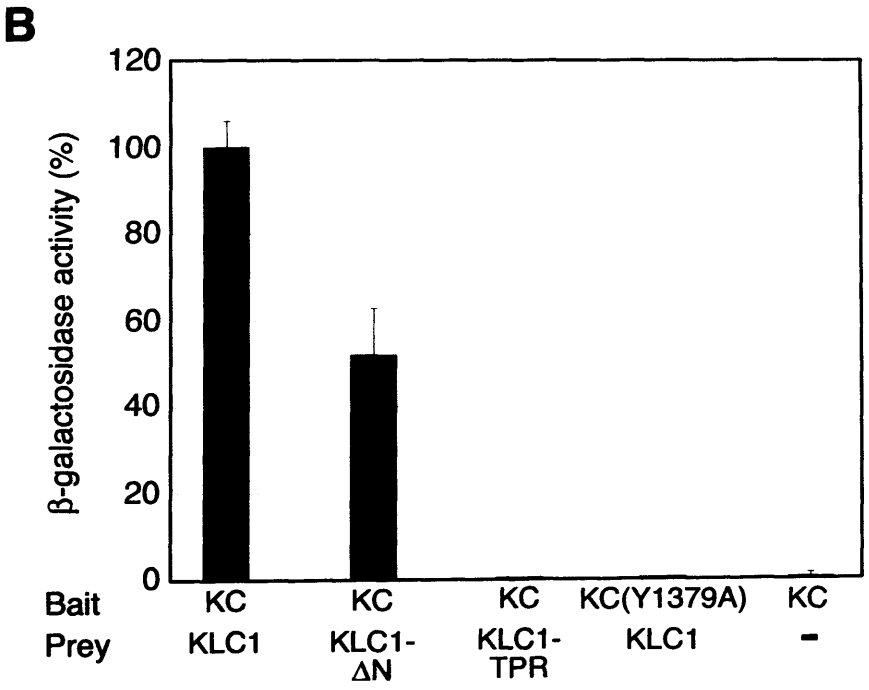
B
120
100
80
60
40
20
0
β-galactosidase activity (%)
Bait
Prey
KC
KLC1
KC
KLC1-ΔN
KC
KLC1-TPR
KC(Y1379A)
KLC1
KC
-

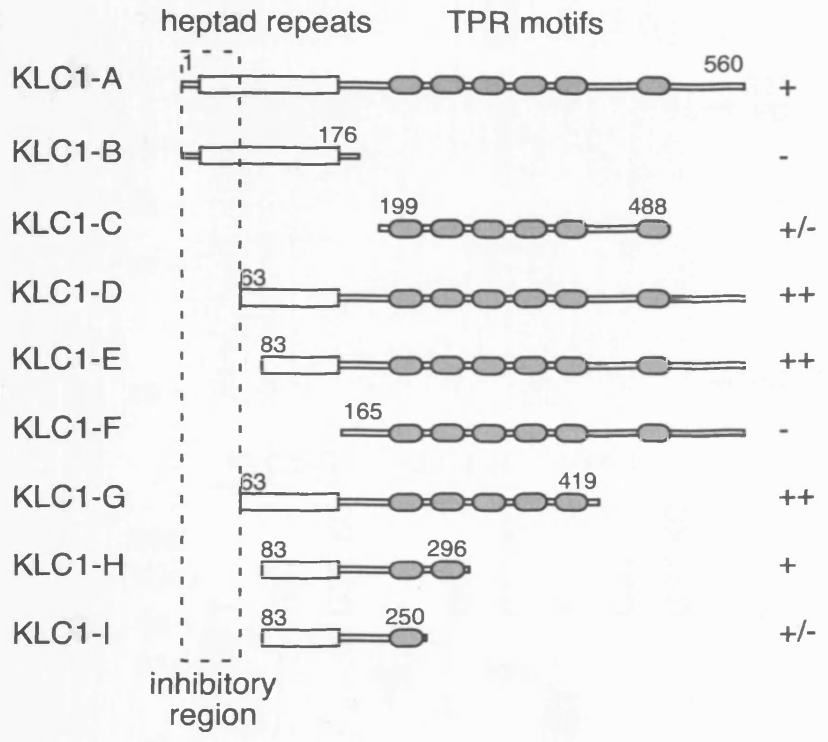

Figure 3-8: *KLC1 mutants used in this study*
Scheme of the KLC1 truncated mutants used in the GST-pull down experiments shown in Figure 3-11. The empty box corresponds to the heptad repeat region, whereas the grey ovals represent the TPR motifs. The putative inhibitory region for the Kidins220-KLC interaction (aa 1-63) is marked by a dashed line. The ability of each mutant to bind Kidins220 is reported on the right: + ≅ 100%, ++ ≅ 200%, +/- ≅ less than 25%, - = no binding.

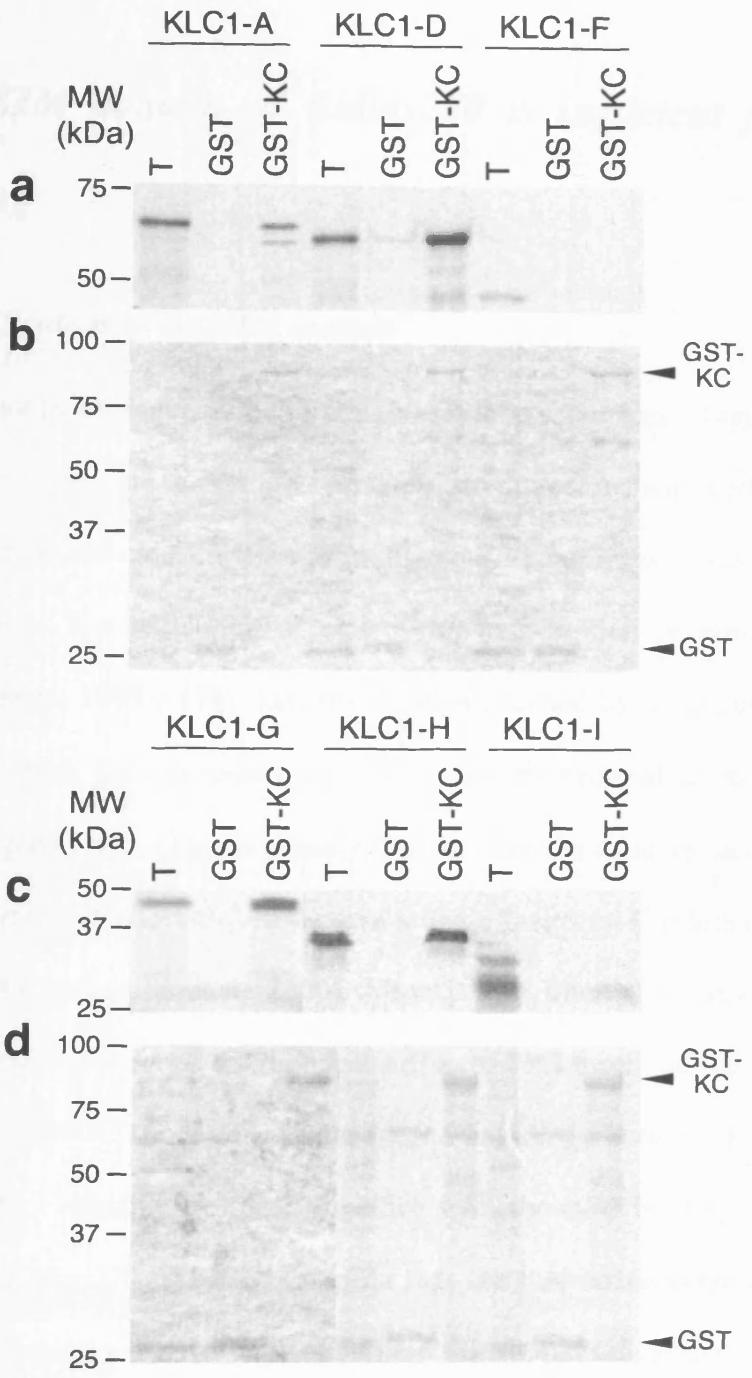

Figure 3-9: *the region 83-296 of KLC1 mediates the binding to Kidins220*
(*a*, *c*) Ability of in vitro [^{35}S]-labelled KLC1 mutants to bind GST-KC. Intensity of the bands was quantified as described in Materials and Methods. 1/25 of the starting in vitro transcription/translation mixes is loaded in T for comparison. (*b*, *d*) Coomassie staining of the SDS-PAGE gels corresponding to the experiments in *a* and *c*, respectively. The GST : GST-KC molar ratio is 2.7 ± 0.4. The amount of GST-KC loaded in different samples is comparable.

3.6 The KIM domain of Kidins220 is sufficient for KLC1 binding

3.6.1 Identification of the KIM domain

TPR motifs are degenerate, 34-amino acid long sequences, often organised in tandem arrays. They are extremely versatile structures, which mediate protein-protein interaction and the formation of multi-protein complexes involved in diverse cellular functions like regulation of cell cycle, transcription or protein transport (Blatch and Lassle, 1999). TPR domains are characterised by a variable number of TPR motifs, which are composed of two α-helices arranged in an antiparallel orientation (Figure 3-10). Ligands usually interact with the concave face (groove) of the TPR domains via a short sequence close to their C-termini (Terlecky et al., 1995; Gatto et al., 2000; Scheufler et al., 2000). Alternatively, internal sequences of partner proteins can bind to the loops that connect different TPR motifs in the TPR domain (Lapouge et al., 2000). The absence of sequence homology between Kidins220 and other known KLC-binding proteins, together with the new binding determinants recognised by Kidins220 on KLC1, suggest that the interaction between these two proteins is mediated by a novel motif. To map this domain, I generated a series of KC deletion mutants (Figure 3-11 A), which I expressed as GST-fusion proteins and tested in pull-down assays using *in vitro* transcribed-translated KLC1 (Figure 3-12 A), or PC12 cell lysates (Figure 3-12 B). In a parallel approach, I performed the same assays using the recombinant GST-KLC1 and *in vitro* translated Kidins220 mutants. The latter strategy was however abandoned in favour of the former, due to

the presence of a number of alternative start codons in the KC mutants, which resulted in multiple bands after *in vitro* translation (data not shown). I was able to identify the region between residues 1356-1395 as sufficient, and 1361-1390 as necessary, for the binding to KLC1. The region 1356-1395 was named KIM, for KLC Interacting Motif (Figure 3-11 B).

A growing number of proteins are known to interact with kinesin light chain. For some of them, the domains responsible for the interaction have been identified. I asked whether KIM bears any similarities with other domains, which have been shown to interact with KLC. As shown in Figure 3-13, different KLC-binding proteins do not share a common amino acid signature. A closer analysis however revealed a loosely conserved 5 amino acid sequence, which could represent the core of the KLC interacting interface (highlighted in Figure 3-13). KIM therefore represents a novel kinesin-1 interacting motif, which specifically binds kinesin-1, as shown by its inability to interact with other kinesins, such as kinesin-3 (Figure 3-12 B). The interaction between KIM and KLC is highly specific, since single-point mutations of several of the amino acid residues of KIM completely abolished the binding to kinesin-1 in GST-pull down. As an example, Figure 3-12 B shows that KIM(Y24A), in which tyrosine 24 (corresponding to residue 1379 of the full-length protein) is mutated to alanine, is unable to bind the kinesin-1 complex. The inhibitory effect of the Y1379A mutation on the binding of KC to KLC1 was confirmed by pairwise yeast two-hybrid analysis, as shown by both number of colonies and β-galactosidase activity (Figure 3-7). A more detailed characterisation of how other KIM mutations affect the binding to KLC1, together with an analysis

of the predicted three dimensional structure of KIM, will be presented in the following chapter.

3.6.2 KIM mediates the recruitment of kinesin-1 in PC12 cells

The experiment described in Figure 3-14 was performed by Dr. V. Neubrand, with constructs that I generated.

All the biochemical experiments described above were carried out with recombinant GST-KC. To confirm the binding to the full length Kidins220 in a cellular context, Dr. V. Neubrand transfected PC12 cells with constructs encoding either the full length EGFP-Kidins220, or a mutant lacking the KIM domain (EGFP-Kidins220-ΔKIM). She then stained the cells with an antibody against KHC, and analysed the distribution of the proteins by confocal microscopy (Figure 3-14). Both the full length Kidins220 (Figure 3-14 *a*) and the ΔKIM mutant (Figure 3-14 *d*) are expressed at the same level in NGF-differentiated PC12 cells, and accumulate in discrete structures upon transfection. However, while Kidins220-positive structures were found both in the cell bodies and in the neurites (Figure 3-14 *a, c*), the majority of Kidins220-ΔKIM was confined to cell bodies (Figure 3-14 *d, f*). A marked overlap of kinesin-1 with EGFP-Kidins220 was observed (Figure 3-14 *a-c* arrowheads, and insets), whereas no co-localisation was found between KHC and the mutant lacking the KIM domain (Figure 3-14 *d-f*, and insets). Altogether, these findings indicate that the KIM domain of Kidins220 is responsible for the recruitment of the kinesin-1 complex both *in vitro* and in neuronal cells.

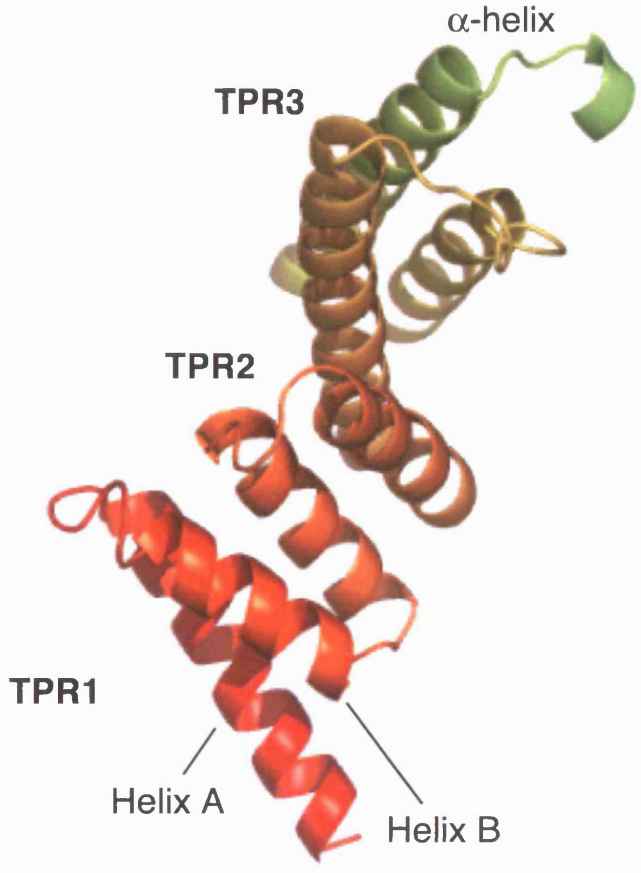

Figure 3-10: *three-dimensional structure of a TPR domain*
Ribbon representation of the TPR domain of *Plasmodium falciparum* FK506-binding protein. Each TPR motif is composed by two antiparallel α-helices (Helix A and Helix B). Adjacent TPR motifs are usually disposed in a parallel fashion, such as sequential α-helices are in an antiparallel orientation. The three TPR motifs, and an additional α-helix, are indicated. This structure prediction was obtained from the Structural Genomics Consortium (SGC) website, http://www.sgc.utoronto.ca/SGC-WebPages/StructureDescription/2FBN.php

Figure 3-11: *Kidins220 mutants used in this study*
(A) Scheme of the Kidins220 mutants used in this study. The ability of each mutant to bind KLC1 is reported on the right (+ = binding, - = no binding). The position of the kinesin-1 interacting motif (KIM) is highlighted by the dashed line. (B) Sequence of KIM (KC-K). The asterisk indicates the tyrosine (residue 1379 of the full-length protein) that is mutated to alanine in KIM(Y24A).

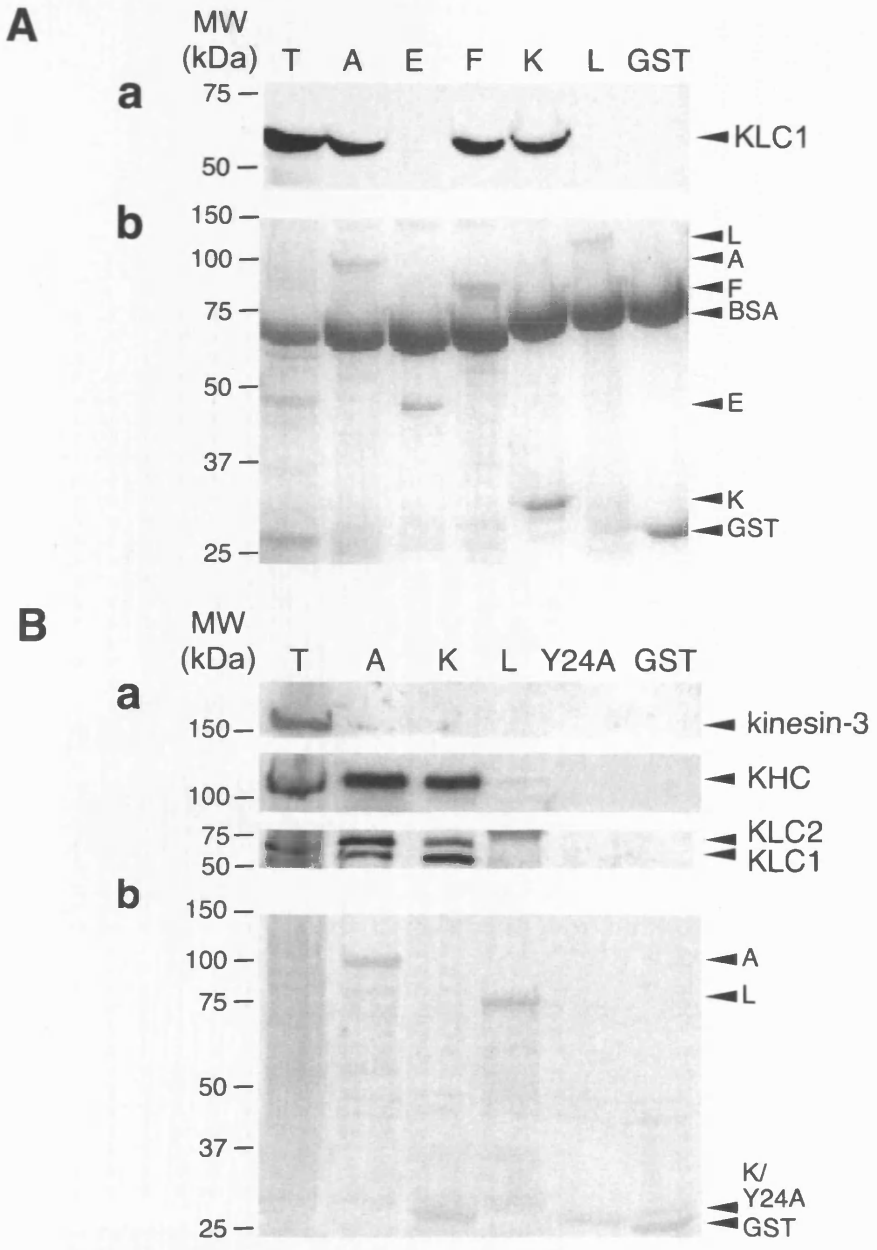

Figure 3-12: *the KLC-Interacting Motif (KIM) is sufficient for the binding of Kidins220 to KLC*

(A) *a.* The ability of some of the KC mutants expressed as GST-fusion proteins to bind *in vitro* [^{35}S]-labelled KLC1 is shown. 1/25 of the starting *in vitro* transcription/translation mix is loaded in T for comparison. *b.* Coomassie staining of the SDS-PAGE gel corresponding to this experiment. The molar ratios of GST versus the different GST-fusion proteins are the following: 7.9 for KC-A, 3.0 for KC-E, 3.3 for KC-F, 1.5 for KC-K and 8.8 for KC-L. (B) *a.* The KIM motif is sufficient to bind the native kinesin-1 motor complex. PC12 cells lysates were incubated with either GST or GST-fusion proteins pre-bound to glutathione-beads, as indicated. The bound material was analysed by Western blot using anti-kinesin 3, anti-KHC and anti-KLC antibodies. T corresponds to 10 µg of total lysate. *b.* Ponceau staining of the nitrocellulose membrane corresponding to this experiment. The molar ratios of GST versus the different GST-fusion proteins are the following: 3.7 for KC-A, 1.1 for KC-K, 2.1 for KC-L, 2.2 for KIM(Y24A). Molar ratios were calculated as described in Materials and Methods.

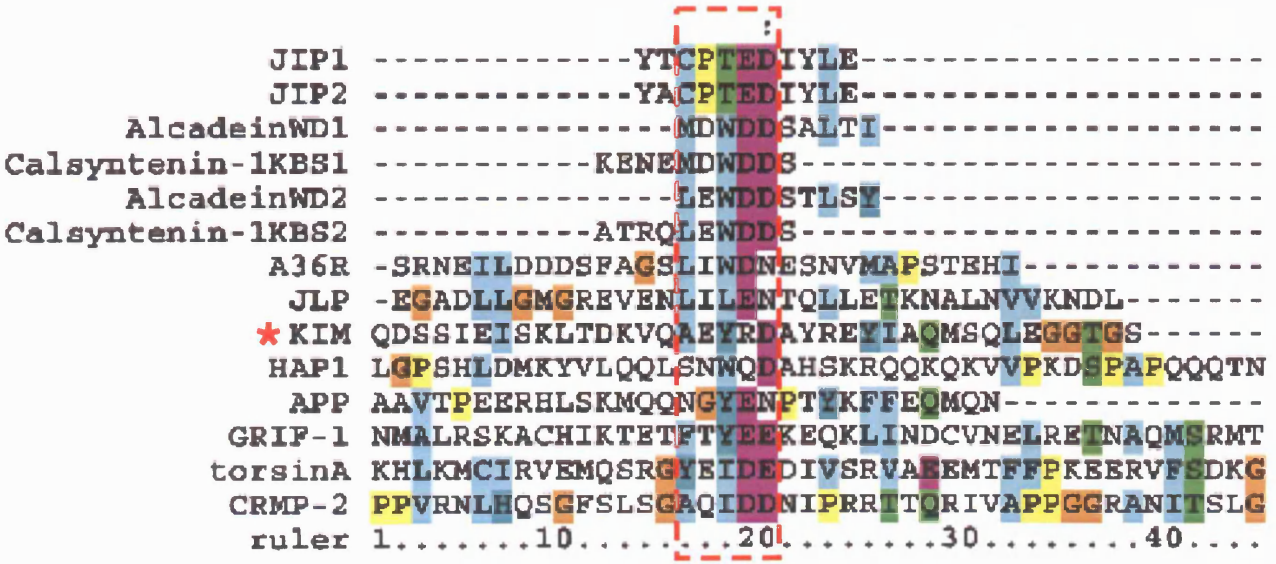

Figure 3-13: *alignment of different KLC-binding sequences*
Local alignment of different KLC-binding sequences revealed a loosely conserved 5 amino acid group, highlighted by the dashed line, which follows the consensus [hydrophobic] - [X] - [hydrophobic] - [acid/charged] - [acid/amine/charged]. The regions of the proteins analysed were as described in the corresponding publications: human JIP1 (aa 701-711) and human JIP2 (aa 814-824) (Verhey et al., 2001); mouse Alcadeinα tryptophan- and aspartic acid-containing sequence (WD)1 (aa 891-900) and WD2 (aa 962-971) (Araki et al., 2007); mouse Calsyntenin-1 KLC1-binding segment (KBS)1 (aa 897-906) and KBS2 (aa 966-979) (Konecna et al., 2006); vaccinia virus A36R (aa 81-111) (Ward and Moss, 2004); mouse JNK-associated leucine zipper protein (JLP, aa 400-434) (Nguyen et al., 2005); rat Huntingtin associated protein-1 (HAP1-A, aa 445-599) (McGuire et al., 2006); human APP (aa 653-695) (Kamal et al., 2000); rat γ-aminobutyric $acid_A$ receptor-interacting factor-1 (GRIF-1, aa 124-283) (Brickley et al., 2005); human torsinA (aa 251-332) (Kamm et al., 2004); human collapsing response mediator protein-2 (CRMP-2, aa 440-572) (Kimura et al., 2005). This alignment was performed with the help of Mike Mitchell, Bioinformatics and Biostatistics Service (CRUK).

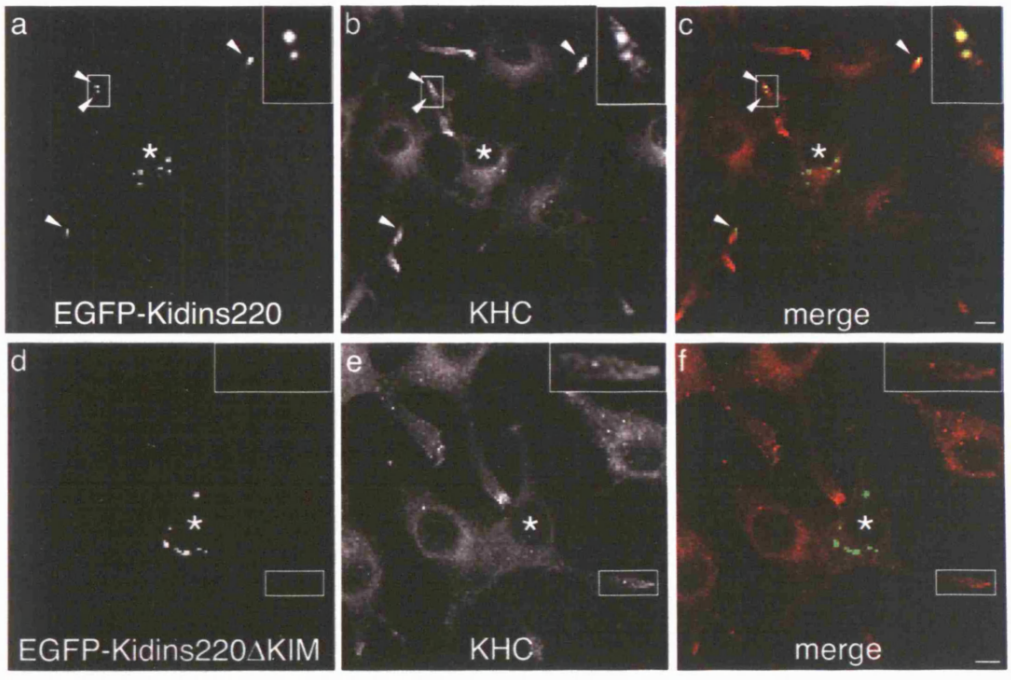

Figure 3-14: *KIM mediates the recruitment of kinesin-1 in PC12 cells*
PC12 cells were transfected with EGFP-Kidins220 (*a-c*) or EGFP-Kidins220-ΔKIM (*d-f*), and stained with anti-KHC antibody (*b*, *e*). Full-length Kidins220-positive puncta are positive for KHC (*c*, arrowheads and inset), whereas there is no significant overlapping between KHC and the mutant lacking the KIM domain (*f*, and inset). Asterisks indicate transfected cells. Scale bars = 5 μm. This experiment was performed by Dr. V. Neubrand.

3.7 Kidins220 is a kinesin-1 specific cargo

3.7.1 Analysis of Kidins220 transport in PC12 cells

The accumulation of Kidins220 at neurite tips implies the existence of an active targeting mechanism responsible for its peripheral localisation in differentiating PC12 cells. To visualise this process in real time, I imaged cells microinjected with a construct encoding EGFP-Kidins220 by time-lapse fluorescent microscopy, as described in Materials and Methods. EGFP-Kidins220 is localised to discrete vesicular structures, which show a bidirectional movement along the neurites. Upon treatment with NGF, these Kidins220-positive carriers accumulate at the tips of growing neuronal processes (Supplemental Video 1), in agreement with the immunofluorescence data on fixed cells. Figure 3-15 A shows a time-series of an EGFP-Kidins220 carrier (arrowhead) moving along a neurite towards the growth cone. The average speed of these carriers is 0.41 ± 0.05 μm/s (Figure 3-15 B), which is compatible with the rate observed for kinesin-1-mediated transport (Woehlke and Schliwa, 2000a; Hirokawa and Takemura, 2005).

Kidins220 is actively transported in PC12 cells, and binds KLC via the KIM motif. On the basis of these results, it is possible that kinesin-1 might be responsible for the intracellular trafficking of Kidins220. If this is the case, the KIM peptide is predicted to have a dominant-negative effect, since its binding to KLC should block the interaction with full-length Kidins220 and impair its transport. To test this hypothesis, I co-injected plasmids encoding EGFP-Kidins220 with constructs encoding either mRFP-tagged KIM or mRFP-KIM(Y24A), and analysed their effect

on the formation and transport of Kidins220-positive structures by time-lapse microscopy. Firstly, I monitored the transport of EGFP-Kidins220 positive structures in the presence of KIM(Y24A), and I compared it to the case where only EGFP-Kidins220 was expressed. I found that the co-expression of KIM(Y24A) did not have any effect on the speed of the moving carriers, whose behaviour was indistinguishable from the control samples (0.45 ± 0.10 μm/s; Figure 3-15 B). In contrast, the average speed of the carriers in cells overexpressing KIM was reduced to 0.16 ± 0.02 μm/s (Figure 3-15 B). However, the number of structures per neurite was unaffected by KIM overexpression (5.69 ± 0.87 structures for cells expressing KIM(Y24A), 5.38 ± 0.93 for cells expressing KIM, Figure 3-15 C), suggesting that the presence of this peptide does not interfere with the biogenesis of the EGFP-Kidins220-positive structures, but rather selectively impairs their trafficking. In agreement with this hypothesis, the average maximum displacement of the EGFP-Kidins220 positive carriers was significantly reduced in KIM-expressing cells in comparison to KIM(Y24A)-microinjected samples (3.5 ± 0.63 μm versus 7.1 ± 1.03 μm, Figure 3-15 D, Supplemental Videos 2 and 3). Quantitative kinetic analysis revealed that in KIM-expressing cells, the vast majority (86%) of the Kidins220-positive structures are stationary (maximum displacement between 0 and 3.9 μm), and only 14% move farther away (Figure 3-15 E, black bars). In contrast, in cells microinjected with a plasmid encoding the inactive KIM(Y24A) mutant, 54% of the particles have a maximum displacement between 0 and 3.9 μm, and the remaining cover longer distances, up to 45 μm (Figure 3-15 E, white bars). Overexpression of KIM, therefore, results in a net increase in the number of structures that are either stationary or undergo only short-range movements.

Altogether, these findings suggest that KIM overexpression has a dominant-negative effect on the transport of Kidins220-positive carriers, causing a reduction in both their maximum displacement and average speed, and support the hypothesis that the trafficking of Kidins220 is mediated by the kinesin-1 complex.

Figure 3-15: *KIM overexpression impairs Kidins220 trafficking in PC12 cells*
(A) EGFP-Kidins220 is transported along neurites in PC12 cells. (*a*) Phase image of a microinjected cell and (*b*) time series of the boxed area. Arrowheads indicate a EGFP-Kidins220-positive moving carrier. Scale bar = 5 μm. (B-E) NGF-treated PC12 cells were co-injected with plasmids driving the expression of EGFP-Kidins220 alone (control) or in combination with either mRFP-KIM, or mRFP-KIM(Y24A). (B) The average speed of EGFP-Kidins220 positive carriers is decreased by mRFP-KIM expression. (C) The average number of EGFP-Kidins220 positive carriers per neurite is not affected by the overexpression of mRFP-KIM. n = 13 neurites were analysed for both conditions. (D) The average maximum displacement of EGFP-Kidins220 positive carriers is reduced in mRFP-KIM-expressing cells. The analysis of the movement of EGFP-Kidins220 positive carriers is shown in (E) (see text and Materials and Methods for details). A 4 μm binning starting from 0 was applied. n = 24 carriers for EGFP-Kidins220 expressing cells, n = 70 carriers for EGFP-Kidins220 and mRFP-KIM expressing cells; n = 74 carriers for EGFP-Kidins220 and mRFP-KIM(Y24A) expressing cells. Movies were acquired from three independent experiments. Error bars represent s.e.m.

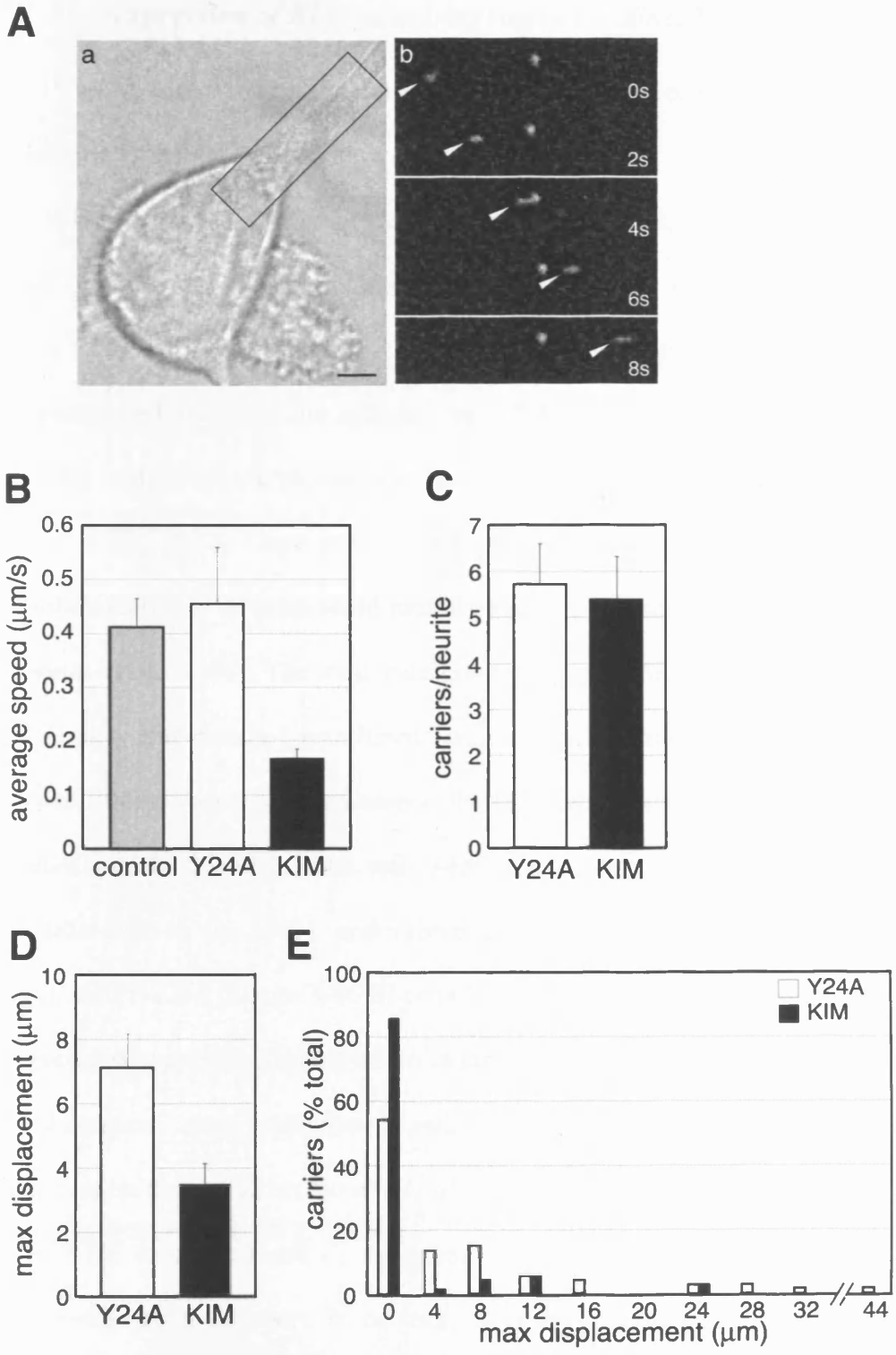
A
a
b
0s
2s
4s
6s
8s
B
average speed (μm/s)
0.6
0.5
0.4
0.3
0.2
0.1
0
control
Y24A
KIM
C
carriers/neurite
7
6
5
4
3
2
1
0
Y24A
KIM
D
max displacement (μm)
10
8
6
4
2
0
Y24A
KIM
E
carriers (% total)
100
80
60
40
20
0
Y24A
KIM
0
4
8
12
16
20
24
28
32
44
max displacement (μm)

3.7.2 *Overexpression of KIM selectively impairs Kidins220 trafficking*

The experiment described in Figure 3-16 was performed by Dr. T. Newsome, with constructs that I generated.

KIM might selectively prevent Kidins220 transport, or it could act as a general inhibitor for kinesin-1-dependent trafficking. In order to discriminate between these two possibilities, Dr. T. Newsome tested whether different forms of kinesin-mediated transport are affected by KIM overexpression. Vaccinia virus reaches the surface of infected cells by exploiting a kinesin-1-dependent mechanism (Rietdorf et al., 2001). Once at the plasma membrane, the virus switches from a microtubule-based to an actin-based motility and then spreads to neighbouring cells (Newsome et al., 2004). The viral membrane protein A36R is required for actin-based motility and kinesin-1 recruitment, which occurs via the TPRs of KLC (Ward and Moss, 2004). Vaccinia virus transport therefore represents an ideal system to test KIM function. To this end, HeLa cells were infected with the vaccinia A36R-YdF strain (Rietdorf et al., 2001), and subsequently transfected with mRFP (Figure 3-16 A), mRFP-KIM (Figure 3-16 B) or mRFP-TPRs (Figure 3-16 C). Extracellular viral particles were then visualised by wide field microscopy in the absence of permeabilisation (see Materials and Methods). Strikingly, mRFP-KIM overexpression did not affect the ability of the virus to reach the plasma membrane (Figure 3-16, compare *b* and *e*), suggesting that mRFP-KIM does not perturb its kinesin-1-dependent transport. In contrast, the overexpression of the TPR domain impaired the transport of the viral particles to the cell periphery (Figure 3-16, compare *b* and *h*). Altogether, these experiments indicate that KIM is not a general

inhibitor of kinesin-1 function, but it rather selectively blocks the recruitment of Kidins220 by interfering with a specific binding site on KLC.

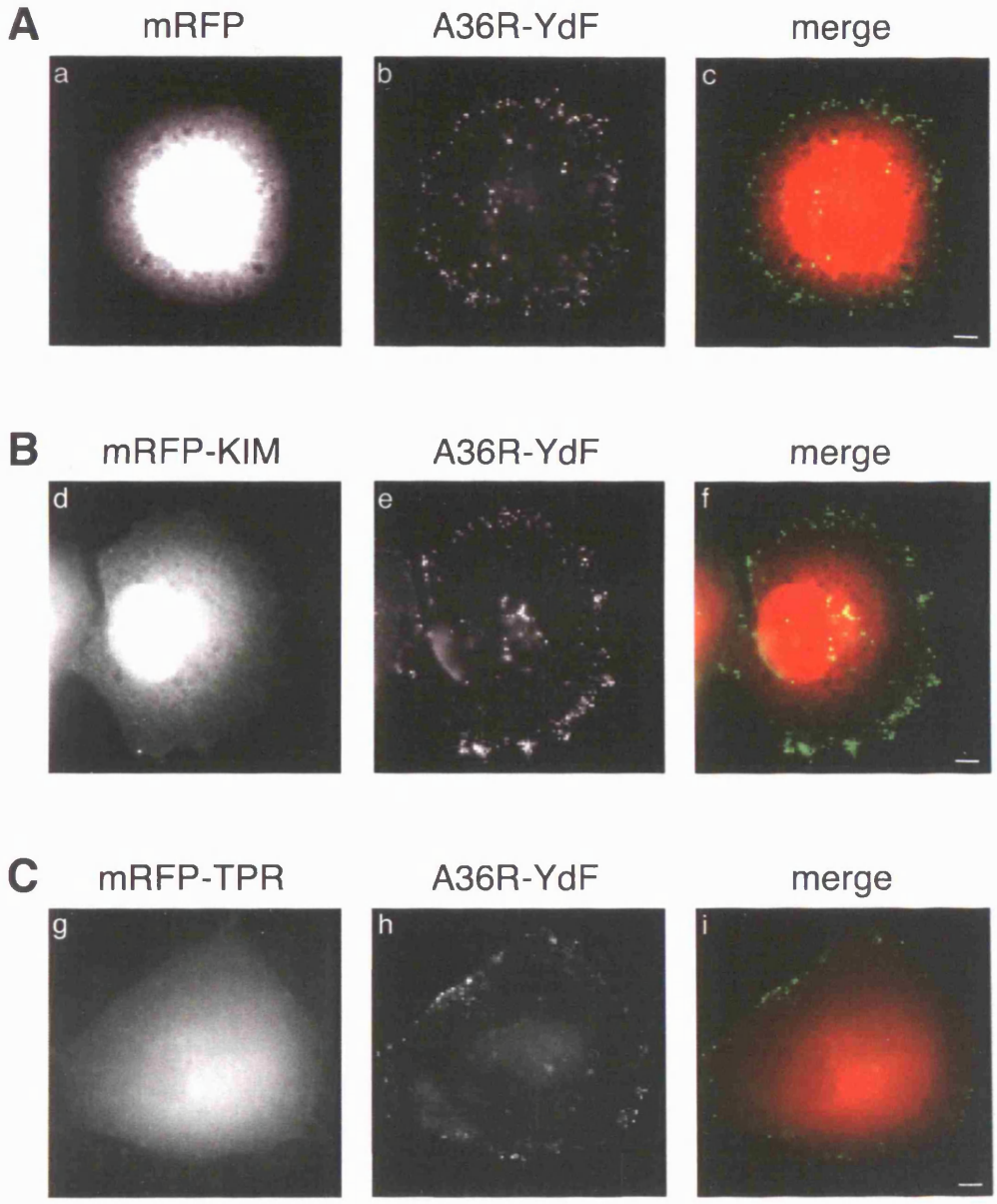

Figure 3-16: *the translocation of vaccinia virus to the plasma membrane is unaffected by KIM*
HeLa cells were infected with the A36R-YdF vaccinia virus strain and 4 h later transfected with mRFP (A), mRFP-KIM (B), or mRFP-TPR (C). After a further 4 h, cells were processed for immunofluorescence in absence of permeabilisation and extracellular virus particles were visualised. The distribution of the virus on the plasma membrane is independent of the overexpression of mRFP-KIM (compare *b* and *e*), whereas it is reduced by the overexpression of the mRFP-TPR domain (compare *b* and *h*). Scale bars = 5 µm. This experiment was performed by Dr. T. Newsome.

3.8 Effects of KIM overexpression

3.8.1 Inhibition of the activation of the MAP kinase pathway

The experiment in Figure 3-17 was performed by Dr. V. Neubrand, with constructs that I generated.

Kidins220 has been linked to NGF signalling and sustained MAPK-activation (Arevalo et al., 2004; Arevalo et al., 2006). These observations prompted us to consider the possibility that the kinesin-1-dependent targeting of Kidins220 plays a role in its signalling function. To test this hypothesis, Dr. V. Neubrand examined the effect of KIM overexpression on the NGF-dependent activation of the MAP kinase pathway. Downregulation of Kidins220 by RNAi has been previously reported to reduce MAPK activation (Arevalo et al., 2004). This approach however does not directly answer the question of whether the kinesin-1 dependent transport of Kidins220 is required for NGF signalling. She therefore chose to tackle this problem by taking a dominant-negative approach, which would allow her to specifically interfere with the kinesin-1-mediated transport of Kidins220, leaving unaffected other interactions in which Kidins220 might be involved, such as those with $p75^{NTR}$ and α-syntrophin. To examine the activation of MAPK, she transfected PC12 cells with either mRFP-KIM or mRFP-KIM(Y24A), and upon short treatment with NGF (5 hours stimulation, see Materials and Methods), cells were stained for the phosphorylated form of MAPK (P-MAPK). As shown in Figure 3-17 A, the P-MAPK labelling was reduced in mRFP-KIM-transfected cells compared to non-transfected cells, whereas the KIM(Y24A) mutant had no significant effect on the

intensity of the staining. Quantitative analysis of the mean fluorescence intensity of these samples revealed that mRFP-KIM-transfected cells showed a reduction of 40% in the P-MAPK staining compared to mRFP-KIM(Y24A)-expressing samples or non-transfected cells (Figure 3-17 B). This result suggests that the kinesin-1-dependent transport of Kidins220 might be required for downstream events in response to NGF stimuli.

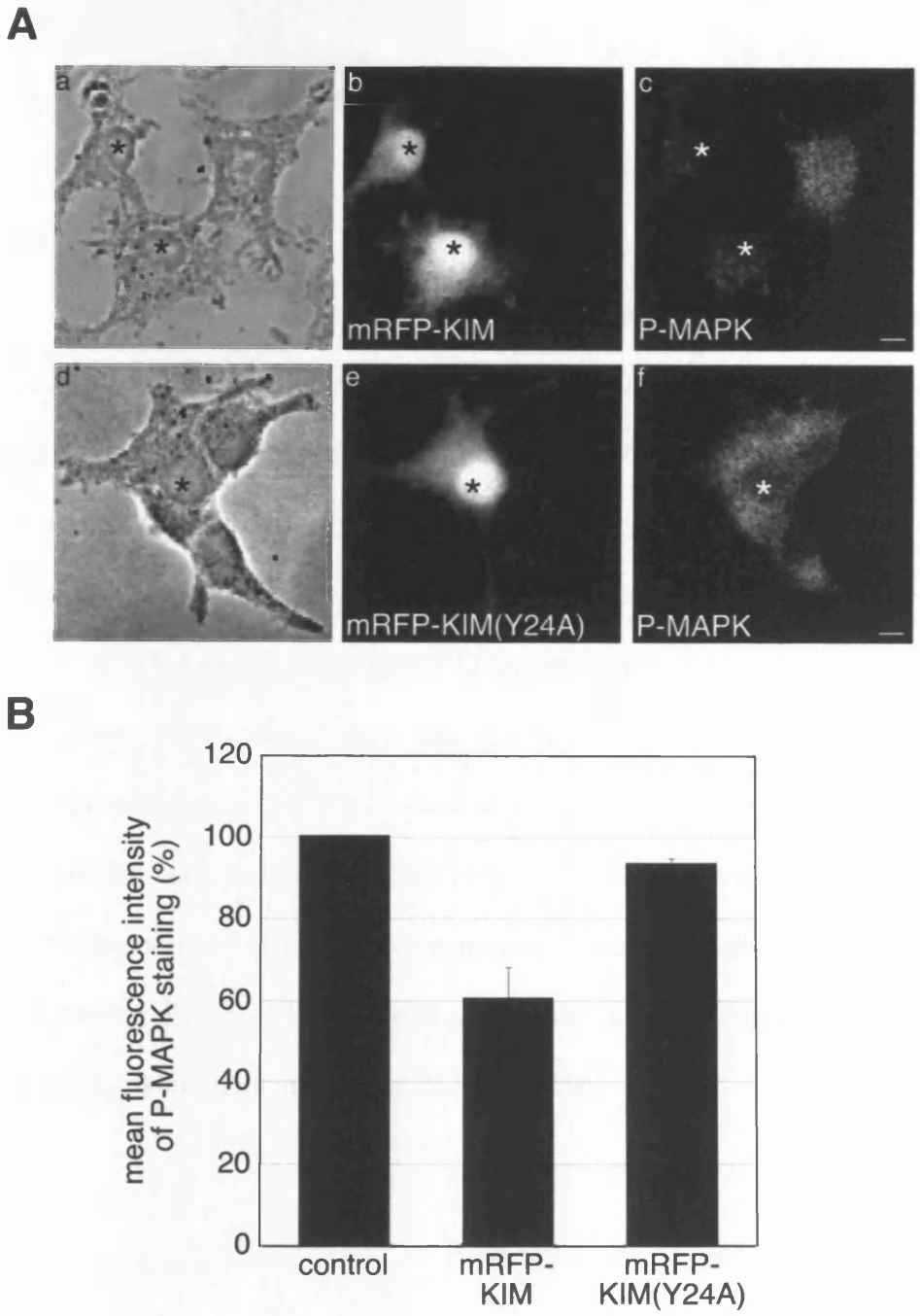

Figure 3-17: *overexpression of KIM reduces the phosphorylation of MAPK in PC12 cells*

(A) PC12 cells were transfected with mRFP-KIM (*a-c*) or mRFP-KIM(Y24A) (*d-f*), then fixed and immunostained for P-MAPK (*c, f*). mRFP-KIM-expressing cells show a reduced P-MAPK staining compared to non-transfected cells and mRFP-KIM(Y24A) expressing cells. Transfected cells are marked with asterisks. Scale bars = 5 µm. (B) The mean fluorescence intensities of untransfected cells and cells overexpressing mRFP-KIM or mRFP-KIM(Y24A) were determined as described in Materials and Methods. mRFP-KIM, n = 74 cells; mRFP-KIM(Y24A), n = 63 cells; non-transfected cells, n = 204 derived from three independent experiments. Error bars represent s.e.m. This experiment was performed by Dr. V. Neubrand.

3.8.2 Inhibition of neuronal differentiation

The experiment in Figure 3-18 was performed by Dr. A. Bracale, with constructs that I generated.

The NGF-mediated activation of the MAPK pathway plays a major role in promoting neuronal differentiation in PC12 cells (Vaudry et al., 2002). In light of the results described above, interfering with Kidins220 transport by KIM overexpression is predicted to reduce or delay the NGF-dependent differentiation of PC12 cells. To test this hypothesis, Dr. A. Bracale transfected undifferentiated PC12 cells with mRFP, mRFP-KIM or mRFP-KIM(Y24A) prior to NGF treatment (Figure 3-18). Cells were fixed after 3 days and differentiation was then quantified. KIM overexpression caused a 40% reduction in the percentage of differentiated cells, whereas the transfection of KIM(Y24A) was ineffective (Figure 3-18 B). These results demonstrate that KIM overexpression interferes with neurite outgrowth in NGF-treated PC12 cells, suggesting that the kinesin-1-dependent transport of Kidins220 participates in neuronal differentiation.

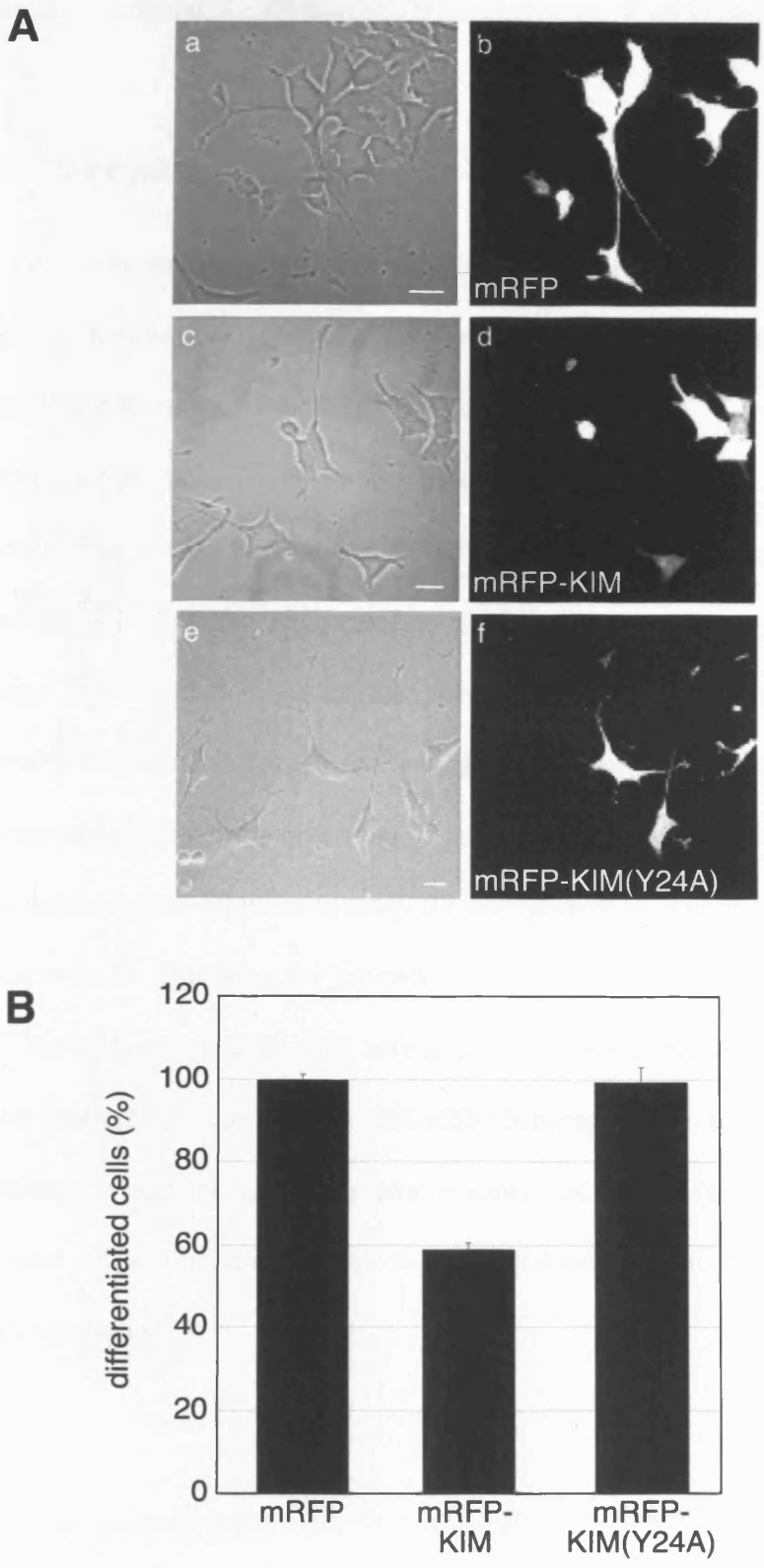

Figure 3-18: *KIM overexpression inhibits neurite outgrowth in PC12 cells*
(A) Undifferentiated PC12 cells were transfected with mRFP (*a*, *b*), mRFP-KIM (*c*, *d*), or mRFP-KIM(Y24A) (*e*, *f*), treated for 3 days with NGF, and analysed by confocal microscopy. Scale bars = 20 µm. (B) The percentage of differentiated cells in each condition is shown. Differentiation in mRFP-expressing cells was set to 100%. Between 50 and 140 cells were counted for each experiment (n = 3). Error bars represent s.e.m. This experiment was performed by Dr. A. Bracale.

3.9 Future perspectives

We have shown that the formation of a complex with the KLC subunit of the kinesin-1 motor complex is required for the transport and intracellular localisation of Kidins220. Furthermore, impairing Kidins220 trafficking by overexpression of the kinesin-1 binding motif (KIM) results in an inhibition of MAPK activation and of neuronal differentiation in response to NGF. We are currently investigating whether Kidins220 could link the neurotrophin receptors to the kinesin-1 complex, thus mediating their correct target to the plasma membrane. To further analyse the relationship between Kidins220 trafficking and neurotrophin receptors, it will be necessary to perform some live imaging experiments with labelled proteins. This kind of approach will allow us to study the co-transport of Kidins220 with Trks, and to characterise its regulation and kinetics.

The analysis of Kidins220 null mice is at present helping us to define how different types of neurons react to Kidins220 depletion. Once this is defined, it will be possible to select the optimal system to analyse Kidins220 trafficking, as well as the effects of its impairment on the establishment of a correct response to neurotrophic stimuli.

Chapter 4 – Modulation of the interaction between Kidins220 and KLC

4 Modulation of the interaction between Kidins220 and KLC

4.1 Introduction

We have shown that the interaction between Kidins220 and KLC is mediated by a short sequence, named KIM, which is located in the carboxy-terminal tail of Kidins220. KIM represents a novel kinesin-interacting motif, as it does not bear any similarities with the sequences of other known kinesin-binding proteins (see Figure 3-13). I was interested in studying in detail the molecular basis of the interaction between Kidins220 and kinesin-1. To better define this new docking interface, I sought to identify amino acid residues in the KIM sequence that are essential for the binding to KLC.

Individual motor proteins are able to transport multiple binding partners in a regulated manner. However, the molecular mechanisms by which motors distinguish and select cargo proteins are still poorly understood. Several recent studies have established that phosphorylation can regulate and coordinate the attachment/detachment of cargoes to specific motors. One of the first studies supporting this notion was by Morfini and colleagues (Morfini et al., 2002), where they demonstrated that phosphorylation of kinesin light chain by GSK3 inhibits anterograde transport in squid axoplasm, by causing the detachment of the motor from membranes. GSK3 might therefore mediate a regulatory switch of kinesin-1 motility, to ensure delivery of cargoes to specific subcellular compartments. Several kinesin-1 interacting proteins have also been shown to undergo phosphorylation. In

the case of vaccinia virus, for example, Src-mediated phosphorylation of the viral protein A36R at the plasma membrane is required to release kinesin-1, and for the subsequent switch to actin-based motility (Newsome et al., 2004). It has also been suggested that phosphorylation modulates the binding of APP to the kinesin-1 complex. The phosphorylated and non-phosphorylated forms of APP are transported into neuronal processes by different pathways. Phosphorylation of APP triggers the formation of a pAPP-JIP-1 complex, which accumulates in neurites independently of the non-phosphorylated APP (Muresan and Muresan, 2005). Analysis of the KIM sequence (http://bioinformatics.lcd-ustc.org/gps_web/index.php, Zhou et al., 2004; Xue et al., 2005) revealed a series of predicted consensus sites for phosphorylation, which are listed in Table 9. On the basis of these considerations, I asked whether the interaction between Kidins220 and kinesin light chain is modulated by phosphorylation.

Table 9: *predicted phosphorylation sites on KIM*

Asterisks mark kinases that have been further analysed in this study. CK1: casein kinase 1; CK2: casein kinase 2; GRK: G protein-coupled receptor kinase; IKK: inhibitor of nuclear factor kappa-B kinase; PKR: interferon-induced, double-stranded RNA-activated protein kinase; PLK: Polo-like kinase; DNA-PK: DNA-dependent protein kinase; ILK: integrin-linked protein kinase; MAPKKK: mitogen-activated protein kinase kinase kinase; ALK: anaplastic lymphoma kinase; CSK: C-Src kinase; EGFR: epidermal growth factor receptor; EPHA: ephrin type-A receptor; EPHB: ephrins type-B receptor; Fer: proto-oncogene tyrosine-protein kinase Fer; Fes: proto-oncogene tyrosine-protein kinase Fes/Fps; FGFR: fibroblast growth factor receptor; Fgr: proto-oncogene tyrosine-protein kinase Fgr; Fyn: proto-oncogene tyrosine-protein kinase Fyn; Yes: proto-oncogene tyrosine-protein kinase Yes; IR: insulin receptor; LYN: tyrosine-protein kinase LYN; PDGFR: platelet-derived growth factor receptor; SRC: proto-oncogene tyrosine-protein kinase Src;

SYK: tyrosine-protein kinase Syk; VEGFR: vascular endothelial growth factor receptor; ZAP-70: zeta-associated protein of 70 kDa; LCK: proto-oncogene tyrosine-protein kinase LCK; RET: proto-oncogene tyrosine-protein kinase receptor ret; ATM: ataxia telangiectasia mutated serine-protein kinase; CaM-II: calcium/calmodulin-dependent protein kinase type II; PAK: p21-activated kinase.

Residue	Kinase	Residue	Kinase
Ser 5	CK1*	Tyr 20	Fyn/Yes*
Ser 5	CK2*	Tyr 20	IR
Ser 5	GRK	Tyr 20	LYN
Ser 5	IKK	Tyr 20	PDGFR
Ser 5	PKR	Tyr 20	SRC*
Ser 5	PLK	Tyr 20	SYK
Ser 6	CK1	Tyr 20	VEGFR
Ser 6	DNA-PK	Tyr 20	ZAP70
Ser 6	PLK	Tyr 24	ALK
Ser 10	PKR	Tyr 24	Fgr
Ser 10	PLK	Tyr 24	LCK
Thr 13	ILK	Tyr 24	LYN
Thr 13	MAPKKK	Tyr 24	RET
Tyr 20	ALK	Tyr 24	SYK
Tyr 20	CSK	Tyr 24	VEGFR
Tyr 20	EGFR	Ser 32	ATM
Tyr 20	EPHA/B	Ser 32	CaM-II
Tyr 20	Fer	Ser 32	CK2*
Tyr 20	Fes	Ser 32	PAK
Tyr 20	FGFR	Ser 32	PLK
Tyr 20	Fgr		

4.2 Molecular basis of the interaction between KIM and KLC

4.2.1 Amino acid sequence and predicted three dimensional structure of KIM

By comparing the sequences of different Kidins220 orthologues, I found that KIM is highly conserved, while the flanking regions are more divergent between

different organisms (Figure 4-1 A, also Figure 1-5). I identified a few residues that are conserved also in *Drosophila* and *C. elegans*, highlighted in Figure 4-1 A.

Figure 4-1 B shows a prediction of the three dimensional structure of KIM, obtained by the Robetta server (http://robetta.bakerlab.org/). KIM, delimited by the arrowheads, is predicted to fold as a helix, while the flanking sequences have an extended structure.

4.2.1.1 Mutation of KIM residues disrupts the binding to KLC1

Taking into consideration the results obtained from the sequence analysis and the structure prediction, I designed the single point-mutants KIM(Q17A) and KIM(Y20P). Both these substitutions are predicted to disrupt the helical structure of KIM, and could therefore affect its ability to bind KLC. In addition, I engineered the triple mutant KIM(Y24A, E26A, Y27A) (Figure 4-2 A). In this mutant protein, the three substitutions are predicted to complement each other to recreate the helix, thus restoring the KLC-binding site. In order to verify our predictions, I expressed all these mutants as GST-fusion proteins and I tested them in GST-pull down assays using [^{35}S]-labelled KLC1. The results of this first set of experiments are reported in Figure 4-2 B. The single-point mutations Q17A and Y20P strongly inhibited the binding to KLC1, in accordance to our predictions. However, I could not detect any binding between the triple mutant and KLC1, suggesting that the three substitutions did not recreate the correct three-dimensional structure required for the interaction.

A

```
                                  ▼  ▼     ▼▼
human          NSQDSSIEISKLTDKVQAEYRDAYREYIAQMSQLEGGPGS
rat            NSQDSSIEISKLTDKVQAEYRDAYREYIAQMSQLEGGTGS
mouse          NSQDSSIEISKLTDKVQAEYRDAYREYIAQMSQLEGGTGS
Danio          NSQESSNEICKLTDKQQAEYRNAYEDYIASMSQLELG---
Drosophila     MEKQVTLEEQMICGTLQTLNEEAYEDVASS-ERPSPTGEM
C.elegans      NATELSIDHKCLMEKLSGMDLTETEGDVNEMHFSHFSSST
```

B

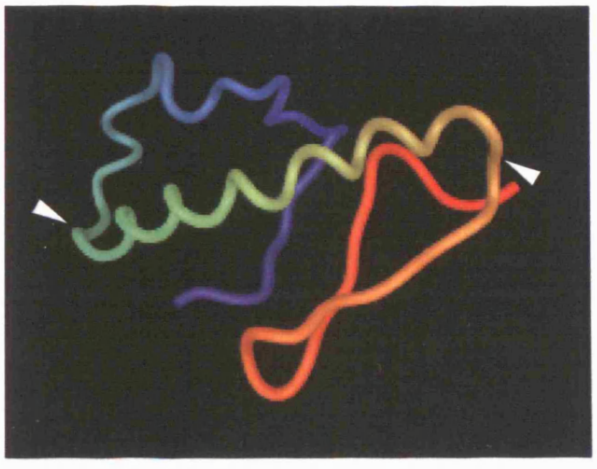

Figure 4-1: *amino acid sequence and three-dimensional structure of KIM*
(A) Alignment of KIM sequences from different organisms. Conserved residues are highlighted. Arrowheads indicate the residues that were mutated to alanine for the GST-pull down experiments in Figure 4-2. Accession numbers are as in Figure 1-12. (B)Prediction of the three-dimensional structure of KIM (http://robetta.bakerlab.org/). KIM (delimited by the arrowheads) is predicted to fold as a helix.

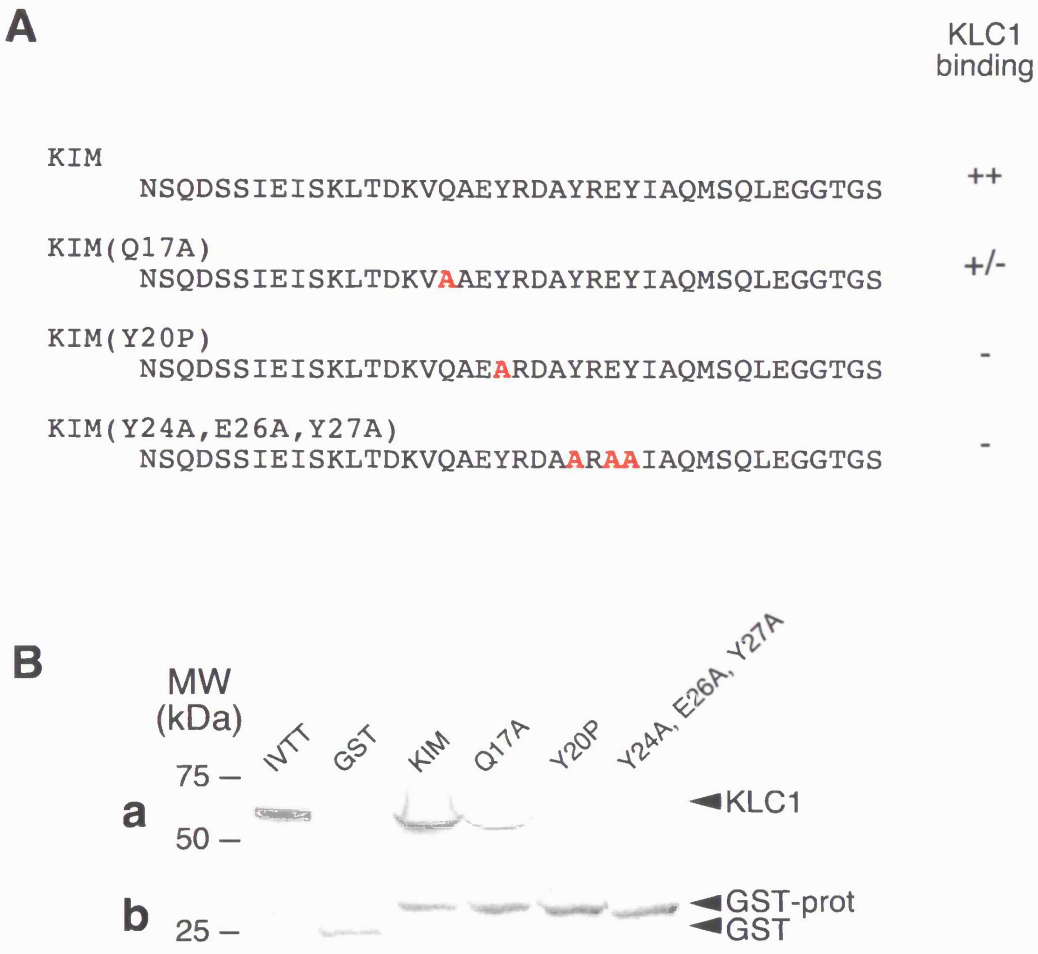

Figure 4-2: *mutations of KIM residues disrupt the binding to KLC1*
(A) Sequences of the KIM mutants used in the GST-pull down experiments shown in (B). The ability of each mutant to bind KLC1 is indicated on the right: ++ ≅ 100%; +/- ≅ 25%; - = no binding. (B) KIM mutants were expressed as GST-fusion proteins, and tested in a GST-pull down assay using *in vitro* [^{35}S]-labeled KLC1. The ability of [^{35}S]-KLC1 to bind different mutant proteins is shown in *a*. The Coomassie-staining of the recombinant GST-proteins is shown in *b*.

4.2.2 *Identification of essential residues by alanine- and phosphorylation-scanning*

To further investigate the molecular basis of the interaction between KIM and KLC, I used peptide arrays, provided by the Peptide Synthesis Laboratory at Cancer Research UK. In the arrays, peptides corresponding to series of specific KIM single point mutations or phosphorylated isoforms were synthesised on a membrane. Membranes were then incubated with purified KLC1, and bound proteins were detected with anti-KLC1 antibodies and HRP-conjugated secondary antibodies, as described in Materials and Methods. The binding of KLC1 to each peptide was quantified, and normalised to the binding to the non-mutated KIM, which was arbitrarily set to 1. In the first array, I analysed the effect of the substitution of each residue to alanine ("alanine scanning", Figure 4-3). This approach allowed me to identify two mutants that showed significant changes in the affinity for KLC1: KIM(E19A), which showed the most pronounced reduction of KLC1 binding, and KIM(E26A), whose binding capacity was massively increased.

We also asked whether phosphorylation might affect the interaction between KIM and KLC1. To this purpose, several peptide arrays were generated, where all the possible combinations of phosphorylated tyrosine, serine and threonine residues were represented ("phosphorylation scanning"). In a first array, I analysed the effect of tyrosine phosphorylation on KLC1 binding (Figure 4-4). I observed that phosphorylation of tyrosine 27 always enhances the interaction between KIM and KLC1, independently of the phosphorylation state of the other two tyrosines. Phosphorylation of both tyrosine 20 and tyrosine 24, on the contrary, has an

inhibitory effect on the binding. I then considered phosphorylation of the serine and threonine residues (Figure 4-5). Phosphorylation of serine 32, and to a lesser extent, phosphorylation of threonine 13, enhances the binding affinity of KLC1. Phosphorylation of serine 6 and serine 10 instead has an inhibitory effect on the interaction. Furthermore, the effect of Ser32 phosphorylation is dominant over phosphorylation of all the other residues.

4.2.2.1 Validation of the results obtained from the peptide array

On the basis of the results obtained from the arrays, I designed the single point mutants KIM(E19A) and KIM(E26A). I expressed these mutants as GST-fusion proteins and I tested them in GST-pull down assays using [^{35}S]-labelled KLC1. The results of this set of experiments are shown in Figure 4-6. KIM(E19A) binds KLC1 poorly, in agreement with the data obtained from the peptide array. Surprisingly, KIM(E26A) also shows a reduced KLC1 binding, suggesting that the result from the peptide array was an artefact, probably due to an altered presentation of the peptide on the supporting membrane, and/or a boosting effect on binding of the membrane itself.

To further investigate the role of phosphorylation in the modulation of the binding between KIM and KLC1, I cloned and expressed the GST-fusion proteins of the three Y-A point mutants: KIM(Y20A), KIM(Y24A) and KIM(Y27A). As shown in Figure 4-6, these mutations completely abolished the binding to kinesin light chain.

4.2.3 Conclusions

I have tried to define the molecular basis of the interaction between Kidins220 and kinesin light chain. To this purpose, I cloned and expressed a series of single-point mutants of the kinesin interacting motif (KIM), and tested their ability to bind KLC1 *in vitro*. I found that all the substitutions had an inhibitory effect on the binding. This could be due to misfolding of the mutant peptides, however, many of the mutations were not predicted to alter the helical structure of KIM. It is possible that the three dimensional organisation of the docking interface between KIM and KLC is crucial for the interaction of these two proteins, and that, as a consequence, subtle changes might impair the binding of these two interacting partners.

All the *in vitro* experiments described in this section were conducted with the recombinant GST-KIM. Although KIM is sufficient for the binding to KLC1, it is possible that in a cellular context, other parts of Kidins220 might help to stabilise the interaction. To better identify the determinants of the binding, therefore, it will be necessary to mutate the same residues in the full-length protein, and repeat the binding assays with native proteins.

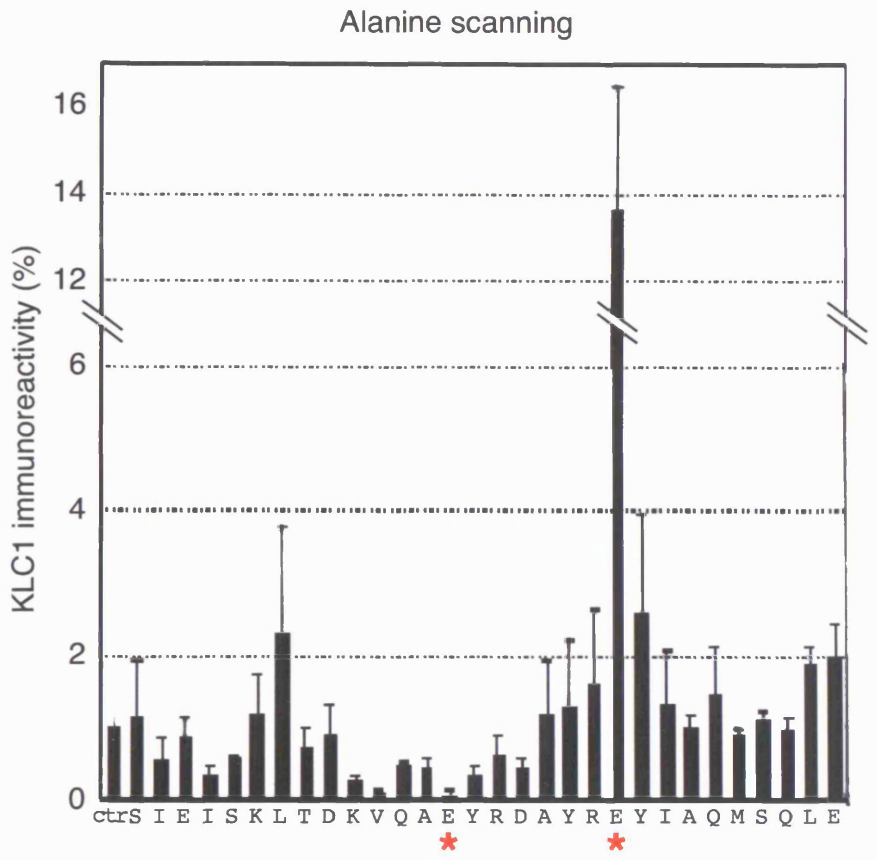

Figure 4-3: *alanine-scanning on KIM*
Array membranes were incubated with purified KLC1, and bound proteins were detected with anti-KLC1 antibodies and HRP-conjugated secondary antibodies. Immunoreactivity was quantified, and results were normalised to the binding of KLC1 to the non-mutated KIM (set to 1). The residues that are mutated to alanine in each peptide are indicated at the bottom of the corresponding bar. Asterisks mark the mutants KIM(E19A) and KIM(E26A), which show the most significant changes in the binding affinity for KLC1. ctr = non mutated KIM; scale bars represent standard error, with n = 2 experiments.

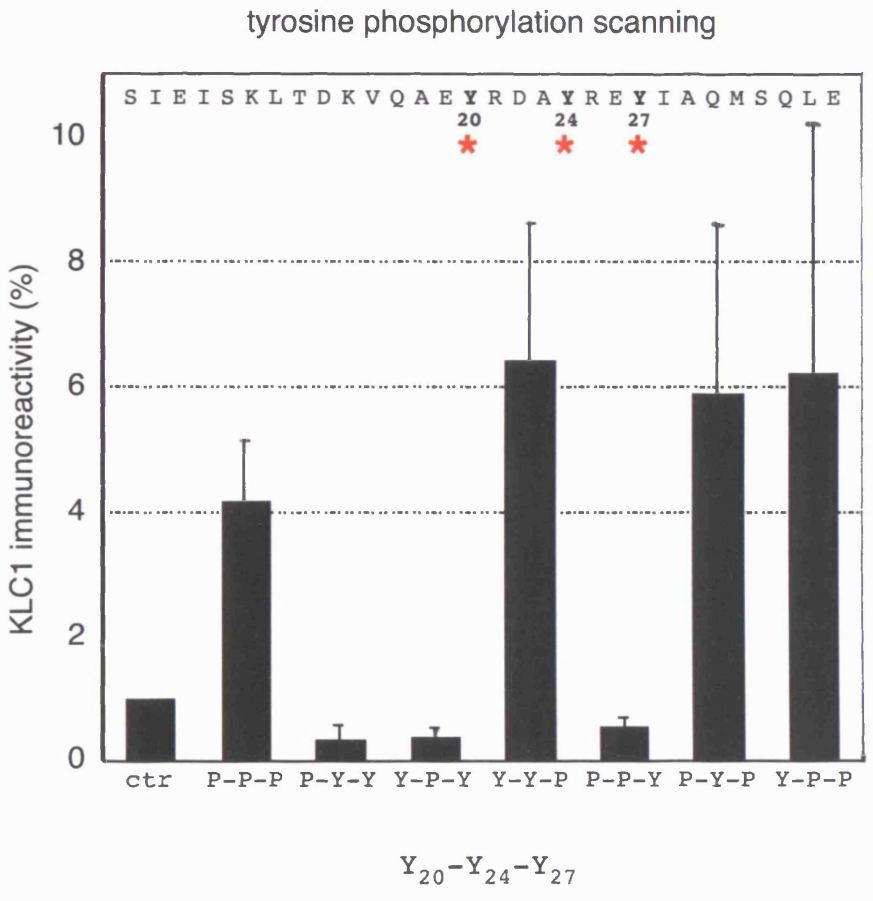

Figure 4-4: *tyrosine phosphorylation scanning on KIM*
Array membranes were incubated with purified KLC1, and bound proteins were detected with anti-KLC1 antibodies and HRP-conjugated secondary antibodies. Immunoreactivity was quantified, and results were normalised to the binding of KLC1 to the non-mutated KIM (set to 1). The three tyrosines in the KIM sequence are marked by asterisks. Phosphorylation of Tyr27 always results in an increased binding affinity, whereas phosphorylation of Tyr20 and Tyr24 seems to impair the interaction. The combination of phosphorylated - non phosphorylated residues present in each peptide is indicated at the bottom of the corresponding bar (P = phosphorylated, Y = non phosphorylated). ctr = non mutated KIM; scale bars represent standard error, with n = 2 experiments.

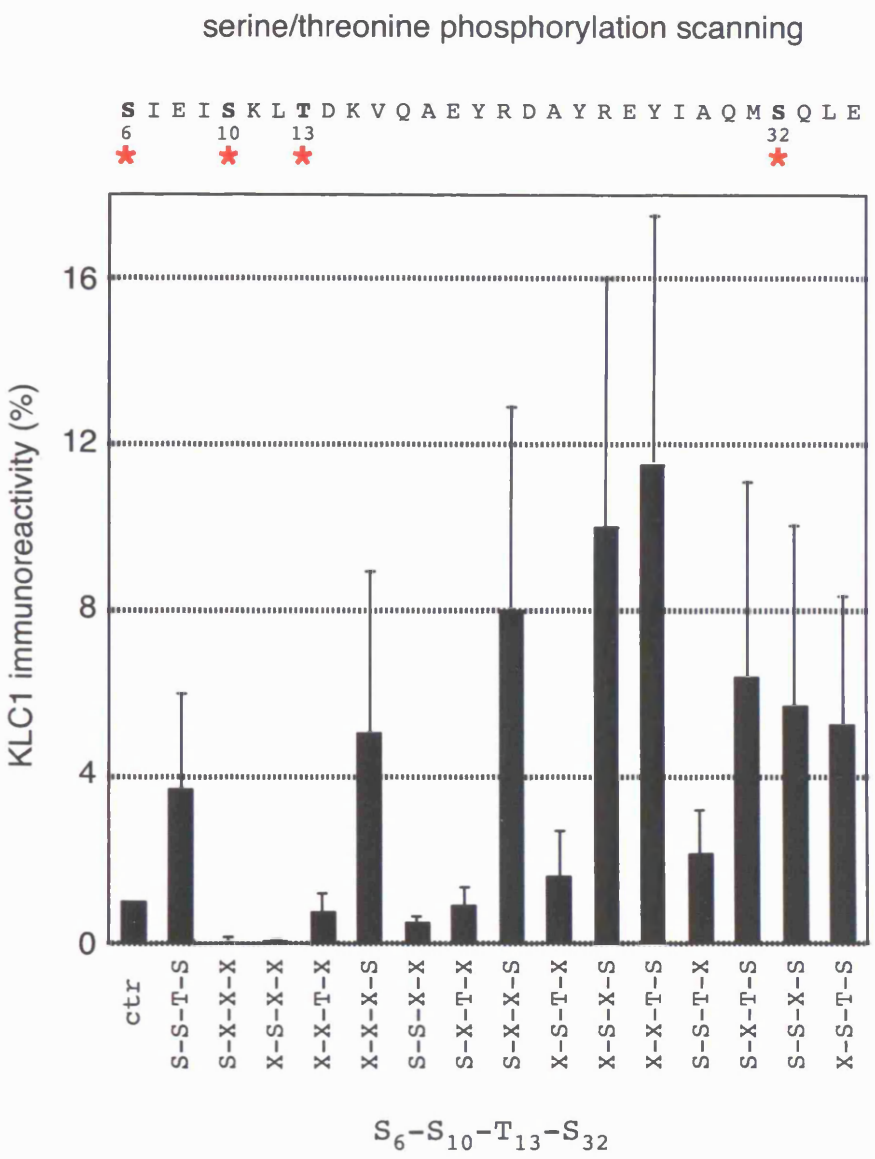

Figure 4-5: *serine/threonine phosphorylation scanning on KIM*
Array membranes were incubated with purified KLC1, and bound proteins were detected with anti-KLC1 antibodies and HRP-conjugated secondary antibodies. Immunoreactivity was quantified, and results were normalised to the binding of KLC1 to the non-mutated KIM (set to 1). The serines and threonines in the KIM sequence are marked by asterisks. Phosphorylation of Ser6 and Ser10 has an inhibitory effect on KLC1 binding, whereas phosphorylation of Thr13 or Ser32 enhances the interaction. The combination of phosphorylated - non phosphorylated residues present in each peptide is indicated at the bottom of the corresponding bar (S, T = phosphorylated, X = non phosphorylated). ctr = non mutated KIM; scale bars represent standard error, with n = 2 experiments.

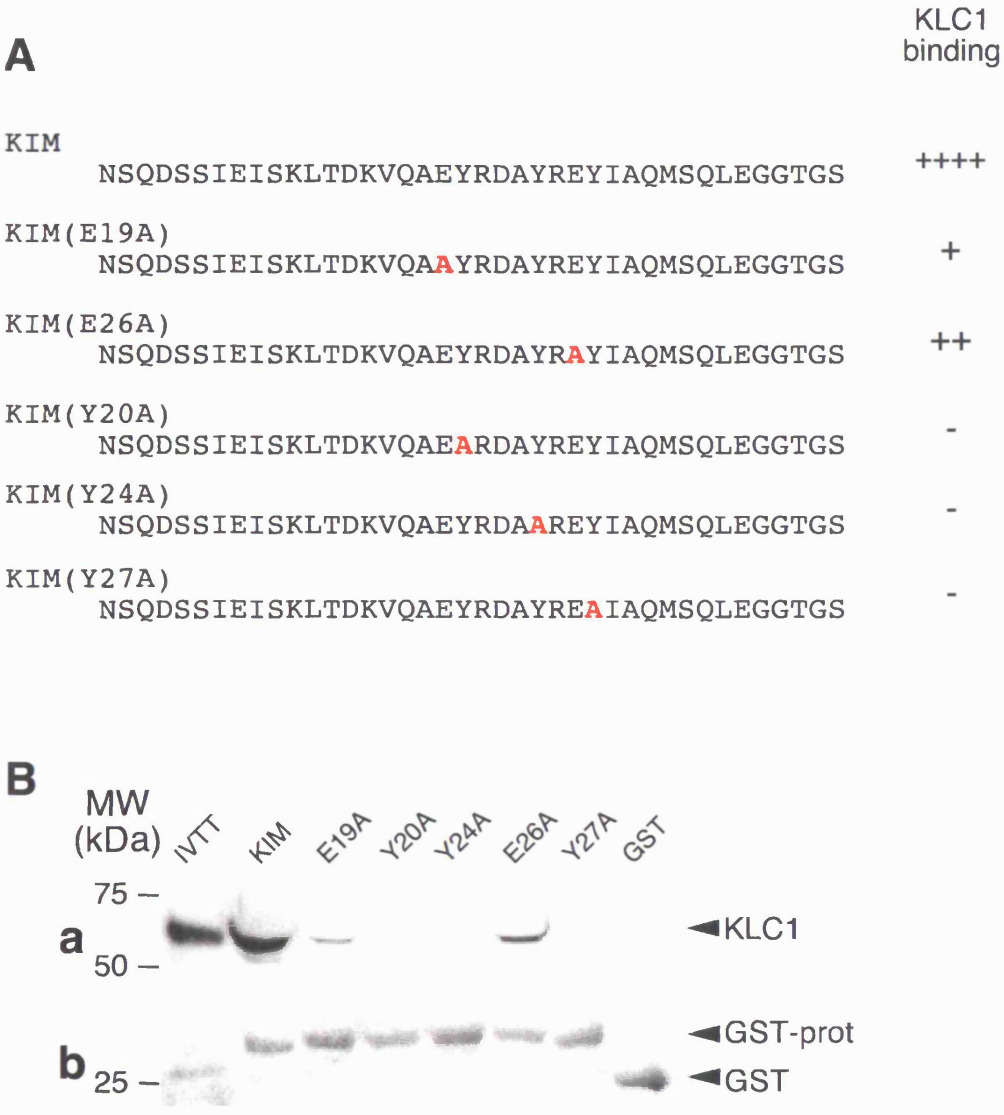

Figure 4-6: *GST-pull down with single point mutants*
(A) Sequence of the KIM mutants used in the GST-pull down experiments shown in (B). The ability of each mutant to bind KLC1 is indicated on the right: ++++ ≅ 100%; ++ ≅ 50%; + ≅ 25%; - ≅ no binding. (B) KIM mutants were expressed as GST-fusion proteins, and tested in a GST-pull down assay using in vitro [^{35}S]-labeled KLC1. The ability of [^{35}S]-KLC1 to bind different mutant proteins is shown in *a*. The Coomassie-staining of the recombinant GST-proteins is shown in *b*.

4.3 Phosphorylation analysis

4.3.1 KIM phosphorylation by Abl kinase

4.3.1.1 *Abl phosphorylates KIM* in vitro

The experiment presented in Figure 4-8 was performed by Dr. T. Newsome, with recombinant GST proteins that I generated.

The data obtained from the phosphorylation scanning suggest that tyrosine phosphorylation might modulate the binding between Kidins220 and KLC1. By analysing the predicted three dimensional structure of KIM, I observed that the aromatic rings of the three tyrosine residues are located close together in the helix, and that they all point to the same direction (Figure 4-7). It is possible that this three dimensional organisation represents a docking site, susceptible to phosphorylation and conformational changes. We therefore tried to identify some kinases that could target KIM.

The Src and Abl superfamilies of tyrosine kinases have been implicated in the modulation of several cellular events, such as cell proliferation, differentiation, survival, adhesion and migration (Thomas and Brugge, 1997). Some members of these kinase families (Fyn, Yes and Src) are predicted to phosphorylated Kidins220 on KIM (see Table 9). Interestingly, Src-mediated phosphorylation of the viral protein A36R mediates the release of kinesin-1 from vaccinia virus particles (Newsome et al., 2004). In addition, phosphorylation of the same protein by Abl has been recently shown to collaborate with Src to stimulate actin-base motility of the viral particles (Newsome et al., 2006). On the basis of these observations, it is

possible that a similar mechanism could modulate the binding between Kidins220 and kinesin-1. Dr. T. Newsome performed an *in vitro* phosphorylation assay on the recombinant GST-KIM, using a panel of kinases belonging to the Src and Abl families (Figure 4-8). He found that KIM is strongly phosphorylated by Abl. As a control, he used the viral protein A36R, a known Abl substrate (Newsome et al., 2006). This result was particularly interesting, as Abl has been suggested to regulate phosphorylation events leading to neuronal differentiation, via a specific interaction with the TrkA receptor (Koch et al., 2000; Yano et al., 2000). Abl would therefore be in the correct cellular context to interact with and phosphorylate Kidins220. On the basis of these data, I decided to study in more detail Abl-mediated phosphorylation of KIM.

4.3.1.2 Abl phosphorylates KIM on tyrosine 20

Analysis of the KIM sequence did not reveal any consensus sites for Abl (I/V/L-**Y**-X-X-P/F, Songyang et al., 1995). I therefore sought to identify which of the three tyrosines is targeted by this kinase. To this purpose, I used the three Y-A mutants described in Figure 4-6 in an *in vitro* phosphorylation assay, where phosphorylated proteins were visualised by [^{32}P]-labelling. As shown in Figure 4-9 A, the mutation Y20A completely abolished the phosphorylation. The mutant KIM(Y27A) also displayed a reduced phosphorylation, whereas the level of phosphorylation of KIM(Y24A) was unaffected. Analysis of the phosphorylated KIM and KIM mutants by autoradiography always revealed a minor band migrating just above GST-KIM (arrow, Figure 4-9 A and B). To understand the nature of this band, I performed a phosphorylation assay with cold ATP, and analysed the

phosphorylated proteins by Western blot, using anti-GST and anti-phospho-tyrosine antibodies (Figure 4-9 B). The upper band is not recognised by either GST (Figure 4-9 B *b*) or phospho-tyrosine (Figure 4-9 B *c*) antibodies. I concluded that it is probably due to phosphorylation of a bacterial product, which co-purifies with GST-KIM and GST-KIM mutant proteins. Altogether, these experiments have shown that *in vitro* Abl phosphorylates KIM preferentially on tyrosine 20, which corresponds to residue 1375 of the full-length Kidins220.

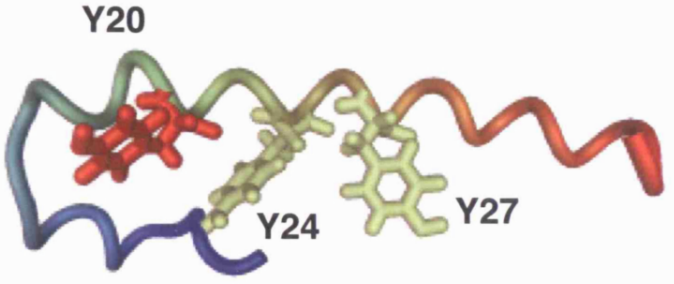

Figure 4-7: *possible orientation of the three tyrosine residues in KIM*
Three dimensional representation of the kinesin-interacting motif. The aromatic rings of the three tyrosines in the KIM sequence are in close proximity, and might represent a docking site susceptible to phosphorylation.

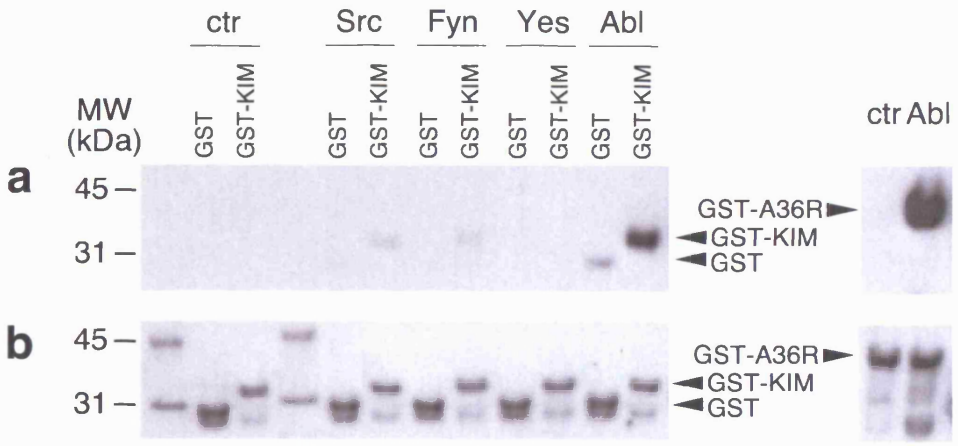

Figure 4-8: *Abl phosphorylates KIM*
KIM is *in vitro* phosphorylated by Abl. GST or recombinant GST-KIM were bound to glutathione-Sepharose beads and subsequently incubated with different kinases, as indicated. Beads were washed and resuspended in loading buffer. Eluted proteins were then analysed by Western blot by using anti-phospho-tyrosine antibodies. Arrowheads indicate the phosphorylation bands (*a*) and the corresponding Ponceau-stained proteins (*b*). In the control lanes ("ctr"), no kinase was added. This experiment was performed by Dr. T. Newsome.

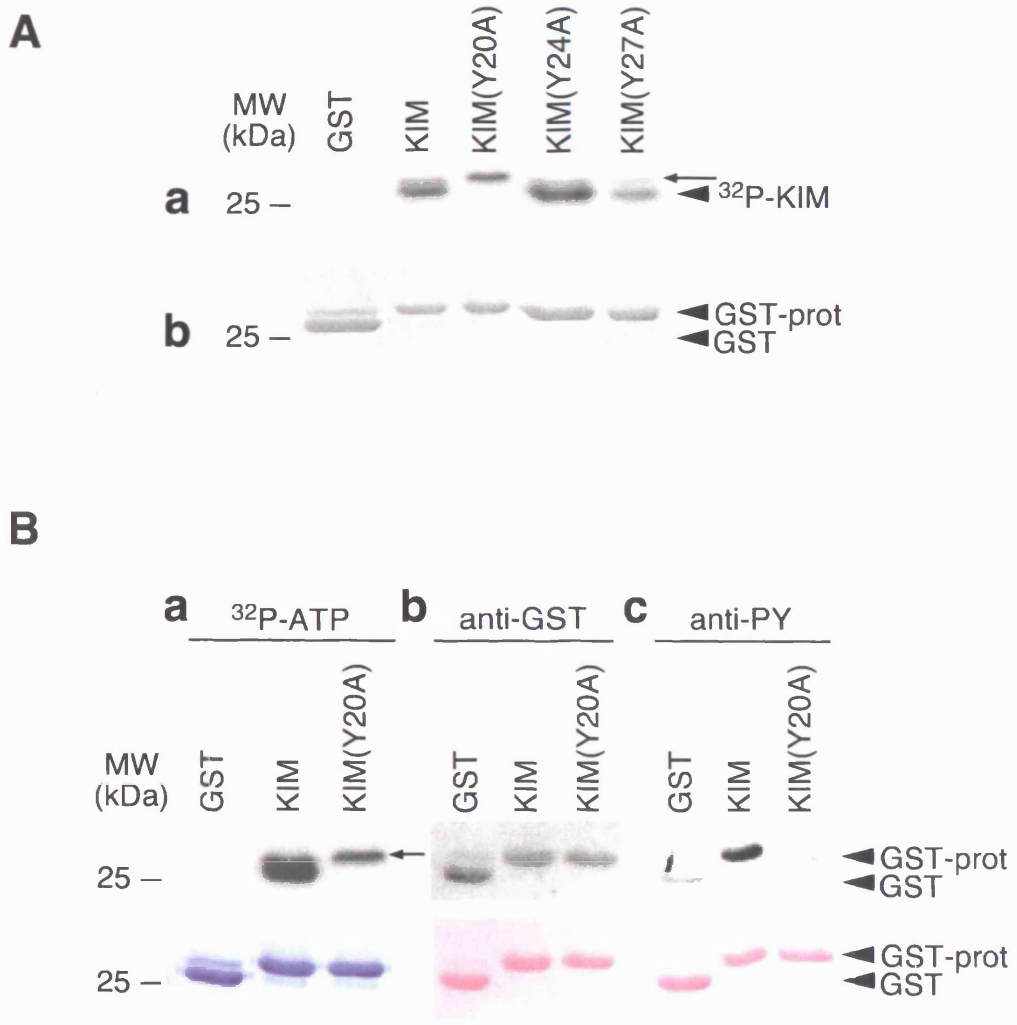

Figure 4-9: *Abl phosphorylates KIM on tyrosine 20*
(A) GST or recombinant GST-KIM mutants were bound to glutathione-Sepharose beads and subsequently incubated with Abl protein tyrosine kinase in presence of Redivue™ [^{32}P]-ATP. Beads were washed and resuspended in loading buffer. Eluted proteins were then analysed by SDS-PAGE and autoradiography. The ability of Abl to phosphorylate different mutant proteins is shown in *a*. The corresponding Coomassie-stained proteins are shown in *b*. (B) GST or recombinant GST-KIM mutants were bound to glutathione-Sepharose beads and subsequently incubated with Abl protein tyrosine kinase in presence of Redivue™ [^{32}P]-ATP (*a*) or with cold ATP only (*b*, *c*). Beads were washed and resuspended in loading buffer. Eluted proteins were then analysed by SDS-PAGE and autoradiography (*a*) or Western blot with anti-GST (*b*) or anti-phosphotyrosine antibodies (*c*). Arrowheads indicate the specific phosphorylation or immunoreactive bands (upper panels) and the corresponding Coomassie- or Ponceau-stained proteins (lower panels). Arrows indicate the unspecific radioactive band.

4.3.1.3 Phosphorylation of KIM abolishes the binding to KLC1

Phosphorylation of KIM might act as a molecular switch that modulates the binding of Kidins220 to the kinesin-1 motor complex. To validate this hypothesis, I phosphorylated the recombinant GST-KIM *in vitro*, and then used the phosphorylated protein in a GST-pull down assay, with [^{35}S]-labelled KLC1 (Figure 4-10). I found that increasing the level of phosphorylation decreased the affinity for KLC1. This is an indication that Abl-mediated phosphorylation of KIM might indeed regulate the binding of Kidins220 to kinesin-1. Phosphorylation could alter the recognition of KIM on the KLC1 docking site or could trigger conformational changes of KIM, that would result in a decreased affinity for KLC1, and the subsequent detachment of Kidins220 from the kinesin-1 complex.

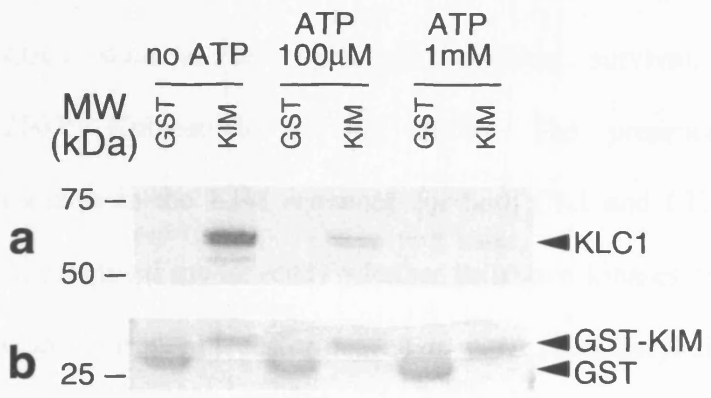

Figure 4-10: *phosphorylation of KIM inhibits KLC1 binding*
GST or recombinant GST-KIM were bound to glutathione-Sepharose beads and incubated with Abl tyrosine kinase in the presence of different concentrations of ATP, as indicated. Phosphorylated proteins were then incubated with in vitro [^{35}S]-labelled KLC1, washed and resuspended in loading buffer. Eluted proteins were analysed by SDS-PAGE and autoradiography. The ability of KLC1 to bind GST-KIM under the different conditions is shown in *a*. The Coomassie staining of the recombinant GST-proteins is shown in *b*.

4.3.2 KIM phosphorylation by casein kinase 1

4.3.2.1 Casein kinase 1 phosphorylates KIM

The serine/threonine specific casein kinase 1 and 2 (CK1 and CK2) are ubiquitously expressed kinases, which are involved in the regulation of diverse cellular processes, such as cell cycle and division, survival, and apoptosis (Litchfield, 2003; Knippschild et al., 2005). The presence of putative phosphorylation sites in the KIM sequence for both CK1 and CK2 (Table 9 and Figure 4-11 A), prompted me to verify whether these two kinases are able to target Kidins220. To this purpose, I performed an *in vitro* phosphorylation assay using recombinant GST-KIM, and purified CK1 and CK2. I found that CK1 strongly phosphorylated KIM, while CK2 did not show any detectable activity (Figure 4-11 B). I concluded that CK1 targets KIM *in vitro*, presumably on Serine 5, which corresponds to residue 1360 of the full length Kidins220.

4.3.2.2 Phosphorylation by casein kinase 1 does not affect KLC1 binding

I have shown that Abl-mediated phosphorylation of KIM inhibits KLC binding. I asked whether also CK1 activity modulates the interaction between Kidins220 and the kinesin-1 complex. To verify this hypothesis, I performed GST-pull down experiments using CK1-phosphorylated GST-KIM, and purified KLC1. As shown in Figure 4-11 C, phosphorylation by CK1 did not affect the ability of KIM to bind KLC1.

Figure 4-11: *KIM phosphorylation by casein kinase 1*

(A) Position of the predicted phosphorylation sites for CK1 (black arrowheads) and CK2 (white arrowheads) on KIM. (B) CK1 phosphorylates KIM. GST or recombinant GST-KIM mutants were bound to glutathione-Sepharose beads and subsequently incubated with CK1 or CK2, as indicated, in the presence of Redivue™ [^{32}P]-ATP. Beads were washed and resuspended in loading buffer. Eluted proteins were then analysed by SDS-PAGE and autoradiography. The ability of CK1 or CK2 to phosphorylate the different proteins is shown in *a*. The corresponding Coomassie-stained proteins are shown in *b*. (C) CK1 phosphorylation does not affect KLC1 binding. GST or recombinant GST-KIM were bound to glutathione-Sepharose beads and incubated with (+) or without (-) CK1 in presence of cold ATP. Proteins were then incubated with 20 μg of purified KLC1, washed and resuspended in loading buffer. Eluted proteins were analysed by SDS-PAGE and Coomassie-staining. Increasing amounts (0.1, 0.2, 0.4, 0.8 μg) of purified KLC1 were loaded on the right, for comparison.

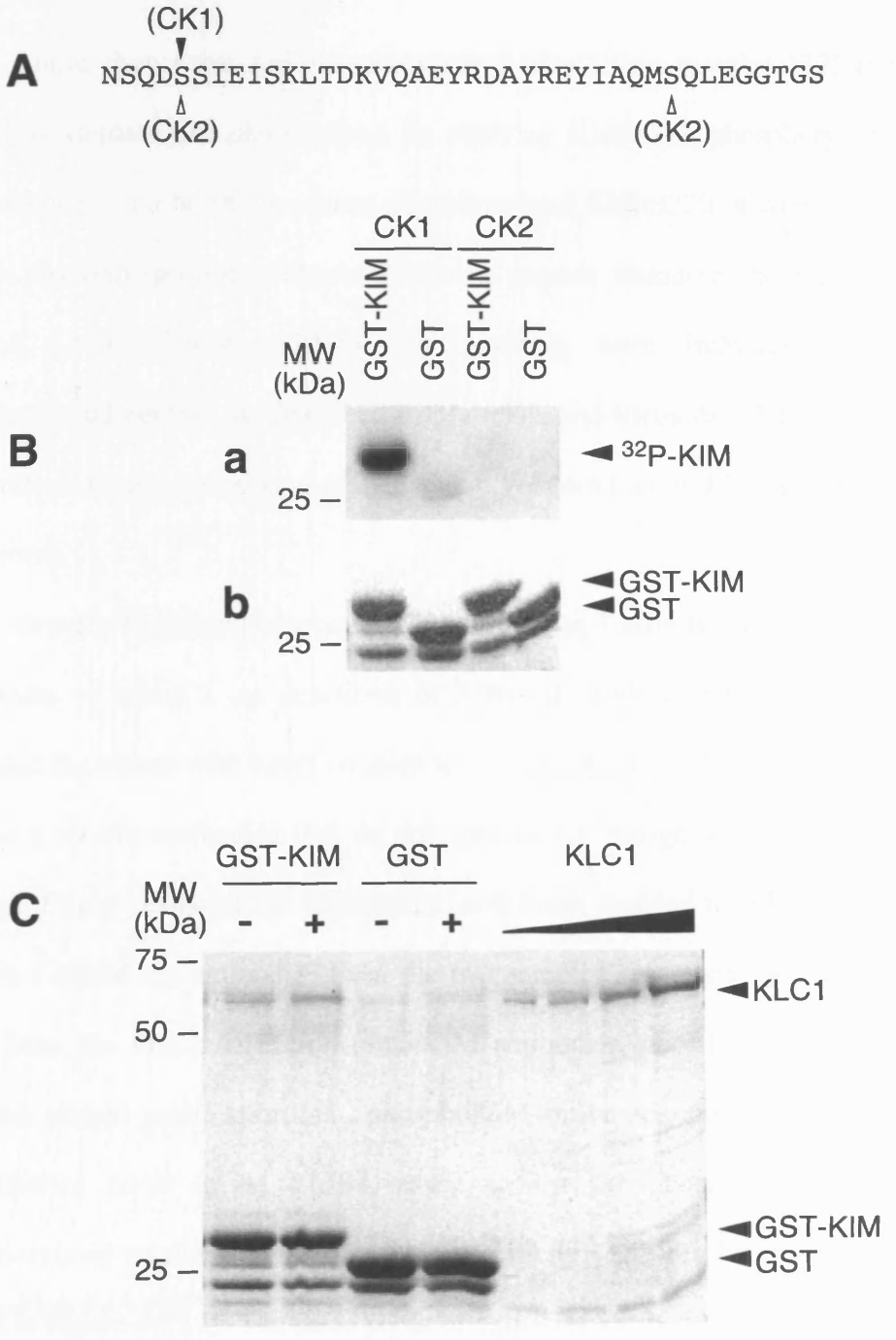
A
(CK1)
NSQDSSIEISKLTDKVQAEYRDAYREYIAQMSQLEGGTGS
(CK2)
(CK2)
B
CK1
CK2
GST-KIM
GST
GST-KIM
GST
MW
(kDa)
a
25 –
32P-KIM
b
25 –
GST-KIM
GST
C
GST-KIM
GST
KLC1
MW
(kDa)
-
+
-
+
75 –
50 –
25 –
KLC1
GST-KIM
GST

4.4 Generation of an antibody against phosphorylated KIM

I have shown that Abl phosphorylates Kidins220 on tyrosine 1375 *in vitro*. I wanted to validate our observations, by studying Kidins220 phosphorylation in a cellular system. To be able to detect phosphorylated Kidins220 *in vivo*, I decided to raise a phospho-specific antibody against a peptide spanning the region around tyrosine 1375 (Figure 4-12 A). Two rabbits were immunised with the phosphorylated peptide, as described in Materials and Methods. The anti-sera from both animals recognised a band of 220 kDa in Western blot on PC12 cell lysate (data not shown).

In order to obtain phospho-specific antibodies, I affinity purified 10 ml of the anti-serum of rabbit 2, as described in Materials and Methods. Briefly, I first incubated the serum with beads coupled to the non-phosphorylated peptide, in order to collect all the antibodies that do not specifically recognise the phosphorylated tyrosine. I then incubated the supernatant with beads coupled to the phosphorylated peptide. I eluted the antibodies from the two samples separately, and created three pools from the first purification (anti-KIM antibodies, pool 1-3), and three pools from the second purification (anti-phosphoKIM antibodies, pool 1-3). I then tested the different pools in an ELISA assay against the phosphorylated and non-phosphorylated peptides, to verify their specificity. The results of this assay are shown in Figure 4-12 B. The three pools of anti-KIM antibodies recognised both the phosphorylated and the unphosphorylated peptide, although less efficiently (Figure 4-12 B *a*). The three pools of anti-phosphoKIM antibodies showed a strong interaction with the phosphorylated peptide, and did not recognise the

unphosphorylated form, even at high concentrations (Figure 4-12 B *b*). On the basis of this assay, I concluded that the anti-phosphoKIM antibodies specifically recognise the phosphorylated tyrosine on the immunising peptide.

I then asked whether the anti-KIM and anti-phosphoKIM antibodies were able to detect native Kidins220. To answer this question, I tested the antibodies in Western blot, using cell lysates from NGF-treated PC12 cells. The anti-KIM antibodies (αKIM) recognised a specific band of 220 kDa, which was competed for by both the phosphorylated and non-phosphorylated peptides (Figure 4-12 C *a*). The anti-phosphoKIM antibodies (αPKIM) recognised a band of higher molecular weight, which was competed for only by the phosphorylated peptide (Figure 4-12 C *b*). The same high molecular weight band was present also in lysates from undifferentiated PC12 cells (data not shown).

Figure 4-12: *generation of an antibody against phosphorylated KIM*

(A) Sequence of the peptide used for the immunisation. The phosphorylated tyrosine corresponds to residue 1375 of the full length Kidins220. (B) Affinity purification of a phospho-specific antibody. A specific anti-serum against the peptide shown in (A) was affinity purified first against the non-posphorylated peptide, and subsequently against the phosphorylated peptide. The two samples were eluted separately and three pools were created for each antibody. The different pools were then tested in an ELISA assay against the phosphorylated (Ph) and non-phosphorylated (unPh) peptides. Anti-KIM antibodies (*a*) could recognise both phosphorylated and non-phosphorylated peptides, whereas anti-phosphoKIM antibodies (*b*) were specific for the phosphorylated form. (C) Test of anti-KIM and anti-phosphoKIM antibodies on PC12 cell lysate (50 μg/lane). The anti-KIM antibody (*a*) recognised a 220 kDa band, that was competed for by both phosphorylated and non-phosphorylated peptides. The anti-phosphoKIM antibody (*b*) recognised a higher band, which was competed for only by the phosphorylated peptide. The Ponceau staining of the membranes corresponding to this experiment is shown in the lower panel.

A


1371
1375
1382
CVQAEYRDAYREY-CONH2
P

B

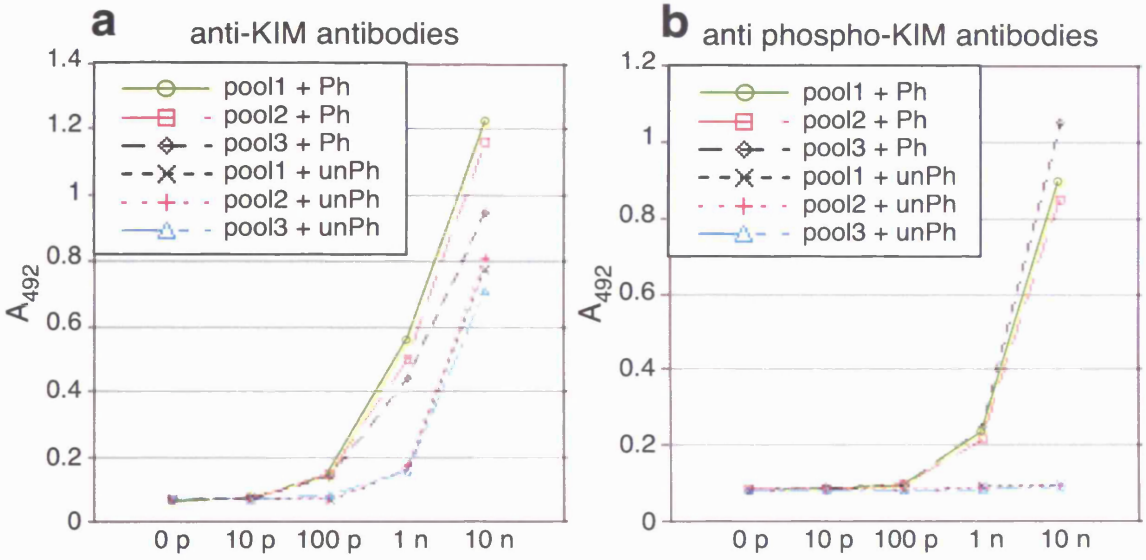
a
anti-KIM antibodies
b
anti phospho-KIM antibodies
pool1 + Ph
pool2 + Ph
pool3 + Ph
pool1 + unPh
pool2 + unPh
pool3 + unPh
A492
0 p
10 p
100 p
1 n
10 n

C

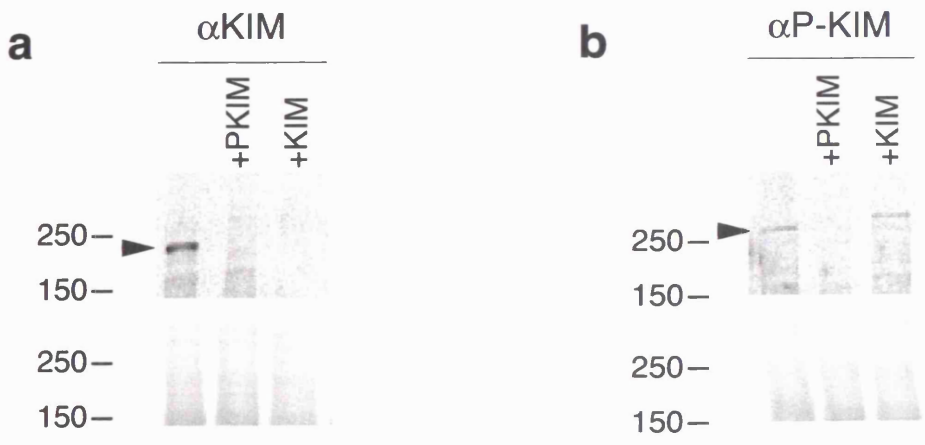
a
αKIM
+PKIM
+KIM
250
150
250
150
b
αP-KIM
+PKIM
+KIM
250
150
250
150

4.5 Future perspectives

On the basis of our *in vitro* experiments, we hypothesise that Abl-mediated phosphorylation of KIM modulates the detachment of the kinesin-1 complex from Kidins220. In order to validate this model, we will need to replicate our observations in a cellular system. To this purpose, it will be necessary to confirm that the high molecular weight band detected by the anti-phosphoKIM antibodies really corresponds to Kidins220, and that this signal is suppressed by Abl inhibitors. Once these results are confirmed, it will be interesting to study the effect of different Abl inhibitors on the trafficking of Kidins220. It will be also important to establish whether the inhibition of Abl activity could affect the ability of Kidins220 to mediate a correct response to neurotrophic stimuli.

Our model (Figure 4-13) predicts that Abl phosphorylation and the subsequent dissociation of Kidins220 from the kinesin-1 complex should take place at the tip of neurites. Once Kidins220 is delivered to the plasma membrane, the binding of neurotrophins would trigger Abl activation and kinesin-1 detachment. To better analyse this mechanism, it will be crucial to selectively target the events occurring at the growth cones. The use of Campenot chambers might help dissecting the molecular basis of our model. This system allows the physical separation of neuronal cell bodies from their processes in different compartments on a culture dish (Campenot, 1977). By using compartmentalised cultures of primary neurons, therefore, it will be possible to target Abl activity specifically at the axon terminals. The Abl inhibitor Gleevec® (also known as STI571 or Imatinib Mesylate), which is currently used to treat chronic myeloid leukemia, would allow the disruption of Abl

function, and the study of how the inhibition of this kinase might affect Kidins220 retrograde trafficking and signalling.

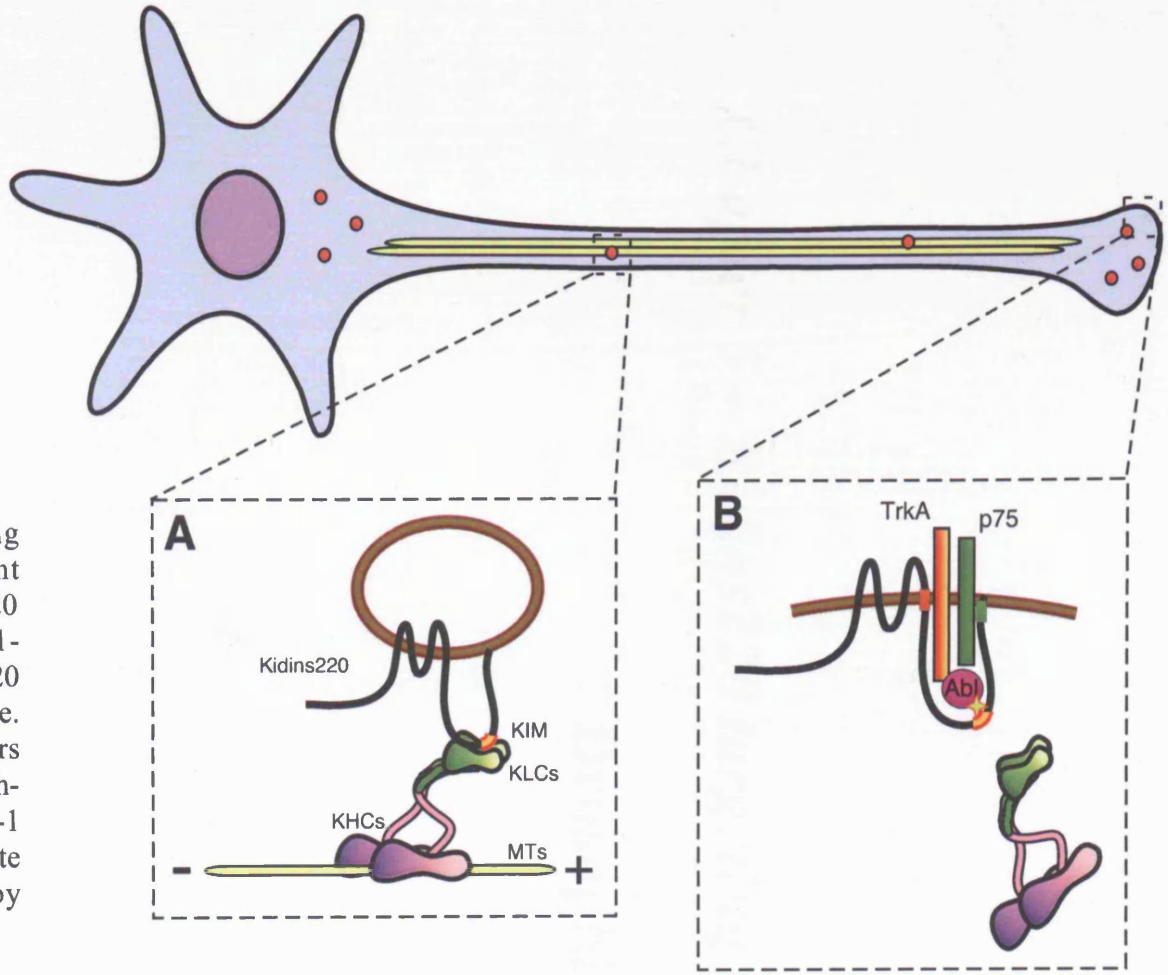

Figure 4-13: *molecular model*
(A) Kidins220 is transported along neurites via a kinesin-1 dependent mechanism. The binding of Kidins220 to KLCs is mediated by the KLC1-Interacting Motif (KIM). (B) Kidins220 is delivered to the membrane surface. The binding of neurotrophins triggers Abl activation and kinesin-1 detachment. The dissociation of the kinesin-1 complex allows Kidins220 to mediate the downstream events triggered by neurotrophic stimuli.

Chapter 5 – Kidins220 targeting in **Drosophila**

5 *Kidins220 targeting in* Drosophila

5.1 *Introduction*

The fruit fly *Drosophila melanogaster* has been used as a model organism in biology for almost a century. Besides being small and easy to maintain, flies have a short life cycle, which allows genetic experiments to be followed over many generations. The fly genome, sequenced in 2000, contains about 14,000 genes on four chromosomes (Adams et al., 2000). During larval stages, many cells undergo S phase without division to increase transcription. Thus, they have large polytene chromosomes, characterised by a "barcode" pattern of light and dark bands, which allows an accurate mapping of genes. By blasting the Kidins220 rat sequence against the *Drosophila* genome, I identified the orthologue of Kidins220, which is located on the right arm of chromosome 2 (2R 57D8-57D11, CG identification number CG 30387, Flybase id FBgn0050387). There are four known alternative transcripts for dKidins220, as illustrated in Figure 5-1 C, which are characterised by progressively shorter N-terminal sequences. As shown in Figure 1-6, *Drosophila* Kidins220 (dKidins220) shares only about 30% homology with the human, rat and mouse sequences, and even less with the *C. elegans* orthologue (26%).

5.2 *Results*

5.2.1 *P-elements*

P elements are transposable elements of *Drosophila* genome. Their general structure is represented in Figure 5-1 A. They are characterised by two terminal

inverted repeats, adjacent to short transposase binding sites, which are needed for efficient transposition. Internally, P elements contain the sequence for a transposase, spread over four exons (O'Hare and Rubin, 1983). "Autonomous" P elements contain the entire transposase gene, and are thus able to mediate their own transposition (Spradling and Rubin, 1982). In "non autonomous" P elements, the transposase gene has internal deletions, so it cannot give a functional product. Mobilisation of non autonomous P elements occurs only in presence of an autonomous P element, which can supply the transposase (Engels, 1984).

In nature, there are *Drosophila* strains that contain P elements ("P strains"), and other strains that do not have any P elements in their genome ("M strains") (Kidwell et al., 1977). It has become common practice to insert artificial P elements into M strains (Spradling and Rubin, 1982), and to select flies according to the location of P element insertion. In artificial P elements, the transposase sequence has been substituted with a marker gene or other genes of interest. This kind of P element behaves as non autonomous, but transposition can be induced at will by providing a transposase. The structure of the artificial P elements used in this work is described in Figure 5-1 B. They contain the wild type *white* gene, which confers red eyes to transgenic flies, under the control of the UAS promoter (Rorth, 1996). GAL4 binding to UAS triggers the transcription of the downstream sequences. When transgenic flies harbouring a P element insertion are crossed with GAL4 expressing lines, transcription is activated from the UAS promoter. This generates chimeric transcripts, which start in the P element sequence and extend into the downstream genomic region. If the P element is inserted inside a coding region, transcription activation might have two opposite effects, depending on the orientation of the

insertion in respect to the surrounding gene. If the P element is inserted in the same orientation as the gene, more mRNA will be transcribed, possibly resulting in protein overexpression. If the P element and the gene are in opposite orientations, transcription activation will generate antisense RNA, which might cause protein knock-down.

I took advantage of the availability of three *Drosophila* strains, with P element insertions mapped inside or in close proximity of the Kidins220 gene (Figure 5-1 C). The strains were purchased from the Bloomington *Drosophila* Stock Centre. In the first strain (GE 14017), the insertion was mapped upstream of the Kidins220 gene. Here, the P element might interfere with promoter regions, causing either up- or down-regulation of transcription. In the second strain (GE 16817), the insertion was located in the promoter region, close to the transcriptional start. Also in this case, the P element could interfere with the promoter region. In addition, if it was inserted in the same orientation as the gene, it could enhance transcription and potentially cause Kidins220 overexpression. However, the orientation of the insertion was not determined for these two strains. In the last strain (GE 14538), the P element is situated inside the first intron, in a sense orientation. Upon GAL4 activation, thus, it would be predicted to trigger overexpression of Kidins220.

5.2.1.1 Lethality crosses and GMR-Gal4 crosses

Balancer chromosomes are "natural" chromosomes with so many rearrangements that their gene array is completely scrambled and they are no longer capable of pairing or recombining with their normal homolog. Recombination is not impossible but very rare, and if it happens it is usually lethal. Strains have been

selected, which contain balancers with dominant markers that can be tracked unambiguously through generations (Greenspan, 2004).

Our P element-containing flies were heterozygous, i.e. they had the insertion in one allele, while the other allele was wild type. P element insertions usually do not have any effects *per se*, however, they can occasionally transpose into an important region of a gene, therefore disrupting the gene function independently of GAL4 activation. In order to verify whether the P elements were affecting dKidins220 espression in our strains, it was necessary to obtain flies homozygous for the insertion. For this purpose, I first crossed our heterozygous flies with a strain carrying balancers for the second chromosome. F1 flies were selected, which displayed the P element marker (red eyes) together with the balancer marker (curly wings). A scheme of this cross is presented in Figure 5-2 A *a*. As a second step, the balanced P element strains were crossed in order to obtain F2 flies homozygous for the P element insertion, selected by the absence of the balancer marker (Figure 5-2 A *b*). For the three strains, homozygous flies were viable and appeared at the expected mendelian ratio, indicating that the P element insertions *per se* did not disrupt any essential region of the dKidins220 gene.

Different *Drosophila* lines are available, expressing GAL4 in a tissue-specific fashion. To study possible phenotypes due to GAL4-driven transcription activation, I used the GMR (*g*lass *m*ultimer *r*eporter)-GAL4 line, where GAL4 expression is restricted to the eye (Hay et al., 1994). Cell fate determination, proliferation and differentiation are all essential processes in the normal eye development. Given that eye functionality is dispensable for viability and fertility of adult flies, it is possible to carry out eye-specific misexpression of genes involved in

several different pathways without interfering with fly development (Hay et al., 1997). GMR-GAL4 flies were crossed with the balanced P element strains. The phenotype was analysed by comparing the eyes of the flies with normal wings (containing the P element) to the eyes of the flies with curly wings (Figure 5-2 B). Unfortunately, I could not detect any macroscopic defect in the eye development, for the three P element strains.

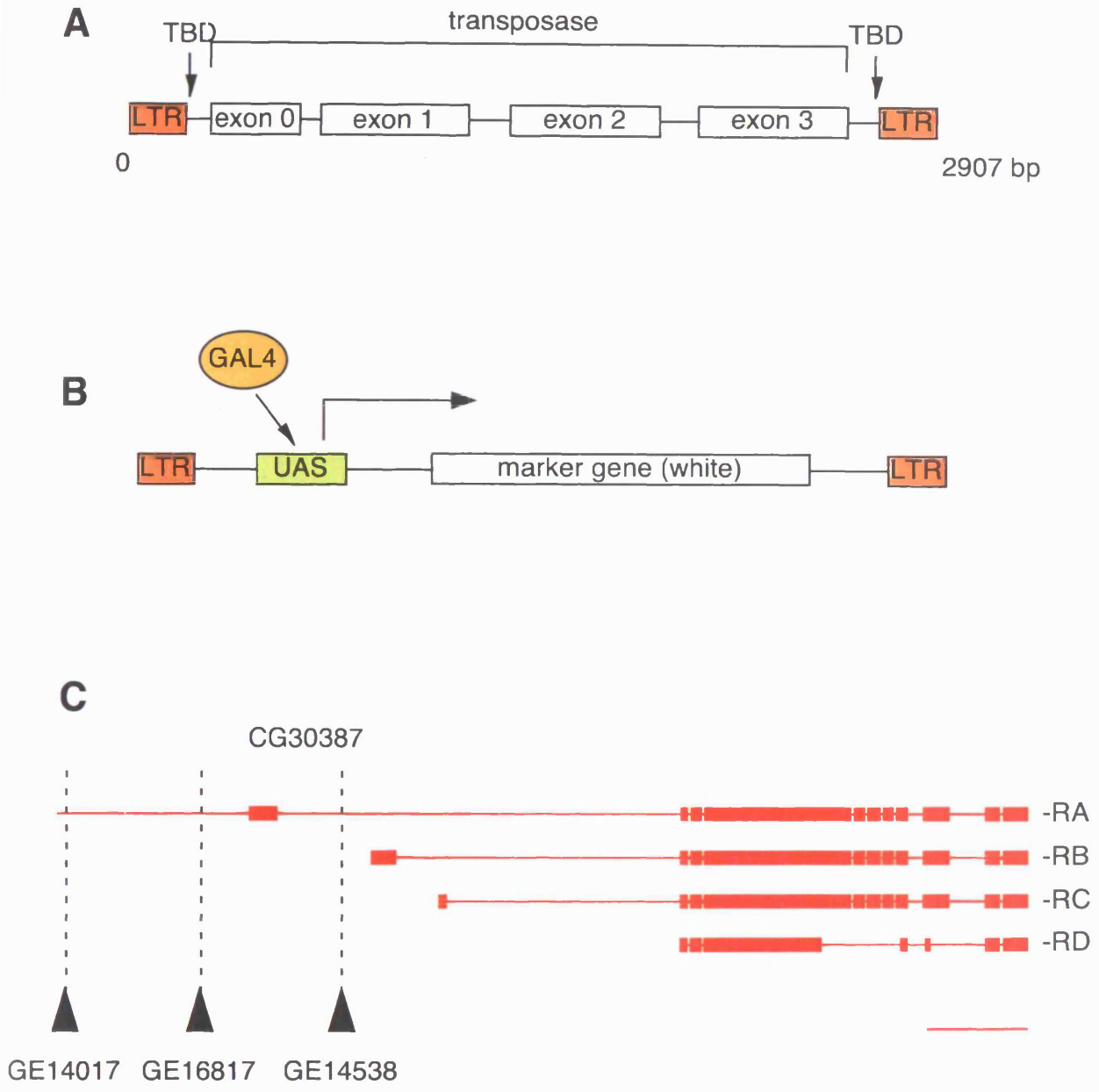

Figure 5-1: *P elements*
(A) An autonomous P element contains the complete sequence for a transposase (exon 0 to 3), flanked by long terminal repeats (LTR). Adjacent to the LTRs, there are two transposase binding domains (TBD). (B) An artificial P element contains a marker gene, in this case the *white* gene, under the control of the UAS (upstream activating sequence) promoter. GAL4 binding to the UAS activates the transcription of the downstream sequences. (C) Scheme of the four transcripts for *Drosophila* Kidins220 (CG30387-RA, -RB, -RC, -RD). The sites of P element insertion are indicated. Scale bar = 10 kb

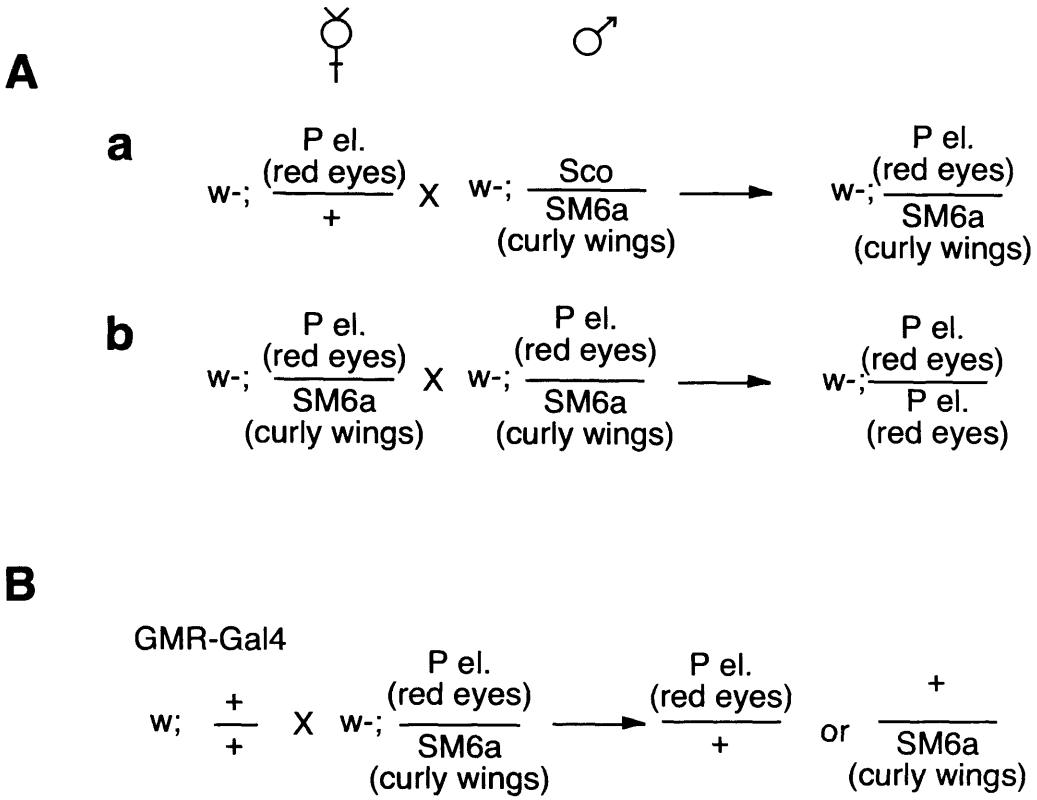

Figure 5-2: *lethality and GAL4 crosses*
(A) Scheme of the lethality crosses. *a.* Heterozygous P element strains were crossed with strains bearing balancers for the second chromosome. F1 flies were selected, which displayed the P element marker (red eyes) together with the balancer (curly wings). *b.* The balanced P element strains were crossed in order to obtain F1 flies homozygous for the P element insertion. (B) Scheme of the GAL4 crosses. Flies expressing GAL4 in the eye (GMR-Gal4 strain) were crossed with the balanced P element strains. The phenotype was analysed by comparing the eyes of the flies with normal wings (P el) to the eyes of the flies with curly wings. w, wild type *white* gene (red eyes); w-, mutant *white* gene (white eyes); Sco, scutoid marker; SM6a, curly wings marker.

5.2.2 RNAi

5.2.2.1 Cloning

In order to knock down Kidins220 in flies, I used an inducible RNAi system based on the pWIZ (*W*hite *I*ntron *Z*ipper) vector (Figure 5-3, adapted from Lee et al., 2003). The pWIZ vector contains two multiple cloning sites (MCS), downstream of the UAS enhancer-promoter and upstream of the SV40 transcription termination site. A 74-nucleotide *white* intron is flanked by the consensus sequence for 5' and 3' splice sites, in between the two MCSs. The *white* intron would be therefore spliced out of the construct upon transcription activation. Any DNA fragment inserted in this vector is fully competent to be spliced as an exon. As a marker, the vector contains the wild type *white* gene, which confers red eyes to transgenic flies.

A typical procedure to make an RNAi construct using the pWIZ vector is illustrated in Figure 5-4. A 500 bp sequence from the cDNA is amplified from genomic DNA and cloned in opposite orientations on each side of the *white* intron (Figure 5-4 B). Upon mating of transgenic flies harbouring the pWIZ gene with flies carrying tissue- or cell-specific GAL4 drivers, the F1 progeny would produce loopless hairpin RNA (Figure 5-4 C), which induces RNAi against target genes in tissue- and cell-specific patterns. The pWIZ construct is injected in embryos derived from a strain carrying the mutant *white* gene (w-), i.e. flies with white eyes. It is therefore possible to identify transgenic flies by the red eyes, conferred by the wild type *white* gene on the pWIZ vector.

In *Drosophila* there are four transcripts for Kidins220. In order to deplete all the isoforms of the protein, I chose a fragment common to all four, as reported in

Figure 5-4 C. The construct was cloned into the pWIZ vector following the strategy presented in Figure 5-4. Details about the cloning procedures are provided in Materials and Methods.

5.2.2.2 Microinjection of embryos and crosses for homozygous pWIZ flies

The microinjection of embryos was performed by Terence Gilbank, CRUK.

The pWIZ construct was injected into about 900 *Drosophila* embryos, from which 14 transgenic lines were obtained. In order to have flies homozygous for the pWIZ insertion, I first crossed each transgenic line with lines carrying balancers for chromosome 2 (*SM6*) and chromosome 3 (*TM6*). By looking at the mendelian ratio of the F1 flies, I was able to determine which chromosome the construct had integrated into. The transgenic line n.69 did not give any progeny when crossed with the balanced flies: a reason for this might be that the pWIZ gene insertion disrupted a gene important for reproduction. I then selected flies with pWIZ/balancer genotype, and by crossing them to each other I were able to obtain homozygotes. The results of this first set of crossings are reported in Table 10.

Table 10: *transgenic lines after pWIZ microinjection*

Transgenic lines obtained from the microinjection of the pWIZ vector. For each line, the chromosome bearing the pWIZ insertion is indicated. Lines used for the RNAi crosses are underlined.

Line	2	8	11	12	16	23	40	47	64	65	67	69	70	76
Chr.	II	II	X	III	III	III	II	III	II	III	II	---	III	II

5.2.2.3 Tissue specific RNAi

Seven selected lines (three bearing the pWIZ insertion in the second chromosome, three in the third chromosome, and one in the X chromosome, underlined in Table 10) were then crossed with flies carrying GAL4 drivers. To verify whether Kidins220 is active at very early stages of development, I chose the *VP16-GAL4* line. In these flies, maternal GAL4 is accumulated in the egg under the influence of the *VP16* promoter (Van Doren et al., 1998) and triggers RNAi only in the first few hours of development. To analyse the role of Kidins220 in the nervous system more specifically, I used the *elav-GAL4* line, in which GAL4 expression is triggered in all neuronal precursors cells by the neuronal specific promoter *elav* (Yao and White, 1994). On the basis of the putative involvement of Kidins220 in neurotrophin and ephrins signalling pathways, some developmental defects of the nervous system were expected. Unfortunately, the analysis of the F1 progeny form these crosses did not reveal any obvious developmental or behavioural phenotypes of the flies. A possible explanation for these negative results is that I did not choose the right moment or the right tissue to induce the RNAi against our protein. Other possibilities to be taken into account are that this gene could be resistant to RNAi, or that the protein has a particularly low turnover rate.

5.2.3 Antibody for Drosophila Kidins220

To verify whether dKidins220 was effectively knocked-down in flies following GAL4 expression, I attempted to raise a dKidins220-specific antibody. To this purpose, two rats were immunised with a peptide corresponding to the last 24 residues of *Drosophila* Kidins220 (Figure 5-5 A). This peptide is common to all the

splice isoforms, and should therefore be able to recognise all the different Kidins220 variants. As shown in Figure 5-5 B, antisera from both animals were able to recognise the peptide in an ELISA assay. Unfortunately, the same antisera failed to give any specific signals when tested in Western blot, using both S2 cells (a haemocyte-derived *Drosophila* cell line) and total embryo lysates (data not shown).

5.3 Conclusions

Little is known about Kidins220 distribution and expression in *Drosophila*. I attempted to target dKidins220 in the *Drosophila* eye, because misexpression of genes in the eye has been proven to be a useful method for the analysis of phenotypes due to alteration of gene function (Hay et al., 1997). However, it is possible that this was not the right system to study dKidins220, and that more overt phenotypes would come from crosses with flies expressing GAL4 in other tissues or at different developmental stages.

P element containing strains can be used to induce local mutagenesis by imprecise excision. This approach is based on the fact that P element excision is often imprecise, and it can leave portions of the P element sequence behind (Voelker et al., 1984; Daniels et al., 1985). It has been estimated that in about 10% of the excision events, some parts of the flanking genomic DNA are also removed. This generates deletions around the original insertion points. If these deletions are large enough, they can cause the knock-out of the surrounding gene. To carry out this strategy, it is necessary to cross homozygous P element-containing flies with a transposase expressing strain (either general or tissue-specific). However, this is a very time consuming approach, which requires the screening of a large number of

flies for several generations. The complete knock-out of the gene is a very rare event, which happens in less then 1% of the excisions. For these reasons, I chose not to follow this line of experimentation.

As an alternative strategy, I decided to attempt the knock down of dKidins220 via an RNAi approach, for which both the expertise and the technical support were available at the LRI. Unfortunately, the knock down of dKidins220 did not give any results from either the *VP16*- or the *elav*-GAL4 crosses, possibly because I did not target dKidins220 at the right stage or in the right tissue. To tackle this problem, one possibility would be to cross dKidins220 transgenic flies with strains expressing GAL4 in different tissues or at different stages of development. The lack of a specific antibody to detect dKidins220 levels, however, made the continuation of this strategy quite problematic. The efficacy of the knock down could be detected by assessing the levels of dKidins220 mRNA in embryos or adult flies, by RT-PCR or *in situ* hybridisation, using dKidins220-specific probes. While conducting these crosses, however, I managed to obtain transgenic ES cell lines, which I planned to use for the conditional knock-out of Kidins220 in mice (discussed in the next section). In the light of the negative results obtained from both the P element strains and the RNAi strategy, I decided not to pursue the fly project any further, but rather to focus on the analysis and characterisation of a Kidins220 knock-out mouse model.

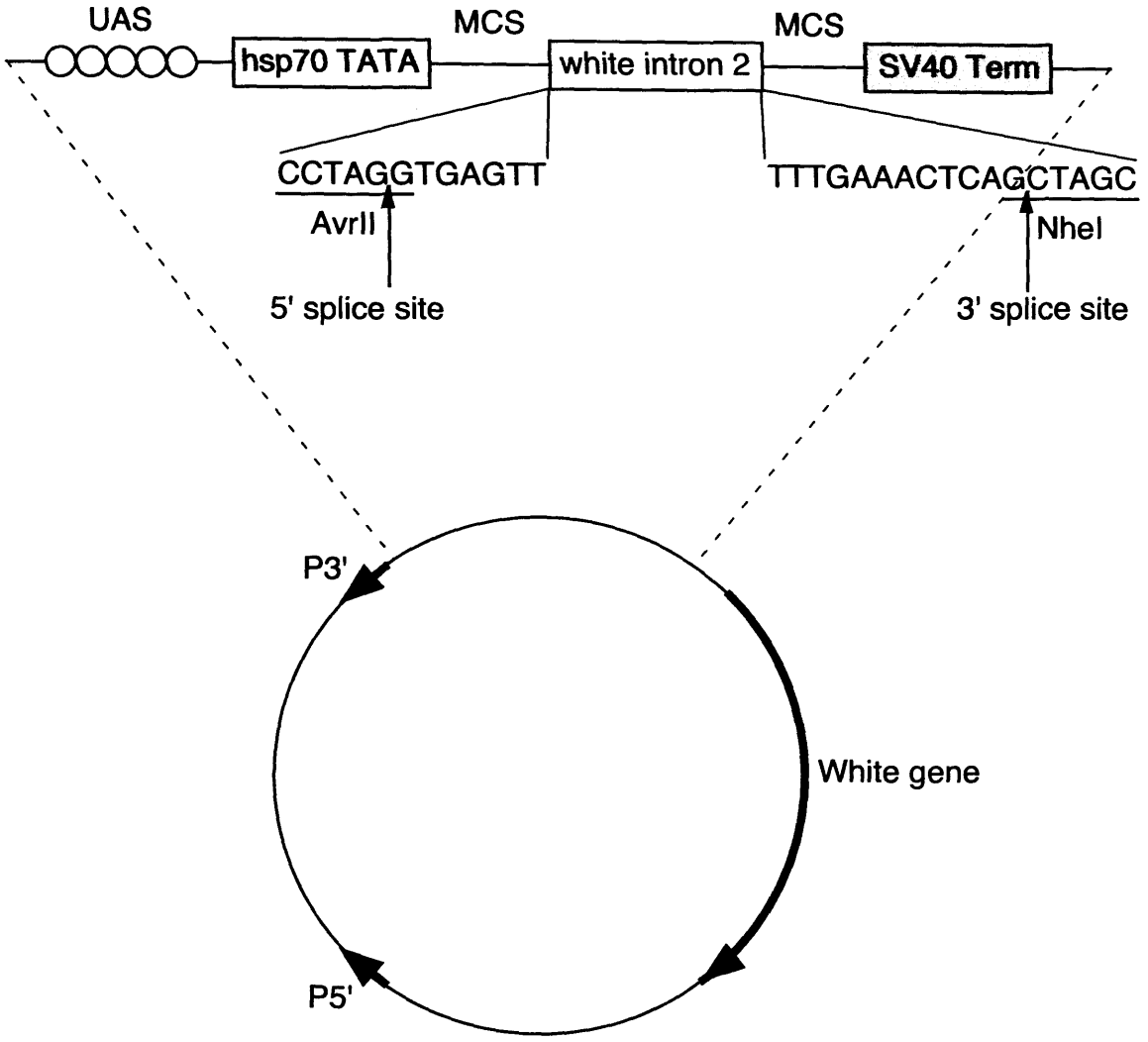

Figure 5-3: *pWIZ vector*
Scheme of the pWIZ (*W*hite *I*ntron *Z*ipper) vector. The MCSs of pWIZ are downstream of the UAS enhancer-promoter and upstream of the SV40 transcription termination site. The 74-nucleotide *white* intron is flanked by the consensus sequence for 5' and 3' splice sites. The inserts were cloned into the AvrII and NheI restriction sites. As a marker, the vector contains the wild type *white* gene, which confers red eyes to transgenic flies.

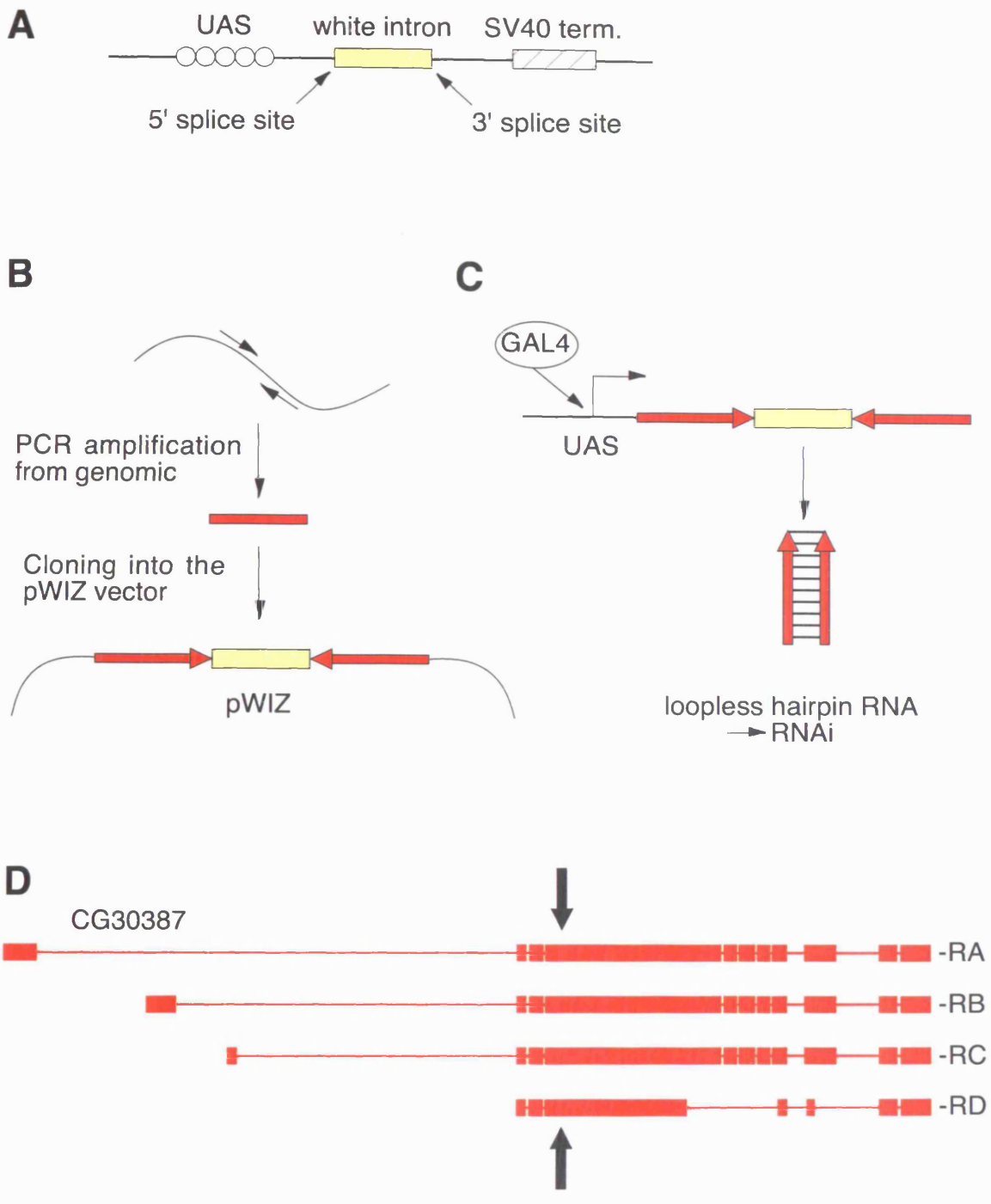

Figure 5-4: *cloning strategy*
(A) Simplified scheme of the pWIZ splicing cassette. (B) Specific inserts are amplified from genomic DNA and cloned in opposite orientations on both sides of the white intron. (C) Upon mating of transgenic flies with flies carrying specific GAL4 drivers, the F1 progeny produces loopless hairpin RNA, which induces RNAi against target genes in tissue- and cell-specific patterns. (D) Scheme of the *Drosophila* Kidins220 transcripts. Arrows indicate the region selected for the cloning.

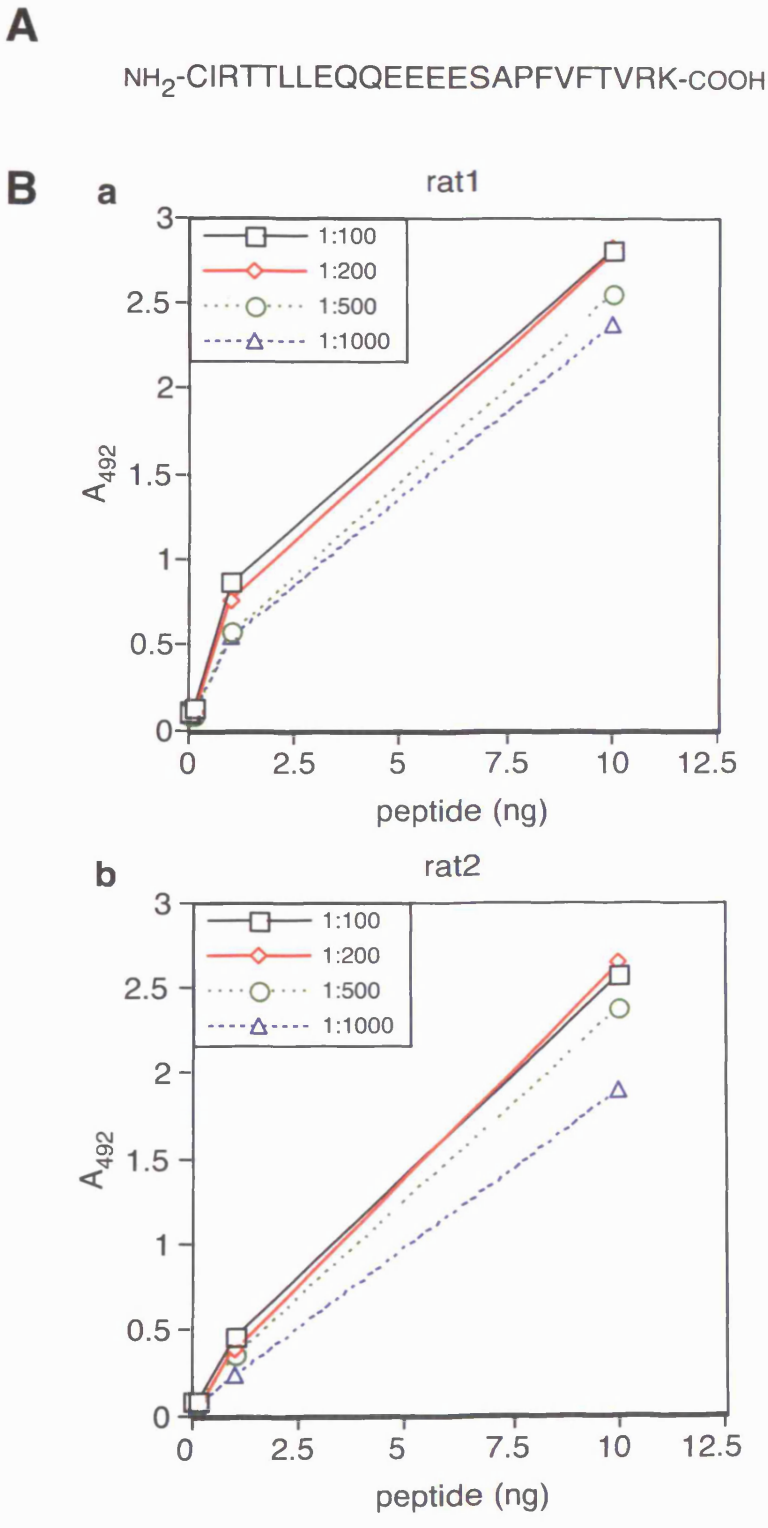

Figure 5-5: *anti dKidins220 antibody*
(A) Sequence of the peptide used for the immunisation, corresponding to residues 1604 to 1626 of dKidins220 (CG30387-RA transcript). (B) Antisera from rat1 (*a*) and rat2 (*b*) recognise the immunising peptide in an ELISA assay.

Chapter 6 –Kidins220 targeting in mouse

6 Kidins220 targeting in mouse

6.1 Introduction

The laboratory mouse (*Mus musculus*) has been used as a model organism since the beginning of the last century. Mouse strains have become of prime importance in biology and medicine, as they often offer the only possibility to model complex human diseases or to test drugs. The physical map of the mouse genome was completed in 2002 (Gregory et al., 2002), revealing that mouse and human genomes are very similar both in terms of size (about 3,000 Mb for the haploid genome) and number of genes (30,000 to 50,000).

The number of mutant mouse strains generated for research purpose is constantly increasing. Mutant strains can derive from ordinary breeding, but more commonly they are the result of genetic manipulation. Genetically altered mice can be knock-in, when foreign genes are inserted in the genome, or knock-out, when the gene of interest is removed or mutated in order to give a non functional product. A common problem when working with knock-out animals, however, is that the elimination of the protein of interest could result in embryonic lethality. This can potentially compromise subsequent studies, especially if death happens at early stages of development. The possibility of obtaining conditional gene ablation in specific tissues and/or at specific stages of development has now made possible to bypass the problem of embryonic lethality, allowing at the same time a more accurate characterisation of loss-of-function phenotypes.

6.2 Cloning strategy

6.2.1 Description of the targeting vector

A bioinformatic analysis, conducted with the help of Michael Mitchell (Bioinformatics and Biostatistic Service, CRUK), allowed me to map the mouse *Kidins220* gene (mKidins220, Unigene name C330002I19Rik) to the region 19422500 – 19507200 of chromosome 12. In order to conditionally delete Kidins220 in mice, I took advantage of a vector (*pFlrt-lacZ.gck*), based on the Cre/lox recombination system, kindly provided by Dr. R.H. Adams (Vascular Development Laboratory, CRUK). This approach relies on the activity of Cre, a recombinase of the P1 bacteriophage, which is able to catalyse DNA recombination at specific recognition sites (loxP sites). When transferred *in vitro* by transfection, or *in vivo* by genetic crosses, Cre mediates the excision of the DNA between the two loxP sites (Sauer and Henderson, 1988). Different mouse lines have been created, which express the Cre recombinase in specific tissues or at precise developmental stages. In the Cre/lox recombination system, the gene of interest is flanked by two loxP sites. By mating lox mice with Cre-expressing animals, it is therefore possible to delete the gene in a controlled fashion. A scheme of the *pFlrt* vector is shown in Figure 6-1 A. In order to generate the final construct, it is necessary to clone and insert into the vector four regions, which will be referred to as short arm, splice acceptor, floxed region, and long arm. A general scheme of the strategy is shown in Figure 6-2. The long and short arm are genomic regions that will recombine with the wild type allele at the 5' and 3' ends, respectively (Figure 6-2 A and B). The floxed region will contain a cDNA-polyA fusion cassette, flanked by two loxP sites. A key feature of

this strategy is the requirement of a restriction site in the cDNA, which has to be unique in the entire targeted genomic region. This site would allow the insertion of the cDNA-polyA cassette into the floxed region (see also Figure 6-6 D). The splice acceptor consists of the first part of the cDNA cassette, fused to a IRES (*i*nternal *r*ibosomal *e*ntry *s*ite)-lacZ-polyA encoding region. Further downstream, the construct contains a neomycin resistance cassette, which provides a means of selection of recombinant ES cells, flanked by two Frt sites. Frt sequences are specifically targeted by the Flp recombinase (McLeod et al., 1986). In a similar way to the Cre/lox system, the neomycin resistance cassette can be removed upon mating of lox animals with Flp expressing mice. In the lox animals (Figure 6-2 B), a complete mRNA is transcribed from the cDNA, under the control of the endogenous promoter, thus generating a full-length functional protein. It needs to be mentioned, however, that transcription from cDNA does not allow the generation of alternative spliced mRNA, as the splicing signals usually present in the pre-mRNA are missing. The lacZ cassette in the lox animals is not transcribed, as transcription ends at the level of the upstream polyA region. When lox mice are crossed with Cre expressing mice, the floxed region is removed, thus generating a knock-out allele (Figure 6-2 C). In this situation, the lacZ gene is expressed under the control of the endogenous promoter, allowing in principle the visualisation of the expression pattern of the protein. The resulting mRNA will be a fusion between the first part of the cDNA cassette, and the lacZ mRNA. The IRES sequence would ensure efficient translation of the β-galactosidase protein. The first part of this mRNA fusion usually does not give any functional products, however it is possible that a short fragment of the original protein is synthesised. If this fragment is sufficiently stable, it could have

detectable biological effects. It is therefore important to verify that no partial fragments of the proteins are produced, which could alter or obscure the loss-of-function phenotype.

Figure 6-1 also shows the polylinker regions of the *pBK-CMV* and *pBS-KS-polyA* vectors. *pBK-CMV* (Figure 6-1 B) was used as intermediate vector, to facilitate the sequencing of the different fragments, before the insertion in *pFlrt*. The cDNA was inserted into *pBS-KS-polyA* (Figure 6-1 C), upstream to the polyA sequence. The cDNA-polyA cassette was then cut and inserted into the floxed regin (Figure 6-6 C). Both vectors were provided by Dr. R.H. Adams.

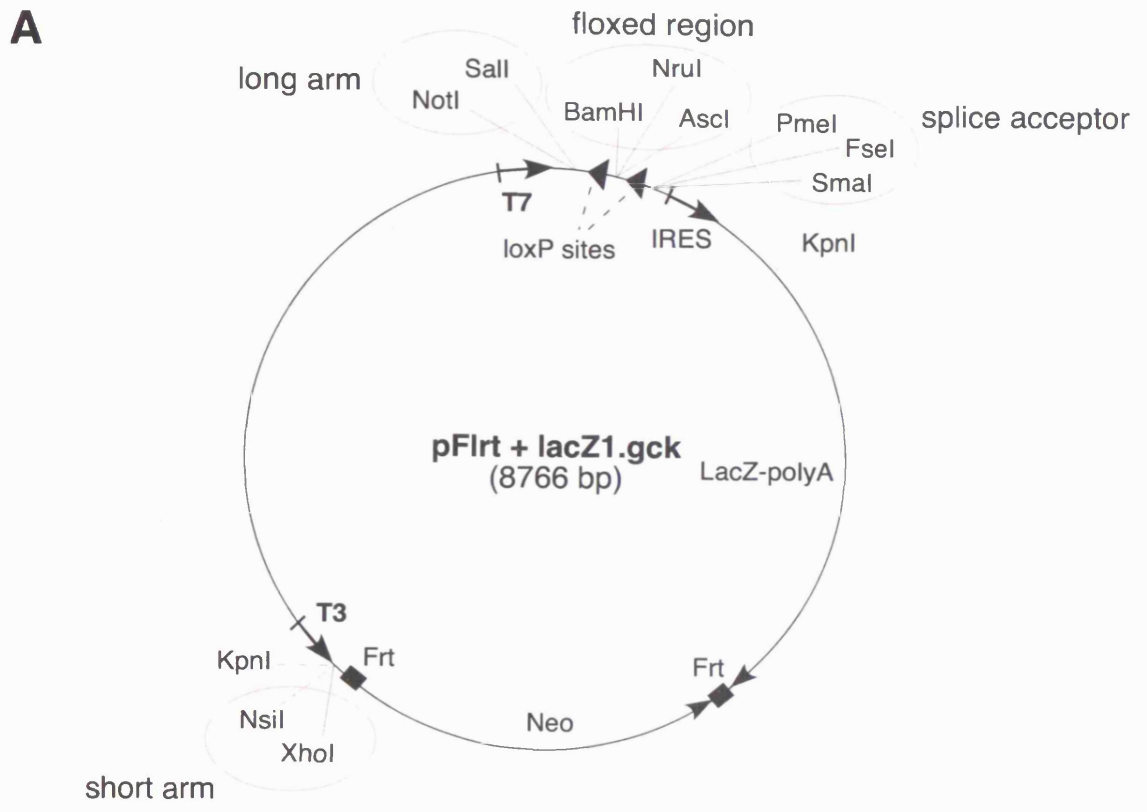

B

pBK-CMV

T7 KpnI BstXI SmaI ApaI NotI XbaI ScaI XhoI HindIII...
...EcoRI BamHI SpeI AccI/SalI PstI BssHII SacI **T3**

C

pBS-KS-polyA

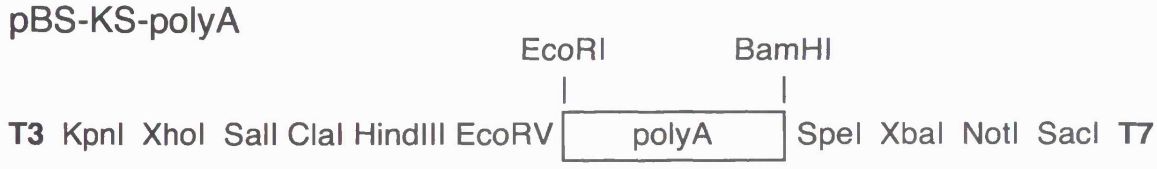

Figure 6-1: *scheme of the vectors used in this work*
(A) Scheme of the *pFlrt* vector. The restriction sites for the insertion of the different regions are indicated. (B) Multiple cloning site region of the *pBK-CMV* vector. (C) Multiple cloning site of the *pBS-KS-polyA* vector. The polyA cassette is indicated. Kidins220 cDNA was inserted into the EcoRV site.

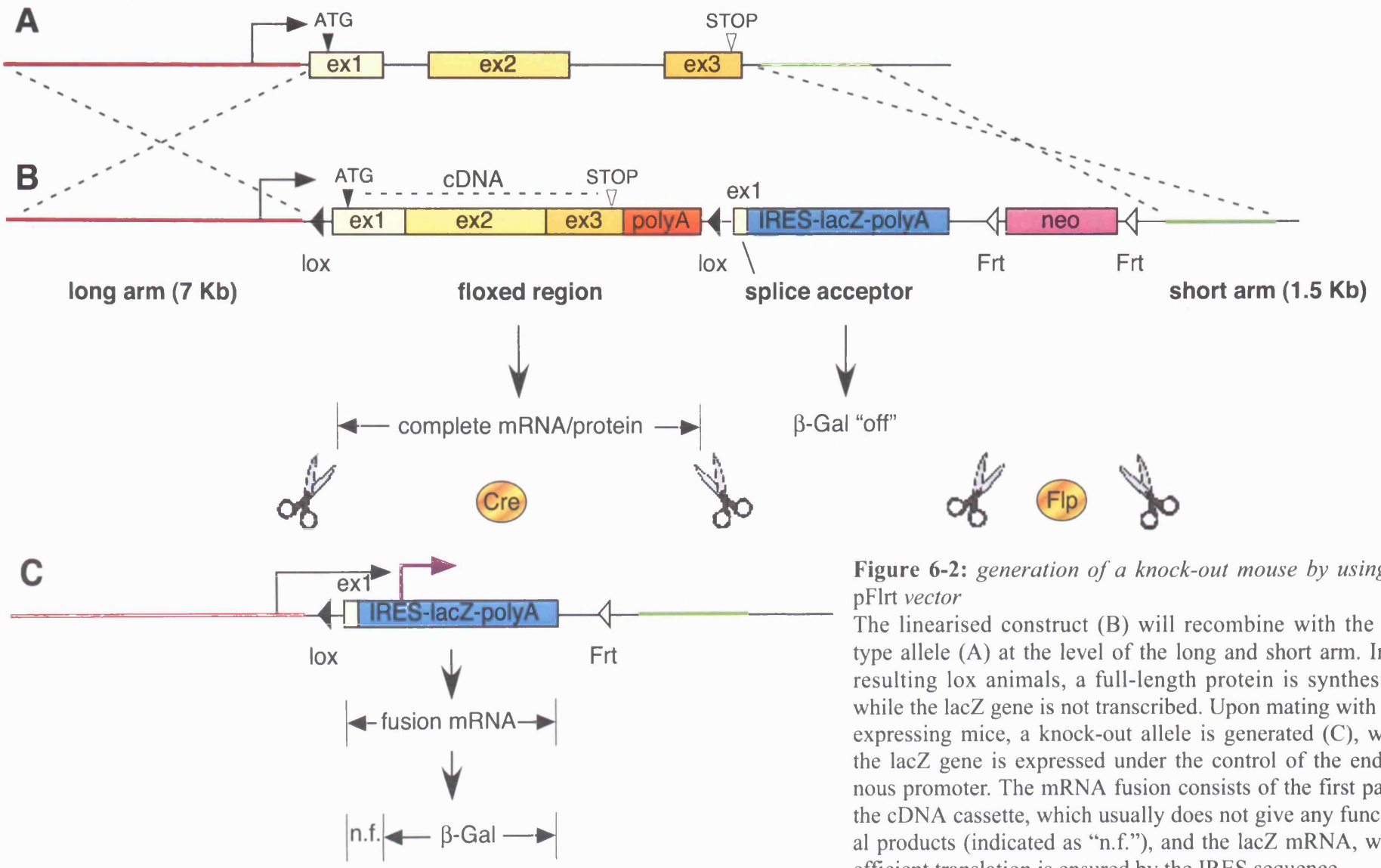

Figure 6-2: *generation of a knock-out mouse by using the* pFlrt *vector*
The linearised construct (B) will recombine with the wild type allele (A) at the level of the long and short arm. In the resulting lox animals, a full-length protein is synthesised, while the lacZ gene is not transcribed. Upon mating with Cre-expressing mice, a knock-out allele is generated (C), where the lacZ gene is expressed under the control of the endogenous promoter. The mRNA fusion consists of the first part of the cDNA cassette, which usually does not give any functional products (indicated as "n.f."), and the lacZ mRNA, whose efficient translation is ensured by the IRES sequence.

6.2.2 *Analysis of mKidins220 genomic map*

The mKidins220 gene is spread over 29 exons, spanning a genomic region of about 90 kb (Figure 6-3). Ideally, the first loxP site should be inserted as close as possible to the beginning of the gene, in order to minimise the length of coding mRNA that will be transcribed in the knock-out allele. However, the N-terminal portion of mKidins220 is coded by several small and dispersed exons, which do not represent a good target region. In addition, a strategy based on the *pFlrt* vector requires the presence of a unique restriction site, as discussed above. By analysing the restriction map of the Kidins220 gene, I identified a NruI site located at the level of exon 16, in a region containing a cluster of exons in relatively close proximity. On the basis of all these considerations, I decided to target the mKidins220 gene at the level of the NruI site (bases 1856-1861 of mKidins mRNA).

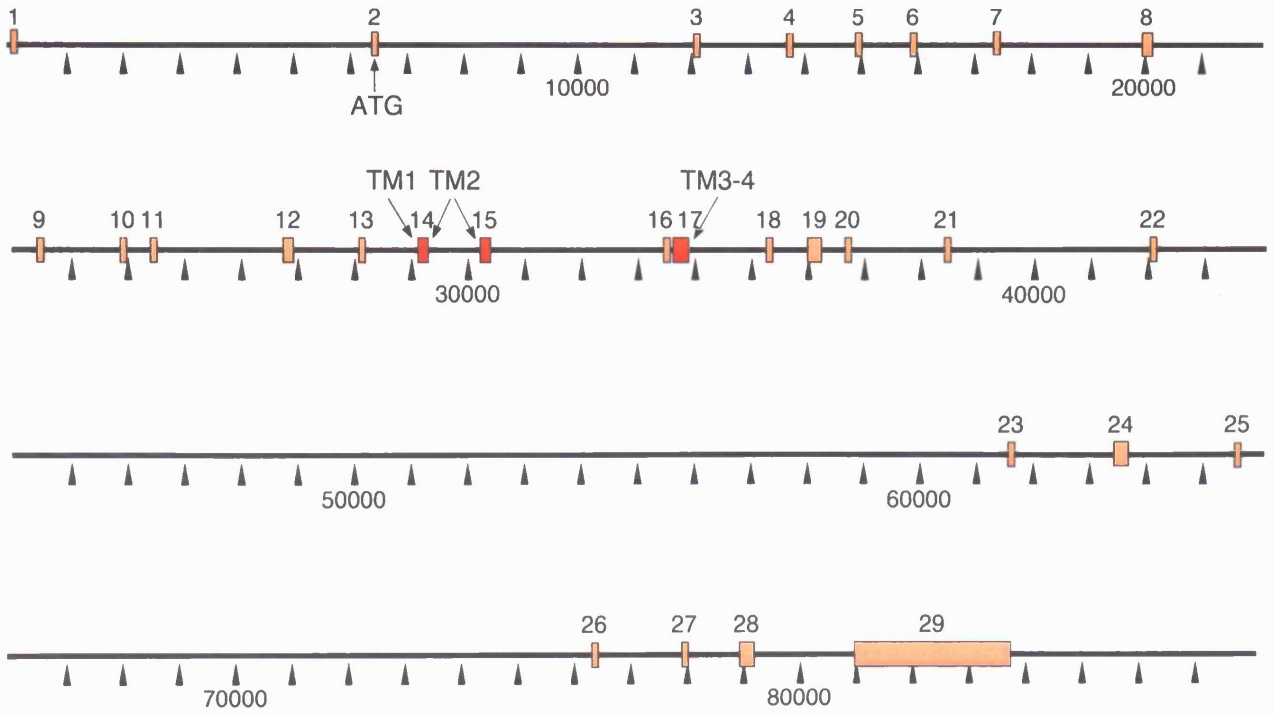

Figure 6-3: m*Kidins220 genomic map*
The mKidins220 gene is spread over 29 exons, spanning a genomic region of about 90 kb. The N-terminal tail of Kidins220 is coded by exon 2 to 13; the four membrane spanning regions are coded by exon 14 to 17. The carboxy terminal tail is coded by 11 small exons (exon 18 to 28) and a final longer exon. Black arrowheads mark 1 kb intervals.

6.2.3 Strategy for the generation of Kidins220 knock-out mice

Figure 6-4 describes the strategy that I followed for the generation of the Kidins220 knock-out mice. The long arm spans a genomic region of about 7 kb, from exon 12 to just before the beginning of exon 16, whereas the short arm spans a 1.5 kb region around exon 18. The cDNA-polyA cassette is fused to exon 16 at the level of the NruI site. The first portion of exon 16 is also present in the splice acceptor region, which is fused to the IRES-lacZ-polyA sequence. In the knock-out allele, the mRNA will be formed by the N-terminal portion of Kidins220 mRNA, fused to the lacZ coding sequence. As discussed in section 6.2.1, this could originate a truncated protein, which would comprise the N-terminal cytoplasmic tail and the first two transmembrane domains of Kidins220.

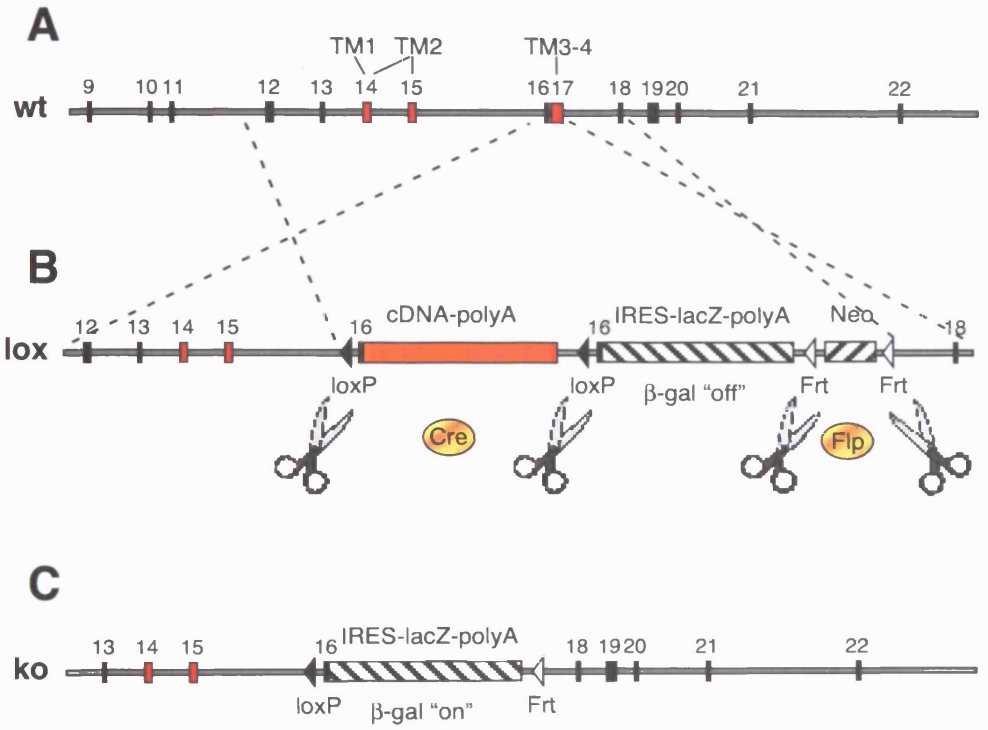

Figure 6-4: *strategy for the generation of Kidins220 knock-out mice*
The linearised *pFlrt* construct (B) would recombine with the wild type allele (A), as indicated. Upon mating with Cre expressing mice, the cDNA is excised, thus generating the knock-out allele (C).

6.3 Identification of IMAGE and PAC clones for mKidins220

6.3.1 Identification of IMAGE clones spanning mKidins220 cDNA

IMAGE (*I*ntegrated *M*olecular *A*nalysis of *G*enomes and their *E*xpression) clones are cDNA clones containing a full length or partial open reading frame. A bioinformatic search conducted with the help of Michael Mitchell (Bioinformatics and Biostatistic Service, CRUK), allowed me to identify four IMAGE clones that were predicted to span different regions of mKidins220 cDNA (see Figure 6-5). The four clones were purchased, and their 5' and 3' regions verified by direct sequencing.

6.3.2 Hybridisation of mouse PAC library

The generation of the final *pFlrt* construct required the amplification of different genomic regions of the mKidins220 gene. To this end, I screened the mouse PAC library RPCI21, with a Kidins220-specific probe. This library was generated from mouse spleen genomic DNA, and consisted of approximately 128,000 clones, with an average insert size of 147 kb.

The screen was performed as described in Materials and Methods, using the 2000 bp insert from the IMAGE clone n.1 (2192152) as probe. The hybridisation of the filters allowed me to identify 2 PAC clones (515-K9 and 542-I24) containing the genomic region corresponding to the mKidins220 gene. These clones were purchased as bacterial stocks, and their DNA was purified as described in Materials

and Methods. It was then necessary to verify whether the two clones covered the entire genomic region needed for the cloning. To this purpose, I designed primers that would amplify single exons of the mKidins220 gene, from exon 9 to exon 22, and performed a series of PCR reactions using DNA from the two PAC clones as template. I obtained PCR bands for all the exons, for both clones (data not shown). I decided to proceed with clone 515-K9.

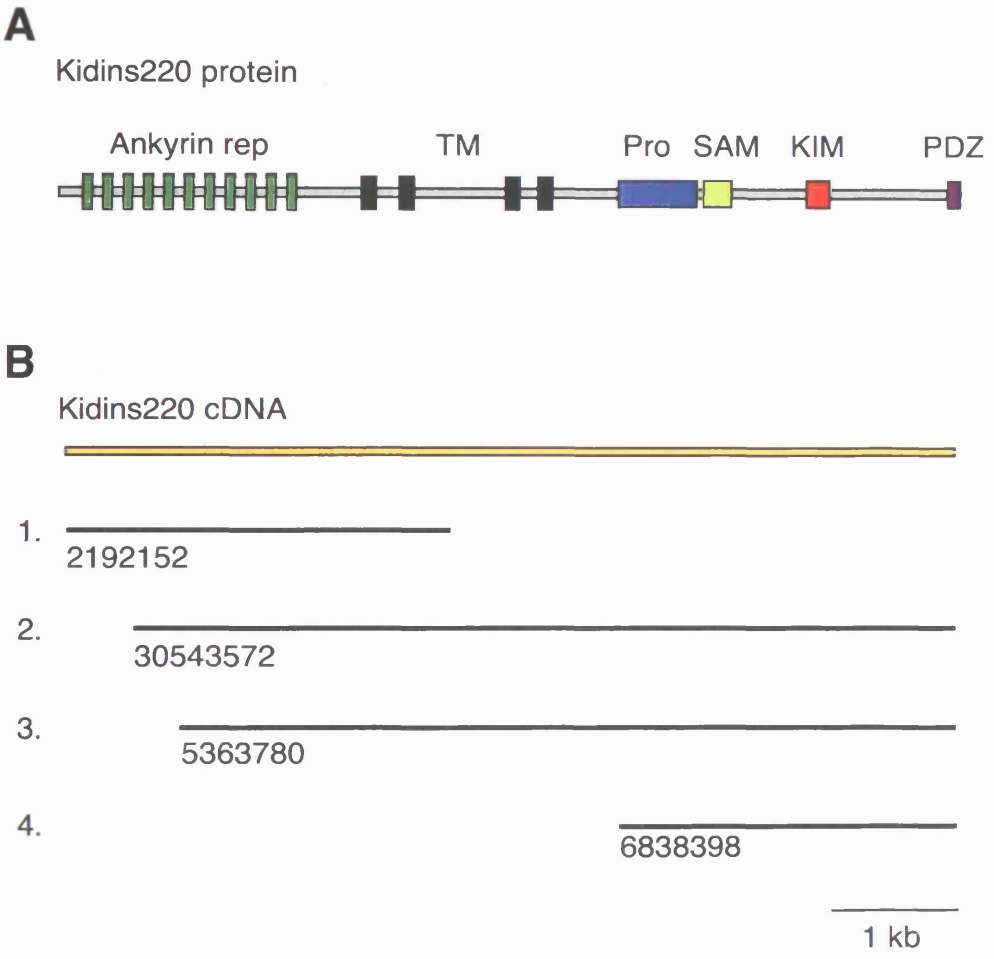

Figure 6-5: *IMAGE clones spanning mKidins220 cDNA*
Schematic representation of the Kidins220 protein (A) and cDNA (B). The black lines indicate the cDNA regions spanned by the four IMAGE clones (accession numbers are indicated). The 5' and 3' regions of each clone were verified by direct sequencing. Ankyrin rep, Ankyrin repeats; TM, transmembrane regions; Pro, proline-rich domain; SAM, SAM domain; KIM, KLC-interacting motif, PDZ, PDZ-binding motif. Scale bar = 1 kb.

6.4 Engineering of the construct

6.4.1 Generation of the different fragments

The short arm, splice acceptor and floxed regions were amplified from the PAC clone 515-K9 with the primers listed in Table 4 (Materials and Methods), using standard PCR procedures. For the amplification of the long arm, the Expand Long Template PCR System (Roche) was used, which is especially formulated to efficiently amplify genomic DNA fragments up to 22 kb. The PCR program used for the amplification of this fragment is described in Table 11. The cDNA sequence comprised between the KpnI (1709) and ApaLI (6854) sites was cut from the IMAGE clone 30543572. The DNA ends were blunted using Mung Bean Nuclease (NEB), and the fragment was then inserted into the EcoRV site of pBS-KS-polyA.

Table 11: *PCR program for the amplification of the long arm*

	Temperature	Time	Cycle n.
Initial denaturation	94°C	2 min	1 X
Denaturation Annealing Elongation	94°C 65°C 68°C	10 s 30 s 6 min	10 X
Denaturation Annealing Elongation	94°C 65°C 68°C	15 s 30 s 6 min + 20 s cycle elongation for each successive cycle	25 X
Final elongation	68°C	7 min	1 X
Cooling	12°C	unlimited time	

6.4.2 *Insertion in pBK-CMV vector and sequencing*

Short arm, splice acceptor, floxed and long arm regions were all first inserted into the *pBK-CMV* vector, using the appropriate restriction sites, as described in Figure 6-6.The cDNA-polyA cassette was cut out the *pBS-KS-polyA* vector and inserted into the floxed region, already in the *pBK-CMV* vector (Figure 6-6 D).

All the exons, splicing consensus sites and the complete cDNA were verified by direct sequencing, and compared to the predicted mKidins220 sequence. For each region, a minimum of 10 different clones were analysed. A number of conservative single-point mutations were identified. Many of these mutations were present in all the clones analysed, and likely represented genetic polymorphisms. For the insertion into the *pFlrt* vector, I selected the clones that had the lower number of conservative mutations.

One single-point mutation was identified, which destroyed the NruI site in the floxed region. Since this site is fundamental for the cDNA insertion, it was necessary to perform a site-directed mutagenesis on the floxed region, to restore the correct sequence. The mutagenesis was performed following standard procedures, with the primers listed in Table 4 (Materials and Methods).

6.4.3 *Insertion in the final vector*

The fragments were inserted into the *pFlrt* vector in the following order: short arm, splice acceptor, floxed-cDNA-polyA, long arm. After each insertion, the product was verified by a series of restriction digestions. The final construct was prepared for electroporation, as described in Materials and Methods.

A

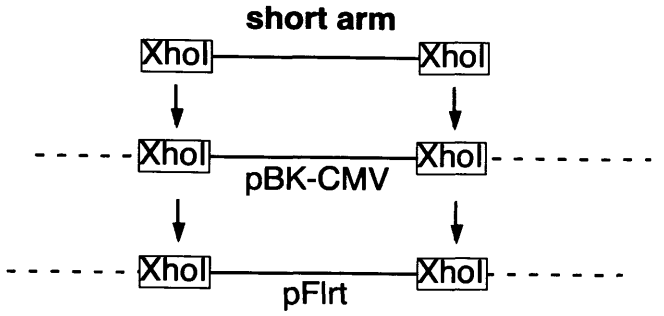
short arm
XhoI
XhoI
XhoI
XhoI
pBK-CMV
XhoI
XhoI
pFlrt

B

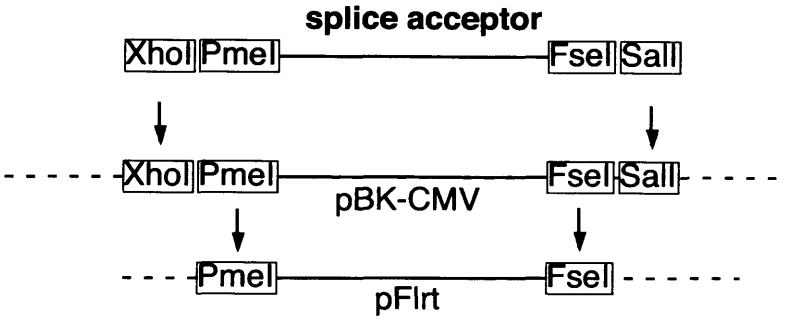
splice acceptor
XhoI
PmeI
FseI
SalI
XhoI
PmeI
FseI
SalI
pBK-CMV
PmeI
FseI
pFlrt

C

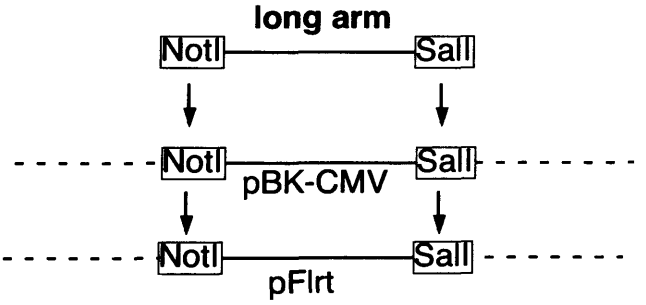
long arm
NotI
SalI
NotI
SalI
pBK-CMV
NotI
SalI
pFlrt

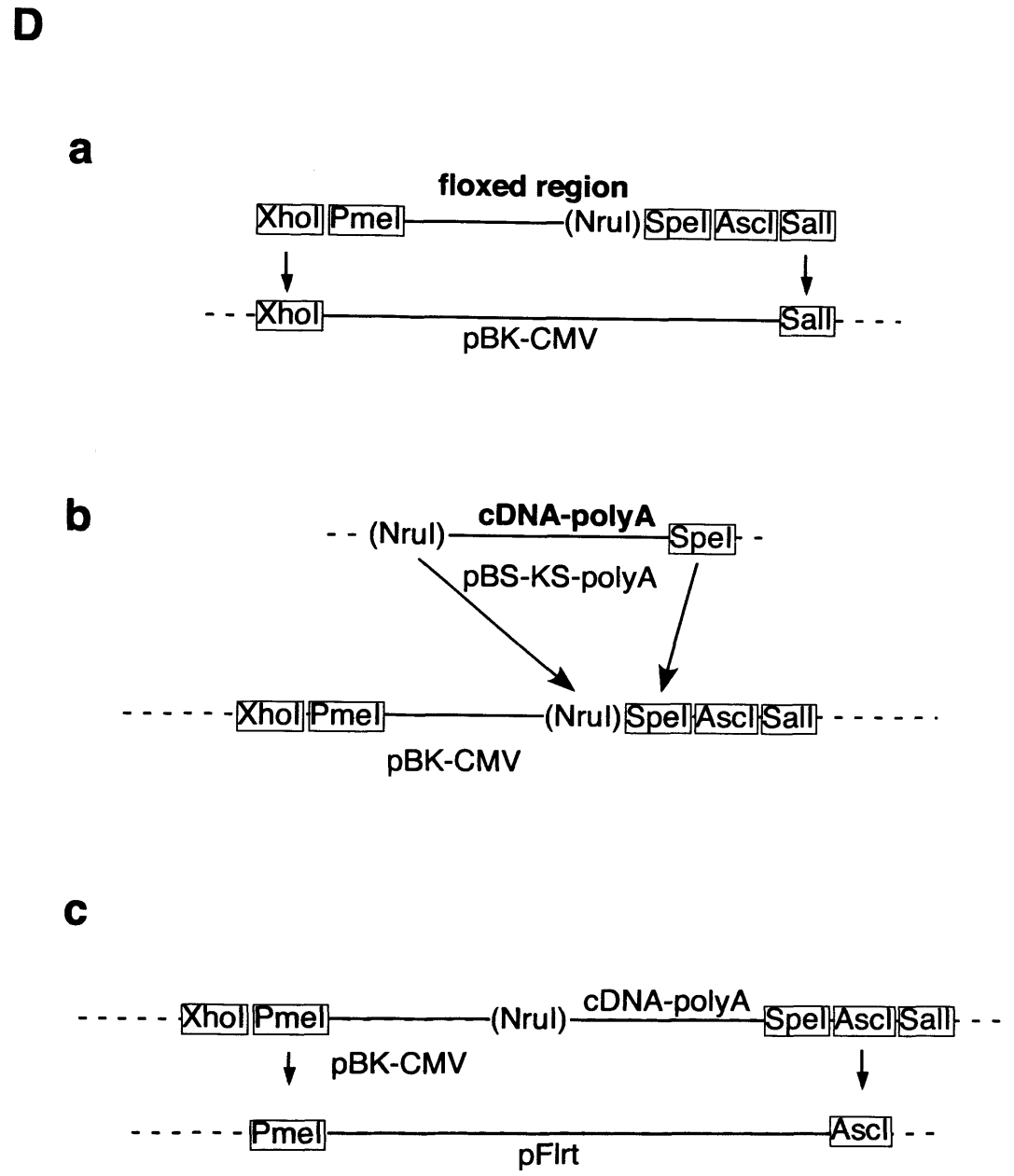

Figure 6-6: *engineering of the construct*
The short arm (A), splice acceptor (B), long arm (C) and floxed (D) regions were amplified from genomic DNA, inserted into the *pBK-CMV* vector, verified by sequencing, and then inserted in the *pFlrt* vector, as described in the text. The cDNA-polyA sequence was inserted into the *pBK-CMV* vector already containing the floxed region (D *b*), prior to insertion of the flox-cDNA-polyA cassette into *pFlrt* (D *c*).

6.5 Generation and identification of transgenic ES cells

ES cell electroporation and maintenance, as well as blastocyst injection and mouse breeding, were carried out by the Transgenic Services Department (Clare Hall laboratories, CRUK). Briefly, male 129 ES cells were electroporated with the linearised *pFlrt* construct, and recombinant clones were identified by using G418, an inhibitor of protein synthesis used to select for cells transfected with the neomycin resistance gene. Single colonies were picked and grown in duplicates in 96 well plates. DNA was isolated from four plates as described in Materials and Methods, and screened by PCR. A first screen was performed with primers that would amplify the short arm recombination site (3' recombination). Positive clones were additionally checked with primers specific for the 5' recombination site (Figure 6-7 A, B). These two PCR screens allowed me to identify three positive ES clones, indicated as 2F8, 4B12, 4E10. These clones were further subjected to Southern blot analysis.

Analysis by Southern blot is based on the fact that recombinant and wild type DNA would give bands of different sizes when digested with appropriate restriction enzymes. It is necessary to perform this type of analysis, to exclude that additional copies of the construct are integrated into non-specific sites. Analysis of the Kidins220 genomic sequence allowed me to identify NheI and SacI as enzymes that would discriminate between DNA fragments corresponding to the wild type and recombinant alleles. NheI digestion was supposed to generate a 17 kb band for the genomic, and an 11 kb band for the recombinant DNA, at the 5' recombination site. SacI digestion would give a 4.3 kb band for the genomic, and 6.3 kb band for the

recombinant DNA. To visualise these bands, I used a probe spanning exon 12 for the 5' recombination, and exon 18 for the 3' recombination, as indicated in Figure 6-7 A. All the three clones showed the correct hybridisation pattern (Figure 6-7 C). Clone 2F8 and 4B12 were selected for blastocyst injection.

6.5.1 Generation of Kidins220 -/- ES cells

ES cells are pluripotent cells that maintain the capability to differentiate into virtually all cell types. In recent years, a number of different protocols have been established, which allow the differentiation of ES cells into specific lineages (Keller, 2005). Dr. M. Golding (Molecular Neuropathobiology laboratory, CRUK) has generated a line of Kidins220 null ES cells. Briefly, homozygous lox/lox cells were generated by treating the parental +/lox line with high concentrations of G418. This approach is based on the assumption that high dosages of this compound selectively allow the survival of clones containing two copies of the neomycin resistance gene. The mechanisms underlying this process are still uncharacterised, and they might involve gene conversion, mitotic recombination or chromosome loss/duplication (Lefebvre et al., 2001). G418-resistant clones would therefore be lox/lox. Single clones were grown in duplicates in 96 well plates and screened by PCR, with primers for the 5' and 3' recombination site (see Figure 6-7 A-B). The efficiency of recombination was unexpectedly high, as almost 100% of the screened colonies (n = 48) had a lox/lox genotype. Figure 6-8 A shows the PCR result obtained from two representative lox/lox clones, indicated as 1F and 5E. In this experiment, the parental 4B12 +/lox line was used as a control. Southern blot analysis confirmed the genotype of the clones (not shown). In order to obtain the knock-out of Kidins220,

clone 5E lox/lox cells were transfected with a plasmid encoding Cre recombinase. Single clones were grown in duplicates and screened by using the KO-specific PCR described in Figure 6-9. I found that about 15% of the clones analysed (n = 96) were positive for the knock-out allele. These clones were subjected to additional PCRs, to verify that the loxed region had been completely removed (not shown). This second screen allowed me to identify one clone that showed a complete removal of both lox alleles. The Kidins220 -/- clone was then expanded and subjected to RT-PCR and Western blot analysis, to verify the deletion of Kidins220 at both the mRNA and protein level (Figure 6-8 B-C). The RT-PCR showed a complete ablation of the Kidins220 mRNA in the Kidins220 -/- line (Figure 6-8 B). As discussed in section 6.8.1, this suggests that the Kidins220 lacZ-mRNA fusion is unstable. Western blot analysis confirmed the ablation of Kidins220 also at the protein level (Figure 6-8 C). A detailed description of the experimental procedures conducted on the ES cell lines is available in the Materials and Methods section.

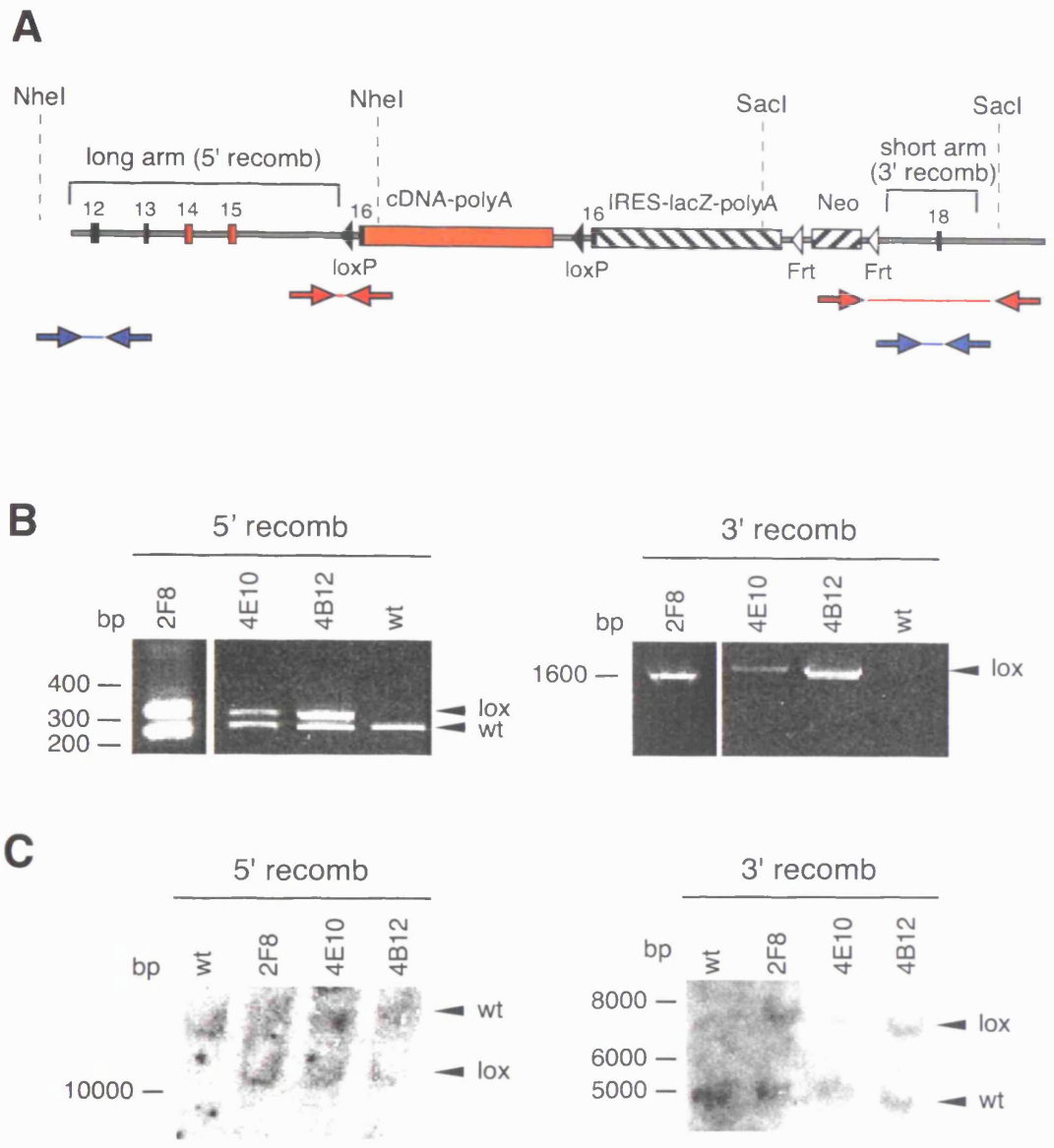

Figure 6-7: *PCR and southern blot on three ES clones*
(A) The position of the probes used for the PCR screen (red arrows) and for the Southern blot (blue arrows), as well as the position of the restriction sites used for the Southern blot, are indicated. (B) PCR for the 5' (left panel) and for the 3' (right panel) recombination site on a wild type clone and the three recombinant ES clones. The 4E10 clone gave weaker bands than the other clones, probably due to the presence of impurities in the starting genomic material, which decreased the efficiency of the PCR reaction. For the 5' PCR we used the primers "long-s fw" and "flox-as rv"; for the 3' PCR we used the primers "pflrt-s-neo fw" and "short-as rv" (primer sequences are available in Table 4, in the Materials and Methods section). (C) Southern blot for the 5' (NheI digestion, left panel) and for the 3' (SacI digestion, right panel) recombination site on a wild type clone and the three recombinant ES clones. In (B) and (C), arrowheads indicate the position of the wild type (wt) and recombinant (lox) bands.

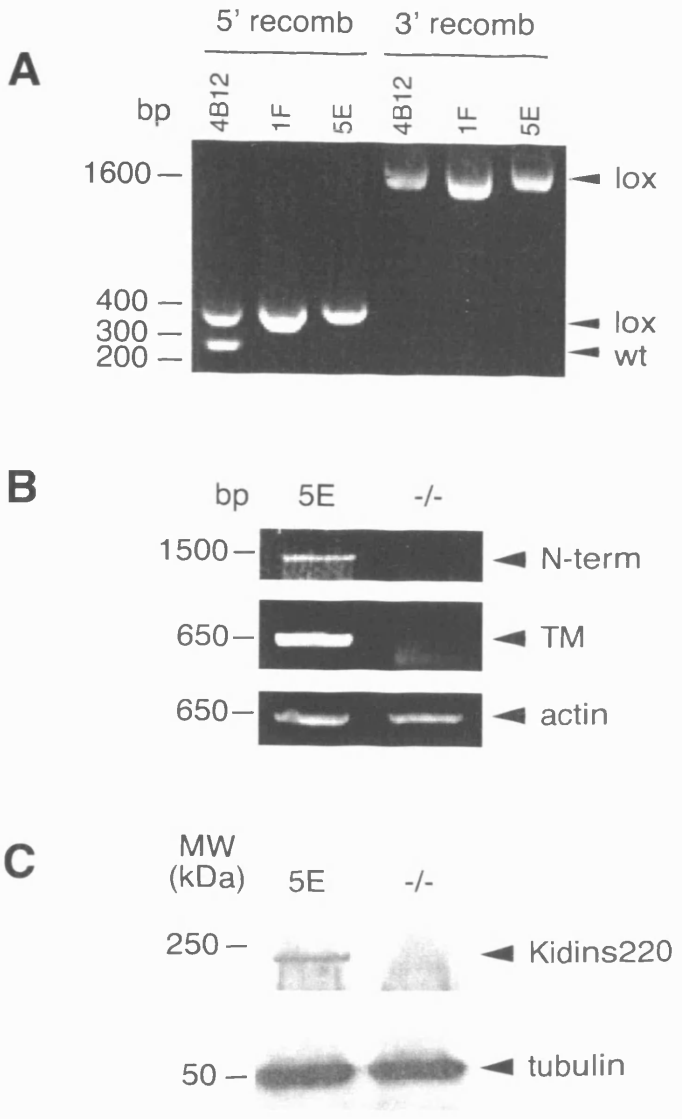

Figure 6-8: *generation of Kidins220 -/- ES cells*
(A) PCR for the 5' (left) and for the 3' (right) recombination site on the parental 4B12 +/lox clone and two lox/lox ES clones (1F and 5E) obtained by G418 selection. (B) The Kidins220-lacZ mRNA fusion is unstable. Total RNA was extracted from the lox/lox 5E and the Kidins220 -/- clones, and cDNA was synthesised following standard procedures (see Materials and Methods). cDNA was then used as the template for PCR reactions using primers specific for the regions encoding the N-terminal portion (N-term) or the transmembrane domains (TM) of Kidins220. For the N-term PCR we used the primers "5' KNAP 136787" and "3' GAP1 142201"; for the TM PCR we used the primers "5' GAP2 142199" and "3' GAP2 142202" (primer sequences are available in Table 4, in the Materials and Methods section). Actin-specific primers were used as a control. (C) The Kidins220 protein is absent in the Kidins220 -/- ES line. Western blot using Kidins220-specific antibodies (top panel) and tubulin antibodies (bottom panel) as a loading control.

6.6 Generation of Kidins220 mutant mice

The selected recombinant ES clones were injected into blastocysts derived from a C57BL6/J female. This strategy allows to recognise chimeric animals by the colour of their fur: 129-derived cells give cream colour, whereas C57BL6/J-derived cells give black colour. Chimeras are given a score on the basis of the percentage of cream (129-derived) colour. Animals that show more than 70% cream colour are likely to give germline transmission of the recombinant allele, and are backcrossed with C57BL6/J females. We obtained 1 male chimera from the 2F8 clone, and 4 male chimeras from the 4B12 clone, which had a score above 70%.

6.7 Crosses

All the crosses described in this section were set up in the clean unit of the Clare Hall laboratories, CRUK.

6.7.1 Generation of lox/lox animals

The 2F8 and 4B12 chimeras were crossed with C57BL6/J females. Litters were genotyped by using the 5' recombination PCR (Figure 6-7 A, B). The number of animals obtained from these crosses, with the corresponding genotype, is shown in Table 12. Both chimeras gave a very good germline transmission, at a rate close to 50%.

+/lox mice derived from both the chimeras were then crossed with each other, in order to obtain lox/lox animals. The percentage of different genotypes in the litters obtained from these crosses was close to the expected one (Table 13),

indicating that the lox allele segregates normally. Furthermore, lox/lox animals are healthy, indicating that the recombination event *per se* does not have any effects on viability. However, no litters were obtained from lox/lox X lox/lox crosses. In the attempt to understand the cause of this problem, the following crosses were set up: 1) +/lox females X lox/lox males; 2) lox/lox females X +/lox males. In the first case, the females showed the same problem than in the lox/lox crosses. Unexpectedly, litters from the second cross showed the expected +/lox : lox/lox ratio. At the moment, we do not have a convincing explanation for this result.

Table 12: *C57BL6/J ♀ X chimera ♂*

Number of animals obtained from the C57BL6/J ♀ X chimera ♂ crosses, with the corresponding genotypes.

	2F8		4B12	
	n. animals	%	n. animals	%
+/+	37	51.4	19	52.8
+/lox	35	48.6	17	47.2
total	72	100	36	100

Table 13: *+/lox ♀ X +/lox ♂*

Number of animals obtained from the +/lox ♀ X +/lox ♂ crosses, with the corresponding genotypes. Expected values are in brackets.

	2F8		4B12	
	n. animals	% (exp)	n. animals	% (exp)
+/+	25	22.32 (25)	48	26.7 (25)
+/lox	60	53.57 (50)	87	48.3 (50)
lox/lox	27	24.11 (25)	45	25 (25)
total	112	100	180	100

6.7.2 *Generation of Kidins220 knock-out animals*

One of the 4B12-derived chimeras, which showed a high efficiency of germline transmission, was bred to females from the PGK-Cre strain, to obtain Kidins220 +/KO animals. In PGK-Cre mice, Cre expression is regulated by the phosphoglycerate kinase (PGK) promoter, which is active in females as early as the diploid primordial germ cells (Lallemand et al., 1998). When PGK-Cre animals are mated with animals carrying the lox allele, the early and ubiquitous activation of the Cre recombinase ensures the complete ablation of the gene of interest. The animals obtained from this cross, with the corresponding genotypes, are listed in Table 14. It is interesting to notice the presence of animals bearing the knock-out allele, which are negative for the Cre transgene. This is due to the activity of maternal Cre, which was shown to be already active in the early, diploid phase of oogenesis (Lallemand et al., 1998). In addition to the PCR for the 5' recombination, the genotype of these animals was confirmed by using another PCR, which would give a band only in the knock-out allele (see Figure 6-9). The Kidins220 +/KO mice were viable and did not show any physical or behavioural defect. It was therefore possible to cross these mice with each other, in order to obtain full knock-out animals.

Kidins220 +/KO animals were fertile, and were able to breed normally. The genotyping of the litters, however, revealed only the presence of wild type (+/+) or heterozygous (+/KO) animals, in a ratio of about 2 : 1 (Table 15). This indicates that the full knock-out of Kidins220 is not viable. As discussed in the following section, knock-out animals die at birth.

Table 14: *PGK-Cre +/- (Kidins220 +/+) ♀ X chimera 4B12 (Kidins220 +/KO) ♂*

Number of animals obtained from the PGK-Cre +/- (Kidins220 +/+) ♀ X chimera 4B12 (Kidins220 +/KO) ♂ crosses, with the corresponding genotypes.

Cre	Kidins220	n. animals	%
+	+/+	7	14.6
+	+/KO	12	25
-	+/+	12	25
-	+/KO	17	35.4
total		48	100

Table 15: *Kidins220 +/KO ♀ X Kidins220 +/KO ♂*

Number of animals obtained from the Kidins220 +/KO ♀ X Kidins220 +/KO ♂ crosses, with the corresponding genotypes. Expected values are in brackets.

	n. animals	% (exp)
+/+	69	30.8 (25)
+/KO	155	69.2 (50)
KO/KO	0	0 (25)
total	224	100

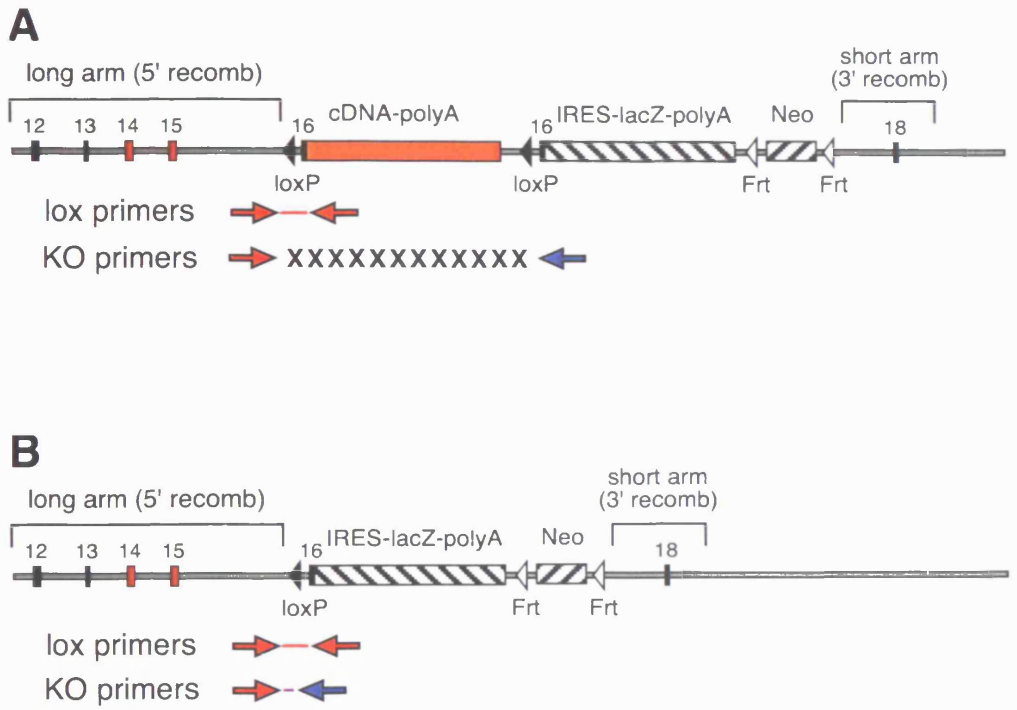

Figure 6-9: *KO-specific PCR*
Scheme of the primers used for the KO-specific PCR. In the lox allele (A), the forward and reverse primers are separated by the cDNA cassette. whereas in the KO allele (B) they are close to each other. By using a PCR cycle with an extension time of 1 min, we obtain a 150 bp band from the KO allele, and no bands from the lox (or wild type) allele. For the lox PCR, we used the primers described in Figure 6-7. For the KO PCR we used the same forward primer ("long-s fw"), with the KO-specific "splice-as" primer (primer sequences are available in Table 4, in the Materials and Methods section). (C) Examples of genotyping on wild type (+/+), knock-out (+/KO) or heterozygous (+/KO) embryos. The "lox" PCR gives a 250 bp band for the wild type allele, and a 350 bp band for the knock-out allele (this PCR does not distinguish between the lox allele and the knock-out allele). The "KO" PCR gives a 150 bp band only in presence of the knock-out allele.

6.8 Analysis of Kidins220 knock-out animals

6.8.1 Validation: RT-PCR and western blot analysis

As first step in the characterisation of the Kidins220 knock-out model, I verified Kidins220 mRNA and protein levels in wild type, heterozygous and knock-out embryos (Figure 6-10). cDNA was prepared from E15 embryos, and analysed by RT-PCR with primers specific for different regions of the Kidins220 transcript. I used primers that would specifically amplify the N-terminal portion of Kidins220 cDNA (N-term, Figure 6-10 A). As discussed above, this portion of the transcript should be present in all the animals, irrespective of their genotype. However, I could not detect any bands for the knock-out embryos, indicating that the Kidins220-lacZ mRNA fusion is probably unstable and consequently degraded. This finding is supported by the fact that all my attempts to visualise Kidins220 expression by β-galactosidase staining have so far been unsuccessful (data not shown). I also used primers specific for the cDNA region encoding the four transmembrane domains (TM), which should be detected only in wild type and heterozygous animals. In accordance with our prediction, I did not amplify any specific bands from the cDNA generated from the KO embryos.

Western blot analysis on brain lysates showed the complete ablation of Kidins220 in the knock-out animals, whereas bands of comparable intensity were detected in the heterozygous and wild type samples (Figure 6-10 B). For this experiment, I used anti-Kidins220 antibodies raised against the C-terminal portion of the protein. As a control, I verified the expression levels of other neuronal proteins

(the neurotrophin receptors TrkB and TrkC), which were found to be unaffected. Unfortunately, no antibodies are available at present, which would recognise the N-terminal tail of Kidins220. It is therefore not possible to assess the presence of a possible truncated fragment of Kidins220 in the knock-out sample, by protein analysis. However, the instability of the Kidins220 lacZ-mRNA suggests that no protein should be produced from the knock-out allele. Altogether, these results indicate that in the knock-out animals Kidins220 is ablated both at a mRNA and protein level.

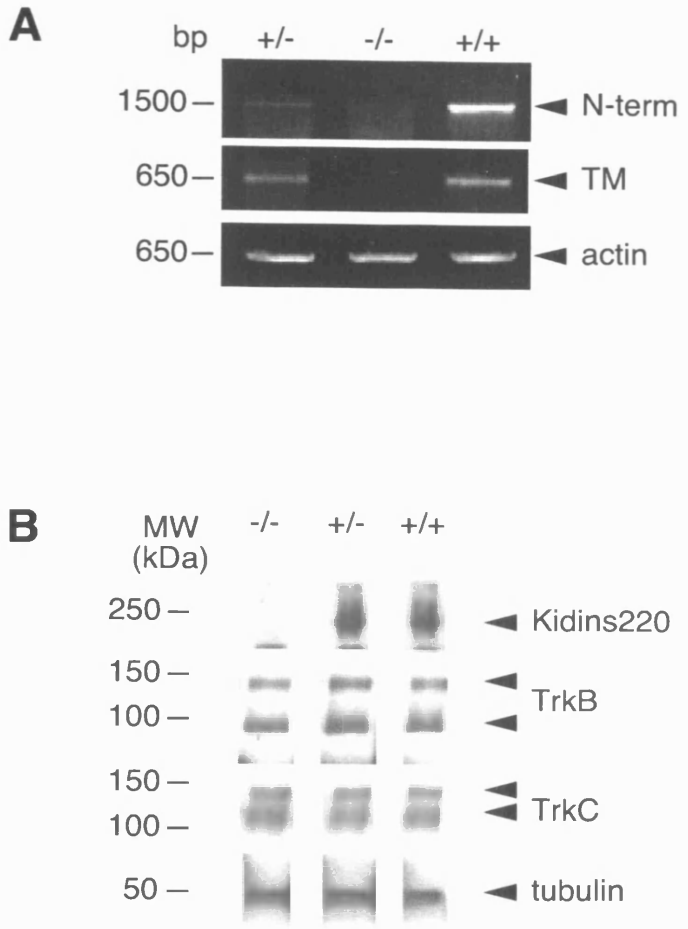

Figure 6-10: *RT-PCR and Western blot on Kidins220 KO embryos*
Kidins220 wild type (+/+), heterozygous (+/-) or knock-out (-/-) embryos were analysed by RT-PCR (A) or Western blot (B). (A) The Kidins220-lacZ mRNA fusion is unstable. Total RNA was extracted from E15 embryos, and cDNA was synthesised following standard procedures (see Materials and Methods). cDNA was then used as template for PCR reactions using primers specific for the regions encoding the N terminal portion (N-term) or the transmembrane domains (TM) of Kidins220 (see Figure 6-8). Actin-specific primers were used as a control. (B) The Kidins220 protein is absent in knock-out animals, whilst the levels of other neuronal proteins are unaffected. Brains from E18.5 embryos were lysed and analysed by Western blot using Kidins220, TrkB and TrkC antibodies. Tubulin antibodies were used to verify that equal amounts of proteins were loaded for each sample.

6.8.2 *Kidins220 knock-out animals die at birth*

As shown in Table 15, genotyping of the litters from the Kidins220 +/KO X Kidins220 +/KO crosses did not detect any knock-out animals at weaning age, suggesting that Kidins220 deletion results in embryonic or perinatal lethality. I therefore tried to determine exactly at which stage of development the knock-out embryos die. I found that the knock-out embryos are undistinguishable from their littermates up to the 15th day of gestation (Figure 6-19 and data not shown). However, by the 18th day they are visibly smaller than their littermates (see Figure 6-11 A). Knock-out animals are alive until the last day of gestation (E19.5), but they die at birth with no macroscopically visible developmental defects, apart from being smaller than their littermates (Figure 6-11 B).

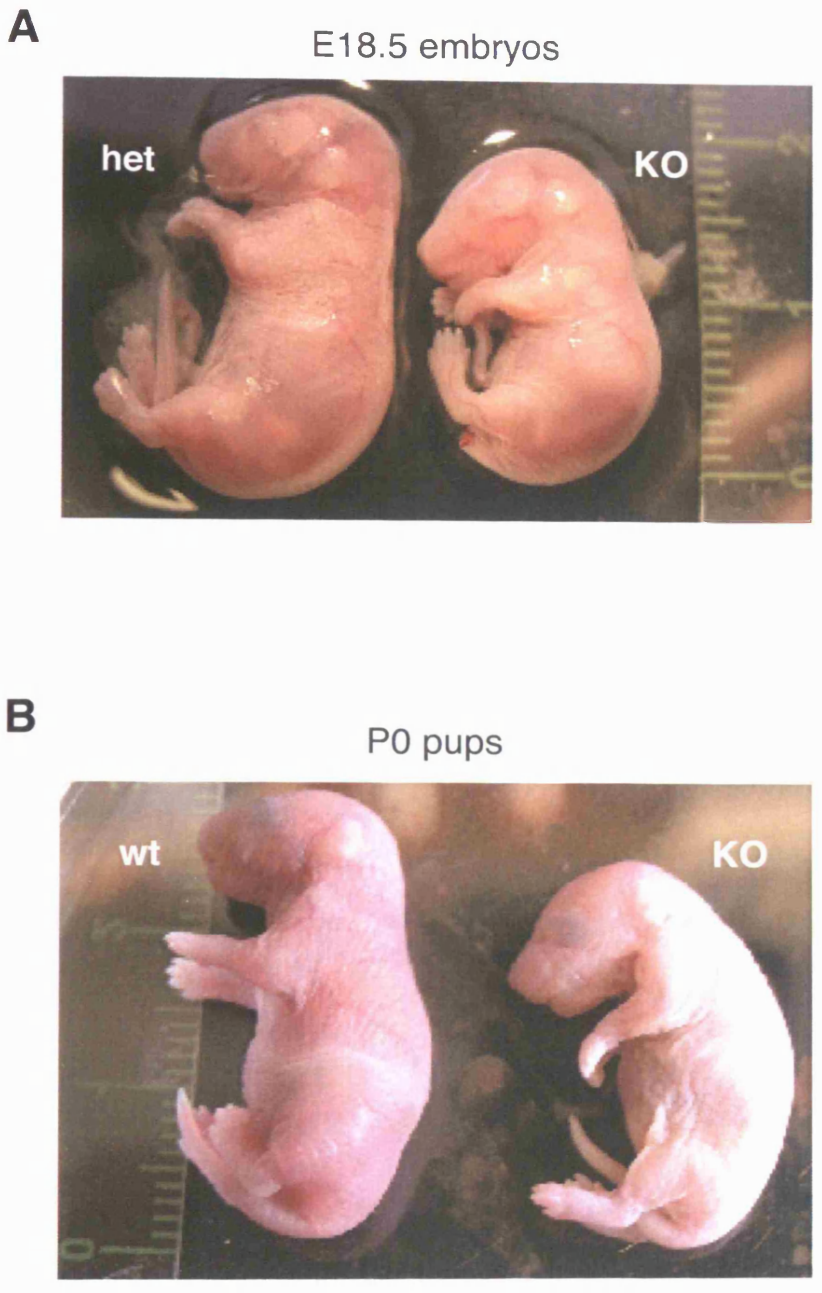

Figure 6-11: *Kidins220 knock-out animals die at birth*
(A) Kidins220 knock-out E18.5 embryos are alive, and smaller than their littermates. (B) Comparison between P0 knock-out and wild type pups. Kidins220 knock-out animals die at birth and are smaller than their littermates. n=10 embryos of each genotype were analysed in (A), n=5 embryos in (B).

6.9 Heart defects in Kidins220 knock-out animals

6.9.1 Histological analysis

The histological analysis presented in Figure 6-12 was performed in the Experimental Pathology Laboratory, under the supervision of Dr. B. Spencer-Dene. I provided the samples, genotyped them and contributed to the analysis of the results.

The external morphology of a Kidins220 knock-out heart is strikingly different from that of a wild type. The most obvious malformation affects the atria, which are dilated and congested (Figure 6-12, compare *a* and *b*, or *c* and *d*, arrowheads). Histological analysis of E19.5 heart sections revealed that the opening in the septum between the right and the left atrium (known as *foramen ovale*) was significantly wider in the knock-out than in the wild type (Figure 6-12, compare *e* and *f*, arrowheads). This could be a consequence of the dilation of the atria. Alternatively, it might indicate the presence of an atrial septal defect (ASD), a pathology characterised by the incomplete closure of the *foramen ovale*. This phenotype would be particularly interesting, as it is reminiscent of the phenotype of NT-3 (Donovan et al., 1996) and TrkC (Tessarollo et al., 1997) null mice. Furthermore, recent evidence has unveiled a role in cardiovascular development also for $p75^{NTR}$ (von Schack et al., 2001). ASD can be unambiguously detected only after birth, when the *foramen ovale* normally obliterates. Due to the fact that the Kidins220 knock-out embryos die at birth, however, it is not possible to verify whether they would display this abnormality. The generation of conditional Kidins220 knock-out animals will hopefully allow a better characterisation of this

heart phenotype. A more careful analysis of the heart tissue revealed defects in the organisation of the ventricle walls (Figure 6-12, compare *g* and *h*). The wild type tissue appears compact, with myocytes organised in parallel fibres. In contrast, the knock-out tissue appears loose and disorganised, with enlarged interstitial spaces between myocytes (Figure 6-12 *h*, arrowheads).

The atria congestion observed in the Kidins220 knock-out animals could be due to inability of the ventricle fibres to contract properly. In support of this hypothesis, the knock-out myocardium appears loose and disorganised. However, lungs recovered post-mortem from P0 pups did not contain any air, thus suggesting that Kidins220 null animals die as a consequence of their inability to breathe, rather than from cardiovascular defects. This could be caused by faulty innervation of the diaphragm, or by defects in the areas of the brain that control breathing. Future analysis will determine the cause of death in the Kidins220 knock-out pups.

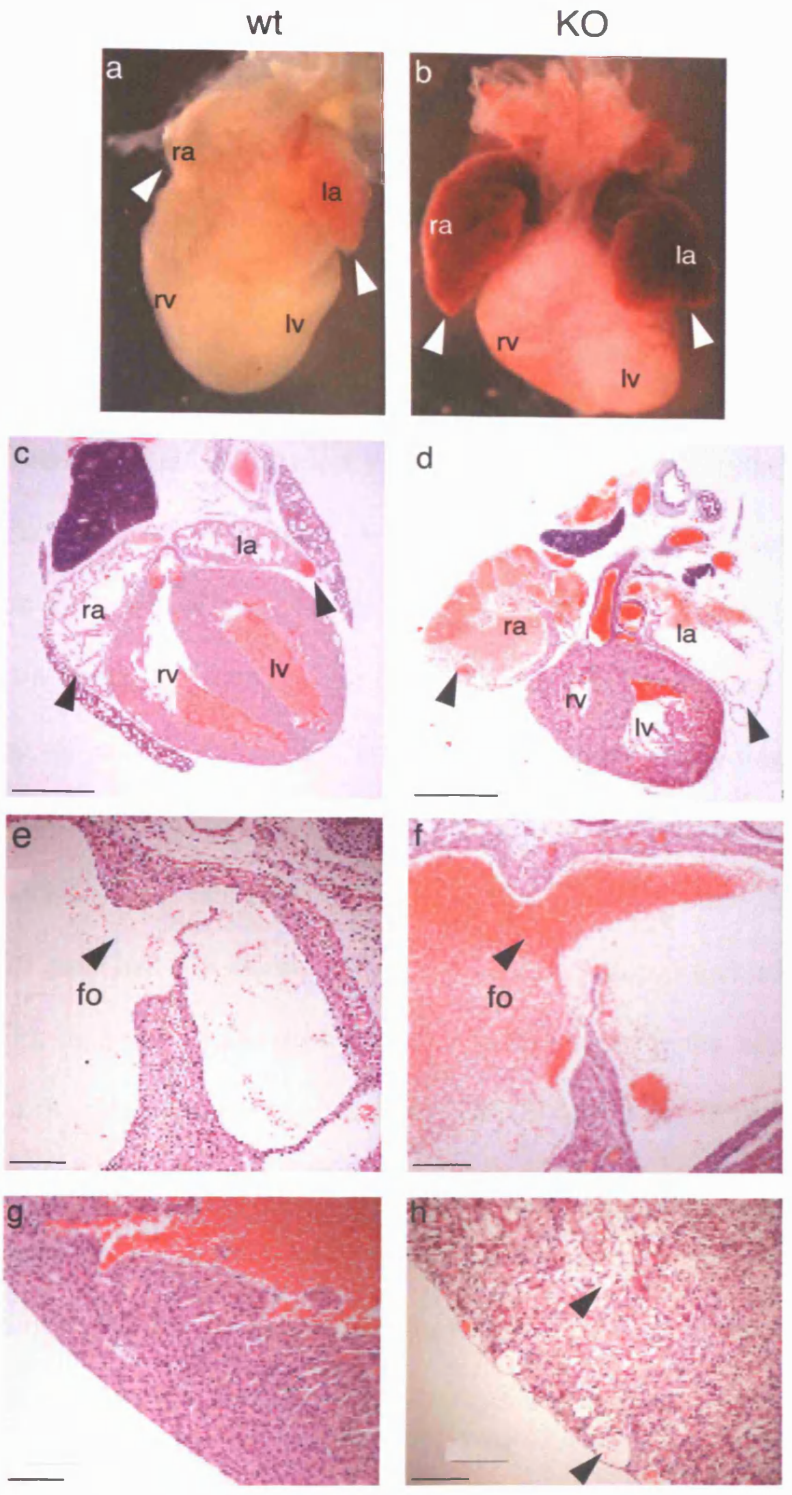

Figure 6-12: *morphological and histological analysis of the Kidins220 knock-out heart*
Three-dimensional view (*a*, *b*) and haematoxylin-eosin staining of paraffin-embedded sections (*c-h*) of wild type (left) and Kidins220 knock-out (right) E19.5 hearts. The knock-out heart shows congested and dilated atria (compare *a* and *b*, *c* and *d*, arrowheads). (*e*, *f*) Enlargement of a region corresponding to the atrial septum. In the knock-out heart the communication between the two atria appears enlarged, suggesting the presence of an atrial septal defect (*f*, arrowhead). (*g-h*) Enlargement of a region of the right ventricle wall. In the knock-out heart, the myocytes appear disorganised and loose, with enlarged interstitial spaces (*h*, arrowheads). ra, right atrium; la, left atrium; rv, right ventricle; lv, left ventricle; fo, *foramen ovale*. Scale bars = 1 mm in *c* and *d*, 200 µm in *e* and *f*, 100 µm in *g* and *h*. This histological analysis was repeated on 2 wild type and 2 knock-out hearts, by Dr. B. Spencer-Dene, Experimental Pathology Laboratory, CRUK.

6.9.2 *Neural crest migration is not affected in Kidins220 knock-out embryos*

Cardiovascular abnormalities in both TrkC and NT-3 null mice are consistent with defects in cardiac neural crest migration (Donovan et al., 1996; Tessarollo et al., 1997). Furthermore, it has been shown that TrkC deletion causes precocious fate restriction of neural crest stem cells, which ultimately results in defects in the outflow tract endothelium (Youn et al., 2003). Cardiac neural crest participate in the patterning of pharyngeal arches and their derivatives, including the aortic arch arteries, and contribute to the formation of the cardiac outflow septum (Kirby and Waldo, 1995). These observations prompted me to ask whether the deletion of the Kidins220 gene has any effects on neural crest migration. I tackled this question by performing *in situ* hybridisation on E9.5 embryos, with the neural crest marker CRABP-I. At this stage of development, CRABP-I localises in the frontonasal mass (FNM), in the mesencephalic trigeminal neurons (MTN), as well as in two neural crest streams, going into the second branchial arch (NC2) and into the heart (NCH) (Leonard et al., 1995). As shown in Figure 6-13, neural crest patterning in the E9.5 knock-out embryos was undistinguishable from the wild type.

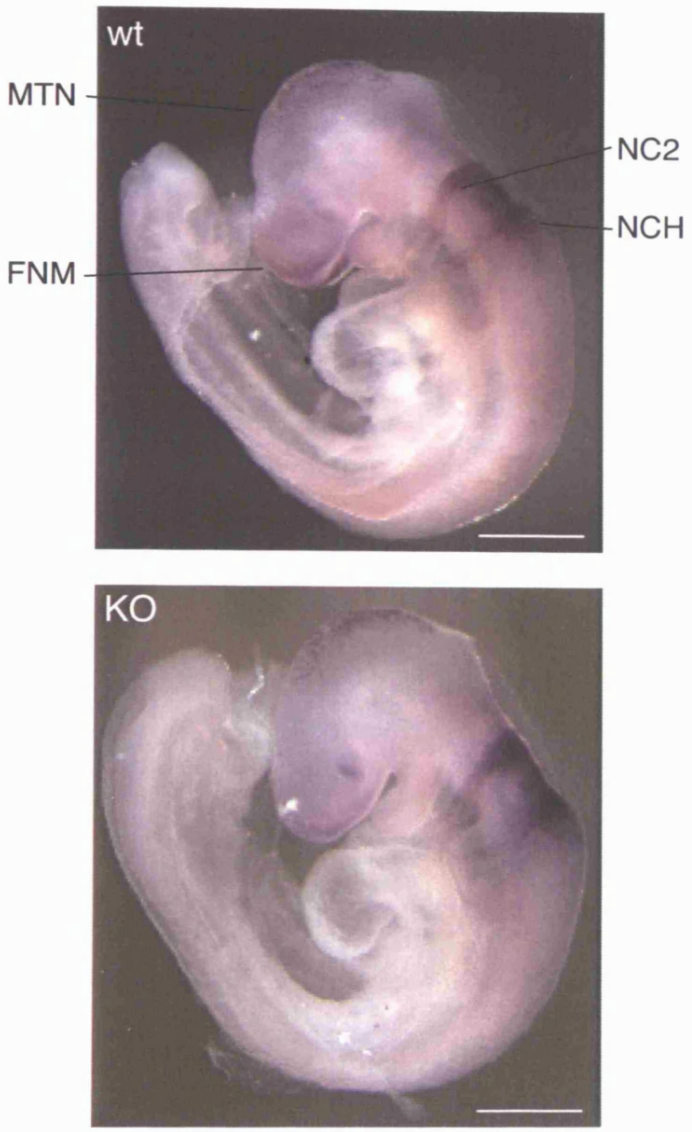

Figure 6-13: *neural crest migration is not affected in Kidins220 knock-out embryos*
In situ hybridisation on E9.5 mouse embryos, with the neural crest marker CRABP-I. The deletion of Kidins220 does not affect neural crest migration at this stage of development. FNM, frontonasal mass; MTN, mesencephalic trigeminal neurons; NC2, neural crest cells streaming into the second branchial arch; NCH, neural crest cells streaming into the heart. Scale bars = 500 μm. n=3 embryos of each genotype were analysed.

6.10Neuronal phenotypes in Kidins220 knock-out mice

6.10.1 Analysis of the Kidins220 knock-out brain

Kidins220 is expressed in a variety of neuronal and non-neuronal tissues, but is particularly enriched in the central and peripheral nervous system (Iglesias et al., 2000; Kong et al., 2001). In the adult rat brain, it has been shown to localise to the mitral cell layer of the olfactory bulb, the Purkinje cell layer of the cerebellum, and the hippocampus ((Kong et al., 2001), information about Kidins220 expression are also available in the Allen Brain Atlas website at http://www.brainatlas.org/aba/index.shtml). I began by conducting a general analysis of the Kidins220 knock-out brain. To this purpose, I dissected and sectioned the brains of E19.5 knock-out and wild type littermates. As shown in Figure 6-14 A, the Kidins220 knock-out brain has a normal morphology, being only slightly smaller than the wild type. By sectioning it along the midline, however, I noticed a pronounced enlargement of the lateral and fourth ventricles (Figure 6-14 C, arrowheads). In addition, the brain as a whole looked less compact, with wide clefts corresponding to the anatomical folds (Figure 6-14 C, arrow).

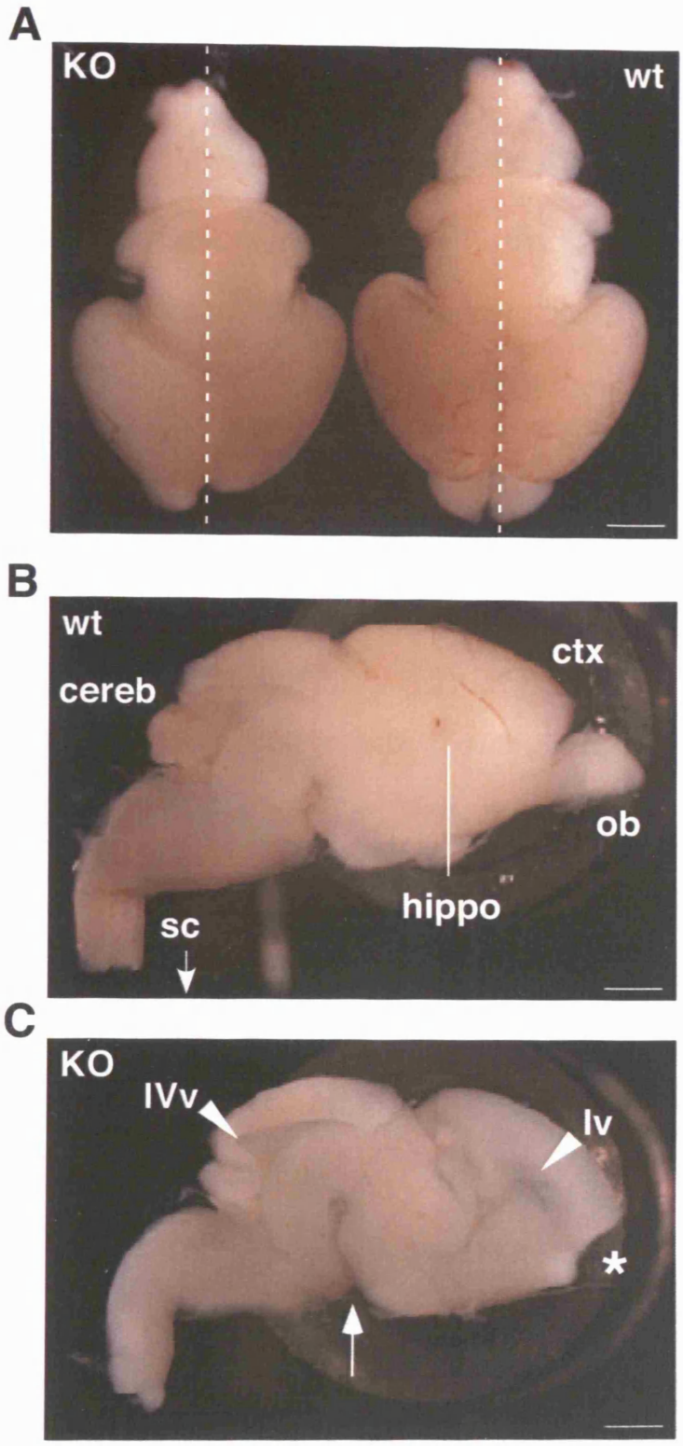

Figure 6-14: *macroscopic appearance of wild type and Kidins220 knock-out brains*
Brains from E19.5 embryos were dissected, fixed as described in Materials and Methods, and analysed. (A) Whole view of a wild type (wt) and knock-out (KO) brain. The knock-out brain appears normal, only slightly smaller than the wild type. The brains were sectioned along the midline, as indicated by the dashed lines. (B, C) Longitudinal sections of the wild type (B) and knock-out (C) brains shown in (A). The knock-out brain displays a pronounced enlargement of the lateral and fourth ventricles (arrowheads), and wide clefts corresponding to anatomical folds (arrow). ob, olfactory bulb; ctx, cortex; hippo, hippocampus; cereb, cerebellum; sc, spinal cord; lv, lateral ventricle; IVv, fourth ventricle. Asterisk: the olfactory bulb was damaged during dissection in this sample. Scale bars = 1 mm. This analysis was repeated on 5 wild type and 5 knock-out brains.

6.10.1.1Specific regions undergo cell death in the Kidins220 knock-out brain

The histological analysis presented in Figure 6-15 and Figure 6-16 was performed in the Experimental Pathology Laboratory, under the supervision of Dr. B. Spencer-Dene. I provided the samples, genotyped them and contributed to the analysis of the results.

One of the main functions of neurotrophins and their receptors is to promote neuronal survival. This is well exemplified by the phenotypes displayed by the corresponding knock-out models, which often show neuronal loss in different regions of the central and peripheral nervous system (Klein et al., 1993; Crowley et al., 1994; Ernfors et al., 1994b; Klein et al., 1994; Smeyne et al., 1994; Carroll et al., 1998). On the basis of these considerations, it is possible that the ablation of Kidins220 would affect specific neuronal populations in the developing brain. To answer this question, a staining for caspase 3, a known marker for apoptotic neurons (Jeon et al., 1999), was performed on sagittal (Figure 6-15) and coronal (Figure 6-16) sections of brains derived from wild type and Kidins220 knock-out E19.5 embryos. From a preliminary analysis, it was possible to identify two distinct caspase 3-positive clusters, in the region leading to the olfactory bulb (Figure 6-15 C and Figure 6-16 B), and in an area corresponding to the thalamic nuclei (Figure 6-15 D and Figure 6-16 C). No significant increase in cell death was detected at the level of either the hippocampus (Figure 6-16 B, arrowheads), or the cerebellum (not shown).

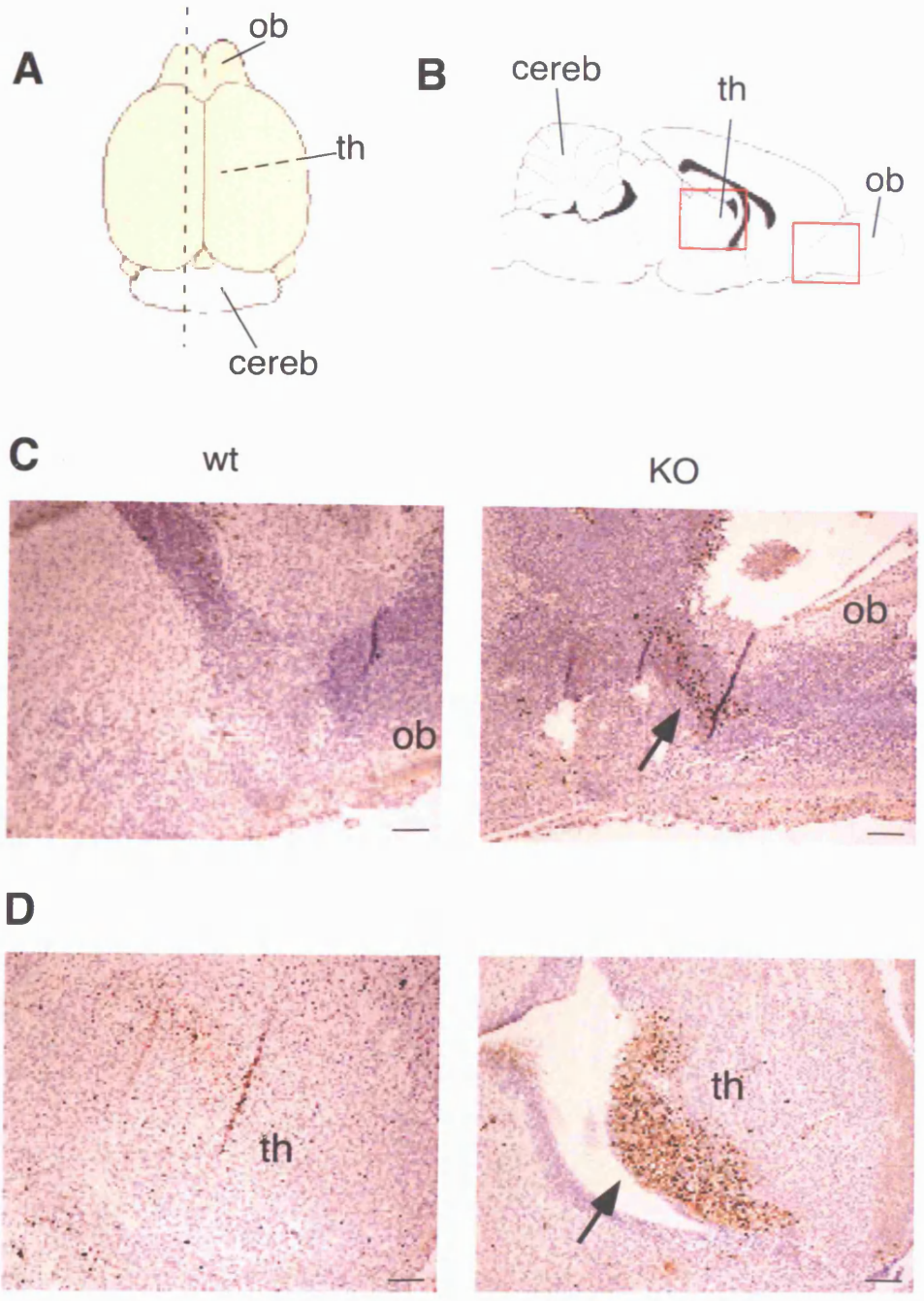

Figure 6-15: *caspase 3-positive regions in sagittal sections of Kidins220 knock-out brain*

Caspase 3 staining of sagittal sections of wild type (C-D, left) and Kidins220 knock-out (C-D, right) E19.5 brains. (A) The plane of section is indicated by the dashed line. (B) The regions approximately corresponding to the images in (C) and (D) are highlighted by the red boxes. We could detect two distinct caspase 3-positive clusters, in the area leading to the olfactory bulb (C) and in a region corresponding to the thalamic nuclei (D). Arrows highlight clusters of dying cells in the knock-out sections. ob, olfactory bulb; th, thalamic region; cereb, cerebellum. Scale bars = 100 μm. This analysis was repeated on 2 wild type and 2 knock-out brains, by Dr. B. Spencer-Dene, Experimental Pathology Laboratory, CRUK.

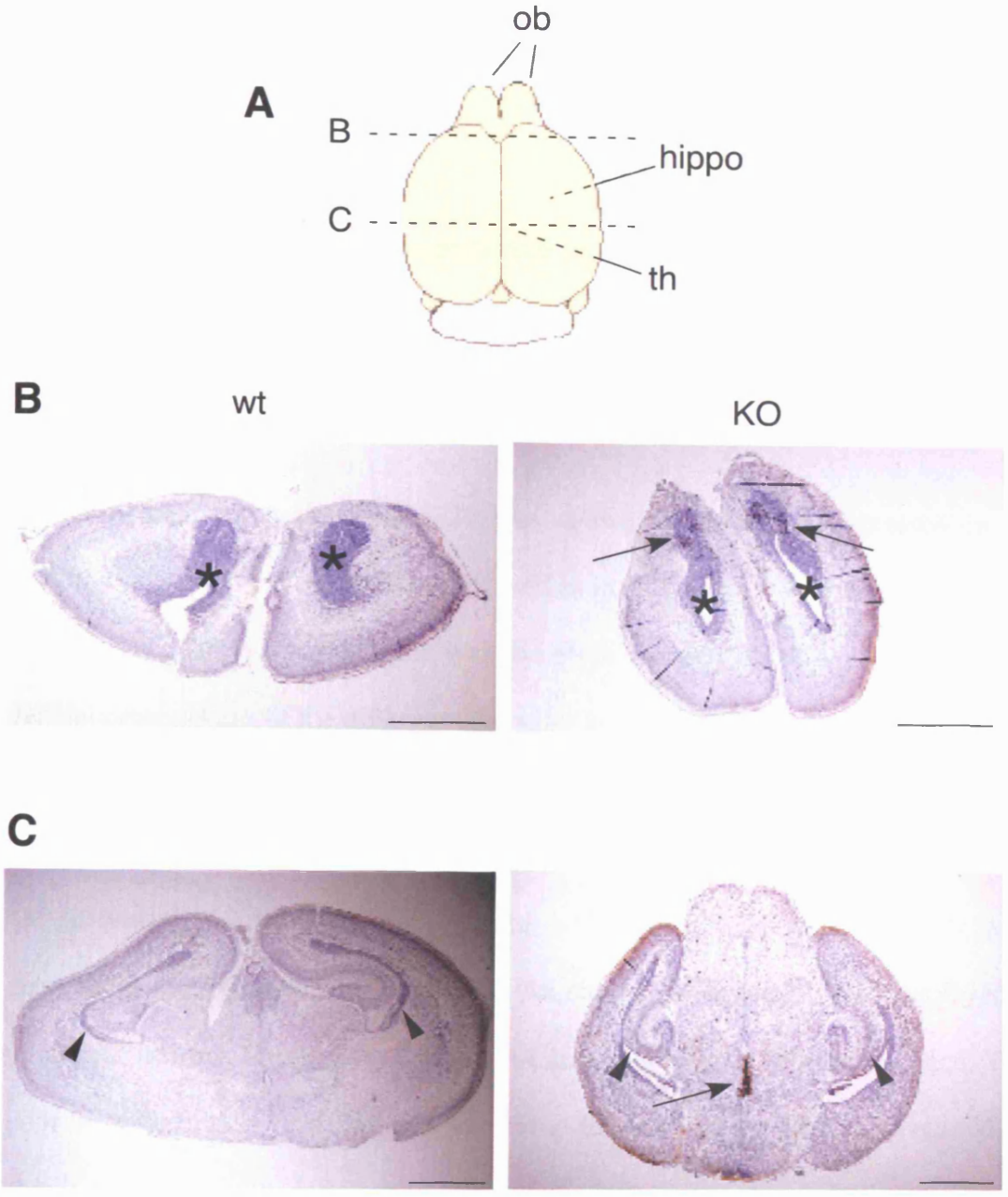

Figure 6-16: *caspase 3-positive regions in coronal sections of Kidins220 knock-out brains*

Caspase 3 staining of coronal sections of wild type (B-C, left) and Kidins220 knock-out (B-C, right) E19.5 brains. (A) The approximate planes of section are indicated by the dashed line. Clusters of caspase 3-positive cells are located in the subependimal zone of the olfactory bulbs (B, arrows), and in the midline thalamic nuclei (C, arrow). Asterisks mark the anterior horns of the lateral ventricle in (B); arrowheads mark the hippocampus in (C). ob, olfactory bulb; hippo, hippocampus; th, thalamic region. Scale bars = 1 mm. This analysis was repeated on 2 wild type and 2 knock-out brains, by Dr. B. Spencer-Dene, Experimental Pathology Laboratory, CRUK.

6.10.1.2Histological analysis of Kidins220 knock-out cerebellum and hippocampus

The histological analysis presented in Figure 6-17 and Figure 6-18 was performed in the Experimental Pathology Laboratory, under the supervision of Dr. B. Spencer-Dene. I provided the samples, genotyped them and contributed to the analysis of the results.

In adult rat brain, Kidins220 was shown to be highly expressed in the Purkinje cell layer of the cerebellum, as well as in all the regions of the hippocampus (Kong et al., 2001). Our analysis was therefore focused on these structures. The general organisation of the different cerebellar layers was not affected by Kidins220 ablation (Figure 6-17 C). However, the expression of the calcium binding protein D-28k (calbindin), which in the cerebellum preferentially labels Purkinje cells (Celio, 1990), was significantly reduced (Figure 6-17 D). Some structural defects were detected in the knock-out hippocampus. As shown in Figure 6-18 C, the layer of pyramidal neurons forming the CA1 - CA4 areas is progressively less defined. This poor layer definition is particularly evident at the level of the dentate gyrus, which shows an increase in cellularity, coupled to a general structural disorganisation (Figure 6-18 C *b* and *b'*, arrowheads).

Figure 6-17: *histological analysis of wild type and Kidins220 knock-out cerebellum*
Haematoxylin-eosin (C) and calbindin (D) staining of sagittal sections of wild tipe (C-D, left) and Kidins220 knock-out (C-D, right) E19.5 cerebellum. (A) The plane of section is indicated by the dashed line. (B) The region approximately corresponding to the images in (C) and (D) is highlighted by the red box. The general organisation of the different cerebellar layers does not seem to be altered in the Kidins220 knock-out (C), however the expression of calbindin, a marker of Purkinje cells, seems to be significantly reduced (D). *a'* and *b'* are enlargements of the boxed regions in C *a* and C *b*, respectively. ob, olfactory bulb; th, thalamic region; cereb, cerebellum; ml, molecular layer; Pl, Purkinje cells layer; gl, granular layer; wm, white matter. Scale bars = 200 μm. This analysis was repeated on 2 wild type and 2 knock-out brains, by Dr. B. Spencer-Dene, Experimental Pathology Laboratory, CRUK.

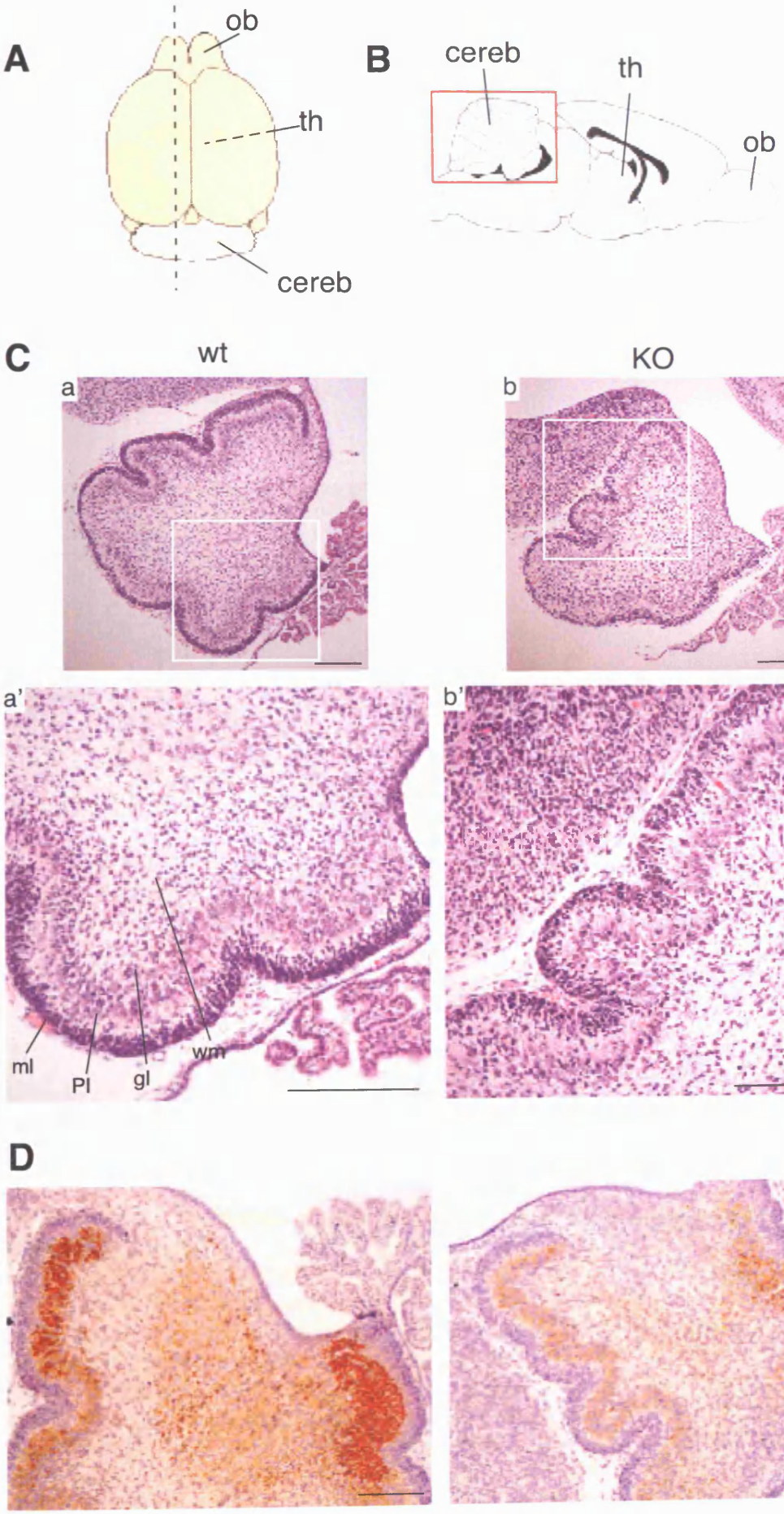
A
ob
th
cereb
B
cereb
th
ob
C
wt
KO
a
b
a'
b'
ml
Pl
gl
wm
D

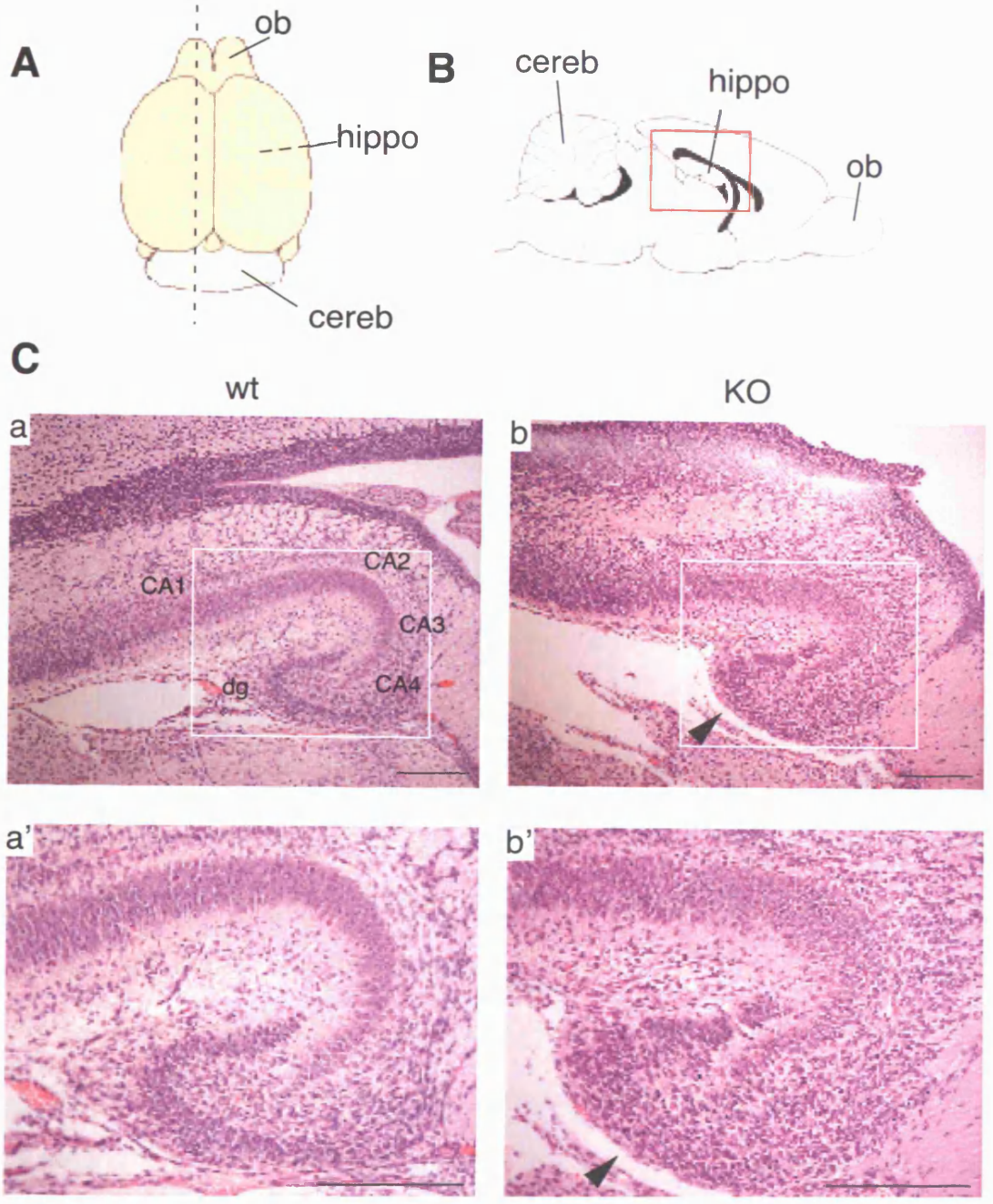

Figure 6-18: *histological analysis of wild type and Kidins220 knock-out hippocampus*

Haematoxylin-eosin staining of sagittal sections of wild type (C, left) or Kidins220 knock-out (C, right) E19.5 hippocampus. (A) The plane of section is indicated by the dashed line. (B) The region approximately corresponding to the images in (C) is highlighted by the red box. (C) The general organisation of the CA1-4 areas is maintained, however, the portion corresponding to the dentate gyrus appears disorganised (arrowhead). *a'* and *b'* are enlargements of the boxed regions in C *a* and C *b*, respectively. ob, olfactory bulb; hippo, hippocampus; cereb, cerebellum; CA1-4, *cornu ammoni* region 1-4; dg, dentate gyrus. Scale bars = 200 µm. This analysis was repeated on 2 wild type and 2 knock-out brains, by Dr. B. Spencer-Dene, Experimental Pathology Laboratory, CRUK.

6.10.2 Analysis of the Kidins220 knock-out spinal cord and dorsal root ganglia

The histological analysis presented in Figure 6-20 was performed in the Experimental Pathology Laboratory, under the supervision of Dr. B. Spencer-Dene. I provided the samples, genotyped them and contributed to the analysis of the results.

DRGs consist of different neuronal subpopulations, characterised by differential expression of Trk receptors. Small nociceptive and thermoreceptive neurons mainly express TrkA, medium-sized mechanoreceptive neurons express TrkB, whereas big proprioceptive neurons express TrkC (Mu et al., 1993). As a consequence, different neuronal groups will require different neurotrophins for their survival. In support of this notion, there is a general correspondence between the knock-out of a single neurotrophin or neurotrophin receptor, and the loss of the related DRG subpopulation (Bibel and Barde, 2000). Kidins220 is highly expressed in spinal cord and dorsal root ganglia at the embryonic stage (Kong et al., 2001). In adult, Kidins220 expression is restricted mainly to medium- and small-sized DRG neurons, and is particularly abundant in the ventral horn of the spinal cord ((Kong et al., 2001), and http://www.brainatlas.org/aba/index.shtml). On the basis of these observations, we decided to analyse the development of these regions in the Kidins220 knock-out animals.

Firstly, I performed whole mount staining of wild type and Kidins220 knock-out embryos, at different stages of development, with a neurofilament-specific antibody. As shown in Figure 6-19, all the main cranial and peripheral nerves developed normally in the Kidins220 knock-out embryos. In particular, DRG

extension and branching did not appear to be grossly affected by Kidins220 deletion (Figure 6-19 A *c-d*, B *c-d*). 1/7 of the embryos analysed displayed axon defasciculation defects (data not shown), however it will be necessary to analyse a higher number of samples in order to determine if this is a low frequence defect or an artifact. In light of the considerations above, I then asked whether Kidins220 deletion would selectively affect one or more groups of DRG neurons. To answer this question, immunostaining of E19.5 and P0 DRG sections were performed, using antibodies specific for TrkA, TrkB and TrkC. A preliminary analysis has shown that no significant reduction in any of the three populations occurs in the Kidins220 knock-out samples, compared to the wild type (data not shown). However, a more careful quantification will be required in order to assess small variations in the numbers of TrkA-, TrkB- or TrkC-positive neurons.

Kidins220 expression is particularly abundant in the ventral horn of the spinal column (Kong et al., 2001), where motor neuron bodies are located. I was therefore interested in determining the effects of Kidins220 ablation on motor neuron survival. To this purpose, E19.5 wild type and knock-out spinal cord sections were stained with antibodies against the homeodomain protein HB9, which is an established marker of motor neurons specification (Saha et al., 1997; Thaler et al., 1999). The presence of HB9-positive cells was assessed in sections taken at the cervical, thoracic and lumbar level of the spine. HB9 strongly stained the nuclei of specific clusters of neurons localised in the ventral side of the column, which I considered *bona fide* motor neurons. It was possible to identify a clear HB9 staining in wild type as well as in knock-out sections taken at both cervical and thoracic level (Figure 6-20 *a-d*). Sections taken from the knock-out lumbar region, in contrast,

showed a clear reduction in the HB9 immunoreactivity compared to the wild type. In those samples, the intensity of the nuclear staining was significantly reduced, and in some cells the signal was exclusively cytoplasmic (Figure 6-20 *e-f*, arrowheads).

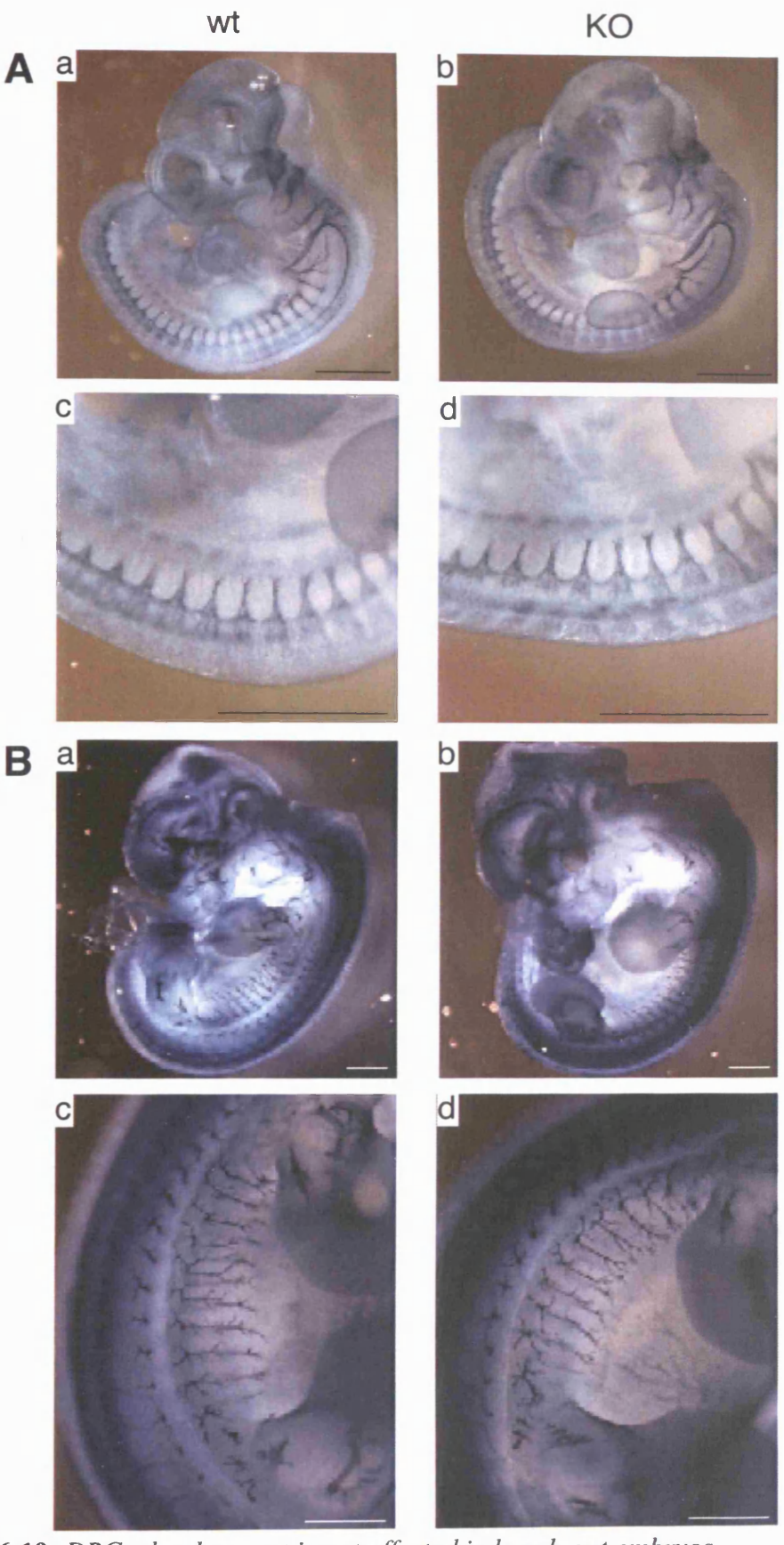

Figure 6-19: *DRGs development is not affected in knock-out embryos*
Whole mount staining of E10.5 (A) and E11.5 (B) wild type (left) and knock-out (right) embryos, with the neurofilament-specific 2H3 antibody. No major differences were visible at either developmental stage. Panels *c* and *d* in (A) and (B) show high magnification images of regions corresponding to DRG. Scale bars = 1 mm. n=7 embryos of each genotype were analysed.

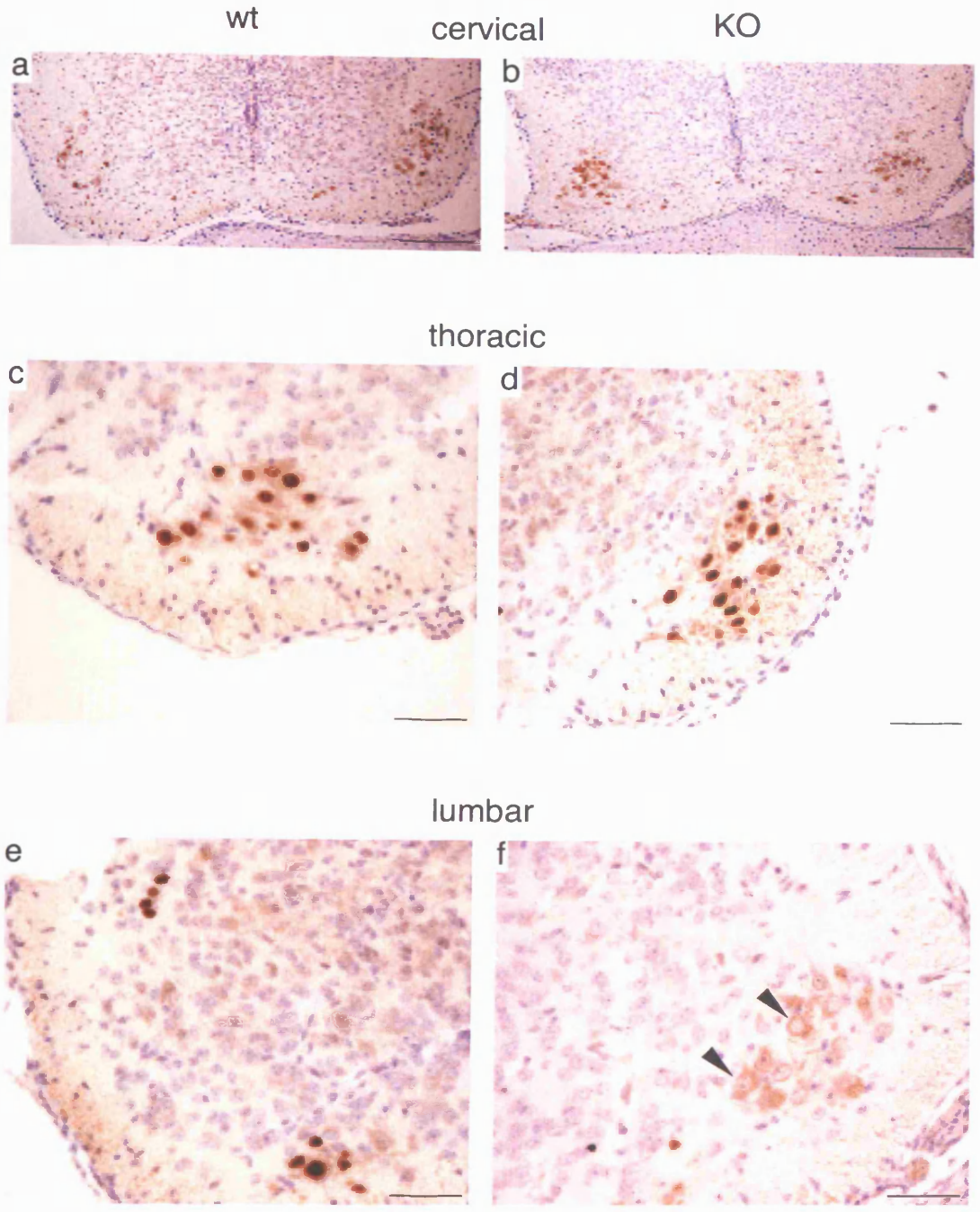

Figure 6-20: *lumbar motor neurons loss in Kidins220 knock-out mice*
HB9 staining of spinal cord sections taken at the cervical (*a*, *b*), thoracic (*c*, *d*) or lumbar (*e*, *f*) level of wild type (*a*, *c*, *e*) or Kidins220 knock-out (*b*, *d*, *f*) E19.5 embryos. Motor neurons are identified by a strong nuclear immunoreactivity. A comparable number of motor neurons were present in wild type and knock-out sections taken at the cervical and thoracic level. Sections taken from the knock-out lumbar region, in contrast, showed a clear reduction in the HB9 immunoreactivity, which in some cells was exclusively cytoplasmic (arrowheads). Scale bars = 100 µm in *a* and *b*, 50 µm in *c-f*. This analysis was repeated on sections prepared from 2 wild type and 2 knock-out embryos, by Dr. B. Spencer-Dene, Experimental Pathology Laboratory, CRUK.

Chapter 7 – Discussion

7 Discussion

7.1 Kinesin-1 mediated trafficking of Kidins220

7.1.1 Kidins220 - a multi-domain protein at the interface between different signalling pathways

In this work, we have demonstrated that the intracellular trafficking of Kidins220 is mediated by the kinesin-1 complex, via a direct interaction of Kidins220 with KLC, and we have characterised in detail the molecular determinants of the binding between these two proteins. The KLC-interacting motif (KIM) of Kidins220 does not bear any sequence similarities with other proteins known to bind KLC (see Figure 3-13). This short stretch of amino acids is located in the central part of the carboxy-terminal tail of Kidins220, a region that has not been involved in the binding to any of the other Kidins220 interactors described to date. Similarly, the portion of KLC interacting with KIM was not previously implicated in cargo recognition. This region spans the central part of the protein, comprising a portion of the heptad repeats, as well as the first two TPR motifs (Figure 3-8). Kidins220 binding therefore does not impair the association of KLC with KHC, and the formation of a functional motor complex. At the same time, KLC could recruit other cargoes via the carboxy-terminal tail, such as the 14-3-3 protein, which binds to the C-terminus of KLC2 (Ichimura et al., 2002). It is possible to speculate that the Kidins220-kinesin-1 module represents a basic scaffold for the assembly of bigger

protein complexes, where single components could associate with KLC as well as with the other domains of Kidins220.

A very similar scenario has been described for the protein *Disrupted-in-schizophrenia-1* (DISC1), which owes its name to the fact that a chromosomal translocation disrupting the *DISC1* gene has been associated with the onset of this disease (Millar et al., 2000). DISC1 is a cytoplasmic protein composed of a N-terminal globular domain, and a C-terminal region folding in a coiled-coil conformation (Millar et al., 2000). A series of proteins have been identified as molecular interactors of DISC1, such as the nuclear distribution gene E-like (NUDEL) protein (Ozeki et al., 2003), the fasciculation and elongation protein ζ-1 (FEZ1) (Miyoshi et al., 2003), and the phosphodiesterase 4B (PDE4B) (Millar et al., 2005). The association of DISC1 with NUDEL or FEZ1 has been shown to play a role in the regulation of neurite outgrowth (Miyoshi et al., 2003; Ozeki et al., 2003), whereas the interaction between DISC1 and PDE4B has been implicated in the modulation of cAMP signalling (Millar et al., 2005). Interestingly, FEZ1 mediates mitochondria transport via a direct interaction with KIF5 in PC12 cells (Fujita et al., 2007), and contributes to the establishment of neuronal polarity by modulating axonal transport of mitochondria in hippocampal neurons (Ikuta et al., 2007).

Two parallel publications from Kaibuchi's group have recently described a new function for DISC1 as a cargo receptor for the kinesin-1 complex. While the N-terminal domain of DISC1 engages the motor complex, the coiled-coil region mediates the interaction with NUDEL (Taya et al., 2007) or the growth factor receptor bound protein 2 (Grb2) (Shinoda et al., 2007). NUDEL is part of a bigger complex, composed of the lissencephaly-1 (LIS1) and 14-3-3ε proteins, which play

an essential role during brain development (Toyo-oka et al., 2003). DISC1 therefore acts as a linker between kinesin-1 and the NUDEL / LIS1 / 14-3-3ε complex, modulating its transport to the axon terminal. It has been suggested that the disruption of DISC1 function may impair neuronal development and lead to psychiatric disorders, such as schizophrenia (Taya et al., 2007). Grb2 is an adaptor molecule that recognises phosphorylated tyrosines in the cytoplasmic domains of Trk receptors, and subsequently recruits a number of proteins involved in the activation of the downstream ERK pathway (MacDonald et al., 2000). DISC1-mediated transport of Grb2 has been shown to play a role in the modulation of NT-3-induced axonal elongation (Shinoda et al., 2007).

Interestingly, DISC1 binds NUDEL, FEZ1, PDBE4 and Grb2 through non-overlapping domains, opening the possibility that this protein can act as a scaffold, assembling different independent complexes in response to specific stimuli. In addition, the association with the kinesin-1 motor would allow the targeting of these complexes to different cellular regions. DISC1 would therefore be responsible for the recruitment as well as the targeting of the different effectors. Figure 7-1 and Figure 7-2 show a schematic representation of the different cellular functions associated with DISC1 and Kidins220, highlighting the similarities in the mechanisms of action of the two proteins. In both cases, these multi-domain proteins are able to recruit different partners, and to link the resulting complexes to the kinesin-1 motor. This is crucial to coordinate the spatial and temporal delivery of different signals. Kidins220 could be simultaneously engaged in interactions with kinesin-1 and a series of other receptor/adaptor proteins. It is therefore possible that Kidins220 links motor proteins to inactive signalling complexes, thus mediating

their targeting to specific domains of the plasma membrane. Once these complexes have been delivered to their final destination, they would become activated upon trophic stimuli, and subsequently recruited to signalling endosomes on the retrograde transport route.

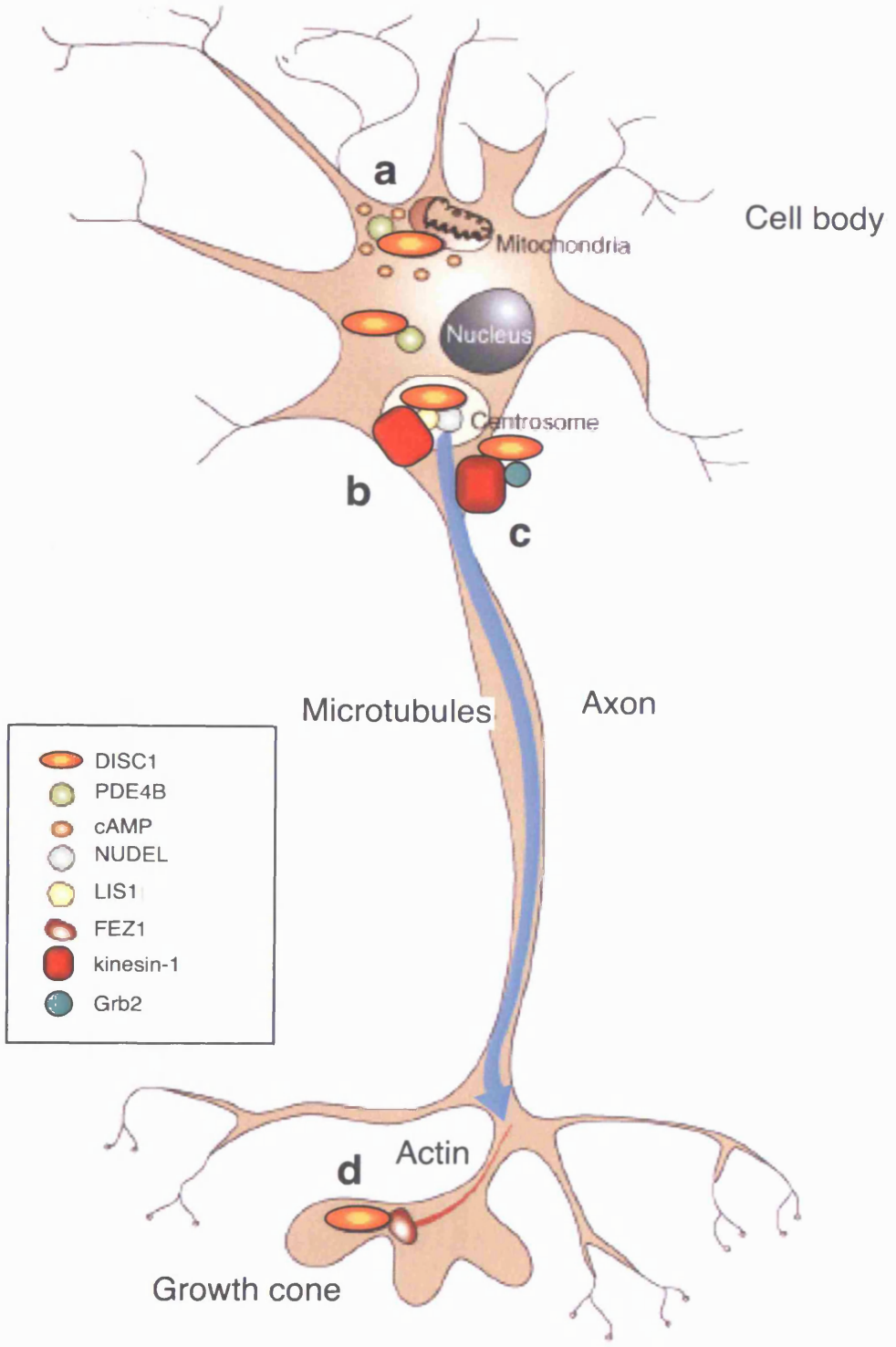

Figure 7-1: *DISC1 mediates the assembly and targeting of different protein complexes through different domains*

Distinct regions of DISC1 mediate the interaction with different proteins, and their localisation to specific cellular compartments. (*a*) Interaction with PDE4B mediates cAMP signalling in the cell body (Millar et al., 2005). Association with kinesin-1 mediates the transport of either the NUDEL / LIS1 / 14-3-3μ complex (Taya et al., 2007) (*b*) or Grb2 (Shinoda et al., 2007) (*c*) to the axon terminal. (*d*) Binding to FEZ1 has been implicated in the process of neurite outgrowth, possibly by modulating actin remodelling at the growth cone (Miyoshi et al., 2003). Adapted from Mackie et al., 2007.

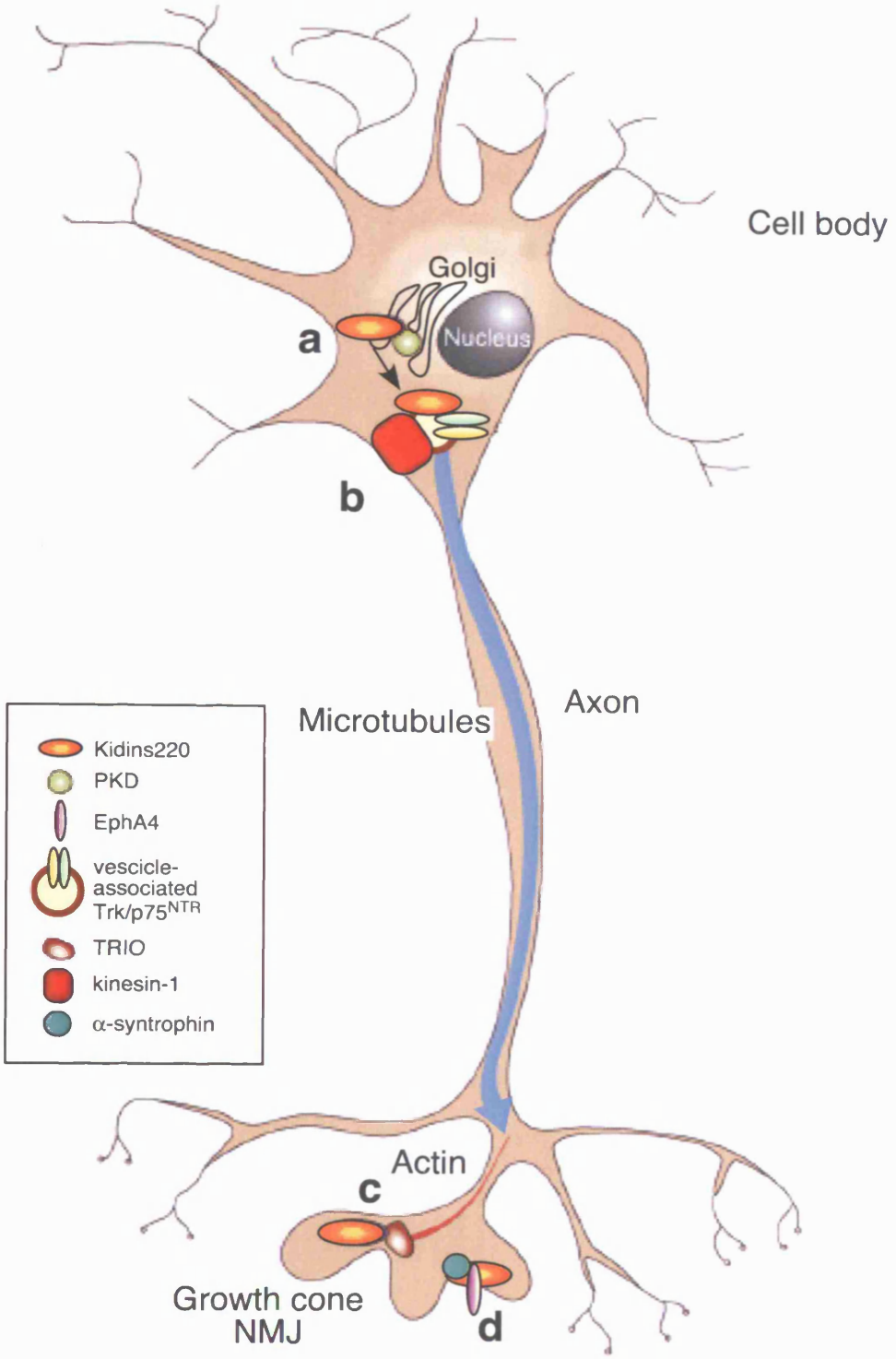

Figure 7-2: *Kidins220 mediates the assembly and targeting of different protein complexes through different domains*

Distinct regions of Kidins220 mediate the interaction with different proteins, and their localisation to specific cellular compartments. (*a*) Interaction with PKD at the level of the trans Golgi network modulates the trafficking of Kidins220 to distinct domains of the plasma membrane (Sanchez-Ruiloba et al., 2006). (*b*) Kidins220 could connect Trk-bearing vesicles to the kinesin-1 motor, thus regulating their anterograde axonal transport. (*c*) The interaction with TRIO could play a role in the actin remodelling processes required for axonal growth. (*d*) The complex between Kidins220, α–syntrophin and EphA4 may coordinate the molecular events leading to synapse development (Luo et al., 2005). Adapted from Mackie et al., 2007.

7.1.2 Is Kidins220 mediating the trafficking of neurotrophin receptors?

Kidins220 constitutively interacts with the neurotrophin receptors Trk and $p75^{NTR}$ (Chang et al., 2004). We have showed that impairing the kinesin-1 mediated transport of Kidins220 reduces the ability of PC12 cells to respond to neurotrophic stimuli (Bracale et al., 2007). These observations prompted us to consider the possibility that Kidins220 might link the kinesin-1 complex to vesicles bearing non-activated neurotrophin receptors, thus modulating their targeting to the plasma membrane. This was a particularly attractive hypothesis, as little is known about the mechanisms regulating the anterograde transport of neurotrophin receptors. To validate this theory, we performed a series of immunoprecipitation experiments on lysates from NGF-differentiated PC12 cells. Even though we could recover Kidins220 with both Trk and $p75^{NTR}$, we were never able to detect a ternary complex between kinesin-1, Kidins220 and $p75^{NTR}$ and/or the Trk receptors (data not shown). It is possible that the connection between Kidins220 and these receptors on transport vesicles is stabilised by additional factors. If this were the case, our biochemical approach would not be effective in detecting the kinesin-1/Kidins220/receptor complex. However, additional evidence against our hypothesis is provided by a recent work, where Sanchez-Ruiloba and co-workers show that impairment of Kidins220 trafficking by overexpression of a kinase dead form of PKD does not affect the cellular localisation of neurotrophin receptors, both in PC12 cells and in primary neurons (Sanchez-Ruiloba et al., 2006). These conclusions however are based exclusively on immunofluroscence data. If Kidins220 were responsible for the transport of only a subset of receptors, the reduction in the surface localisation of

these molecules might not be detectable by this method. To validate our model, we will need to follow different approaches, as discussed in section 7.3.

In any case, alternative hypotheses must be taken into consideration. A possible alternative scenario would be that the binding of the kinesin-1 complex and of the neurotrophin receptors to Kidins220 is mutually exclusive. In this case, Kidins220 could become available for the interaction with the receptors only after the detachment of kinesin-1. As a consequence, Kidins220 would be fully competent to act as a scaffolding protein for neurotrophin signalling only after its delivery to the neurite terminals. As discussed in the next paragraph, this step might be modulated by phosphorylation.

7.2 Modulation of Kidins220 trafficking by phosphorylation

7.2.1 Abl phosphorylation might mediate the release of the kinesin-1 complex from Kidins220

Our *in vitro* evidence shows that Abl-mediated phosphorylation of Kidins220 at the level of the KIM sequence decreases the binding affinity for KLC (Figure 4-10). On the basis of these observations, we considered the possibility that phosphorylation might mediate the dissociation of the kinesin-1 motor complex from Kidins220, once it has been delivered to its final destination. We formulated two possible hypotheses. In the first scenario, Kidins220 would be transported to the axon terminal independently of the neurotrophin receptors (Figure 7-3 A, step 1). A second possibility is that Kidins220 and the neurotrophin receptors are anterogradely transported in the same carriers, but KLC binding to Kidins220 creates a sterical

hindrance that prevents its direct interaction with the receptors. In this situation, additional factors might link Kidins220 and the receptors on the same transport vesicle (Figure 7-3 B, step 1). This would also provide an explanation about why we could not immunoprecipitate kinesin-1 with the Kidins220/neurotrophin receptor complex. Once these Kidins220-bearing vesicles have reached their destination, Abl-mediated phosphorylation might trigger the detachment of the motor. Kinesin-1 detachment might be a prerequisite for the fusion of the cargo with the plasma membrane or a peripheral endosomal compartment. At the same time, the disengagement of kinesin-1 would free Kidins220 to come into contact with the receptors, immediately prior or after plasma membrane fusion at the axon terminal (Figure 7-3 A and B, steps 2-3).

As discussed in the Introduction, phosphorylation is a common way to modulate the attachment/detachment of molecular motors from their cargoes. Phosphorylation can directly target the motors, as shown for kinesin-1 (Sato-Yoshitake et al., 1992; Morfini et al., 2002), cytoplasmic dynein (Addinall et al., 2001), and myosin V (Karcher et al., 2001), as well as the cargo proteins themselves. In the latter case, phosphorylation of the cargo can determine the release of the motor, as demonstrated for the viral protein A36R (Newsome et al., 2004), or can modulate the recruitment of the cargo to different transport routes, as shown for APP/pAPP (Muresan and Muresan, 2005). Kidins220 phosphorylation might therefore mediate the release of the kinesin-1 complex, thus allowing Kidins220 to interact with the neurotrophin receptors.

7.2.2 *A link between Abl and neurotrophins?*

The Abl family of non-receptor tyrosine kinases is composed of Abelson tyrosine kinase (Abl) and the Abl-related gene (Arg). Abl is a conserved and ubiquitous protein, which has been implicated in diverse cellular processes such as regulation of cell growth and survival, response to oxidative stress and DNA damage, modulation of actin dynamics and cell migration. It has been reported to interact with several proteins, such as membrane receptors and signalling adaptors, transcription factors, and cytoskeletal proteins (Van Etten, 1999). Abl has been extensively studied because of its association with chronic myeloid leukaemia and a subset of acute lymphocytic leukaemia, where it is expressed as a Bcr-Abl fusion protein, a constitutively active tyrosine kinase (Advani and Pendergast, 2002). Many years of intense medical research have led to the development of Gleevec® (also known as STI571 or Imatinib Mesylate), which specifically inhibits Bcr-Abl kinase activity, and is currently used to treat chronic myeloid leukaemia as well as a subset of gastrointestinal stromal tumours (detailed information about this compound and its use as anti-cancer drug are available at http://www.glivec.com/content/home.jsp). For our purposes, the use of Gleevec® would allow us to specifically target Abl function, and to study how the inhibition of this kinase might affect Kidins220 function at the axon terminal, as discussed in section 7.3. In recent years, evidence has been accumulating about the role played by Abl in regulating neuronal morphogenesis and synaptic function. Early experiments in *Drosophila* indicated that members of the Abl family are required for axonal outgrowth and pathfinding during development (Gertler et al., 1989). Many studies have now characterised in detail the interactions between Abl and a number of neuronal receptors, including

TrkA (Koch et al., 2000; Yano et al., 2000), and the EphB2 receptor (Yu et al., 2001). However, it is still unclear whether Abl activity is involved in the intracellular pathways initiated by NGF or ephrin-B1 stimuli. Although many of the mechanisms regulating growth cone motility and axon guidance have now been elucidated, it is still not completely understood how extracellular guidance cues can coordinate the changes in actin dynamics that are required to control growth cone remodelling. This was partially answered by four studies, which independently identified Trio as an Abl interactor, and implicated the Abl/Trio complex in the signalling network regulating axon guidance during *Drosophila* development (Awasaki et al., 2000; Bateman et al., 2000; Liebl et al., 2000; Newsome et al., 2000). This complex was later found to act downstream of the netrin receptor *Frazzled* (Fra) (Forsthoefel et al., 2005).

Our data and future investigation might contribute to the understanding of this poorly characterised aspect of neuronal development. As discussed in the Introduction, different regions of Kidins220 mediate the interaction with Trio, neurotrophin and ephrin receptors. We suggest that Kidins220 could represent the missing link connecting extracellular neurotrophic stimuli to cytoskeletal rearrangements. In addition to its role in promoting the sustained activation of the MAPK pathway (Arevalo et al., 2004), Kidins220 could couple Trk activation to actin remodelling in the growth cone, via the interaction with Trio. In this context, Abl could on one side mediate the detachment of Kidins220 from kinesin-1, and additionally modulate the interaction between Kidins220 and Trio.

Figure 7-3: *different possibilities for the modulation of Kidins220 trafficking*
(A) Kidins220 is anterogradely transported in carriers devoid of neurotrophin receptors (1). Once at the axon terminal, Abl phosphorylation triggers the detachment of the kinesin-1 motor (2), thus enabling Kidins220 to interact with neurotrophin receptors at the plasma membrane (3). (B) Kidins220 and neurotrophin receptors are present on the same transport vesicles, but the binding to kinesin-1 prevents Kidins220 from interacting with the receptors. It is possible that intermediate factors might link Kidins220 and the receptors on the same vesicles (1). Once at the axon terminal, Abl phosphorylation triggers the detachment of the kinesin-1 motor and of the hypothetical additional factors (2), thus enabling Kidins220 to interact with the neurotrophin receptors, immediately prior or after plasma membrane fusion (3).

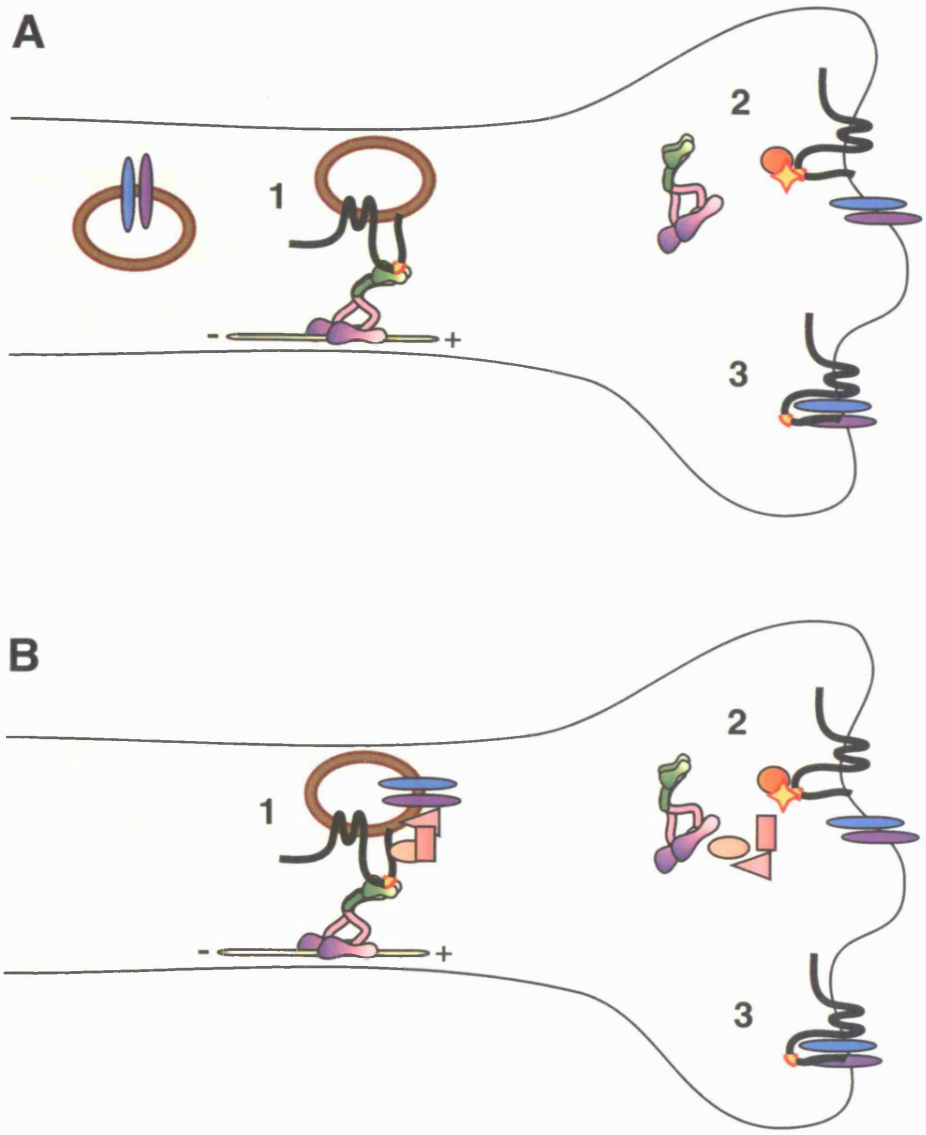
A
1
2
3
-
+
B
1
2
3
-
+
Kidins220 (the KIM domain is highlighted)
kinesin-1 complex (KHC in pink, KLC in green)
microtubules
Abl
Trks/p75NTR receptors
hypothetical additional factors
phosphorylation

7.3 Future perspectives – 1

As discussed in section 7.1.1, the ability of Kidins220 to interact with different adaptor and receptor proteins, as well as with molecular motors like the kinesin-1 complex, makes it a suitable candidate as a component of signalling endosomes. The nature and dynamics of Kidins220-bearing vesicles could be analysed by employing live imaging techniques on primary neurons. It would be interesting to determine whether Kidins220 and neurotrophin receptors are present on the same carriers, and whether the extent of their association is influenced by neurotrophic treatment.

Moreover, it would also be interesting to study the effect of Abl inhibition on Kidins220 trafficking and targeting. If our model is correct, Abl inhibition would be expected to cause an accumulation of Kidins220-positive structures at the neurite tip, due to the inability of Kidins220 to detach from the kinesin-1 motor. As a consequence, Kidins220-positive structures could fail to fuse with the plasma membrane or other peripheral compartments. Alternatively, Kidins220 could interact with the Trk receptors but, due to the steric hindrance caused by kinesin-1, would not be able to recruit the appropriate downstream effectors (i.e. CrkL). The next step would therefore be to analyse the activation of the intracellular pathways triggered by neurotrophins, during Abl inhibition. However, Abl can interact with many different proteins, and has been implicated in a wide range of essential biological processes (Van Etten, 1999). It will therefore be crucial to spatially and temporally restrict Abl inactivation, in order to target the neurotrophin-dependent pathways with maximal specificity. For instance, the use of compartmentalised cultures of primary

neurons (Campenot, 1977) would allow Abl inhibition specifically at the axon terminal. In this situation, the ability of the cells to respond to neurotrophic stimuli should be partially impaired. As shown by the work of Arevalo and colleagues, inhibition of Kidins220 function selectively affects the activation of the MAPK pathway (Arevalo et al., 2004). Therefore, if the Kidins220-dependent response to neurotrophins relies on Abl activity, MAPK activation should be preferentially affected, rather than PLC or Akt signalling, during Abl inhibition. The ability of Abl-inhibited cells to respond to different neurotrophins could therefore be assessed by measuring the level of activation of MAPK-specific intracellular effectors.

The availability of Kidins220-deficient cell lines will benefit the analysis of the molecular mechanisms regulating Kidins220 trafficking. The Kidins220 -/- ES line will be particularly useful for overexpression studies of different specific Kidins220 mutants, such as those lacking the KLC-binding domain or the Abl phosphorylation site. It will be of particular interest to establish whether the knock-out of Kidins220 affects the ability of the ES cells to differentiate into neuronal lineages, and whether the expression of specific Kidins220 mutants can rescue such phenotypes.

7.4 Nervous system development in Kidins220 KO animals

7.4.1 Kidins220 and cell adhesion

7.4.1.1 Ventricle enlargement in the Kidins220 knock-out brain

The most striking feature of the Kidins220 knock-out brain is the abnormal enlargement of the lateral ventricles (Figure 6-14). A similar brain phenotype has

been associated with malfunctioning of the neuronal adhesion molecules NCAM (Weinhold et al., 2005) and L1 (Dahme et al., 1997; Fransen et al., 1998). Both NCAM and L1 belong to the immunoglobulin superfamily, and are involved in important processes in nervous system development, such as the modulation of axon outgrowth and fasciculation, neuronal migration and survival, and regeneration after trauma (reviewed in Maness and Schachner, 2007). The polysialyltransferase-mediated transfer of poly-α2,8-sialic acid (polySia) to NCAM is known to modulate neurogenesis, migration, axonal outgrowth and synaptic plasticity (Kleene and Schachner, 2004). PolySia deficient mice show a severe neurodevelopmental phenotype, including brain wiring defects and a progressive hydrocephalus, with the consequent abnormal enlargement of brain ventricles. The deletion of NCAM in polySia null animals completely rescue the hydrocephalus phenotype, thus indicating that this defect is mainly due to a gain of function of NCAM in absence of polySia. On the basis of these data, the authors propose that polySia could act by preventing premature contacts between NCAM molecules, on the plane of the membrane or between adjacent cells (Weinhold et al., 2005).

Several independent studies have described and characterised the hydrocephalus phenotype in L1-deficient mice (Dahme et al., 1997; Fransen et al., 1998; Demyanenko et al., 1999). The ventricle dilation observed in the L1 knock-out animals was suggested to be due to defective neuronal extension, or cell loss in specific regions of the brain, which would determine the onset of hydrocephalus as a consequence of the reduced cerebral mass (Fransen et al., 1998). A mouse model has been recently generated, in which the sixth Ig domain of L1 has been deleted (Itoh et al., 2004). This modification was shown to disrupt homophilic interactions between

L1 molecules, leaving the binding to other molecules unaffected. Interestingly, neuronal development was not affected in these animals, but they developed hydrocephalus when back-crossed onto the inbred C57BL/6 background. These data indicate that the onset of hydrocephalus in L1 null mice is associated at least partially with the loss of homophilic interactions between L1 molecules (Itoh et al., 2004). Similar to what has been suggested for the L1-null mice (Fransen et al., 1998), the ventricle enlargement in the Kidins220 knock-out brain could be the consequence of a loss of cerebral mass. This could be due to impaired proliferation of neuronal progenitors, and/or to increased cell death of specific neuronal subpopulations. In order to better understand the mechanisms underlying this ventricle phenotype, we plan to follow the development of the knock-out brain in detail. To this purpose, we will perform immunohistochemistry on sections from brains taken at different developmental stages, using markers specific for cell death and cell proliferation.

7.4.1.2 Cell death in the olfactory bulb

High levels of Kidins220 expression were detected in the mitral layer of the adult rat olfactory bulb (Kong et al., 2001). We observed an apoptotic region localised to the subependymal zone of the olfactory bulb of Kidins220 knock-out animals, adjacent to the lateral ventricle (Figure 6-15 and Figure 6-16). During the development of the rodent olfactory bulb, some neuronal populations are generated prenatally, while others are generated after birth. Mitral and tufted cells belong to the former category, whereas granule and periglomerular cells belong to the latter (Bayer, 1983). Granule and periglomerular cells originate from the subventricular

zone (SVZ) of the olfactory bulb, which is located close to the anterior horn of the lateral ventricle. To reach their final destination, neuronal precursors migrate tangentially along a precisely defined route denominated rostral migratory stream (RMS) (Luskin, 1993).

The phenotype observed in the Kidins220 knock-out brains is reminiscent of defects found in the NCAM knock-out mice, where the olfactory bulb is significantly smaller than the wild type (Cremer et al., 1994). These animals show a reduction in granule cells number, and a corresponding accumulation of granule cells precursors in the SVZ, the origin of their migration (Tomasiewicz et al., 1993). Subsequent studies demonstrated that this phenotype is due to impaired tangential migration of the precursor cells, which is dependent on the presence of the NCAM-conjugated polySia molecule (Hu et al., 1996). Further insights into the role played by polySia-NCAM in this process have been uncovered in a recent work, where polySia-NCAM was shown to promote the survival of the neuronal precursors in the olfactory bulb via two parallel mechanisms. On one side, polySia-NCAM facilitates the binding of BDNF to TrkB, and at the same time it downregulates the expression of $p75^{NTR}$, thus inhibiting the pro-apoptotic cascades initiated by this receptor (Gascon et al., 2007).

PolySia-NCAM had already been implicated in the modulation of BDNF signalling in hippocampal (Muller et al., 2000) as well as in cortical neurons (Vutskits et al., 2001). It therefore seems that the functional relationship between NCAM and BDNF/TrkB might represent a pro-survival mechanism common to different classes of neurons. NCAM can act as an alternative receptor for the glial-derived neurotrophic factor (GDNF), independently of its natural receptor Ret. GDNF signalling through NCAM was shown to promote Schwann cell migration

and axonal growth in hippocampal and cortical neurons (Paratcha et al., 2003). It has been proposed that NCAM could also play a similar role in the BDNF/TrkB pathway. In this case, NCAM would present BDNF to TrkB at the cell surface, thus facilitating the ligand-receptor interaction and the activation of the downstream signalling cascades (Muller et al., 2000; Vutskits et al., 2001; Gascon et al., 2007).

Although to date no interactions between Kidins220 and cell adhesion molecules have been demonstrated, the similarities between the brain phenotype in the Kidins220, L1 and NCAM knock-out mice suggest that Kidins220 might be involved in the modulation of cell-cell interactions during neuronal development. The involvement of NCAM in the BDNF-induced signalling pathways provides additional support to a model where Kidins220 acts downstream of TrkB, as discussed below.

Kidins220 could control the molecular events required for axon pathfinding and migration in response to neurotrophic stimuli, via its specific interaction with Trio. This idea is supported by the analysis of the brain defects displayed by Trio knock-out mice. The ablation of Trio results in the abnormal organisation of the dentate gyrus and the mitral cell layer of the olfactory bulb (O'Brien et al., 2000), which closely resembles the phenotype of the Kidins220 deficient animals (see Figure 6-15, Figure 6-16, Figure 6-18). We suggest that Kidins220 might play an important role in the correct migration and positioning of specific neuronal populations. In this scenario, the interaction between Kidins220 and Trio would be functional to translate signals from neurotrophin receptors and/or adhesion molecules, into the cytoskeletal remodelling events required for growth cone migration and axon pathfinding.

7.4.2 *Kidins220 in the cerebellum: Ca^{2+} signalling*

Kidins220 is highly expressed in the Purkinje cells of adult rat cerebellum (Kong et al., 2001, and http://www.brainatlas.org/aba/index.shtml), however the analysis of cerebellar morphology in E19.5 Kidins220 knock-out brains failed to reveal major defects in the development of this structure (Figure 6-17). To identify more subtle changes in the Purkinje layer, we monitored the expression of calbindin, a well-established marker of Purkinje cells (Celio, 1990), which was markedly reduced in the knock-out sample, compared to the wild type (Figure 6-17). Calbindin is a calcium binding protein that exerts a protective effect on neurons, by preventing the accumulation of toxic levels of free calcium (Chard et al., 1993). Calbindin-deficient mice show ataxia and impaired motor coordination, which are linked to alteration of calcium signalling in the dendritic compartment of Purkinje cells (Airaksinen et al., 1997). The selective knock-out of calbindin in Purkinje cells confirmed the role of this protein in modulating the synaptic activity required for motor coordination (Barski et al., 2003). The reduced levels of calbindin in the Kidins220 knock-out Purkinje cells might indicate defects in calcium signalling and/or synaptic activity in this neuronal population. Because of the early lethality of the Kidins220 knock-out mice, more insights into the role of Kidins220 in adult cerebellar physiology might be obtained by selectively targeting this protein in Purkinje cells.

7.4.3 Kidins220 in the BDNF/TrkB signalling pathways

7.4.3.1 Developmental defects in the hippocampus and thalamus

The hippocampus of Kidins220 null animals shows some structural defects, such as a poorly defined pyramidal cell layer, and a general disorganisation of the region corresponding to the dentate gyrus, coupled to an increase in cellularity (Figure 6-18). These defects suggest a link between Kidins220 and the BDNF/TrkB pathways. As discussed in section 1.4.2.3 (Introduction), deletion of either BDNF or TrkB compromises both hippocampal morphology and functionality (Korte et al., 1995; Patterson et al., 1996; Minichiello et al., 1999; Pozzo-Miller et al., 1999). A very recent study has analysed in detail the developmental and activity-dependent regulation of Kidins220 in rat hippocampal neurons (Cortes et al., 2007). In this work, the authors showed an inverse relationship between Kidins220 expression levels and synaptic activity of cultured neurons. Kidins220 expression is relatively high during active neurite extension soon after plating, and progressively decreases at later points, when the growth rate slows down as the neurons mature. Interestingly, it was possible to alter Kidins220 levels even in older cultures, by inhibiting or stimulating synaptic activity via pharmacological treatments, as well as by BDNF treatment. The knock-down of Kidins220 via RNAi induced premature synapse maturation, but this effect was limited to early time points after plating (Cortes et al., 2007).

The morphological defects in the Kidins220 knock-out hippocampus are most evident in the dentate gyrus area, which displayed an increased in cellularisation, coupled to a general disorganisation of its characteristic arrow-

shaped cell layer. This observation is particularly interesting, as TrkB deletion was shown to cause high levels of apoptosis in this region (Alcantara et al., 1997). The neuronal populations of the dentate gyrus generated postnatally showed the most abundant cell death, thus suggesting that this particular subset of neurons develops a more selective dependence on TrkB-mediated trophic stimuli (Alcantara et al., 1997). As for the cerebellar neurons, the lethality caused by the full Kidins220 deletion prevents us from analysing the events that take place during postnatal development. The generation of conditional knock-out animals will allow the characterisation of the role of Kidins220 in the adult and ageing hippocampus.

The hypothesis of a connection between Kidins220 and the BDNF-TrkB signalling pathways is further corroborated by the finding of a precisely defined apoptotic area, corresponding to the thalamic region, in E19.5 Kidins220 knock-out brains (Figure 6-15 and Figure 6-16). As described in section 1.4.2.3 (Introduction), thalamic neurons develop a specific dependence on cortex-derived BDNF, at late stages of embryonic development (Lotto et al., 2001). It is therefore possible to speculate that Kidins220 might promote the survival of one or more subpopulations of thalamic neurons, by modulating their response to BDNF, via its interaction with TrkB.

Besides these observations, other biochemical data have linked Kidins220 to the TrkB-mediated signalling pathways. Kidins220 interacts with the TrkB receptors (Arevalo et al., 2004), and it is rapidly phosphorylated after BDNF treatment (Kong et al., 2001). In addition, a dominant negative portion of Kidins220 was shown to impair BDNF-mediated MAPK activation in cortical neurons (Arevalo et al., 2004).

It will be interesting to test the ability of hippocampal and thalamic neurons lacking Kidins220 to respond to BDNF stimulation, as well as to other neurotrophins.

7.4.3.2 Loss of lumbar motor neurons

Staining of spinal cord sections for the motor neuron-specific marker HB9 revealed a reduction of the nuclear immunoreactivity in the knock-out samples, compared to the wild type, in particular at the lumbar level (Figure 6-20). Motor neuron development is a complex process that requires the spatial and temporal coordination of different signalling pathways at different developmental stages. Motor neuron specification initially requires the establishment of a Sonic hedgehog (Shh) gradient along the dorso-ventral axis of the spinal cord. These initial motor neuron progenitors would subsequently differentiate into different pools, with different target specificity (reviewed in Jessell, 2000). Later steps of motor neuron diversification rely on the orchestrated activity of growth factors such as hepatocyte growth factor / scatter factor HGF/SF (Ebens et al., 1996), GDNF (Airaksinen and Saarma, 2002), transforming growth factor α (TGFα) (Boillee et al., 2001), cardiotrophin-1 (CT-1) (Oppenheim et al., 2001), and many others. Amongst these players, the BDNF/TrkB pathway seems to be essential during the early stages of development, when BDNF secreted by dorsal interneurons stimulates the proliferation and differentiation of motor neuron precursors, located in the ventral side of the neural tube (Jungbluth et al., 1997). The homeodomain factor HB9 is expressed in a subset of MNs, namely all the hindbrain and spinal cord MNs with a ventral axonal projection (v-MNs) (Thaler et al., 1999). Its expression is already detectable at the onset of MN neurogenesis, around E9, and is maintained during the

post-mitotic stage. HB9 has been shown to behave as a transcriptional repressor, actively preventing neuronal precursors from differentiating into interneurons (Arber et al., 1999; Thaler et al., 1999). The reduction of the nuclear HB9 staining in the Kidins220 knock-out lumbar MNs might indicate a defect in the differentation of v-MNs. Future studies will assess whether there is a difference in the ratio between different MN subpopulations in the wild type and knock-out embryos.

Mice deficient for the TrkB receptor show a marked reduction in the number of motor neurons in the facial nucleus, as well as in the lumbar region (Klein et al., 1993). This is in accordance with the results of several studies, which have identified BDNF as a primary modulator of motor neuron survival and regeneration after injury (Oppenheim et al., 1992; Sendtner et al., 1992; Yan et al., 1992; Henderson et al., 1993; Koliatsos et al., 1993). Although a precise quantification of motor neuron numbers in wild type and knock-out samples has not been performed as yet, our preliminary data suggest that the Kidins220 knock-out mice might also exhibit a reduction of motor neurons in the lumbar region (Figure 6-20). As for the hippocampal and thalamic neurons, motor neuron cultures derived from Kidins220 knock-out embryos will provide more insights about the role of Kidins220 in the modulation of BDNF-dependent survival.

7.4.4 Kidins220 in DRG development

Whole mount staining of E10.5 and E11.5 Kidins220 knock-out embryos did not reveal any major defects in DRG branching or pathfinding (Figure 6-19). In addition, staining for TrkA, TrkB and TrkC receptors on DRG sections from E19.5 embryos did not show prominent cell loss in any of the three subpopulations (data

not shown). The biogenesis of the different classes of DRG neurons, as well as their neurotrophin dependence, has been extensively studied. It is now known that large (TrkB/TrkC-positive) neurons are born around E9.5, whereas small TrkA-expressing neurons are generated around E10.5 of mouse embryonic development (Ma et al., 1999). A study by White and colleagues showed that at E11.5 virtually all DRG neurons express TrkC mRNA, and display a strict NT-3/TrkC survival dependence. By E13.5 TrkC expression is massively downregulated, and at this stage DRG neurons rely on NGF/TrkA signalling (White et al., 1996). A similar analysis for TrkB/BDNF dependence has not been performed to date. However, experiments conducted on mice bearing combined Trk deletions (*trkA-/-;trkB-/-*, *trkA-/-;trkC-/-*, and *trkB-/-;trkC-/-*) revealed that by postnatal day 1, DRG loss has already occurred in all the genotypes (Minichiello et al., 1995).

Published data have described a very strong expression of Kidins220 in rat embryonic DRGs, as well as in small- and medium-sized neurons in adult DRGs (Kong et al., 2001). It is possible that the stages chosen for the whole mount staining were too early in development to reveal specific neuronal death due to Kidins220 deletion. An accurate analysis of the Kidins220 knock-out DRGs has not been conducted as yet. A detailed quantification of the TrkA-, TrkB- and TrkC-positive neurons in the knock-out and wild type samples might reveal a partial reduction in one or more of these populations.

7.5 Heart defects in Kidins220 KO animals

7.5.1 Is Kidins220 a major player of the NT-3/TrkC pathway?

The morphology of the Kidins220 knock-out heart is severely affected. Analysis of heart sections from E19.5 embryos revealed enlarged and congested atria, as well as a defective organisation of the ventricular walls. In addition, the opening between the atria (*foramen ovale*) was significally wider in the knock-out samples than the wild type, suggesting the presence of an atrial septal defect (ASD, Figure 6-12).

Defects in heart development were found in both NT-3 (Donovan et al., 1996) and TrkC (Tessarollo et al., 1997) null mice. Kidins220 has been shown to interact with all three Trk receptors (Arevalo et al., 2004), as well as with $p75^{NTR}$ (Chang et al., 2004). However, up to now all the studies have focused on the characterisation of the role of Kidins220 in the NGF/TrkA and BDNF/TrkB pathways, while the involvement of Kidins220 in NT-3/TrkC signalling is still unexplored. Our observations suggest that Kidins220 might mediate the signalling cascades downstream of TrkC, during heart development. At this stage of our analysis, it is not possible to establish if the ASD is due to a real developmental defect, or if it is only a consequence of the abnormal ventricle dilation. In both the NT-3 and TrkC knock-out mice, the heart phenotype is consistent with defects in neural crest migration and differentiation (Donovan et al., 1996; Tessarollo et al., 1997). *In situ* hybridisation on E9.5 embryos did not reveal any defects in neural crest patterning in the Kidins220 knock-out embryos (Figure 6-13). It is possible that Kidins220 deletion affects only a small subset of neural crest cells, which could not

be detected by this method. Alternatively, the defect might only manifest itself at later stages of development. A careful analysis of the Kidins220 expression pattern in wild type embryos will be crucial to characterise its distribution in neural crest-derived structures, at different developmental stages. In this regard, the optimisation of Kidins220-specific probes by *in situ* hybridisation, on a range of embryonic as well as adult tissues, is underway.

The ventricle wall phenotype might indicate a problem in cell adhesion. As discussed in section 7.4.1, several defects of the Kidins220 knock-out brain suggest the involvement of Kidins220 in the molecular events mediated by the neuronal adhesion molecules NCAM and L1. NCAM expression has been documented in several non-neuronal structures, including neural crest cells (Thiery et al., 1982). NCAM immunoreactivity is detectable at early stages of neural crest generation, it then gradually disappears during migration, and reappears at the sites of ganglia formation (Thiery et al., 1982; Akitaya and Bronner-Fraser, 1992). Interestingly, NCAM expression was detected in several neural crest-derived structures of the developing heart (Okagawa et al., 1995). In the course of our future studies, it will be important to establish whether a defect in cell adhesion underlies both the neuronal and cardiac phenotype in the Kidins220 knock-out animals.

7.6 Kidins220 deletion causes embryonic lethality

As discussed in section 6.9.1, lungs recovered post-mortem from P0 Kidins220 knock-out pups do not contain air, suggesting that respiratory failure is the primary cause of death in the knock-out embryos. This could be due to defective innervation of the diaphragm, or alternatively, to developmental defects in the

medulla oblongata, the area of the brain stem that controls breathing. To understand which of these two events is responsible for the death of the Kidins220 knock-out animals, we will firstly examine diaphragm innervation. We will also perform an immunohistochemical analysis of the brain stem region, to verify whether specific populations of brain stem motor neurons undergo cell death during embryonic development, thus compromising the correct onset of breathing at birth.

7.7 Future perspectives – 2

7.7.1 Kidins220 during evolution

The data discussed above support the notion that Kidins220 acts as modulator of the neurotrophin signalling pathways. However, Kidins220 orthologues are also found in lower organisms, namely *Drosophila* and *C. elegans*, which lack a canonical neurotrophin/Trk system. Although the *Drosophila* and *C. elegans* orthologues share a low degree of homology with their vertebrate counterparts (Figure 1-6), it is possible that Kidins220 would exert a similar function in these organisms, by interacting with different receptors involved in neuronal development.

Kidins220 is involved in the modulation of EphA4 signalling at the NMJ, via its interaction with α-syntrophin (Luo et al., 2005). Ephrins and Eph receptors play a key role in fundamental processes such as neuronal development and angiogenesis (Pasquale, 2005), and their orthologues have been identified in organisms ranging from vertebrates to sponges (Drescher, 2002). Sequencing of the *C. elegans* genome revealed one Eph receptor (VAB-1) and four putative ephrin ligands (EFN 1-4) (consortium, 1998), whereas only one Eph receptor (Dek) and one ligand (D-ephrin)

have been identified in *Drosophila* (Scully et al., 1999; Bossing and Brand, 2002). In both organisms, the Eph/ephrin pathways have been implicated in neuronal development and morphogenesis (George et al., 1998; Scully et al., 1999; Bossing and Brand, 2002). Kidins220 modulates both the ephrin/Eph and Nt/Trk signalling pathways via distinct amino acid signatures in its carboxy-terminal region (Kong et al., 2001; Arevalo et al., 2004; Luo et al., 2005). Interestingly, the carboxy-terminal tail is the portion of Kidins220 that is most divergent between different organisms (see Figure 1-5). On the basis of these observations, we suggest that Kidins220 might have a common function in vertebrates and invertebrates, as a modulator of Eph/ephrin signalling, and that its role in the Nt/Trk pathways could be a specific acquisition of vertebrates.

7.7.2 Different Trks for different functions

Several studies have mainly focused on the role of Kidins220 in the signalling pathways triggered by NGF stimulation (Iglesias et al., 2000; Arevalo et al., 2004; Arevalo et al., 2006; Bracale et al., 2007), only marginally characterising the involvement of this protein in the cellular responses triggered by BDNF (Kong et al., 2001; Arevalo et al., 2004; Arevalo et al., 2006; Cortes et al., 2007). It is presently unknown whether Kidins220 can modulate the activation of intracellular cascades in response to NT-3 stimuli. A preliminary analysis of the phenotypes displayed by the Kidins220 knock-out mice has delineated an unexpectedly complex role for this protein during mouse development, which is summarised in Figure 7-4. The heart phenotype, possibly related to defects in neural crest migration, strongly resembles the defects of TrkC or NT-3 deficient mice (Figure 7-4 c)(Donovan et al.,

1996; Tessarollo et al., 1997). This would implicate Kidins220 in the TrkC-mediated events that modulate heart development. The defects in hippocampal morphology, the cell death in the thalamic region, as well as the possible reduction of motor neuron survival, all point towards a defective neuronal response to BDNF (Figure 7-4 b). None of the phenotypes analysed so far have specifically suggested a defective response to TrkA- or $p75^{NTR}$-mediated signals. However, it is likely that future studies will reveal other deficiencies, which have escaped this preliminary analysis, linking Kidins220 to these receptors. Culture of primary neurons derived from knock-out and wild-type animals will allow a precise biochemical characterisation of the signalling pathways mediated by Kidins220, in the context of neuronal survival and differentiation. Our observations suggest that Kidins220 is a multifunctional protein, which is able to recruit different adaptors depending on the cellular environment and on the specific Trk receptor that initiates the signal.

The enlargement of the brain ventricles and the cell death in specific regions of the olfactory bulb shifted the focus of our attention from neurotrophin signalling to cell adhesion. As discussed in section 7.4.1, these phenotypes are remarkably similar to the ones shown by both NCAM and L1 null mice (Figure 7-4 a) (Cremer et al., 1994; Dahme et al., 1997; Weinhold et al., 2005). It will be interesting to test the ability of Kidins220 knock-out neurons to grow on different substrates. Furthermore, this might give new insights on the mechanisms underlying the functional relationship between NCAM and the BDNF/TrkB pathway.

The early lethality of the Kidins220 knock-out animals has so far prevented the analysis of postnatal developmental processes, and also precluded any behavioural tests. The conditional deletion of Kidins220 will allow us to perform a

more accurate characterisation of the role of this protein in specific neuronal subpopulations. Several mouse lines expressing Cre recombinase under the control of neuronal-specific promoters are presently available. For example, in the nestin-Cre line the *Cre* gene is expressed under the control of the nestin promoter, which is ubiquitously active in the CNS (Zimmerman et al., 1994). The use of this line would allow us to focus our analysis on the brain and spinal cord, avoiding the complications associated with the cardiac phenotype. An even more specific targeting could by achieved by using the CaMKII-Cre line. In these animals, the *Cre* gene is under the control of the CamKII promoter, which is activated only in selected regions of the forebrain (mainly cortex and hippocampus), during the postnatal period (Tsien et al., 1996; Dragatsis and Zeitlin, 2000). This line would be particularly useful to study the role of Kidins220 in the adult hippocampus. The function of Kidins220 in cerebellar physiology could be analysed by using the L7-Cre line, where *Cre* expression is driven by the Purkinje cells-specific L7 promoter (Barski et al., 2000). Some of these lines are presently available at Cancer Research UK.

The characterisation of the heart phenotype could also benefit from the use of Cre-mediated conditional gene targeting. The involvement of Kidins220 in the development of neural crest-derived structures could be analysed by using Cre lines that exploit neural crest specific promoters such as Sox10, which would target all undifferentiated neural crest precursors (Mollaaghababa and Pavan, 2003), and Wnt1, which would more specifically affect cranial neural crest cells (Echelard et al., 1994). Another possibility would be to perform neural crest explants, to determine the effect of Kidins220 deletion on the ability of these cells to migrate and

differentiate in response to neurotrophic stimuli, similarly to what has been described for TrkC (Youn et al., 2003).

7.7.3 Kidins220 and Eph / ephrin signalling

Our preliminary analysis of the Kidins220 knock-out animals did not reveal any strong similarities to the Eph / ephrin null mouse models. The cardiac defects displayed by the EphB4 and ephrinB2 knock-out mice are much more severe than in the Kidins220 null mice (Gerety et al., 1999). In addition, we could not reveal any defects in neural crest migration in E9.5 Kidins220 knock-out embryos (Figure 6-13), whereas the knock-out of ephrin-B2 results in the absence or reduction of the neural crest population migrating along the second branchial arch (Adams et al., 2001). Altogether, these findings suggest that different molecular mechanisms underlie the heart defects in these two mouse models. Future studies will ascertain whether Kidins220 deletion affects topographic processes such as retinotectal mapping and MN innervation of limb muscles, as well as axon guidance of commissural neurons in the brain and corticospinal tract. Eph / ephrin signalling has been implicated in the development and functioning of hippocampal neurons, as discussed in section 1.6.3.4. It will be crucial to investigate the role of Kidins220 in Eph / ephrin dependent processes such as the clustering and activation of NMDA receptor at synapses, or dendritic spine formation (Dalva et al., 2000; Ethell et al., 2001; Takasu et al., 2002).

Recent studies have described a role for Kidins220 in the modulation of EphA4 signalling at the NMJ (Luo et al., 2005). As previously discussed, these findings support the hypothesis that Kidins220 might have a common function in

vertebrates and invertebrates, as a regulator of the ephrin/Eph signalling pathways during neuronal development. The availability of Kidins220 knock-out mice will provide the opportunity to study the role of this protein in the development and maintenance of the NMJ. The characterisation of Eph signalling in wild type and knock-out NMJs will shed more light on the molecular mechanisms connecting Kidins220 to the Eph-mediated intracellular cascades.

7.8 Conclusive remarks

With reference to the hypotheses and objectives described in section 1.8, I believe that I have fully achieved the objectives set for this thesis. In particular, I have demonstrated that:

1. The intracellular trafficking of Kidins220 is mediated by the kinesin-1 complex, via a direct interaction of Kidins220 with KLC. The KLC-interacting motif (KIM) of Kidins220 is necessary and sufficient for the binding to a region of KLC spanning half of the heptad repeats and the first two TPRs. The kinetic of Kidins220 trafficking is consistent with a kinesin-1-mediated transport. Impairment of Kidins220 transport affects the ability of PC12 cells to respond to NGF stimuli (Chapter 3).
2. The Abl kinase phosphorylates Kidins220 on tyrosine 1375, which lays within the KIM sequence. Abl-mediated phosphorylation inhibits the binding of KIM to KLC (Chapter 4).
3. A preliminary analysis of the phenotypes displayed by the Kidins220 knock-out animals suggests that Kidins220 might play multiple roles

during development, acting downstream of different Trk receptors in different tissues. In addition, Kidins220 might be involved in mediating cell adhesion, possibly via a functional interaction with adhesion molecules such as NCAM (Chapter 6).

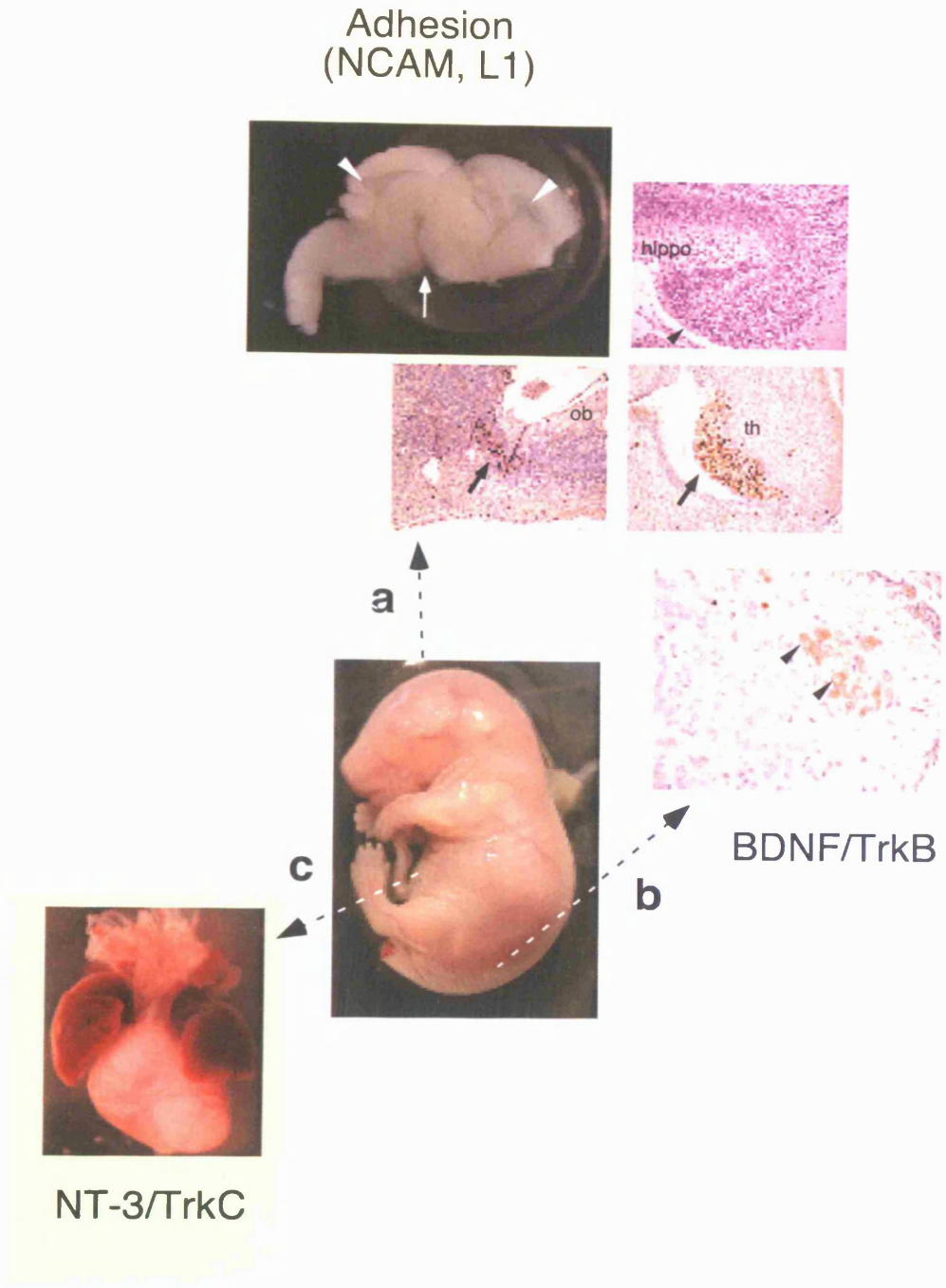

Figure 7-4: *schematic representation of the main developmental defects displayed by the Kidins220 knock-out animals*
(*a*) The enlargement of the brain ventricles and the cell death in the olfactory bulb suggest a link between Kidins220 and cell adhesion molecules such as NCAM and L1. (*b*) The defects in the hippocampus, the cell death in the thalamic region, and the loss of lumbar motor neurons point towards a role for Kidins220 in the BDNF/TrkB signalling pathways. (*c*) Heart malformations are reminiscent of defects present in TrkC and NT-3 null mice.

Chapter 8 – References

8 References

Adams, M. D., Celniker, S. E., Holt, R. A., Evans, C. A., Gocayne, J. D., Amanatides, P. G., Scherer, S. E., Li, P. W., Hoskins, R. A., Galle, R. F., et al. (2000). The genome sequence of Drosophila melanogaster. Science 287, 2185-2195.

Adams, R. H., Diella, F., Hennig, S., Helmbacher, F., Deutsch, U., and Klein, R. (2001). The cytoplasmic domain of the ligand ephrinB2 is required for vascular morphogenesis but not cranial neural crest migration. Cell 104, 57-69.

Adams, R. H., Wilkinson, G. A., Weiss, C., Diella, F., Gale, N. W., Deutsch, U., Risau, W., and Klein, R. (1999). Roles of ephrinB ligands and EphB receptors in cardiovascular development: demarcation of arterial/venous domains, vascular morphogenesis, and sprouting angiogenesis. Genes Dev 13, 295-306.

Addinall, S. G., Mayr, P. S., Doyle, S., Sheehan, J. K., Woodman, P. G., and Allan, V. J. (2001). Phosphorylation by cdc2-CyclinB1 kinase releases cytoplasmic dynein from membranes. J Biol Chem 276, 15939-15944.

Advani, A. S., and Pendergast, A. M. (2002). Bcr-Abl variants: biological and clinical aspects. Leuk Res 26, 713-720.

Airaksinen, M. S., Eilers, J., Garaschuk, O., Thoenen, H., Konnerth, A., and Meyer, M. (1997). Ataxia and altered dendritic calcium signaling in mice carrying a targeted null mutation of the calbindin D28k gene. Proc Natl Acad Sci U S A 94, 1488-1493.

Airaksinen, M. S., and Saarma, M. (2002). The GDNF family: signalling, biological functions and therapeutic value. Nat Rev Neurosci 3, 383-394.

Aizawa, H., Sekine, Y., Takemura, R., Zhang, Z., Nangaku, M., and Hirokawa, N. (1992). Kinesin family in murine central nervous system. J Cell Biol 119, 1287-1296.

Akitaya, T., and Bronner-Fraser, M. (1992). Expression of cell adhesion molecules during initiation and cessation of neural crest cell migration. Dev Dyn 194, 12-20.

Alcantara, S., Frisen, J., del Rio, J. A., Soriano, E., Barbacid, M., and Silos-Santiago, I. (1997). TrkB signaling is required for postnatal survival of CNS neurons and protects hippocampal and motor neurons from axotomy-induced cell death. J Neurosci 17, 3623-3633.

Aoki, M., Yamashita, T., and Tohyama, M. (2004). EphA receptors direct the differentiation of mammalian neural precursor cells through a mitogen-activated protein kinase-dependent pathway. J Biol Chem 279, 32643-32650.

Araki, Y., Kawano, T., Taru, H., Saito, Y., Wada, S., Miyamoto, K., Kobayashi, H., Ishikawa, H. O., Ohsugi, Y., Yamamoto, T., et al. (2007). The novel cargo Alcadein induces vesicle association of kinesin-1 motor components and activates axonal transport. Embo J 26, 1475-1486.

Aravind, L., Iyer, L. M., Leipe, D. D., and Koonin, E. V. (2004). A novel family of P-loop NTPases with an unusual phyletic distribution and transmembrane segments inserted within the NTPase domain. Genome Biol 5, R30.

Arber, S., Han, B., Mendelsohn, M., Smith, M., Jessell, T. M., and Sockanathan, S. (1999). Requirement for the homeobox gene Hb9 in the consolidation of motor neuron identity. Neuron 23, 659-674.

Arevalo, J. C., Pereira, D. B., Yano, H., Teng, K. K., and Chao, M. V. (2006). Identification of a switch in neurotrophin signaling by selective tyrosine phosphorylation. J Biol Chem 281, 1001-1007.

Arevalo, J. C., Yano, H., Teng, K. K., and Chao, M. V. (2004). A unique pathway for sustained neurotrophin signaling through an ankyrin-rich membrane-spanning protein. Embo J 23, 2358-2368.

Awasaki, T., Saito, M., Sone, M., Suzuki, E., Sakai, R., Ito, K., and Hama, C. (2000). The Drosophila trio plays an essential role in patterning of axons by regulating their directional extension. Neuron 26, 119-131.

Baas, P. W., Deitch, J. S., Black, M. M., and Banker, G. A. (1988). Polarity orientation of microtubules in hippocampal neurons: uniformity in the axon and nonuniformity in the dendrite. Proc Natl Acad Sci U S A 85, 8335-8339.

Bannai, H., Inoue, T., Nakayama, T., Hattori, M., and Mikoshiba, K. (2004). Kinesin dependent, rapid, bi-directional transport of ER sub-compartment in dendrites of hippocampal neurons. J Cell Sci 117, 163-175.

Barde, Y. A. (1994). Neurotrophic factors: an evolutionary perspective. J Neurobiol 25, 1329-1333.

Barski, J. J., Dethleffsen, K., and Meyer, M. (2000). Cre recombinase expression in cerebellar Purkinje cells. Genesis 28, 93-98.

Barski, J. J., Hartmann, J., Rose, C. R., Hoebeek, F., Morl, K., Noll-Hussong, M., De Zeeuw, C. I., Konnerth, A., and Meyer, M. (2003). Calbindin in cerebellar Purkinje cells is a critical determinant of the precision of motor coordination. J Neurosci 23, 3469-3477.

Bateman, J., Shu, H., and Van Vactor, D. (2000). The guanine nucleotide exchange factor trio mediates axonal development in the Drosophila embryo. Neuron 26, 93-106.

Batut, J., Howell, M., and Hill, C. S. (2007). Kinesin-mediated transport of Smad2 is required for signaling in response to TGF-beta ligands. Dev Cell 12, 261-274.

Bayer, S. A. (1983). 3H-thymidine-radiographic studies of neurogenesis in the rat olfactory bulb. Exp Brain Res 50, 329-340.

Beattie, E. C., Howe, C. L., Wilde, A., Brodsky, F. M., and Mobley, W. C. (2000). NGF signals through TrkA to increase clathrin at the plasma membrane and enhance clathrin-mediated membrane trafficking. J Neurosci 20, 7325-7333.

Beg, A. A., Sommer, J. E., Martin, J. H., and Scheiffele, P. (2007). alpha2-Chimaerin is an essential EphA4 effector in the assembly of neuronal locomotor circuits. Neuron 55, 768-778.

Bellanger, J. M., Astier, C., Sardet, C., Ohta, Y., Stossel, T. P., and Debant, A. (2000). The Rac1- and RhoG-specific GEF domain of Trio targets filamin to remodel cytoskeletal actin. Nat Cell Biol 2, 888-892.

Benito-Gutierrez, E., Garcia-Fernandez, J., and Comella, J. X. (2006). Origin and evolution of the Trk family of neurotrophic receptors. Mol Cell Neurosci 31, 179-192.

Benito-Gutierrez, E., Nake, C., Llovera, M., Comella, J. X., and Garcia-Fernandez, J. (2005). The single AmphiTrk receptor highlights increased complexity

of neurotrophin signalling in vertebrates and suggests an early role in developing sensory neuroepidermal cells. Development 132, 2191-2202.

Bentley, C. A., and Lee, K. F. (2000). p75 is important for axon growth and schwann cell migration during development. J Neurosci 20, 7706-7715.

Bhattacharyya, A., Watson, F. L., Pomeroy, S. L., Zhang, Y. Z., Stiles, C. D., and Segal, R. A. (2002). High-resolution imaging demonstrates dynein-based vesicular transport of activated Trk receptors. J Neurobiol 51, 302-312.

Bibel, M., and Barde, Y. A. (2000). Neurotrophins: key regulators of cell fate and cell shape in the vertebrate nervous system. Genes Dev 14, 2919-2937.

Bilderback, T. R., Gazula, V. R., Lisanti, M. P., and Dobrowsky, R. T. (1999). Caveolin interacts with Trk A and p75(NTR) and regulates neurotrophin signaling pathways. J Biol Chem 274, 257-263.

Blasius, T. L., Cai, D., Jih, G. T., Toret, C. P., and Verhey, K. J. (2007). Two binding partners cooperate to activate the molecular motor Kinesin-1. J Cell Biol 176, 11-17.

Blatch, G. L., and Lassle, M. (1999). The tetratricopeptide repeat: a structural motif mediating protein-protein interactions. Bioessays 21, 932-939.

Boillee, S., Cadusseau, J., Coulpier, M., Grannec, G., and Junier, M. P. (2001). Transforming growth factor alpha: a promoter of motoneuron survival of potential biological relevance. J Neurosci 21, 7079-7088.

Bonni, A., Ginty, D. D., Dudek, H., and Greenberg, M. E. (1995). Serine 133-phosphorylated CREB induces transcription via a cooperative mechanism that may confer specificity to neurotrophin signals. Mol Cell Neurosci 6, 168-183.

Bossing, T., and Brand, A. H. (2002). Dephrin, a transmembrane ephrin with a unique structure, prevents interneuronal axons from exiting the Drosophila embryonic CNS. Development 129, 4205-4218.

Bowman, A. B., Kamal, A., Ritchings, B. W., Philp, A. V., McGrail, M., Gindhart, J. G., and Goldstein, L. S. (2000). Kinesin-dependent axonal transport is mediated by the sunday driver (SYD) protein. Cell 103, 583-594.

Bracale, A., Cesca, F., Neubrand, V. E., Newsome, T. P., Way, M., and Schiavo, G. (2007). Kidins220/ARMS is transported by a kinesin-1-based mechanism likely to be involved in neuronal differentiation. Mol Biol Cell 18, 142-152.

Brady, S. T. (1985). A novel brain ATPase with properties expected for the fast axonal transport motor. Nature 317, 73-75.

Brady, S. T., Pfister, K. K., and Bloom, G. S. (1990). A monoclonal antibody against kinesin inhibits both anterograde and retrograde fast axonal transport in squid axoplasm. Proc Natl Acad Sci U S A 87, 1061-1065.

Brendza, R. P., Serbus, L. R., Duffy, J. B., and Saxton, W. M. (2000). A function for kinesin I in the posterior transport of oskar mRNA and Staufen protein. Science 289, 2120-2122.

Brickley, K., Smith, M. J., Beck, M., and Stephenson, F. A. (2005). GRIF-1 and OIP106, members of a novel gene family of coiled-coil domain proteins: association in vivo and in vitro with kinesin. J Biol Chem 280, 14723-14732.

Brown, D. A., and London, E. (1998). Functions of lipid rafts in biological membranes. Annu Rev Cell Dev Biol 14, 111-136.

Bruckner, K., Labrador, J. P., Scheiffele, P., Herb, A., Seeburg, P. H., and Klein, R. (1999). EphrinB ligands recruit GRIP family PDZ adaptor proteins into raft membrane microdomains. Neuron 22, 511-524.

Bruckner, K., Pasquale, E. B., and Klein, R. (1997). Tyrosine phosphorylation of transmembrane ligands for Eph receptors. Science 275, 1640-1643.

Bunn, R. C., Jensen, M. A., and Reed, B. C. (1999). Protein interactions with the glucose transporter binding protein GLUT1CBP that provide a link between GLUT1 and the cytoskeleton. Mol Biol Cell 10, 819-832.

Burack, M. A., Silverman, M. A., and Banker, G. (2000). The role of selective transport in neuronal protein sorting. Neuron 26, 465-472.

Burke, R. D., Angerer, L. M., Elphick, M. R., Humphrey, G. W., Yaguchi, S., Kiyama, T., Liang, S., Mu, X., Agca, C., Klein, W. H., et al. (2006). A genomic view of the sea urchin nervous system. Dev Biol 300, 434-460.

Cabrera-Poch, N., Sanchez-Ruiloba, L., Rodriguez-Martinez, M., and Iglesias, T. (2004). Lipid raft disruption triggers protein kinase C and Src-dependent protein kinase D activation and Kidins220 phosphorylation in neuronal cells. J Biol Chem 279, 28592-28602.

Campbell, R. E., Tour, O., Palmer, A. E., Steinbach, P. A., Baird, G. S., Zacharias, D. A., and Tsien, R. Y. (2002). A monomeric red fluorescent protein. Proc Natl Acad Sci U S A 99, 7877-7882.

Campenot, R. B. (1977). Local control of neurite development by nerve growth factor. Proc Natl Acad Sci U S A 74, 4516-4519.

Campenot, R. B., and MacInnis, B. L. (2004). Retrograde transport of neurotrophins: fact and function. J Neurobiol 58, 217-229.

Carninci, P., Kasukawa, T., Katayama, S., Gough, J., Frith, M. C., Maeda, N., Oyama, R., Ravasi, T., Lenhard, B., Wells, C., et al. (2005). The transcriptional landscape of the mammalian genome. Science 309, 1559-1563.

Carroll, P., Lewin, G. R., Koltzenburg, M., Toyka, K. V., and Thoenen, H. (1998). A role for BDNF in mechanosensation. Nat Neurosci 1, 42-46.

Carter, N., Nakamoto, T., Hirai, H., and Hunter, T. (2002). EphrinA1-induced cytoskeletal re-organization requires FAK and p130(cas). Nat Cell Biol 4, 565-573.

Cavalli, V., Kujala, P., Klumperman, J., and Goldstein, L. S. (2005). Sunday Driver links axonal transport to damage signaling. J Cell Biol 168, 775-787.

Celio, M. R. (1990). Calbindin D-28k and parvalbumin in the rat nervous system. Neuroscience 35, 375-475.

Chang, M. S., Arevalo, J. C., and Chao, M. V. (2004). Ternary complex with Trk, p75, and an ankyrin-rich membrane spanning protein. J Neurosci Res 78, 186-192.

Chao, M. V. (2003). Neurotrophins and their receptors: a convergence point for many signalling pathways. Nat Rev Neurosci 4, 299-309.

Chard, P. S., Bleakman, D., Christakos, S., Fullmer, C. S., and Miller, R. J. (1993). Calcium buffering properties of calbindin D28k and parvalbumin in rat sensory neurones. J Physiol 472, 341-357.

Chen, Z. Y., Sun, C., Reuhl, K., Bergemann, A., Henkemeyer, M., and Zhou, R. (2004). Abnormal hippocampal axon bundling in EphB receptor mutant mice. J Neurosci 24, 2366-2374.

Cheng, H. J., Nakamoto, M., Bergemann, A. D., and Flanagan, J. G. (1995). Complementary gradients in expression and binding of ELF-1 and Mek4 in development of the topographic retinotectal projection map. Cell 82, 371-381.

Chung, H. J., Jan, Y. N., and Jan, L. Y. (2006). Polarized axonal surface expression of neuronal KCNQ channels is mediated by multiple signals in the KCNQ2 and KCNQ3 C-terminal domains. Proc Natl Acad Sci U S A 103, 8870-8875.

Clary, D. O., and Reichardt, L. F. (1994). An alternatively spliced form of the nerve growth factor receptor TrkA confers an enhanced response to neurotrophin 3. Proc Natl Acad Sci U S A 91, 11133-11137.

Conover, J. C., Erickson, J. T., Katz, D. M., Bianchi, L. M., Poueymirou, W. T., McClain, J., Pan, L., Helgren, M., Ip, N. Y., Boland, P., and et al. (1995). Neuronal deficits, not involving motor neurons, in mice lacking BDNF and/or NT4. Nature 375, 235-238.

consortium, T. C. e. s. (1998). Genome sequence of the nematode C. elegans: a platform for investigating biology. Science 282, 2012-2018.

Cortes, R. Y., Arevalo, J. C., Magby, J. P., Chao, M. V., and Plummer, M. R. (2007). Developmental and activity-dependent regulation of ARMS/Kidins220 in cultured rat hippocampal neurons. Dev Neurobiol 67, 1687-1698.

Coy, D. L., Hancock, W. O., Wagenbach, M., and Howard, J. (1999). Kinesin's tail domain is an inhibitory regulator of the motor domain. Nat Cell Biol 1, 288-292.

Cremer, H., Lange, R., Christoph, A., Plomann, M., Vopper, G., Roes, J., Brown, R., Baldwin, S., Kraemer, P., Scheff, S., and et al. (1994). Inactivation of the N-CAM gene in mice results in size reduction of the olfactory bulb and deficits in spatial learning. Nature 367, 455-459.

Crowley, C., Spencer, S. D., Nishimura, M. C., Chen, K. S., Pitts-Meek, S., Armanini, M. P., Ling, L. H., McMahon, S. B., Shelton, D. L., Levinson, A. D., and et al. (1994). Mice lacking nerve growth factor display perinatal loss of sensory and sympathetic neurons yet develop basal forebrain cholinergic neurons. Cell 76, 1001-1011.

Dahme, M., Bartsch, U., Martini, R., Anliker, B., Schachner, M., and Mantei, N. (1997). Disruption of the mouse L1 gene leads to malformations of the nervous system. Nat Genet 17, 346-349.

Dalva, M. B., Takasu, M. A., Lin, M. Z., Shamah, S. M., Hu, L., Gale, N. W., and Greenberg, M. E. (2000). EphB receptors interact with NMDA receptors and regulate excitatory synapse formation. Cell 103, 945-956.

Daniels, S. B., McCarron, M., Love, C., and Chovnick, A. (1985). Dysgenesis-induced instability of rosy locus transformation in Drosophila melanogaster: analysis of excision events and the selective recovery of control element deletions. Genetics 109, 95-117.

Das, A. K., Cohen, P. W., and Barford, D. (1998). The structure of the tetratricopeptide repeats of protein phosphatase 5: implications for TPR-mediated protein-protein interactions. Embo J 17, 1192-1199.

Davies, A. M., Lee, K. F., and Jaenisch, R. (1993). p75-deficient trigeminal sensory neurons have an altered response to NGF but not to other neurotrophins. Neuron 11, 565-574.

Davis, R. J. (2000). Signal transduction by the JNK group of MAP kinases. Cell 103, 239-252.

Davy, A., Gale, N. W., Murray, E. W., Klinghoffer, R. A., Soriano, P., Feuerstein, C., and Robbins, S. M. (1999). Compartmentalized signaling by GPI-anchored ephrin-A5 requires the Fyn tyrosine kinase to regulate cellular adhesion. Genes Dev 13, 3125-3135.

De Vos, K., Severin, F., Van Herreweghe, F., Vancompernolle, K., Goossens, V., Hyman, A., and Grooten, J. (2000). Tumor necrosis factor induces hyperphosphorylation of kinesin light chain and inhibits kinesin-mediated transport of mitochondria. J Cell Biol 149, 1207-1214.

Deacon, S. W., Serpinskaya, A. S., Vaughan, P. S., Lopez Fanarraga, M., Vernos, I., Vaughan, K. T., and Gelfand, V. I. (2003). Dynactin is required for bidirectional organelle transport. J Cell Biol 160, 297-301.

Debant, A., Serra-Pages, C., Seipel, K., O'Brien, S., Tang, M., Park, S. H., and Streuli, M. (1996). The multidomain protein Trio binds the LAR transmembrane tyrosine phosphatase, contains a protein kinase domain, and has separate rac-specific and rho-specific guanine nucleotide exchange factor domains. Proc Natl Acad Sci U S A 93, 5466-5471.

Dehal, P., Satou, Y., Campbell, R. K., Chapman, J., Degnan, B., De Tomaso, A., Davidson, B., Di Gregorio, A., Gelpke, M., Goodstein, D. M., et al. (2002). The draft genome of Ciona intestinalis: insights into chordate and vertebrate origins. Science 298, 2157-2167.

Deinhardt, K., Salinas, S., Verastegui, C., Watson, R., Worth, D., Hanrahan, S., Bucci, C., and Schiavo, G. (2006). Rab5 and Rab7 control endocytic sorting along the axonal retrograde transport pathway. Neuron 52, 293-305.

Delcroix, J. D., Valletta, J. S., Wu, C., Hunt, S. J., Kowal, A. S., and Mobley, W. C. (2003). NGF signaling in sensory neurons: evidence that early endosomes carry NGF retrograde signals. Neuron 39, 69-84.

Demyanenko, G. P., Tsai, A. Y., and Maness, P. F. (1999). Abnormalities in neuronal process extension, hippocampal development, and the ventricular system of L1 knockout mice. J Neurosci 19, 4907-4920.

Diefenbach, R. J., Diefenbach, E., Douglas, M. W., and Cunningham, A. L. (2002). The heavy chain of conventional kinesin interacts with the SNARE proteins SNAP25 and SNAP23. Biochemistry 41, 14906-14915.

Diefenbach, R. J., Diefenbach, E., Douglas, M. W., and Cunningham, A. L. (2004). The ribosome receptor, p180, interacts with kinesin heavy chain, KIF5B. Biochem Biophys Res Commun 319, 987-992.

Dong, H., O'Brien, R. J., Fung, E. T., Lanahan, A. A., Worley, P. F., and Huganir, R. L. (1997). GRIP: a synaptic PDZ domain-containing protein that interacts with AMPA receptors. Nature 386, 279-284.

Donovan, M. J., Hahn, R., Tessarollo, L., and Hempstead, B. L. (1996). Identification of an essential nonneuronal function of neurotrophin 3 in mammalian cardiac development. Nat Genet 14, 210-213.

Dottori, M., Hartley, L., Galea, M., Paxinos, G., Polizzotto, M., Kilpatrick, T., Bartlett, P. F., Murphy, M., Kontgen, F., and Boyd, A. W. (1998). EphA4 (Sek1) receptor tyrosine kinase is required for the development of the corticospinal tract. Proc Natl Acad Sci U S A 95, 13248-13253.

Dowling, P., Ming, X., Raval, S., Husar, W., Casaccia-Bonnefil, P., Chao, M., Cook, S., and Blumberg, B. (1999). Up-regulated p75NTR neurotrophin receptor on glial cells in MS plaques. Neurology 53, 1676-1682.

Dragatsis, I., and Zeitlin, S. (2000). CaMKIIalpha-Cre transgene expression and recombination patterns in the mouse brain. Genesis 26, 133-135.

Drescher, U. (2002). Eph family functions from an evolutionary perspective. Curr Opin Genet Dev 12, 397-402.

Drescher, U., Kremoser, C., Handwerker, C., Loschinger, J., Noda, M., and Bonhoeffer, F. (1995). In vitro guidance of retinal ganglion cell axons by RAGS, a 25 kDa tectal protein related to ligands for Eph receptor tyrosine kinases. Cell 82, 359-370.

Ebens, A., Brose, K., Leonardo, E. D., Hanson, M. G., Jr., Bladt, F., Birchmeier, C., Barres, B. A., and Tessier-Lavigne, M. (1996). Hepatocyte growth

factor/scatter factor is an axonal chemoattractant and a neurotrophic factor for spinal motor neurons. Neuron 17, 1157-1172.

Eberhart, J., Swartz, M. E., Koblar, S. A., Pasquale, E. B., and Krull, C. E. (2002). EphA4 constitutes a population-specific guidance cue for motor neurons. Dev Biol 247, 89-101.

Echelard, Y., Vassileva, G., and McMahon, A. P. (1994). Cis-acting regulatory sequences governing Wnt-1 expression in the developing mouse CNS. Development 120, 2213-2224.

Elowe, S., Holland, S. J., Kulkarni, S., and Pawson, T. (2001). Downregulation of the Ras-mitogen-activated protein kinase pathway by the EphB2 receptor tyrosine kinase is required for ephrin-induced neurite retraction. Mol Cell Biol 21, 7429-7441.

Engels, W. R. (1984). A trans-acting product needed for P factor transposition in Drosophila. Science 226, 1194-1196.

Ernfors, P., Henschen, A., Olson, L., and Persson, H. (1989). Expression of nerve growth factor receptor mRNA is developmentally regulated and increased after axotomy in rat spinal cord motoneurons. Neuron 2, 1605-1613.

Ernfors, P., Lee, K. F., and Jaenisch, R. (1994a). Mice lacking brain-derived neurotrophic factor develop with sensory deficits. Nature 368, 147-150.

Ernfors, P., Lee, K. F., Kucera, J., and Jaenisch, R. (1994b). Lack of neurotrophin-3 leads to deficiencies in the peripheral nervous system and loss of limb proprioceptive afferents. Cell 77, 503-512.

Estrach, S., Schmidt, S., Diriong, S., Penna, A., Blangy, A., Fort, P., and Debant, A. (2002). The Human Rho-GEF trio and its target GTPase RhoG are involved in the NGF pathway, leading to neurite outgrowth. Curr Biol 12, 307-312.

Ethell, I. M., Irie, F., Kalo, M. S., Couchman, J. R., Pasquale, E. B., and Yamaguchi, Y. (2001). EphB/syndecan-2 signaling in dendritic spine morphogenesis. Neuron 31, 1001-1013.

Farinas, I., Yoshida, C. K., Backus, C., and Reichardt, L. F. (1996). Lack of neurotrophin-3 results in death of spinal sensory neurons and premature differentiation of their precursors. Neuron 17, 1065-1078.

Feldheim, D. A., Kim, Y. I., Bergemann, A. D., Frisen, J., Barbacid, M., and Flanagan, J. G. (2000). Genetic analysis of ephrin-A2 and ephrin-A5 shows their requirement in multiple aspects of retinocollicular mapping. Neuron 25, 563-574.

Fields, S., and Song, O. (1989). A novel genetic system to detect protein-protein interactions. Nature 340, 245-246.

Flanagan, J. G., and Vanderhaeghen, P. (1998). The ephrins and Eph receptors in neural development. Annu Rev Neurosci 21, 309-345.

Flenniken, A. M., Gale, N. W., Yancopoulos, G. D., and Wilkinson, D. G. (1996). Distinct and overlapping expression patterns of ligands for Eph-related receptor tyrosine kinases during mouse embryogenesis. Dev Biol 179, 382-401.

Foletti, D. L., Prekeris, R., and Scheller, R. H. (1999). Generation and maintenance of neuronal polarity: mechanisms of transport and targeting. Neuron 23, 641-644.

Forsthoefel, D. J., Liebl, E. C., Kolodziej, P. A., and Seeger, M. A. (2005). The Abelson tyrosine kinase, the Trio GEF and Enabled interact with the Netrin receptor Frazzled in Drosophila. Development 132, 1983-1994.

Fransen, E., D'Hooge, R., Van Camp, G., Verhoye, M., Sijbers, J., Reyniers, E., Soriano, P., Kamiguchi, H., Willemsen, R., Koekkoek, S. K., et al. (1998). L1 knockout mice show dilated ventricles, vermis hypoplasia and impaired exploration patterns. Hum Mol Genet 7, 999-1009.

Friedman, D. S., and Vale, R. D. (1999). Single-molecule analysis of kinesin motility reveals regulation by the cargo-binding tail domain. Nat Cell Biol 1, 293-297.

Frischknecht, F., Moreau, V., Rottger, S., Gonfloni, S., Reckmann, I., Superti-Furga, G., and Way, M. (1999). Actin-based motility of vaccinia virus mimics receptor tyrosine kinase signalling. Nature 401, 926-929.

Fujita, T., Maturana, A. D., Ikuta, J., Hamada, J., Walchli, S., Suzuki, T., Sawa, H., Wooten, M. W., Okajima, T., Tatematsu, K., et al. (2007). Axonal guidance protein FEZ1 associates with tubulin and kinesin motor protein to transport mitochondria in neurites of NGF-stimulated PC12 cells. Biochem Biophys Res Commun 361, 605-610.

Gale, N. W., Holland, S. J., Valenzuela, D. M., Flenniken, A., Pan, L., Ryan, T. E., Henkemeyer, M., Strebhardt, K., Hirai, H., Wilkinson, D. G., et al. (1996). Eph receptors and ligands comprise two major specificity subclasses and are reciprocally compartmentalized during embryogenesis. Neuron 17, 9-19.

Gascon, E., Vutskits, L., Jenny, B., Durbec, P., and Kiss, J. Z. (2007). PSA-NCAM in postnatally generated immature neurons of the olfactory bulb: a crucial role in regulating p75 expression and cell survival. Development 134, 1181-1190.

Gatto, G. J., Jr., Geisbrecht, B. V., Gould, S. J., and Berg, J. M. (2000). Peroxisomal targeting signal-1 recognition by the TPR domains of human PEX5. Nat Struct Biol 7, 1091-1095.

George, S. E., Simokat, K., Hardin, J., and Chisholm, A. D. (1998). The VAB-1 Eph receptor tyrosine kinase functions in neural and epithelial morphogenesis in C. elegans. Cell 92, 633-643.

Gerety, S. S., Wang, H. U., Chen, Z. F., and Anderson, D. J. (1999). Symmetrical mutant phenotypes of the receptor EphB4 and its specific transmembrane ligand ephrin-B2 in cardiovascular development. Mol Cell 4, 403-414.

Gertler, F. B., Bennett, R. L., Clark, M. J., and Hoffmann, F. M. (1989). Drosophila abl tyrosine kinase in embryonic CNS axons: a role in axonogenesis is revealed through dosage-sensitive interactions with disabled. Cell 58, 103-113.

Ghanekar, Y., and Lowe, M. (2005). Protein kinase D: activation for Golgi carrier formation. Trends Cell Biol 15, 511-514.

Gho, M., McDonald, K., Ganetzky, B., and Saxton, W. M. (1992). Effects of kinesin mutations on neuronal functions. Science 258, 313-316.

Gindhart, J. G., Jr., Desai, C. J., Beushausen, S., Zinn, K., and Goldstein, L. S. (1998). Kinesin light chains are essential for axonal transport in Drosophila. J Cell Biol 141, 443-454.

Gindhart, J. G., Jr., and Goldstein, L. S. (1996). Tetratrico peptide repeats are present in the kinesin light chain. Trends Biochem Sci 21, 52-53.

Ginty, D. D., Bonni, A., and Greenberg, M. E. (1994). Nerve growth factor activates a Ras-dependent protein kinase that stimulates c-fos transcription via phosphorylation of CREB. Cell 77, 713-725.

Ginty, D. D., and Segal, R. A. (2002). Retrograde neurotrophin signaling: Trk-ing along the axon. Curr Opin Neurobiol 12, 268-274.

Glater, E. E., Megeath, L. J., Stowers, R. S., and Schwarz, T. L. (2006). Axonal transport of mitochondria requires milton to recruit kinesin heavy chain and is light chain independent. J Cell Biol 173, 545-557.

Goldstein, L. S., and Yang, Z. (2000). Microtubule-based transport systems in neurons: the roles of kinesins and dyneins. Annu Rev Neurosci 23, 39-71.

Greenspan, R. J. (2004). Fly Pushing - The Theory and Practise of Drosophila Genetics, second edition edn (New York: CSHL Press).

Gregory, S. G., Sekhon, M., Schein, J., Zhao, S., Osoegawa, K., Scott, C. E., Evans, R. S., Burridge, P. W., Cox, T. V., Fox, C. A., et al. (2002). A physical map of the mouse genome. Nature 418, 743-750.

Gross, S. P., Welte, M. A., Block, S. M., and Wieschaus, E. F. (2002). Coordination of opposite-polarity microtubule motors. J Cell Biol 156, 715-724.

Grunwald, I. C., Korte, M., Wolfer, D., Wilkinson, G. A., Unsicker, K., Lipp, H. P., Bonhoeffer, T., and Klein, R. (2001). Kinase-independent requirement of EphB2 receptors in hippocampal synaptic plasticity. Neuron 32, 1027-1040.

Gu, C., Jan, Y. N., and Jan, L. Y. (2003). A conserved domain in axonal targeting of Kv1 (Shaker) voltage-gated potassium channels. Science 301, 646-649.

Gudkov, A. V., Kazarov, A. R., Thimmapaya, R., Axenovich, S. A., Mazo, I. A., and Roninson, I. B. (1994). Cloning mammalian genes by expression selection of genetic suppressor elements: association of kinesin with drug resistance and cell immortalization. Proc Natl Acad Sci U S A 91, 3744-3748.

Gyoeva, F. K., Bybikova, E. M., and Minin, A. A. (2000). An isoform of kinesin light chain specific for the Golgi complex. J Cell Sci 113 (Pt 11), 2047-2054.

Hallbook, F., Lundin, L. G., and Kullander, K. (1998). Lampetra fluviatilis neurotrophin homolog, descendant of a neurotrophin ancestor, discloses the early molecular evolution of neurotrophins in the vertebrate subphylum. J Neurosci 18, 8700-8711.

Hamburger, V. (1975). Cell death in the development of the lateral motor column of the chick embryo. J Comp Neurol 160, 535-546.

Hapner, S. J., Boeshore, K. L., Large, T. H., and Lefcort, F. (1998). Neural differentiation promoted by truncated trkC receptors in collaboration with p75(NTR). Dev Biol 201, 90-100.

Hay, B. A., Maile, R., and Rubin, G. M. (1997). P element insertion-dependent gene activation in the Drosophila eye. Proc Natl Acad Sci U S A 94, 5195-5200.

Hay, B. A., Wolff, T., and Rubin, G. M. (1994). Expression of baculovirus P35 prevents cell death in Drosophila. Development 120, 2121-2129.

Heerssen, H. M., Pazyra, M. F., and Segal, R. A. (2004). Dynein motors transport activated Trks to promote survival of target-dependent neurons. Nat Neurosci 7, 596-604.

Heerssen, H. M., and Segal, R. A. (2002). Location, location, location: a spatial view of neurotrophin signal transduction. Trends Neurosci 25, 160-165.

Helmbacher, F., Schneider-Maunoury, S., Topilko, P., Tiret, L., and Charnay, P. (2000). Targeting of the EphA4 tyrosine kinase receptor affects dorsal/ventral pathfinding of limb motor axons. Development 127, 3313-3324.

Henderson, C. E., Camu, W., Mettling, C., Gouin, A., Poulsen, K., Karihaloo, M., Rullamas, J., Evans, T., McMahon, S. B., Armanini, M. P., and et al. (1993). Neurotrophins promote motor neuron survival and are present in embryonic limb bud. Nature 363, 266-270.

Henkemeyer, M., Itkis, O. S., Ngo, M., Hickmott, P. W., and Ethell, I. M. (2003). Multiple EphB receptor tyrosine kinases shape dendritic spines in the hippocampus. J Cell Biol 163, 1313-1326.

Henkemeyer, M., Orioli, D., Henderson, J. T., Saxton, T. M., Roder, J., Pawson, T., and Klein, R. (1996). Nuk controls pathfinding of commissural axons in the mammalian central nervous system. Cell 86, 35-46.

Heumann, R., Schwab, M., and Thoenen, H. (1981). A second messenger required for nerve growth factor biological activity? Nature 292, 838-840.

Hidalgo, A. (2002). Interactive nervous system development: control of cell survival in Drosophila. Trends Neurosci 25, 365-370.

Higgins, C. F., Gallagher, M. P., Mimmack, M. L., and Pearce, S. R. (1988). A family of closely related ATP-binding subunits from prokaryotic and eukaryotic cells. Bioessays 8, 111-116.

Higuchi, H., Yamashita, T., Yoshikawa, H., and Tohyama, M. (2003). PKA phosphorylates the p75 receptor and regulates its localization to lipid rafts. Embo J 22, 1790-1800.

Hirai, H., Maru, Y., Hagiwara, K., Nishida, J., and Takaku, F. (1987). A novel putative tyrosine kinase receptor encoded by the eph gene. Science 238, 1717-1720.

Hirokawa, N., and Takemura, R. (2004). Molecular motors in neuronal development, intracellular transport and diseases. Curr Opin Neurobiol 14, 564-573.

Hirokawa, N., and Takemura, R. (2005). Molecular motors and mechanisms of directional transport in neurons. Nat Rev Neurosci 6, 201-214.

Holland, S. J., Gale, N. W., Mbamalu, G., Yancopoulos, G. D., Henkemeyer, M., and Pawson, T. (1996). Bidirectional signalling through the EPH-family receptor Nuk and its transmembrane ligands. Nature 383, 722-725.

Hollenbeck, P. J. (1989). The distribution, abundance and subcellular localization of kinesin. J Cell Biol 108, 2335-2342.

Hollenbeck, P. J. (1993). Phosphorylation of neuronal kinesin heavy and light chains in vivo. J Neurochem 60, 2265-2275.

Homma, N., Takei, Y., Tanaka, Y., Nakata, T., Terada, S., Kikkawa, M., Noda, Y., and Hirokawa, N. (2003). Kinesin superfamily protein 2A (KIF2A) functions in suppression of collateral branch extension. Cell 114, 229-239.

Hoogenraad, C. C., Milstein, A. D., Ethell, I. M., Henkemeyer, M., and Sheng, M. (2005). GRIP1 controls dendrite morphogenesis by regulating EphB receptor trafficking. Nat Neurosci 8, 906-915.

Horiguchi, K., Hanada, T., Fukui, Y., and Chishti, A. H. (2006). Transport of PIP3 by GAKIN, a kinesin-3 family protein, regulates neuronal cell polarity. J Cell Biol 174, 425-436.

Howe, C. L., and Mobley, W. C. (2004). Signaling endosome hypothesis: A cellular mechanism for long distance communication. J Neurobiol 58, 207-216.

Howe, C. L., Valletta, J. S., Rusnak, A. S., and Mobley, W. C. (2001). NGF signaling from clathrin-coated vesicles: evidence that signaling endosomes serve as a platform for the Ras-MAPK pathway. Neuron 32, 801-814.

Hu, H., Tomasiewicz, H., Magnuson, T., and Rutishauser, U. (1996). The role of polysialic acid in migration of olfactory bulb interneuron precursors in the subventricular zone. Neuron 16, 735-743.

Huang, C. S., Zhou, J., Feng, A. K., Lynch, C. C., Klumperman, J., DeArmond, S. J., and Mobley, W. C. (1999). Nerve growth factor signaling in caveolae-like domains at the plasma membrane. J Biol Chem 274, 36707-36714.

Huang, E. J., and Reichardt, L. F. (2003). Trk receptors: roles in neuronal signal transduction. Annu Rev Biochem 72, 609-642.

Hurd, D. D., and Saxton, W. M. (1996). Kinesin mutations cause motor neuron disease phenotypes by disrupting fast axonal transport in Drosophila. Genetics 144, 1075-1085.

Ichimura, T., Wakamiya-Tsuruta, A., Itagaki, C., Taoka, M., Hayano, T., Natsume, T., and Isobe, T. (2002). Phosphorylation-dependent interaction of kinesin light chain 2 and the 14-3-3 protein. Biochemistry 41, 5566-5572.

Iglesias, T., Cabrera-Poch, N., Mitchell, M. P., Naven, T. J., Rozengurt, E., and Schiavo, G. (2000). Identification and cloning of Kidins220, a novel neuronal substrate of protein kinase D. J Biol Chem 275, 40048-40056.

Ikuta, J., Maturana, A., Fujita, T., Okajima, T., Tatematsu, K., Tanizawa, K., and Kuroda, S. (2007). Fasciculation and elongation protein zeta-1 (FEZ1) participates in the polarization of hippocampal neuron by controlling the mitochondrial motility. Biochem Biophys Res Commun 353, 127-132.

Inomata, H., Nakamura, Y., Hayakawa, A., Takata, H., Suzuki, T., Miyazawa, K., and Kitamura, N. (2003). A scaffold protein JIP-1b enhances amyloid precursor protein phosphorylation by JNK and its association with kinesin light chain 1. J Biol Chem 278, 22946-22955.

Irie, F., and Yamaguchi, Y. (2002). EphB receptors regulate dendritic spine development via intersectin, Cdc42 and N-WASP. Nat Neurosci 5, 1117-1118.

Itoh, K., Cheng, L., Kamei, Y., Fushiki, S., Kamiguchi, H., Gutwein, P., Stoeck, A., Arnold, B., Altevogt, P., and Lemmon, V. (2004). Brain development in mice lacking L1-L1 homophilic adhesion. J Cell Biol 165, 145-154.

Iwasato, T., Katoh, H., Nishimaru, H., Ishikawa, Y., Inoue, H., Saito, Y. M., Ando, R., Iwama, M., Takahashi, R., Negishi, M., and Itohara, S. (2007). Rac-GAP alpha-chimerin regulates motor-circuit formation as a key mediator of EphrinB3/EphA4 forward signaling. Cell 130, 742-753.

Jaaro, H., Beck, G., Conticello, S. G., and Fainzilber, M. (2001). Evolving better brains: a need for neurotrophins? Trends Neurosci 24, 79-85.

Jacobson, C., Schnapp, B., and Banker, G. A. (2006). A change in the selective translocation of the Kinesin-1 motor domain marks the initial specification of the axon. Neuron 49, 797-804.

Jeon, B. S., Kholodilov, N. G., Oo, T. F., Kim, S. Y., Tomaselli, K. J., Srinivasan, A., Stefanis, L., and Burke, R. E. (1999). Activation of caspase-3 in developmental models of programmed cell death in neurons of the substantia nigra. J Neurochem 73, 322-333.

Jones, K. R., Farinas, I., Backus, C., and Reichardt, L. F. (1994). Targeted disruption of the BDNF gene perturbs brain and sensory neuron development but not motor neuron development. Cell 76, 989-999.

Junco, A., Bhullar, B., Tarnasky, H. A., and van der Hoorn, F. A. (2001). Kinesin light-chain KLC3 expression in testis is restricted to spermatids. Biol Reprod 64, 1320-1330.

Jungbluth, S., Koentges, G., and Lumsden, A. (1997). Coordination of early neural tube development by BDNF/trkB. Development 124, 1877-1885.

Kalil, K., and Dent, E. W. (2005). Touch and go: guidance cues signal to the growth cone cytoskeleton. Curr Opin Neurobiol 15, 521-526.

Kamal, A., Almenar-Queralt, A., LeBlanc, J. F., Roberts, E. A., and Goldstein, L. S. (2001). Kinesin-mediated axonal transport of a membrane compartment containing beta-secretase and presenilin-1 requires APP. Nature 414, 643-648.

Kamal, A., Stokin, G. B., Yang, Z., Xia, C. H., and Goldstein, L. S. (2000). Axonal transport of amyloid precursor protein is mediated by direct binding to the kinesin light chain subunit of kinesin-I. Neuron 28, 449-459.

Kamm, C., Boston, H., Hewett, J., Wilbur, J., Corey, D. P., Hanson, P. I., Ramesh, V., and Breakefield, X. O. (2004). The early onset dystonia protein torsinA interacts with kinesin light chain 1. J Biol Chem 279, 19882-19892.

Kanai, Y., Dohmae, N., and Hirokawa, N. (2004). Kinesin transports RNA: isolation and characterization of an RNA-transporting granule. Neuron 43, 513-525.

Kanai, Y., Okada, Y., Tanaka, Y., Harada, A., Terada, S., and Hirokawa, N. (2000). KIF5C, a novel neuronal kinesin enriched in motor neurons. J Neurosci 20, 6374-6384.

Karcher, R. L., Deacon, S. W., and Gelfand, V. I. (2002). Motor-cargo interactions: the key to transport specificity. Trends Cell Biol 12, 21-27.

Karcher, R. L., Roland, J. T., Zappacosta, F., Huddleston, M. J., Annan, R. S., Carr, S. A., and Gelfand, V. I. (2001). Cell cycle regulation of myosin-V by calcium/calmodulin-dependent protein kinase II. Science 293, 1317-1320.

Katoh, H., Yasui, H., Yamaguchi, Y., Aoki, J., Fujita, H., Mori, K., and Negishi, M. (2000). Small GTPase RhoG is a key regulator for neurite outgrowth in PC12 cells. Mol Cell Biol 20, 7378-7387.

Kawano, Y., Yoshimura, T., Tsuboi, D., Kawabata, S., Kaneko-Kawano, T., Shirataki, H., Takenawa, T., and Kaibuchi, K. (2005). CRMP-2 is involved in kinesin-1-dependent transport of the Sra-1/WAVE1 complex and axon formation. Mol Cell Biol 25, 9920-9935.

Kay, B. K., Williamson, M. P., and Sudol, M. (2000). The importance of being proline: the interaction of proline-rich motifs in signaling proteins with their cognate domains. Faseb J 14, 231-241.

Keller, G. (2005). Embryonic stem cell differentiation: emergence of a new era in biology and medicine. Genes Dev 19, 1129-1155.

Kernie, S. G., Liebl, D. J., and Parada, L. F. (2000). BDNF regulates eating behavior and locomotor activity in mice. Embo J 19, 1290-1300.

Khodjakov, A., Lizunova, E. M., Minin, A. A., Koonce, M. P., and Gyoeva, F. K. (1998). A specific light chain of kinesin associates with mitochondria in cultured cells. Mol Biol Cell 9, 333-343.

Kidwell, M. G., Kidwell, J. F., and Sved, J. A. (1977). Hybrid Dysgenesis in DROSOPHILA MELANOGASTER: A Syndrome of Aberrant Traits Including Mutation, Sterility and Male Recombination. Genetics 86, 813-833.

Kimura, T., Watanabe, H., Iwamatsu, A., and Kaibuchi, K. (2005). Tubulin and CRMP-2 complex is transported via Kinesin-1. J Neurochem 93, 1371-1382.

Kirby, M. L., and Waldo, K. L. (1995). Neural crest and cardiovascular patterning. Circ Res 77, 211-215.

Kleene, R., and Schachner, M. (2004). Glycans and neural cell interactions. Nat Rev Neurosci 5, 195-208.

Klein, R., Silos-Santiago, I., Smeyne, R. J., Lira, S. A., Brambilla, R., Bryant, S., Zhang, L., Snider, W. D., and Barbacid, M. (1994). Disruption of the neurotrophin-3 receptor gene trkC eliminates la muscle afferents and results in abnormal movements. Nature 368, 249-251.

Klein, R., Smeyne, R. J., Wurst, W., Long, L. K., Auerbach, B. A., Joyner, A. L., and Barbacid, M. (1993). Targeted disruption of the trkB neurotrophin receptor gene results in nervous system lesions and neonatal death. Cell 75, 113-122.

Knippschild, U., Gocht, A., Wolff, S., Huber, N., Lohler, J., and Stoter, M. (2005). The casein kinase 1 family: participation in multiple cellular processes in eukaryotes. Cell Signal 17, 675-689.

Koch, A., Mancini, A., Stefan, M., Niedenthal, R., Niemann, H., and Tamura, T. (2000). Direct interaction of nerve growth factor receptor, TrkA, with non-receptor tyrosine kinase, c-Abl, through the activation loop. FEBS Lett 469, 72-76.

Koliatsos, V. E., Clatterbuck, R. E., Winslow, J. W., Cayouette, M. H., and Price, D. L. (1993). Evidence that brain-derived neurotrophic factor is a trophic factor for motor neurons in vivo. Neuron 10, 359-367.

Konecna, A., Frischknecht, R., Kinter, J., Ludwig, A., Steuble, M., Meskenaite, V., Indermuhle, M., Engel, M., Cen, C., Mateos, J. M., et al. (2006). Calsyntenin-1 docks vesicular cargo to kinesin-1. Mol Biol Cell 17, 3651-3663.

Kong, H., Boulter, J., Weber, J. L., Lai, C., and Chao, M. V. (2001). An evolutionarily conserved transmembrane protein that is a novel downstream target of neurotrophin and ephrin receptors. J Neurosci 21, 176-185.

Korte, M., Carroll, P., Wolf, E., Brem, G., Thoenen, H., and Bonhoeffer, T. (1995). Hippocampal long-term potentiation is impaired in mice lacking brain-derived neurotrophic factor. Proc Natl Acad Sci U S A 92, 8856-8860.

Kramarcy, N. R., and Sealock, R. (2000). Syntrophin isoforms at the neuromuscular junction: developmental time course and differential localization. Mol Cell Neurosci 15, 262-274.

Krause, M., Dent, E. W., Bear, J. E., Loureiro, J. J., and Gertler, F. B. (2003). Ena/VASP proteins: regulators of the actin cytoskeleton and cell migration. Annu Rev Cell Dev Biol 19, 541-564.

Kruger, R. P., Aurandt, J., and Guan, K. L. (2005). Semaphorins command cells to move. Nat Rev Mol Cell Biol 6, 789-800.

Kullander, K., Croll, S. D., Zimmer, M., Pan, L., McClain, J., Hughes, V., Zabski, S., DeChiara, T. M., Klein, R., Yancopoulos, G. D., and Gale, N. W. (2001). Ephrin-B3 is the midline barrier that prevents corticospinal tract axons from recrossing, allowing for unilateral motor control. Genes Dev 15, 877-888.

Kullander, K., and Klein, R. (2002). Mechanisms and functions of Eph and ephrin signalling. Nat Rev Mol Cell Biol 3, 475-486.

Kuruvilla, R., Ye, H., and Ginty, D. D. (2000). Spatially and functionally distinct roles of the PI3-K effector pathway during NGF signaling in sympathetic neurons. Neuron 27, 499-512.

Lallemand, Y., Luria, V., Haffner-Krausz, R., and Lonai, P. (1998). Maternally expressed PGK-Cre transgene as a tool for early and uniform activation of the Cre site-specific recombinase. Transgenic Res 7, 105-112.

Lalli, G., Herreros, J., Osborne, S. L., Montecucco, C., Rossetto, R., and Schiavo, G. (1999). Functional characterisation of tetanus and botulinum neurotoxins binding domains. J Cell Sci 112, 2715-2724.

Landmesser, L. (1978). The distribution of motoneurones supplying chick hind limb muscles. J Physiol 284, 371-389.

Lapouge, K., Smith, S. J., Walker, P. A., Gamblin, S. J., Smerdon, S. J., and Rittinger, K. (2000). Structure of the TPR domain of p67phox in complex with Rac.GTP. Mol Cell 6, 899-907.

Lee, F. S., Kim, A. H., Khursigara, G., and Chao, M. V. (2001). The uniqueness of being a neurotrophin receptor. Curr Opin Neurobiol 11, 281-286.

Lee, K. D., and Hollenbeck, P. J. (1995). Phosphorylation of kinesin in vivo correlates with organelle association and neurite outgrowth. J Biol Chem 270, 5600-5605.

Lee, K. F., Davies, A. M., and Jaenisch, R. (1994). p75-deficient embryonic dorsal root sensory and neonatal sympathetic neurons display a decreased sensitivity to NGF. Development 120, 1027-1033.

Lee, K. F., Li, E., Huber, L. J., Landis, S. C., Sharpe, A. H., Chao, M. V., and Jaenisch, R. (1992). Targeted mutation of the gene encoding the low affinity NGF receptor p75 leads to deficits in the peripheral sensory nervous system. Cell 69, 737-749.

Lee, Y. S., and Carthew, R. W. (2003). Making a better RNAi vector for Drosophila: use of intron spacers. Methods 30, 322-329.

Lefebvre, L., Dionne, N., Karaskova, J., Squire, J. A., and Nagy, A. (2001). Selection for transgene homozygosity in embryonic stem cells results in extensive loss of heterozygosity. Nat Genet 27, 257-258.

Leonard, L., Horton, C., Maden, M., and Pizzey, J. A. (1995). Anteriorization of CRABP-I expression by retinoic acid in the developing mouse central nervous system and its relationship to teratogenesis. Dev Biol 168, 514-528.

Li, J., Mahajan, A., and Tsai, M. D. (2006). Ankyrin repeat: a unique motif mediating protein-protein interactions. Biochemistry 45, 15168-15178.

Liebl, D. J., Mbiene, J. P., and Parada, L. F. (1999). NT4/5 mutant mice have deficiency in gustatory papillae and taste bud formation. Dev Biol 213, 378-389.

Liebl, E. C., Forsthoefel, D. J., Franco, L. S., Sample, S. H., Hess, J. E., Cowger, J. A., Chandler, M. P., Shupert, A. M., and Seeger, M. A. (2000). Dosage-sensitive, reciprocal genetic interactions between the Abl tyrosine kinase and the putative GEF trio reveal trio's role in axon pathfinding. Neuron 26, 107-118.

Lin, D. C., Quevedo, C., Brewer, N. E., Bell, A., Testa, J. R., Grimes, M. L., Miller, F. D., and Kaplan, D. R. (2006). APPL1 associates with TrkA and GIPC1 and is required for nerve growth factor-mediated signal transduction. Mol Cell Biol 26, 8928-8941.

Ling, S. C., Fahrner, P. S., Greenough, W. T., and Gelfand, V. I. (2004). Transport of Drosophila fragile X mental retardation protein-containing

ribonucleoprotein granules by kinesin-1 and cytoplasmic dynein. Proc Natl Acad Sci U S A 101, 17428-17433.

Litchfield, D. W. (2003). Protein kinase CK2: structure, regulation and role in cellular decisions of life and death. Biochem J 369, 1-15.

Liu, P., Ying, Y., Ko, Y. G., and Anderson, R. G. (1996). Localization of platelet-derived growth factor-stimulated phosphorylation cascade to caveolae. J Biol Chem 271, 10299-10303.

Liu, X., Ernfors, P., Wu, H., and Jaenisch, R. (1995). Sensory but not motor neuron deficits in mice lacking NT4 and BDNF. Nature 375, 238-241.

Lotto, R. B., Asavaritikrai, P., Vali, L., and Price, D. J. (2001). Target-derived neurotrophic factors regulate the death of developing forebrain neurons after a change in their trophic requirements. J Neurosci 21, 3904-3910.

Lou, X., Yano, H., Lee, F., Chao, M. V., and Farquhar, M. G. (2001). GIPC and GAIP form a complex with TrkA: a putative link between G protein and receptor tyrosine kinase pathways. Mol Biol Cell 12, 615-627.

Lu, Q., Sun, E. E., Klein, R. S., and Flanagan, J. G. (2001). Ephrin-B reverse signaling is mediated by a novel PDZ-RGS protein and selectively inhibits G protein-coupled chemoattraction. Cell 105, 69-79.

Luo, S., Chen, Y., Lai, K. O., Arevalo, J. C., Froehner, S. C., Adams, M. E., Chao, M. V., and Ip, N. Y. (2005). α-Syntrophin regulates ARMS localization at the neuromuscular junction and enhances EphA4 signaling in an ARMS-dependent manner. J Cell Biol 169, 813-824.

Luskin, M. B. (1993). Restricted proliferation and migration of postnatally generated neurons derived from the forebrain subventricular zone. Neuron 11, 173-189.

Luukko, K., Moshnyakov, M., Sainio, K., Saarma, M., Sariola, H., and Thesleff, I. (1996). Expression of neurotrophin receptors during rat tooth development is developmentally regulated, independent of innervation, and suggests functions in the regulation of morphogenesis and innervation. Dev Dyn 206, 87-99.

Ma, Q., Fode, C., Guillemot, F., and Anderson, D. J. (1999). Neurogenin1 and neurogenin2 control two distinct waves of neurogenesis in developing dorsal root ganglia. Genes Dev 13, 1717-1728.

Ma, S., and Chisholm, R. L. (2002). Cytoplasmic dynein-associated structures move bidirectionally in vivo. J Cell Sci 115, 1453-1460.

MacDonald, J. I., Gryz, E. A., Kubu, C. J., Verdi, J. M., and Meakin, S. O. (2000). Direct binding of the signaling adapter protein Grb2 to the activation loop tyrosines on the nerve growth factor receptor tyrosine kinase, TrkA. J Biol Chem 275, 18225-18233.

MacInnis, B. L., and Campenot, R. B. (2002). Retrograde support of neuronal survival without retrograde transport of nerve growth factor. Science 295, 1536-1539.

Macioce, P., Gambara, G., Bernassola, M., Gaddini, L., Torreri, P., Macchia, G., Ramoni, C., Ceccarini, M., and Petrucci, T. C. (2003). Beta-dystrobrevin interacts directly with kinesin heavy chain in brain. J Cell Sci 116, 4847-4856.

Mackie, S., Millar, J. K., and Porteous, D. J. (2007). Role of DISC1 in neural development and schizophrenia. Curr Opin Neurobiol 17, 95-102.

Majdan, M., Lachance, C., Gloster, A., Aloyz, R., Zeindler, C., Bamji, S., Bhakar, A., Belliveau, D., Fawcett, J., Miller, F. D., and Barker, P. A. (1997). Transgenic mice expressing the intracellular domain of the p75 neurotrophin receptor undergo neuronal apoptosis. J Neurosci 17, 6988-6998.

Marshall, C. J. (1995). Specificity of receptor tyrosine kinase signaling: transient versus sustained extracellular signal-regulated kinase activation. Cell 80, 179-185.

Martin, M., Ahern-Djamali, S. M., Hoffmann, F. M., and Saxton, W. M. (2005). Abl tyrosine kinase and its substrate Ena/VASP have functional interactions with kinesin-1. Mol Biol Cell 16, 4225-4230.

Martin, M., Iyadurai, S. J., Gassman, A., Gindhart, J. G., Jr., Hays, T. S., and Saxton, W. M. (1999). Cytoplasmic dynein, the dynactin complex, and kinesin are interdependent and essential for fast axonal transport. Mol Biol Cell 10, 3717-3728.

Martin, S. C., Marazzi, G., Sandell, J. H., and Heinrich, G. (1995). Five Trk receptors in the zebrafish. Dev Biol 169, 745-758.

Martin, S. C., Sandell, J. H., and Heinrich, G. (1998). Zebrafish TrkC1 and TrkC2 receptors define two different cell populations in the nervous system during the period of axonogenesis. Dev Biol 195, 114-130.

Matsuda, S., Matsuda, Y., and D'Adamio, L. (2003). Amyloid beta protein precursor (AbetaPP), but not AbetaPP-like protein 2, is bridged to the kinesin light

chain by the scaffold protein JNK-interacting protein 1. J Biol Chem 278, 38601-38606.

McCart, A. E., Mahony, D., and Rothnagel, J. A. (2003). Alternatively spliced products of the human kinesin light chain 1 (KNS2) gene. Traffic 4, 576-580.

McGuire, J. R., Rong, J., Li, S. H., and Li, X. J. (2006). Interaction of Huntingtin-associated protein-1 with kinesin light chain: implications in intracellular trafficking in neurons. J Biol Chem 281, 3552-3559.

McLeod, M., Craft, S., and Broach, J. R. (1986). Identification of the crossover site during FLP-mediated recombination in the Saccharomyces cerevisiae plasmid 2 microns circle. Mol Cell Biol 6, 3357-3367.

Meng, Y. X., Wilson, G. W., Avery, M. C., Varden, C. H., and Balczon, R. (1997). Suppression of the expression of a pancreatic beta-cell form of the kinesin heavy chain by antisense oligonucleotides inhibits insulin secretion from primary cultures of mouse beta-cells. Endocrinology 138, 1979-1987.

Menzel, P., Valencia, F., Godement, P., Dodelet, V. C., and Pasquale, E. B. (2001). Ephrin-A6, a new ligand for EphA receptors in the developing visual system. Dev Biol 230, 74-88.

Miao, H., Burnett, E., Kinch, M., Simon, E., and Wang, B. (2000). Activation of EphA2 kinase suppresses integrin function and causes focal-adhesion-kinase dephosphorylation. Nat Cell Biol 2, 62-69.

Miki, H., Setou, M., Kaneshiro, K., and Hirokawa, N. (2001). All kinesin superfamily protein, KIF, genes in mouse and human. Proc Natl Acad Sci U S A 98, 7004-7011.

Millar, J. K., Pickard, B. S., Mackie, S., James, R., Christie, S., Buchanan, S. R., Malloy, M. P., Chubb, J. E., Huston, E., Baillie, G. S., et al. (2005). DISC1 and PDE4B are interacting genetic factors in schizophrenia that regulate cAMP signaling. Science 310, 1187-1191.

Millar, J. K., Wilson-Annan, J. C., Anderson, S., Christie, S., Taylor, M. S., Semple, C. A., Devon, R. S., Clair, D. M., Muir, W. J., Blackwood, D. H., and Porteous, D. J. (2000). Disruption of two novel genes by a translocation co-segregating with schizophrenia. Hum Mol Genet 9, 1415-1423.

Mineo, C., James, G. L., Smart, E. J., and Anderson, R. G. (1996). Localization of epidermal growth factor-stimulated Ras/Raf-1 interaction to caveolae membrane. J Biol Chem 271, 11930-11935.

Ming, G., Song, H., Berninger, B., Inagaki, N., Tessier-Lavigne, M., and Poo, M. (1999). Phospholipase C-gamma and phosphoinositide 3-kinase mediate cytoplasmic signaling in nerve growth cone guidance. Neuron 23, 139-148.

Minichiello, L., Korte, M., Wolfer, D., Kuhn, R., Unsicker, K., Cestari, V., Rossi-Arnaud, C., Lipp, H. P., Bonhoeffer, T., and Klein, R. (1999). Essential role for TrkB receptors in hippocampus-mediated learning. Neuron 24, 401-414.

Minichiello, L., Piehl, F., Vazquez, E., Schimmang, T., Hokfelt, T., Represa, J., and Klein, R. (1995). Differential effects of combined trk receptor mutations on dorsal root ganglion and inner ear sensory neurons. Development 121, 4067-4075.

Miyoshi, K., Honda, A., Baba, K., Taniguchi, M., Oono, K., Fujita, T., Kuroda, S., Katayama, T., and Tohyama, M. (2003). Disrupted-In-Schizophrenia 1, a candidate gene for schizophrenia, participates in neurite outgrowth. Mol Psychiatry 8, 685-694.

Mok, H., Shin, H., Kim, S., Lee, J. R., Yoon, J., and Kim, E. (2002). Association of the kinesin superfamily motor protein KIF1Balpha with postsynaptic density-95 (PSD-95), synapse-associated protein-97, and synaptic scaffolding molecule PSD-95/discs large/zona occludens-1 proteins. J Neurosci 22, 5253-5258.

Mollaaghababa, R., and Pavan, W. J. (2003). The importance of having your SOX on: role of SOX10 in the development of neural crest-derived melanocytes and glia. Oncogene 22, 3024-3034.

Morfini, G., Szebenyi, G., Elluru, R., Ratner, N., and Brady, S. T. (2002). Glycogen synthase kinase 3 phosphorylates kinesin light chains and negatively regulates kinesin-based motility. Embo J 21, 281-293.

Morris, R. L., and Hollenbeck, P. J. (1993). The regulation of bidirectional mitochondrial transport is coordinated with axonal outgrowth. J Cell Sci 104 (Pt 3), 917-927.

Mu, X., Silos-Santiago, I., Carroll, S. L., and Snider, W. D. (1993). Neurotrophin receptor genes are expressed in distinct patterns in developing dorsal root ganglia. J Neurosci 13, 4029-4041.

Muller, D., Djebbara-Hannas, Z., Jourdain, P., Vutskits, L., Durbec, P., Rougon, G., and Kiss, J. Z. (2000). Brain-derived neurotrophic factor restores long-term potentiation in polysialic acid-neural cell adhesion molecule-deficient hippocampus. Proc Natl Acad Sci U S A 97, 4315-4320.

Muresan, Z., and Muresan, V. (2005). Coordinated transport of phosphorylated amyloid-ß-precursor protein and c-Jun NH2-terminal kinase-interacting protein-1. J Cell Biol 171, 615-625.

Murray, S. S., Bartlett, P. F., and Cheema, S. S. (1999). Differential loss of spinal sensory but not motor neurons in the p75NTR knockout mouse. Neurosci Lett 267, 45-48.

Musch, A. (2004). Microtubule organization and function in epithelial cells. Traffic 5, 1-9.

Myers, K. A., and Baas, P. W. (2007). Kinesin-5 regulates the growth of the axon by acting as a brake on its microtubule array. J Cell Biol 178, 1081-1091.

Nakagawa, T., Setou, M., Seog, D., Ogasawara, K., Dohmae, N., Takio, K., and Hirokawa, N. (2000). A novel motor, KIF13A, transports mannose-6-phosphate receptor to plasma membrane through direct interaction with AP-1 complex. Cell 103, 569-581.

Nakata, T., and Hirokawa, N. (1995). Point mutation of adenosine triphosphate-binding motif generated rigor kinesin that selectively blocks anterograde lysosome membrane transport. J Cell Biol 131, 1039-1053.

Nakata, T., and Hirokawa, N. (2003). Microtubules provide directional cues for polarized axonal transport through interaction with kinesin motor head. J Cell Biol 162, 1045-1055.

Nangaku, M., Sato-Yoshitake, R., Okada, Y., Noda, Y., Takemura, R., Yamazaki, H., and Hirokawa, N. (1994). KIF1B, a novel microtubule plus end-directed monomeric motor protein for transport of mitochondria. Cell 79, 1209-1220.

Nascimento, A. A., Roland, J. T., and Gelfand, V. I. (2003). Pigment cells: a model for the study of organelle transport. Annu Rev Cell Dev Biol 19, 469-491.

Newsome, T. P., Scaplehorn, N., and Way, M. (2004). SRC mediates a switch from microtubule- to actin-based motility of vaccinia virus. Science 306, 124-129.

Newsome, T. P., Schmidt, S., Dietzl, G., Keleman, K., Asling, B., Debant, A., and Dickson, B. J. (2000). Trio combines with dock to regulate Pak activity during photoreceptor axon pathfinding in Drosophila. Cell 101, 283-294.

Newsome, T. P., Weisswange, I., Frischknecht, F., and Way, M. (2006). Abl collaborates with Src family kinases to stimulate actin-based motility of vaccinia virus. Cell Microbiol 8, 233-241.

Nguyen, Q., Lee, C. M., Le, A., and Reddy, E. P. (2005). JLP associates with kinesin light chain 1 through a novel leucine zipper-like domain. J Biol Chem 280, 30185-30191.

Nishimura, T., Kato, K., Yamaguchi, T., Fukata, Y., Ohno, S., and Kaibuchi, K. (2004). Role of the PAR-3-KIF3 complex in the establishment of neuronal polarity. Nat Cell Biol 6, 328-334.

Nonaka, S., Tanaka, Y., Okada, Y., Takeda, S., Harada, A., Kanai, Y., Kido, M., and Hirokawa, N. (1998). Randomization of left-right asymmetry due to loss of nodal cilia generating leftward flow of extraembryonic fluid in mice lacking KIF3B motor protein. Cell 95, 829-837.

Nourry, C., Grant, S. G., and Borg, J. P. (2003). PDZ domain proteins: plug and play! Sci STKE 2003, RE7.

Nusser, N., Gosmanova, E., Zheng, Y., and Tigyi, G. (2002). Nerve growth factor signals through TrkA, phosphatidylinositol 3-kinase, and Rac1 to inactivate

RhoA during the initiation of neuronal differentiation of PC12 cells. J Biol Chem 277, 35840-35846.

O'Brien, S. P., Seipel, K., Medley, Q. G., Bronson, R., Segal, R., and Streuli, M. (2000). Skeletal muscle deformity and neuronal disorder in Trio exchange factor-deficient mouse embryos. Proc Natl Acad Sci U S A 97, 12074-12078.

O'Hare, K., and Rubin, G. M. (1983). Structures of P transposable elements and their sites of insertion and excision in the Drosophila melanogaster genome. Cell 34, 25-35.

Offman, M. N., Fitzjohn, P. W., and Bates, P. A. (2006). Developing a move-set for protein model refinement. Bioinformatics 22, 1838-1845.

Ohta, K., Iwamasa, H., Drescher, U., Terasaki, H., and Tanaka, H. (1997). The inhibitory effect on neurite outgrowth of motoneurons exerted by the ligands ELF-1 and RAGS. Mech Dev 64, 127-135.

Okada, Y., Yamazaki, H., Sekine-Aizawa, Y., and Hirokawa, N. (1995). The neuron-specific kinesin superfamily protein KIF1A is a unique monomeric motor for anterograde axonal transport of synaptic vesicle precursors. Cell 81, 769-780.

Okagawa, H., Nakagawa, M., and Simada, M. (1995). Immunolocalization of N-CAM in the heart of the early developing rat embryo. Anat Rec 243, 261-271.

Oppenheim, R. W., Wiese, S., Prevette, D., Armanini, M., Wang, S., Houenou, L. J., Holtmann, B., Gotz, R., Pennica, D., and Sendtner, M. (2001). Cardiotrophin-1, a muscle-derived cytokine, is required for the survival of subpopulations of developing motoneurons. J Neurosci 21, 1283-1291.

Oppenheim, R. W., Yin, Q. W., Prevette, D., and Yan, Q. (1992). Brain-derived neurotrophic factor rescues developing avian motoneurons from cell death. Nature 360, 755-757.

Orioli, D., Henkemeyer, M., Lemke, G., Klein, R., and Pawson, T. (1996). Sek4 and Nuk receptors cooperate in guidance of commissural axons and in palate formation. Embo J 15, 6035-6049.

Ozeki, Y., Tomoda, T., Kleiderlein, J., Kamiya, A., Bord, L., Fujii, K., Okawa, M., Yamada, N., Hatten, M. E., Snyder, S. H., et al. (2003). Disrupted-in-Schizophrenia-1 (DISC-1): mutant truncation prevents binding to NudE-like (NUDEL) and inhibits neurite outgrowth. Proc Natl Acad Sci U S A 100, 289-294.

Palacios, I. M., and St Johnston, D. (2002). Kinesin light chain-independent function of the Kinesin heavy chain in cytoplasmic streaming and posterior localisation in the Drosophila oocyte. Development 129, 5473-5485.

Palko, M. E., Coppola, V., and Tessarollo, L. (1999). Evidence for a role of truncated trkC receptor isoforms in mouse development. J Neurosci 19, 775-782.

Paratcha, G., Ledda, F., and Ibanez, C. F. (2003). The neural cell adhesion molecule NCAM is an alternative signaling receptor for GDNF family ligands. Cell 113, 867-879.

Pasquale, E. B. (2005). Eph receptor signalling casts a wide net on cell behaviour. Nat Rev Mol Cell Biol 6, 462-475.

Patterson, S. L., Abel, T., Deuel, T. A., Martin, K. C., Rose, J. C., and Kandel, E. R. (1996). Recombinant BDNF rescues deficits in basal synaptic

transmission and hippocampal LTP in BDNF knockout mice. Neuron 16, 1137-1145.

Peiro, S., Comella, J. X., Enrich, C., Martin-Zanca, D., and Rocamora, N. (2000). PC12 cells have caveolae that contain TrkA. Caveolae-disrupting drugs inhibit nerve growth factor-induced, but not epidermal growth factor-induced, MAPK phosphorylation. J Biol Chem 275, 37846-37852.

Penzes, P., Beeser, A., Chernoff, J., Schiller, M. R., Eipper, B. A., Mains, R. E., and Huganir, R. L. (2003). Rapid induction of dendritic spine morphogenesis by trans-synaptic ephrinB-EphB receptor activation of the Rho-GEF kalirin. Neuron 37, 263-274.

Pilling, A. D., Horiuchi, D., Lively, C. M., and Saxton, W. M. (2006). Kinesin-1 and Dynein are the primary motors for fast transport of mitochondria in Drosophila motor axons. Mol Biol Cell 17, 2057-2068.

Polleux, F., Whitford, K. L., Dijkhuizen, P. A., Vitalis, T., and Ghosh, A. (2002). Control of cortical interneuron migration by neurotrophins and PI3-kinase signaling. Development 129, 3147-3160.

Pozzo-Miller, L. D., Gottschalk, W., Zhang, L., McDermott, K., Du, J., Gopalakrishnan, R., Oho, C., Sheng, Z. H., and Lu, B. (1999). Impairments in high-frequency transmission, synaptic vesicle docking, and synaptic protein distribution in the hippocampus of BDNF knockout mice. J Neurosci 19, 4972-4983.

Pulido, D., Campuzano, S., Koda, T., Modolell, J., and Barbacid, M. (1992). Dtrk, a Drosophila gene related to the trk family of neurotrophin receptors, encodes a novel class of neural cell adhesion molecule. Embo J 11, 391-404.

Qiao, F., and Bowie, J. U. (2005). The many faces of SAM. Sci STKE 2005, re7.

Rahman, A., Friedman, D. S., and Goldstein, L. S. (1998). Two kinesin light chain genes in mice. Identification and characterization of the encoded proteins. J Biol Chem 273, 15395-15403.

Rahman, A., Kamal, A., Roberts, E. A., and Goldstein, L. S. (1999). Defective kinesin heavy chain behavior in mouse kinesin light chain mutants. J Cell Biol 146, 1277-1288.

Reck-Peterson, S. L., Yildiz, A., Carter, A. P., Gennerich, A., Zhang, N., and Vale, R. D. (2006). Single-molecule analysis of dynein processivity and stepping behavior. Cell 126, 335-348.

Reed, N. A., Cai, D., Blasius, T. L., Jih, G. T., Meyhofer, E., Gaertig, J., and Verhey, K. J. (2006). Microtubule acetylation promotes kinesin-1 binding and transport. Curr Biol 16, 2166-2172.

Reilein, A. R., Tint, I. S., Peunova, N. I., Enikolopov, G. N., and Gelfand, V. I. (1998). Regulation of organelle movement in melanophores by protein kinase A (PKA), protein kinase C (PKC), and protein phosphatase 2A (PP2A). J Cell Biol 142, 803-813.

Rice, D. S., and Curran, T. (2001). Role of the reelin signaling pathway in central nervous system development. Annu Rev Neurosci 24, 1005-1039.

Rico, B., Xu, B., and Reichardt, L. F. (2002). TrkB receptor signaling is required for establishment of GABAergic synapses in the cerebellum. Nat Neurosci 5, 225-233.

Rietdorf, J., Ploubidou, A., Reckmann, I., Holmstrom, A., Frischknecht, F., Zettl, M., Zimmermann, T., and Way, M. (2001). Kinesin-dependent movement on microtubules precedes actin-based motility of vaccinia virus. Nat Cell Biol 3, 992-1000.

Riol-Blanco, L., Iglesias, T., Sanchez-Sanchez, N., de la Rosa, G., Sanchez-Ruiloba, L., Cabrera-Poch, N., Torres, A., Longo, I., Garcia-Bordas, J., Longo, N., et al. (2004). The neuronal protein Kidins220 localizes in a raft compartment at the leading edge of motile immature dendritic cells. Eur J Immunol 34, 108-118.

Rivera, J., Chu, P. J., Lewis, T. L., Jr., and Arnold, D. B. (2007). The role of Kif5B in axonal localization of Kv1 K(+) channels. Eur J Neurosci 25, 136-146.

Rorth, P. (1996). A modular misexpression screen in Drosophila detecting tissue-specific phenotypes. Proc Natl Acad Sci U S A 93, 12418-12422.

Rosales, C. R., Osborne, K. D., Zuccarino, G. V., Scheiffele, P., and Silverman, M. A. (2005). A cytoplasmic motif targets neuroligin-1 exclusively to dendrites of cultured hippocampal neurons. Eur J Neurosci 22, 2381-2386.

Ross, J. L., Wallace, K., Shuman, H., Goldman, Y. E., and Holzbaur, E. L. (2006). Processive bidirectional motion of dynein-dynactin complexes in vitro. Nat Cell Biol 8, 562-570.

Roux, P. P., and Barker, P. A. (2002). Neurotrophin signaling through the p75 neurotrophin receptor. Prog Neurobiol 67, 203-233.

Ruvkun, G., and Hobert, O. (1998). The taxonomy of developmental control in Caenorhabditis elegans. Science 282, 2033-2041.

Saha, M. S., Miles, R. R., and Grainger, R. M. (1997). Dorsal-ventral patterning during neural induction in Xenopus: assessment of spinal cord regionalization with xHB9, a marker for the motor neuron region. Dev Biol 187, 209-223.

Saiki, R. K., Gelfand, D. H., Stoffel, S., Scharf, S. J., Higuchi, R., Horn, G. T., Mullis, K. B., and Erlich, H. A. (1988). Primer-directed enzymatic amplification of DNA with a thermostable DNA polymerase. Science 239, 487-491.

Sampo, B., Kaech, S., Kunz, S., and Banker, G. (2003). Two distinct mechanisms target membrane proteins to the axonal surface. Neuron 37, 611-624.

Sanchez-Ruiloba, L., Cabrera-Poch, N., Rodriguez-Martinez, M., Lopez-Menendez, C., Jean-Mairet, R. M., Higuero, A. M., and Iglesias, T. (2006). Protein kinase D intracellular localization and activity control kinase D-interacting substrate of 220-kDa traffic through a postsynaptic density-95/discs large/zonula occludens-1-binding motif. J Biol Chem 281, 18888-18900.

Sato-Yoshitake, R., Yorifuji, H., Inagaki, M., and Hirokawa, N. (1992). The phosphorylation of kinesin regulates its binding to synaptic vesicles. J Biol Chem 267, 23930-23936.

Sauer, B., and Henderson, N. (1988). Site-specific DNA recombination in mammalian cells by the Cre recombinase of bacteriophage P1. Proc Natl Acad Sci U S A 85, 5166-5170.

Saxena, S., Bucci, C., Weis, J., and Kruttgen, A. (2005). The small GTPase Rab7 controls the endosomal trafficking and neuritogenic signaling of the nerve growth factor receptor TrkA. J Neurosci 25, 10930-10940.

Saxton, W. M., Hicks, J., Goldstein, L. S., and Raff, E. C. (1991). Kinesin heavy chain is essential for viability and neuromuscular functions in Drosophila, but mutants show no defects in mitosis. Cell 64, 1093-1102.

Scheufler, C., Brinker, A., Bourenkov, G., Pegoraro, S., Moroder, L., Bartunik, H., Hartl, F. U., and Moarefi, I. (2000). Structure of TPR domain-peptide complexes: critical elements in the assembly of the Hsp70-Hsp90 multichaperone machine. Cell 101, 199-210.

Schmelz, M., Sodeik, B., Ericsson, M., Wolffe, E. J., Shida, H., Hiller, G., and Griffiths, G. (1994). Assembly of vaccinia virus: the second wrapping cisterna is derived from the trans Golgi network. J Virol 68, 130-147.

Schnapp, B. J. (2003). Trafficking of signaling modules by kinesin motors. J Cell Sci 116, 2125-2135.

Scully, A. L., McKeown, M., and Thomas, J. B. (1999). Isolation and characterization of Dek, a Drosophila eph receptor protein tyrosine kinase. Mol Cell Neurosci 13, 337-347.

Seiler, S., Kirchner, J., Horn, C., Kallipolitou, A., Woehlke, G., and Schliwa, M. (2000). Cargo binding and regulatory sites in the tail of fungal conventional kinesin. Nat Cell Biol 2, 333-338.

Seitz, A., Kojima, H., Oiwa, K., Mandelkow, E. M., Song, Y. H., and Mandelkow, E. (2002). Single-molecule investigation of the interference between kinesin, tau and MAP2c. Embo J 21, 4896-4905.

Sendtner, M., Holtmann, B., Kolbeck, R., Thoenen, H., and Barde, Y. A. (1992). Brain-derived neurotrophic factor prevents the death of motoneurons in newborn rats after nerve section. Nature 360, 757-759.

Setou, M., Nakagawa, T., Seog, D. H., and Hirokawa, N. (2000). Kinesin superfamily motor protein KIF17 and mLin-10 in NMDA receptor-containing vesicle transport. Science 288, 1796-1802.

Setou, M., Seog, D. H., Tanaka, Y., Kanai, Y., Takei, Y., Kawagishi, M., and Hirokawa, N. (2002). Glutamate-receptor-interacting protein GRIP1 directly steers kinesin to dendrites. Nature 417, 83-87.

Shamah, S. M., Lin, M. Z., Goldberg, J. L., Estrach, S., Sahin, M., Hu, L., Bazalakova, M., Neve, R. L., Corfas, G., Debant, A., and Greenberg, M. E. (2001). EphA receptors regulate growth cone dynamics through the novel guanine nucleotide exchange factor ephexin. Cell 105, 233-244.

Shao, Y., Akmentin, W., Toledo-Aral, J. J., Rosenbaum, J., Valdez, G., Cabot, J. B., Hilbush, B. S., and Halegoua, S. (2002). Pincher, a pinocytic chaperone for nerve growth factor/TrkA signaling endosomes. J Cell Biol 157, 679-691.

Shin, H., Wyszynski, M., Huh, K. H., Valtschanoff, J. G., Lee, J. R., Ko, J., Streuli, M., Weinberg, R. J., Sheng, M., and Kim, E. (2003). Association of the kinesin motor KIF1A with the multimodular protein liprin-alpha. J Biol Chem 278, 11393-11401.

Shinoda, T., Taya, S., Tsuboi, D., Hikita, T., Matsuzawa, R., Kuroda, S., Iwamatsu, A., and Kaibuchi, K. (2007). DISC1 regulates neurotrophin-induced axon elongation via interaction with Grb2. J Neurosci 27, 4-14.

Simons, K., and Toomre, D. (2000). Lipid rafts and signal transduction. Nat Rev Mol Cell Biol 1, 31-39.

Skoufias, D. A., Cole, D. G., Wedaman, K. P., and Scholey, J. M. (1994). The carboxyl-terminal domain of kinesin heavy chain is important for membrane binding. J Biol Chem 269, 1477-1485.

Smeyne, R. J., Klein, R., Schnapp, A., Long, L. K., Bryant, S., Lewin, A., Lira, S. A., and Barbacid, M. (1994). Severe sensory and sympathetic neuropathies in mice carrying a disrupted Trk/NGF receptor gene. Nature 368, 246-249.

Sodergren, E., Weinstock, G. M., Davidson, E. H., Cameron, R. A., Gibbs, R. A., Angerer, R. C., Angerer, L. M., Arnone, M. I., Burgess, D. R., Burke, R. D., et al. (2006). The genome of the sea urchin Strongylocentrotus purpuratus. Science 314, 941-952.

Sofroniew, M. V., Howe, C. L., and Mobley, W. C. (2001). Nerve growth factor signaling, neuroprotection, and neural repair. Annu Rev Neurosci 24, 1217-1281.

Soldati, T., and Schliwa, M. (2006). Powering membrane traffic in endocytosis and recycling. Nat Rev Mol Cell Biol 7, 897-908.

Spradling, A. C., and Rubin, G. M. (1982). Transposition of cloned P elements into Drosophila germ line chromosomes. Science 218, 341-347.

Steinberg, G., and Schliwa, M. (1995). The Neurospora organelle motor: a distant relative of conventional kinesin with unconventional properties. Mol Biol Cell 6, 1605-1618.

Stenmark, H., and Olkkonen, V. M. (2001). The Rab GTPase family. Genome Biol 2, REVIEWS3007.

Stock, M. F., Guerrero, J., Cobb, B., Eggers, C. T., Huang, T. G., Li, X., and Hackney, D. D. (1999). Formation of the compact confomer of kinesin requires a COOH-terminal heavy chain domain and inhibits microtubule-stimulated ATPase activity. J Biol Chem 274, 14617-14623.

Stoilov, P., Castren, E., and Stamm, S. (2002). Analysis of the human TrkB gene genomic organization reveals novel TrkB isoforms, unusual gene length, and splicing mechanism. Biochem Biophys Res Commun 290, 1054-1065.

Stowell, J. N., and Craig, A. M. (1999). Axon/dendrite targeting of metabotropic glutamate receptors by their cytoplasmic carboxy-terminal domains. Neuron 22, 525-536.

Strohmaier, C., Carter, B. D., Urfer, R., Barde, Y. A., and Dechant, G. (1996). A splice variant of the neurotrophin receptor trkB with increased specificity for brain-derived neurotrophic factor. Embo J 15, 3332-3337.

Stucky, C. L., DeChiara, T., Lindsay, R. M., Yancopoulos, G. D., and Koltzenburg, M. (1998). Neurotrophin 4 is required for the survival of a subclass of hair follicle receptors. J Neurosci 18, 7040-7046.

Su, Q., Cai, Q., Gerwin, C., Smith, C. L., and Sheng, Z. H. (2004). Syntabulin is a microtubule-associated protein implicated in syntaxin transport in neurons. Nat Cell Biol 6, 941-953.

Suzuki, S., Numakawa, T., Shimazu, K., Koshimizu, H., Hara, T., Hatanaka, H., Mei, L., Lu, B., and Kojima, M. (2004). BDNF-induced recruitment of TrkB

receptor into neuronal lipid rafts: roles in synaptic modulation. J Cell Biol 167, 1205-1215.

Takasu, M. A., Dalva, M. B., Zigmond, R. E., and Greenberg, M. E. (2002). Modulation of NMDA receptor-dependent calcium influx and gene expression through EphB receptors. Science 295, 491-495.

Tanaka, Y., Kanai, Y., Okada, Y., Nonaka, S., Takeda, S., Harada, A., and Hirokawa, N. (1998). Targeted disruption of mouse conventional kinesin heavy chain, kif5B, results in abnormal perinuclear clustering of mitochondria. Cell 93, 1147-1158.

Taniuchi, M., Clark, H. B., and Johnson, E. M., Jr. (1986). Induction of nerve growth factor receptor in Schwann cells after axotomy. Proc Natl Acad Sci U S A 83, 4094-4098.

Tansey, M. G., Baloh, R. H., Milbrandt, J., and Johnson, E. M., Jr. (2000). GFRalpha-mediated localization of RET to lipid rafts is required for effective downstream signaling, differentiation, and neuronal survival. Neuron 25, 611-623.

Taya, S., Shinoda, T., Tsuboi, D., Asaki, J., Nagai, K., Hikita, T., Kuroda, S., Kuroda, K., Shimizu, M., Hirotsune, S., et al. (2007). DISC1 regulates the transport of the NUDEL/LIS1/14-3-3epsilon complex through kinesin-1. J Neurosci 27, 15-26.

Terada, S., Kinjo, M., and Hirokawa, N. (2000). Oligomeric tubulin in large transporting complex is transported via kinesin in squid giant axons. Cell 103, 141-155.

Terlecky, S. R., Nuttley, W. M., McCollum, D., Sock, E., and Subramani, S. (1995). The Pichia pastoris peroxisomal protein PAS8p is the receptor for the C-terminal tripeptide peroxisomal targeting signal. Embo J 14, 3627-3634.

Tessarollo, L., Tsoulfas, P., Donovan, M. J., Palko, M. E., Blair-Flynn, J., Hempstead, B. L., and Parada, L. F. (1997). Targeted deletion of all isoforms of the trkC gene suggests the use of alternate receptors by its ligand neurotrophin-3 in neuronal development and implicates trkC in normal cardiogenesis. Proc Natl Acad Sci U S A 94, 14776-14781.

Thaler, C. D., and Haimo, L. T. (1990). Regulation of organelle transport in melanophores by calcineurin. J Cell Biol 111, 1939-1948.

Thaler, J., Harrison, K., Sharma, K., Lettieri, K., Kehrl, J., and Pfaff, S. L. (1999). Active suppression of interneuron programs within developing motor neurons revealed by analysis of homeodomain factor HB9. Neuron 23, 675-687.

Thiery, J. P., Duband, J. L., Rutishauser, U., and Edelman, G. M. (1982). Cell adhesion molecules in early chicken embryogenesis. Proc Natl Acad Sci U S A 79, 6737-6741.

Thomas, S. M., and Brugge, J. S. (1997). Cellular functions regulated by Src family kinases. Annu Rev Cell Dev Biol 13, 513-609.

Tienari, P. J., De Strooper, B., Ikonen, E., Simons, M., Weidemann, A., Czech, C., Hartmann, T., Ida, N., Multhaup, G., Masters, C. L., et al. (1996). The beta-amyloid domain is essential for axonal sorting of amyloid precursor protein. Embo J 15, 5218-5229.

Tomasiewicz, H., Ono, K., Yee, D., Thompson, C., Goridis, C., Rutishauser, U., and Magnuson, T. (1993). Genetic deletion of a neural cell adhesion molecule variant (N-CAM-180) produces distinct defects in the central nervous system. Neuron 11, 1163-1174.

Toyo-oka, K., Shionoya, A., Gambello, M. J., Cardoso, C., Leventer, R., Ward, H. L., Ayala, R., Tsai, L. H., Dobyns, W., Ledbetter, D., et al. (2003). 14-3-3epsilon is important for neuronal migration by binding to NUDEL: a molecular explanation for Miller-Dieker syndrome. Nat Genet 34, 274-285.

Toyoshima, I., Yu, H., Steuer, E. R., and Sheetz, M. P. (1992). Kinectin, a major kinesin-binding protein on ER. J Cell Biol 118, 1121-1131.

Tsai, M. Y., Morfini, G., Szebenyi, G., and Brady, S. T. (2000). Release of kinesin from vesicles by hsc70 and regulation of fast axonal transport. Mol Biol Cell 11, 2161-2173.

Tsien, J. Z., Chen, D. F., Gerber, D., Tom, C., Mercer, E. H., Anderson, D. J., Mayford, M., Kandel, E. R., and Tonegawa, S. (1996). Subregion- and cell type-restricted gene knockout in mouse brain. Cell 87, 1317-1326.

Urfer, R., Tsoulfas, P., O'Connell, L., Shelton, D. L., Parada, L. F., and Presta, L. G. (1995). An immunoglobulin-like domain determines the specificity of neurotrophin receptors. Embo J 14, 2795-2805.

Valdez, G., Akmentin, W., Philippidou, P., Kuruvilla, R., Ginty, D. D., and Halegoua, S. (2005). Pincher-mediated macroendocytosis underlies retrograde signaling by neurotrophin receptors. J Neurosci 25, 5236-5247.

Vale, R. D., Reese, T. S., and Sheetz, M. P. (1985). Identification of a novel force-generating protein, kinesin, involved in microtubule-based motility. Cell 42, 39-50.

Valetti, C., Wetzel, D. M., Schrader, M., Hasbani, M. J., Gill, S. R., Kreis, T. E., and Schroer, T. A. (1999). Role of dynactin in endocytic traffic: effects of dynamitin overexpression and colocalization with CLIP-170. Mol Biol Cell 10, 4107-4120.

Van Doren, M., Williamson, A. L., and Lehmann, R. (1998). Regulation of zygotic gene expression in Drosophila primordial germ cells. Curr Biol 8, 243-246.

Van Etten, R. A. (1999). Cycling, stressed-out and nervous: cellular functions of c-Abl. Trends Cell Biol 9, 179-186.

van Kesteren, R. E., Fainzilber, M., Hauser, G., van Minnen, J., Vreugdenhil, E., Smit, A. B., Ibanez, C. F., Geraerts, W. P., and Bulloch, A. G. (1998). Early evolutionary origin of the neurotrophin receptor family. Embo J 17, 2534-2542.

Varsano, T., Dong, M. Q., Niesman, I., Gacula, H., Lou, X., Ma, T., Testa, J. R., Yates, J. R., 3rd, and Farquhar, M. G. (2006). GIPC is recruited by APPL to peripheral TrkA endosomes and regulates TrkA trafficking and signaling. Mol Cell Biol 26, 8942-8952.

Vaudry, D., Stork, P. J., Lazarovici, P., and Eiden, L. E. (2002). Signaling pathways for PC12 cell differentiation: making the right connections. Science 296, 1648-1649.

Verhey, K. J., Lizotte, D. L., Abramson, T., Barenboim, L., Schnapp, B. J., and Rapoport, T. A. (1998). Light chain-dependent regulation of Kinesin's interaction with microtubules. J Cell Biol 143, 1053-1066.

Verhey, K. J., Meyer, D., Deehan, R., Blenis, J., Schnapp, B. J., Rapoport, T. A., and Margolis, B. (2001). Cargo of kinesin identified as JIP scaffolding proteins and associated signaling molecules. J Cell Biol 152, 959-970.

Verhey, K. J., and Rapoport, T. A. (2001). Kinesin carries the signal. Trends Biochem Sci 26, 545-550.

Voelker, R. A., Greenleaf, A. L., Gyurkovics, H., Wisely, G. B., Huang, S. M., and Searles, L. L. (1984). Frequent Imprecise Excision among Reversions of a P Element-Caused Lethal Mutation in Drosophila. Genetics 107, 279-294.

von Schack, D., Casademunt, E., Schweigreiter, R., Meyer, M., Bibel, M., and Dechant, G. (2001). Complete ablation of the neurotrophin receptor p75NTR causes defects both in the nervous and the vascular system. Nat Neurosci 4, 977-978.

Vutskits, L., Djebbara-Hannas, Z., Zhang, H., Paccaud, J. P., Durbec, P., Rougon, G., Muller, D., and Kiss, J. Z. (2001). PSA-NCAM modulates BDNF-dependent survival and differentiation of cortical neurons. Eur J Neurosci 13, 1391-1402.

Wahl, S., Barth, H., Ciossek, T., Aktories, K., and Mueller, B. K. (2000). Ephrin-A5 induces collapse of growth cones by activating Rho and Rho kinase. J Cell Biol 149, 263-270.

Wang, H. U., and Anderson, D. J. (1997). Eph family transmembrane ligands can mediate repulsive guidance of trunk neural crest migration and motor axon outgrowth. Neuron 18, 383-396.

Wang, H. U., Chen, Z. F., and Anderson, D. J. (1998). Molecular distinction and angiogenic interaction between embryonic arteries and veins revealed by ephrin-B2 and its receptor Eph-B4. Cell 93, 741-753.

Ward, B. M., and Moss, B. (2004). Vaccinia virus A36R membrane protein provides a direct link between intracellular enveloped virions and the microtubule motor kinesin. J Virol 78, 2486-2493.

Waterman-Storer, C. M., Karki, S. B., Kuznetsov, S. A., Tabb, J. S., Weiss, D. G., Langford, G. M., and Holzbaur, E. L. (1997). The interaction between cytoplasmic dynein and dynactin is required for fast axonal transport. Proc Natl Acad Sci U S A 94, 12180-12185.

Watson, F. L., Heerssen, H. M., Bhattacharyya, A., Klesse, L., Lin, M. Z., and Segal, R. A. (2001). Neurotrophins use the Erk5 pathway to mediate a retrograde survival response. Nat Neurosci 4, 981-988.

Weaver, C., Farr, G. H., 3rd, Pan, W., Rowning, B. A., Wang, J., Mao, J., Wu, D., Li, L., Larabell, C. A., and Kimelman, D. (2003). GBP binds kinesin light chain and translocates during cortical rotation in Xenopus eggs. Development 130, 5425-5436.

Wegmeyer, H., Egea, J., Rabe, N., Gezelius, H., Filosa, A., Enjin, A., Varoqueaux, F., Deininger, K., Schnutgen, F., Brose, N., et al. (2007). EphA4-dependent axon guidance is mediated by the RacGAP alpha2-chimaerin. Neuron 55, 756-767.

Weinhold, B., Seidenfaden, R., Rockle, I., Muhlenhoff, M., Schertzinger, F., Conzelmann, S., Marth, J. D., Gerardy-Schahn, R., and Hildebrandt, H. (2005). Genetic ablation of polysialic acid causes severe neurodevelopmental defects rescued by deletion of the neural cell adhesion molecule. J Biol Chem 280, 42971-42977.

Welch, M. D., Mallavarapu, A., Rosenblatt, J., and Mitchison, T. J. (1997). Actin dynamics in vivo. Curr Opin Cell Biol 9, 54-61.

Welte, M. A., Gross, S. P., Postner, M., Block, S. M., and Wieschaus, E. F. (1998). Developmental regulation of vesicle transport in Drosophila embryos: forces and kinetics. Cell 92, 547-557.

West, A. E., Neve, R. L., and Buckley, K. M. (1997). Identification of a somatodendritic targeting signal in the cytoplasmic domain of the transferrin receptor. J Neurosci 17, 6038-6047.

White, F. A., Silos-Santiago, I., Molliver, D. C., Nishimura, M., Phillips, H., Barbacid, M., and Snider, W. D. (1996). Synchronous onset of NGF and TrkA survival dependence in developing dorsal root ganglia. J Neurosci 16, 4662-4672.

Wilkinson, D. G. (2001). Multiple roles of EPH receptors and ephrins in neural development. Nat Rev Neurosci 2, 155-164.

Winberg, M. L., Tamagnone, L., Bai, J., Comoglio, P. M., Montell, D., and Goodman, C. S. (2001). The transmembrane protein Off-track associates with Plexins and functions downstream of Semaphorin signaling during axon guidance. Neuron 32, 53-62.

Woehlke, G., and Schliwa, M. (2000a). Directional motility of kinesin motor proteins. Biochim Biophys Acta 1496, 117-127.

Woehlke, G., and Schliwa, M. (2000b). Walking on two heads: the many talents of kinesin. Nat Rev Mol Cell Biol 1, 50-58.

Wood, S. J., Pritchard, J., and Sofroniew, M. V. (1990). Re-expression of Nerve Growth Factor Receptor after Axonal Injury Recapitulates a Developmental Event in Motor Neurons: Differential Regulation when Regeneration is Allowed or Prevented. Eur J Neurosci 2, 650-657.

Wozniak, M. J., and Allan, V. J. (2006). Cargo selection by specific kinesin light chain 1 isoforms. Embo J 25, 5457-5468.

Wozniak, M. J., Melzer, M., Dorner, C., Haring, H. U., and Lammers, R. (2005). The novel protein KBP regulates mitochondria localization by interaction with a kinesin-like protein. BMC Cell Biol 6, 35.

Wu, C., Butz, S., Ying, Y.-S., and Anderson, R. (1997). Tyrosine kinase receptors concentrated in caveolae like domains from neuronal plasma membrane. Journal of Biological Chemistry 272, 3554-3559.

Wu, C., Lai, C. F., and Mobley, W. C. (2001). Nerve growth factor activates persistent Rap1 signaling in endosomes. J Neurosci 21, 5406-5416.

Xia, C. H., Roberts, E. A., Her, L. S., Liu, X., Williams, D. S., Cleveland, D. W., and Goldstein, L. S. (2003). Abnormal neurofilament transport caused by targeted disruption of neuronal kinesin heavy chain KIF5A. J Cell Biol 161, 55-66.

Xu, B., Gottschalk, W., Chow, A., Wilson, R. I., Schnell, E., Zang, K., Wang, D., Nicoll, R. A., Lu, B., and Reichardt, L. F. (2000a). The role of brain-derived neurotrophic factor receptors in the mature hippocampus: modulation of long-term potentiation through a presynaptic mechanism involving TrkB. J Neurosci 20, 6888-6897.

Xu, B., Zang, K., Ruff, N. L., Zhang, Y. A., McConnell, S. K., Stryker, M. P., and Reichardt, L. F. (2000b). Cortical degeneration in the absence of neurotrophin signaling: dendritic retraction and neuronal loss after removal of the receptor TrkB. Neuron 26, 233-245.

Xu, Q., Alldus, G., Holder, N., and Wilkinson, D. G. (1995). Expression of truncated Sek-1 receptor tyrosine kinase disrupts the segmental restriction of gene expression in the Xenopus and zebrafish hindbrain. Development 121, 4005-4016.

Yaar, M., Zhai, S., Pilch, P. F., Doyle, S. M., Eisenhauer, P. B., Fine, R. E., and Gilchrest, B. A. (1997). Binding of beta-amyloid to the p75 neurotrophin receptor induces apoptosis. A possible mechanism for Alzheimer's disease. J Clin Invest 100, 2333-2340.

Yan, Q., Elliott, J., and Snider, W. D. (1992). Brain-derived neurotrophic factor rescues spinal motor neurons from axotomy-induced cell death. Nature 360, 753-755.

Yanagisawa, M., Kaverina, I. N., Wang, A., Fujita, Y., Reynolds, A. B., and Anastasiadis, P. Z. (2004). A novel interaction between kinesin and p120 modulates p120 localization and function. J Biol Chem 279, 9512-9521.

Yang, J., and Li, T. (2005). The ciliary rootlet interacts with kinesin light chains and may provide a scaffold for kinesin-1 vesicular cargos. Exp Cell Res 309, 379-389.

Yang, J., Liu, X., Yue, G., Adamian, M., Bulgakov, O., and Li, T. (2002). Rootletin, a novel coiled-coil protein, is a structural component of the ciliary rootlet. J Cell Biol 159, 431-440.

Yano, H., and Chao, M. V. (2004). Mechanisms of neurotrophin receptor vesicular transport. J Neurobiol 58, 244-257.

Yano, H., Cong, F., Birge, R. B., Goff, S. P., and Chao, M. V. (2000). Association of the Abl tyrosine kinase with the Trk nerve growth factor receptor. J Neurosci Res 59, 356-364.

Yano, H., Lee, F. S., Kong, H., Chuang, J., Arevalo, J., Perez, P., Sung, C., and Chao, M. V. (2001). Association of Trk neurotrophin receptors with components of the cytoplasmic dynein motor. J Neurosci 21, RC125.

Yao, K. M., and White, K. (1994). Neural specificity of elav expression: defining a Drosophila promoter for directing expression to the nervous system. J Neurochem 63, 41-51.

Ye, H., Kuruvilla, R., Zweifel, L. S., and Ginty, D. D. (2003). Evidence in support of signaling endosome-based retrograde survival of sympathetic neurons. Neuron 39, 57-68.

Yokoyama, N., Romero, M. I., Cowan, C. A., Galvan, P., Helmbacher, F., Charnay, P., Parada, L. F., and Henkemeyer, M. (2001). Forward signaling mediated by ephrin-B3 prevents contralateral corticospinal axons from recrossing the spinal cord midline. Neuron 29, 85-97.

Youn, Y. H., Feng, J., Tessarollo, L., Ito, K., and Sieber-Blum, M. (2003). Neural crest stem cell and cardiac endothelium defects in the TrkC null mouse. Mol Cell Neurosci 24, 160-170.

Yu, H. H., Zisch, A. H., Dodelet, V. C., and Pasquale, E. B. (2001). Multiple signaling interactions of Abl and Arg kinases with the EphB2 receptor. Oncogene 20, 3995-4006.

Zarrinpar, A., Bhattacharyya, R. P., and Lim, W. A. (2003). The structure and function of proline recognition domains. Sci STKE 2003, RE8.

Zhang, Y., Moheban, D. B., Conway, B. R., Bhattacharyya, A., and Segal, R. A. (2000). Cell surface Trk receptors mediate NGF-induced survival while internalized receptors regulate NGF-induced differentiation. J Neurosci 20, 5671-5678.

Zhou, R. (1997). Regulation of topographic projection by the Eph family receptor Bsk (EphA5) and its ligands. Cell Tissue Res 290, 251-259.

Zimmerman, L., Parr, B., Lendahl, U., Cunningham, M., McKay, R., Gavin, B., Mann, J., Vassileva, G., and McMahon, A. (1994). Independent regulatory elements in the nestin gene direct transgene expression to neural stem cells or muscle precursors. Neuron 12, 11-24.

Zweifel, L. S., Kuruvilla, R., and Ginty, D. D. (2005). Functions and mechanisms of retrograde neurotrophin signalling. Nat Rev Neurosci 6, 615-625.